Early-Type Galaxies And Their Sometimes Not So Old Globular Clusters

Maren Hempel

SIGILL·UNIVERSITAT·LUDOVIC·MAXIM·

München 2004

Early-Type Galaxies and Their Sometimes Not So Old Globular Clusters

Maren Hempel

Dissertation
an der Fakultät für Physik
der Ludwig–Maximilians–Universität
München

vorgelegt von
Maren Hempel
aus Karl-Marx-Stadt

München, 17.08.2004

Erstgutachter: Prof. Dr. Ralf Bender
Zweitgutachter: Prof. Dr. Andreas Burkert
Tag der mündlichen Prüfung: 15.10.2004

The most exciting phrase to hear in science, the one that heralds new discoveries,
is not 'Eureka!' (I found it!), but 'That's funny...'.
Isaac Asimov (1920- 1992)

Contents

1 Introduction 2

1.1 Formation and Evolution of Galaxies . . . 3

1.2 Early-Type Galaxies . . . 3

1.2.1 Galaxy Formation Scenarios . . . 4

1.2.1.1 Monolithic Collapse . . . 4

1.2.1.2 Hierarchical Merging . . . 5

1.2.2 Age determination of Stellar Populations . . . 8

1.2.2.1 At Our Doorstep . . . 8

1.2.2.2 In our Neighborhood and Beyond . . . 9

1.2.2.3 Single Stellar Population Models . . . 11

1.2.3 Globular Cluster Systems . . . 14

1.2.3.1 Formation of Globular Clusters . . . 15

1.2.3.2 Globular Cluster Systems . . . 16

1.2.4 Scientific Goals . . . 18

References . . . 21

2 Extragalactic Globular Clusters in the Near Infrared: IV. Quantifying the Age Structure using Monte-Carlo Simulations 28

2.1 Introduction . . . 30

2.2 Modeling of color distributions . . . 31

2.2.1 Overview of the method . . . 31

2.2.2 Input parameters to the simulation . . . 33

2.2.3 Variables of the simulation . . . 33

2.2.4 Monte-Carlo simulation to get a set of primary colors . . . 34

2.2.5 Determination of the second color and observational errors . . . 35

2.3 Quantifying the age structure . . . 35

2.3.1 Cumulative age distribution . . . 35

2.3.2 The comparison with observed data: χ^2-test . . . 37

2.3.3 Comparison of different SSP models . . . 38

2.4 Potential caveats . . . 39

2.4.1 Contamination with background objects 39
2.4.2 Stability of contamination correction 42
2.4.3 Is there a significant intermediate age cluster population? 43
2.5 Results for observed systems 46
2.5.1 NGC 5846 and NGC 4365 48
2.5.2 M87 and NGC 7192 49
2.6 Discussion and conclusions 50
References 54

3 Extragalactic Globular Clusters in the Near Infrared:
III. NGC 5846 and NGC 7192
Quantifying the age distribution of sub-populations 58
3.1 Introduction 60
3.2 Observations and Data Reduction 62
3.2.1 VLT/ISAAC Near–Infrared Data 62
3.2.1.1 Photometry 63
3.2.2 HST/WFPC2 Optical Data 63
3.2.3 Selection criteria 64
3.3 Color-color diagrams for NGC 5846 and NGC 7192 64
3.3.1 NGC 5846 65
3.3.2 NGC 7192 67
3.4 Determining the age structure from color-color diagrams 68
3.4.1 Color distributions 68
3.4.2 Cumulative age structure 71
3.4.2.1 Artificial data sets 72
3.4.2.2 Observed data sets 73
3.4.3 Contamination of background objects 74
3.5 Conclusions and future work 74
3.5.1 Conclusions 74
3.5.2 Future work on age dating 77
References 78

4 Intermediate-age Globular Clusters in early-type Galaxies
Better age determinations by adding U-band observations to the V,I,K datasets 80
4.1 Introduction 82
4.2 VLT/FORS1 U-band Photometry 83
4.2.1 Observations 83
4.2.2 Photometry 84
4.3 Combined U,V,I,K photometry 85

4.3.1 NGC 4365 85
4.3.2 NGC 5846 86
4.3.3 Color-color diagrams for NGC 4365 and NGC 5846 87
4.4 Age sub-populations 93
4.4.1 Cumulative Age Distribution 93
4.4.2 Impact of the sample size 93
4.4.3 Age structures in NGC 4365 and NGC 5846 94
4.5 Discussion and Summary 96
References 98

5 Extragalactic Globular Clusters in the Near Infrared V.: IC 4051 and NGC 3311 100
5.1 Introduction 102
5.2 Observations and Data Reduction 104
5.2.1 Optical data: HST/WFPC2 104
5.2.2 Near-Infrared Data: HST/NICMOS2 106
5.2.2.1 IC 4051 106
5.2.2.2 NGC 3311 107
5.3 Results 108
5.3.1 Color-Color Distributions 108
5.3.1.1 IC 4051 108
5.3.1.2 NGC 3311 111
5.3.2 Cumulative Age Distribution 112
5.4 Metallicity Distribution 119
5.5 Summary 124
References 125

6 Influence of the various Single Stellar Population models 128
6.1 Introduction 129
6.2 Comparison Single Stellar Population Models 129
6.2.1 Model Settings: Size of the reference sample 133
References 139

7 Globular Cluster Systems *vs.* Globular Cluster Systems 140
7.1 Introduction 142
7.2 Age Structure in Globular Cluster Systems 143
7.2.1 Modification in the Monte-Carlo Simulations 143
7.3 Galaxy Sample 143
7.3.1 Cluster Galaxies 145

    - 7.3.2 Group galaxies . . . 150
    - 7.3.3 Isolated Galaxies . . . 151
- References . . . 155

8 Summary **158**

- 8.1 Synopsis . . . 159
- 8.2 Outlook . . . 160

List of Figures

1.1 Cosmic time line 2
1.2 Hubble tuning fork 4
1.3 Sketch of merger tree 6
1.4 Antennae galaxy- example of a galaxy merger 7
1.5 NGC 4365 velocity map 7
1.6 NGC 3311 core 8
1.7 Color-magnitude diagram 47Tuc 9
1.8 Lick Index System 10
1.9 Color and Lick Index Models 11
1.10 Balmer lines vs. Age 12
1.11 Mg_b-Age Dependency 12
1.12 Early-type galaxy & globular cluster 15
1.13 Globular cluster M80 16
1.14 Color distribution in NGC 1399 19

2.1 Color-color diagram NGC 5846 32
2.2 Color -color diagrams for various SSP models 34
2.3 Least square fit to model isochrones 36
2.4 Cumulative age distribution in early-type galaxies 37
2.5 Self consistency test for χ^2-test 38
2.6 Color-color diagrams: globular cluster systems *vs.* HDF-S 40
2.7 Selection effects on HDF-S color-color diagram 41
2.8 Cumulative age distribution of HDF-S objects 42
2.9 Background correction effect on the cumulative age distribution in NGC 5846 43
2.10 Cumulative age distribution for various globular cluster systems 44
2.11 Age distribution in simulated systems 45
2.12 Effect of sample size on χ^2-test results 46
2.13 Stability test for different model sizes 47
2.14 Cumulative age distribution in dependence on SSP models 48
2.15 50%- age in observed globular cluster systems 49
2.16 Photometric and spectroscopic ages 50

2.17 χ^2-test for NGC 5846 and NGC 4365 51
2.18 χ^2-test for NGC 5846, assuming the "old" population to be 10 Gyr 52
2.19 Results of the χ^2-test for M87 and NGC 7192 52
2.20 Age resolution for different color combinations 53

3.1 Field of view for NGC 5846 and NGC 7192 62
3.2 V vs. $(V-K)$ color-magnitude diagram for NGC 5846 65
3.3 $(V-I)$ vs. $(V-K)$ color-color diagram for NGC5846 66
3.4 V vs. $(V-K)$ color-magnitude diagram for NGC 7192 67
3.5 $(V-I)$ vs. $(V-K)$ color-color diagram for NGC 7192 68
3.6 SSP isochrone fit for $(V-I)$ vs. $(V-K)$ 70
3.7 Color distribution and cumulative age distribution for modeled systems 71
3.8 Cumulative age distribution in dependency on relative size of sub-populations 72
3.9 Cumulative age distribution for GCS in different galaxies 73
3.10 Color-color diagram for Hubble-Deep-Field objects 75
3.11 Cumulative age distribution for Hubble-Deep-Field objects 75
3.12 Contribution of background galaxies to the cumulative age distribution of NGC 5846 76

4.1 Color gradient for different colo combinations 83
4.2 Detection limits for U-band observations 86
4.3 U vs. $(U-K)$ color-magnitude diagram for NGC 4365 87
4.4 Color-color diagrams for NGC 4365 88
4.5 U vs. $(U-K)$ color-magnitude diagram for NGC 5846 89
4.6 Color-color diagrams for NGC 5846 90
4.7 Field of view for combined optical and near-infrared observations 91
4.8 U-band luminosity distribution for NGC 4365 and NGC 5846 92
4.9 Cumulative age distribution in NGC 4365 and NGC 5846 94
4.10 Stability of χ^2-tests using $(U-I) vs. (V-K)$ based age distributions 95
4.11 χ^2- test results for NGC 4365 and NGC 5846 96

5.1 Comparison between *psf* and *aperture* photometry 105
5.2 V *vs.* $(V-H)$ color-magnitude diagram for IC 4051 109
5.3 $(V-I)$ *vs.* $(V-H)$ color-color diagram for IC 4051 110
5.4 Gaussian fit to the $(V-H)$ color distribution in IC 4051 111
5.5 Radial distribution of the IC 4051 globular clusters 112
5.6 V *vs.*$(V-H)$ color-magnitude diagram for NGC 3311 113
5.7 $(V-I)$ *vs.* $(V-H)$ color-color diagram for NGC 3311 114
5.8 Simulation of color-color diagrams and the resulting age distribution 115
5.9 Cumulative age distribution in NGC 3311 and IC 4051 116
5.10 χ^2- test result for NGC 3311 117

5.11 χ^2-test for IC 4051 118
5.12 Metallicity distribution in IC 4051 121
5.13 Metallicity distribution in NGC 3311 122
5.14 Gaussian fit to metallicity distribution 123

6.1 Cumulative age distribution using various SSP models 130
6.2 χ^2-test galaxies vs. Vazdekis SSP models 131
6.3 χ^2-test galaxies *vs.* Maraston SSP model 132
6.4 χ^2-test galaxies using corresponding model sizes 134
6.5 Cumulative age distribution 1 135
6.6 Cumulative age distribution 2 136
6.7 Cumulative age distribution 3 137
6.8 Cumulative age distribution 4 138

7.1 M87 and NGC 3311 144
7.2 NGC 7192 & NGC 3115 145
7.3 NGC 5846, IC 4051 and NGC 4365 145
7.4 Cumulative age distribution for cluster galaxies 147
7.5 χ^2- contour plot for M87, NGC 4478, NGC 3311 149
7.6 Cumulative age distribution for cluster galaxies 151
7.7 χ^2- contour plot for M87, NGC 4478, NGC 3311 153
7.8 Cumulative age distribution for isolated galaxies 154
7.9 χ^2- contour plot for NGC 7192 and NGC 3115 154

List of Tables

3.1 General informations on NGC 5846 and NGC 7192 61
3.2 Fit parameter for SSP model isochrones 69

4.1 General galaxy informations 84

5.1 General informations about NGC 3311 and IC 4051 104
5.2 Exposure times 105
5.3 Mean Color versus Radius for IC 4051 113

1 Introduction

In the 18th century Immanuel Kant and Alexander von Humboldt proposed that the elliptical and spiral shaped nebulae, found in the nigth sky, are “world islands” similar to our own Milky Way (Kant 1755). Nevertheless, not until the 1920’s Edwin Hubble proved that even the closest one, the Andromeda Nebula, is not part of the Milky Way but a galaxy on its own (Hubble 1929; Hubble 1936). Only for a few decades we have known that there are in fact hundreds of billions of those galaxies. Since Hubble, our knowledge about galaxies has been growing immensely, but with each discovery more questions arise. Although more and more details on the structure and kinematics of the different types of galaxies are found, some of the most fundamental question in galaxy research still need to be answered, such as: ”How and when do galaxies form?”. The availability of space based and large ground based telescopes allows us nowadays to investigate galaxies which sent out their first light up to ≈13 Gyr ago and thus contain information about the very early stages of the Universe, which we are now able to describe in its major steps (Figure 1.1).

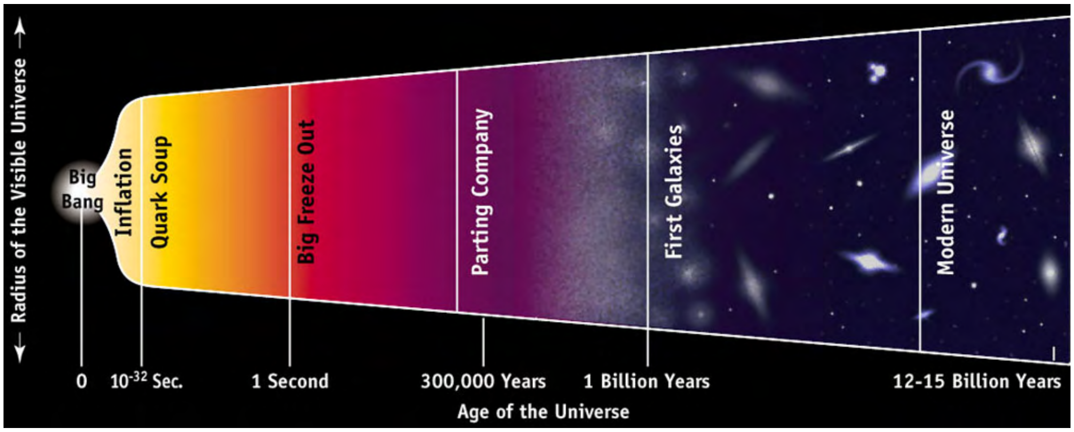
Radius of the Visible Universe
Big Bang
Inflation
Quark Soup
Big Freeze Out
Parting Company
First Galaxies
Modern Universe
0
10^{-32} Sec.
1 Second
300,000 Years
1 Billion Years
12-15 Billion Years
Age of the Universe

Fig. 1.1.— Based on observations taken with ground and space based telescopes our picture about the evolution of the Universe is very detailed and the major events, like the beginning of galaxy formation is timed back to about 1 Gyr after the Big Bang. Copyright, © 1995: Board of Trustees, University of Illinois

1.1 Formation and Evolution of Galaxies

Galaxies are among the most beautiful objects found on the sky and their variety in appearance gives rise to some of the most urgent questions in astronomical research. How do galaxies form and at which point in the formation process is the path set leading to an elliptical or spiral galaxy (see Figure 1.2)? Morphological features, e.g. spiral arms, disks, bars versus bulges and dynamical parameters, such as velocity dispersion compared to the galaxy's rotation velocity lead to the conclusion that these two major types of galaxies are formed in different processes and that their evolution follows different scenarios. Prime targets for the investigation of spiral galaxies are our own Milky Way and the Andromeda galaxy M31, the dominant members of the Local Group of galaxies. Due to the short distance to the Milky Way objects as well as to our nearest giant neighbour M31, observational data are available in an unexceeded wealth and with an unique accuracy. The situation looks quite different for elliptical galaxies, especially for their giant representatives, as the latter are not found in the Local Group at all. Nevertheless, they play an important role in the evolution of the large scale structure in the Universe, as galaxy clusters, which contain most of the baryonic mass in the Universe, are dominated by a small number of giant elliptical galaxies, sometimes even by a single cD galaxy. Thus the formation and evolution of elliptical galaxies has attracted a lot of attention and will also be the general subject of this thesis.

1.2 Early-Type Galaxies

Elliptical galaxies group into three fundamental categories, giant, compact and dwarf ellipticals (Bender, Burstein & Faber 1992; Bender, Burstein & Faber 1993). Considering the large mass range covered by the different categories and the large variety in morphologies, surprisingly simple relations have been found between physical and observed galaxy parameters, described for instance by the **fundamental plane** (FP, e.g. Dressler et al. 1987; Djorgovski & Davis 1987; Djorgovski, Pahre & Carvalho 1996; Burstein et al. 1997), which links the central velocity dispersion σ, the effective surface brightness and the effective radius of a given galaxy to each other. Other examples of such relations are the color-magnitude relation (e.g. Faber 1973; Bower, Lucey & Ellis 1992) and the Faber-Jackson relation (Faber & Jackson 1976; Binney & Tremaine 1994). Taken from the general validity of those relations the formation and evolution of elliptical galaxies could be assumed to be rather simple and global. In contrast to those a number of features are found in early-type galaxies which hint to a more diverse formation, which might in fact not be restricted in time at all (Chiosi & Carraro 2002 and references therein).

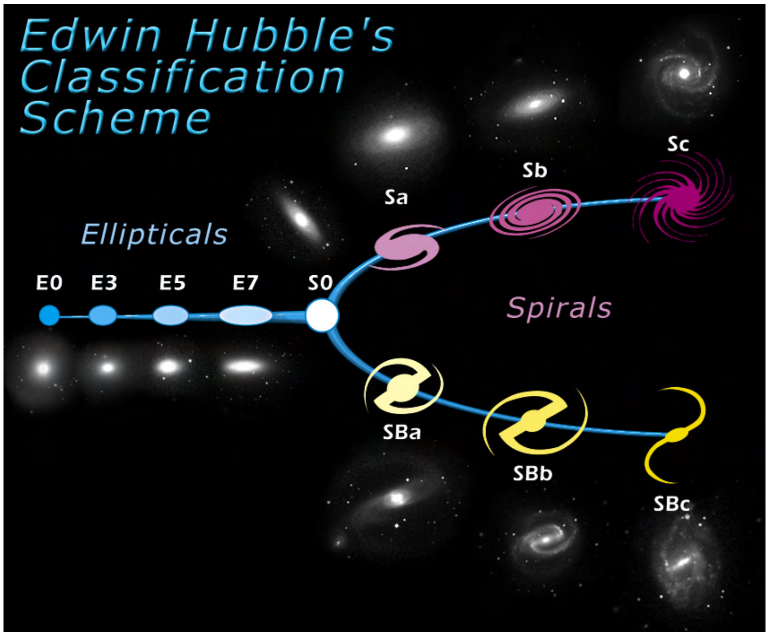

Fig. 1.2.— The classification system for galaxies introduced by Hubble sees elliptical galaxies as young objects, moving along the tuning fork as they age. Consequently elliptical galaxies are classified as “early-type” galaxies, whereas spirals, supposedly old objects, are called “late-type” galaxies. Although an evolution from a non-rotating system, as elliptical galaxies, into rotating, spiral galaxies has been proven wrong, the notation of “early” and “late” type galaxies is still used. Besides the two main classes the “Irregular galaxies” and the “Dwarf galaxies” (elliptical or spiral) complete the galaxy classification. Credit Sloan Digitizes Sky Survey/ Sky Server.

1.2.1 Galaxy Formation Scenarios

Basically two different scenarios for galaxy formation are distinguished, the monolithic collapse and hierarchical merging. Both scenarios are able to explain specific galaxy features, but will fail for others. Despite the huge observational effort during the last decades we are still far from knowing how exactly galaxies form, i.e. which parameters set the conditional framework and to which degree we will be able to generalize galaxy formation scenarios. In the following both scenarios will be described in more detail and pro’s and con’s with respect to galaxy properties will be discussed.

1.2.1.1 Monolithic Collapse

As the name tells the monolithic collapse model sees galaxies as the result of a single burst of star formation at early epochs (at redshifts $z > 2$ or even $z>3$) followed a passive evolution afterward (see Chiosi & Carraro 2002 and references therein). The first feature, star formation at high redshifts, has been proven by various surveys (e.g. Steidel et al. 1996; Renzini & Cimatti 1999; Shapley et al. 2003; D'Odorico & Molaro 2004). The progenitors of the galaxies in this scenario are giant gas clouds (e.g. Eggen, Lynden-Bell & Sandage 1962; Larson 1974). In dependence on the time scale during which the gas is processed into stars and on the amount of angular momentum in the gas cloud either disk or spheroidal galaxies are formed. Observational evidence for this scenario is provided by the above mentioned fundamental plane (Renzini & Ciotti 1993), the color-magnitude relation, the Faber-Jackson relation and the Mg-σ relation (e.g. Colless et al. 1999).

The uniformity of early-type galaxies with respect to the parameters of the fundamental plane (e.g. Djorgovski & Davis 1987; Dressler et al. 1987) is an often used argument for early-type galaxy formation by a monolithic collapse. Based on the age and metallicity dependence of the Mg_b line index (spectral feature of Mg), the small spread in the Mg_b-σ relation in early-type galaxies can be translated into a small dispersion in age (t) and metallicity ($Z/Z_\odot$), assuming a fixed velocity dispersion σ (Colless et al. 1999). The synchronicity in the star formation history of ellipticals is best accounted for by star formation at redshifts $z \gtrapprox 2$.

With more and more data becoming available on specific galaxies and growing galaxy sample, it is realised that the single burst scenario needs to be modified or even complemented by an alternative. For example, the spatial distribution of the metallicity ($Z/Z_\odot$ or [Fe/H], e.g. Carroll & Ostlie 1996) in early-type galaxies derived for a collapse scenario, shows a gradient which is too steep compared to the observed values (e.g. Davies, Sadler & Peletier 1993). In a scenario where the galaxy is built by conglomeration of formerly independent gas clumps the resulting metallicity gradient matches the observations much better (e.g. Larson 1976). Such a scenario represents the first step towards galaxy formation by hierarchical merging of gaseous or stellar substructures.

1.2.1.2 Hierarchical Merging

An alternative scenario to form early-type galaxies is via hierarchical merging, in which sub-units, e.g. galaxies or gas assemble over an extended period and form larger and larger structures. As sketched in Figure 1.3 there is virtually no redshift limit for these merger events to occur, neither the relative size of the sub-units. The most interesting consequence of this scenario with respect to this thesis is that it allows, even predicts the co-existence of multiple stellar populations.

Since the early 70's numerical simulations were developed to improve our understanding of how in interacting galaxies the morphology of the merger remnant and the dynamics of the merger process are related (e.g. Toomre & Toomre 1972; Wright 1972). In dependence on various parameters, such as mass ratio between the merging galaxies, the direction of their approach or the inclination between the galactic planes, the evolution of the merger remnant in time was modeled. Large similarities to observed galaxy merges like the"Antennae" galaxy (see Figure 1.4)

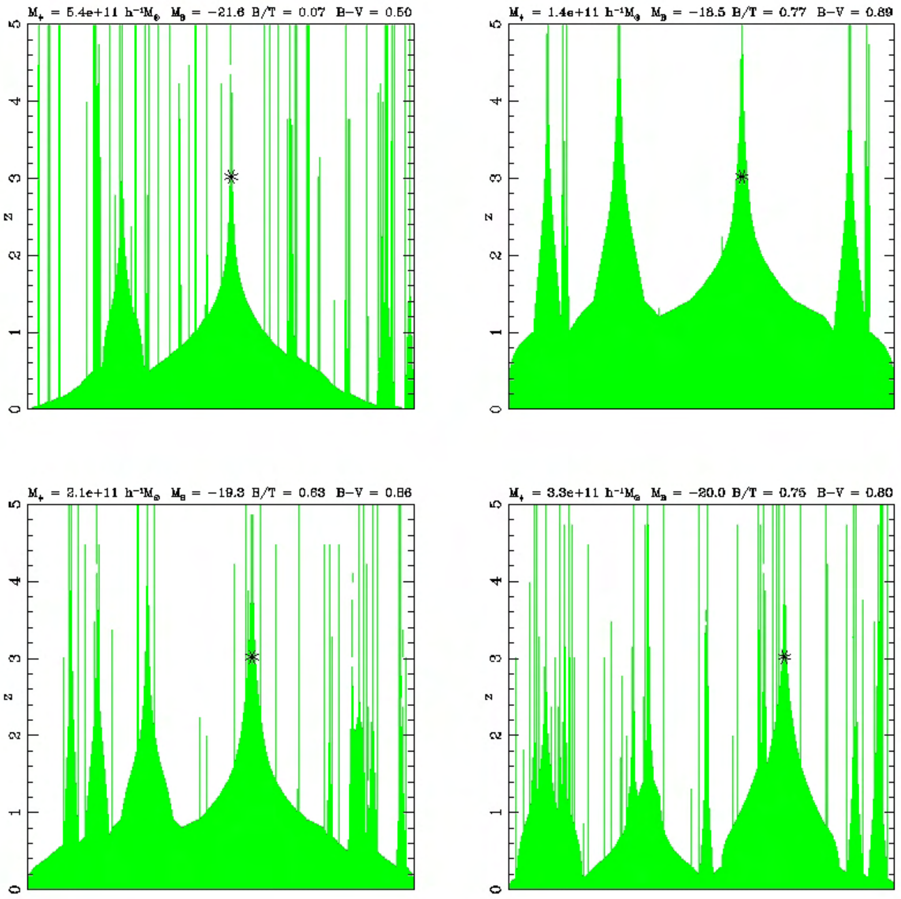

Fig. 1.3.— Merger trees of the star formation history in elliptical galaxies (Baugh, Cole & Frenk 1998; Baugh, Cole & Frenk 1996) of different mass, B-band luminosity, bulge to total light ratio (B-band) and $(B - V)$ color (given on top of each panel). The progenitor of the galaxies is marked by a star, the width of each branch is proportional to the stellar mass at the time.

were obtained.

The simulations of gravitational clustering of cold dark matter halos has seen a lot of progress and allows the calculation of more and more details for the merger remnant (e.g. Kauffmann, White & Guiderdoni 1993; Cole et al. 2000), including parameters such as the luminosity functions, mean galaxy colors or chemical evolution.

The observational support for the merger scenario is manifold. For example, the existence of kinematically decoupled cores (counter- or co-rotating) is hard to explain by the collapse scenario, but has been found in many galaxies, e.g. in NGC 4365 (see Figure 1.5 and Surma & Bender 1995; Davies et al. 2001) or IC 4051 (Mehlert et al. 1998). A similar argument is given by the existence of gaseous disk or dust shells, e.g. found in NGC 5846 (e.g. Goudfrooij & Trichnieri 1998) or NGC 3311 (e.g. Västerberg, Lindblad, Jorsater 1991; Grillmair et al. 1994), shown in Figure 1.6. In general,

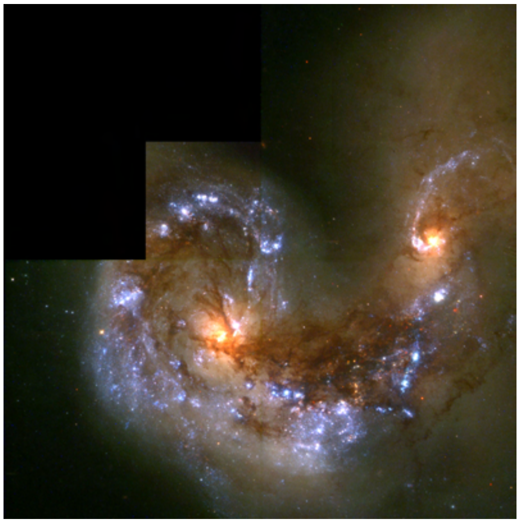

Fig. 1.4.— Example of a galaxy- galaxy merger event. The Antennae galaxy, NGC 4038/39 is one of the prime targets for investigating the processes during a major merger event. The bright blue star clusters are the result of the newly ignited star formation during the merger. Credit: Brad Whitmore (STScI and NASA).

the morphology of a galaxy depends on the number of merger events. Examples of ongoing merger and accretion events can be found in Arp & Madore (1987) or Sandage & Bedke (1994). Individual cases are discussed by Schweizer (1990); Ibata, Gilmore & Irwin (1995); Schweizer & Seitzer (1998); or Goudfrooij et al. (2000, 2001a,b).

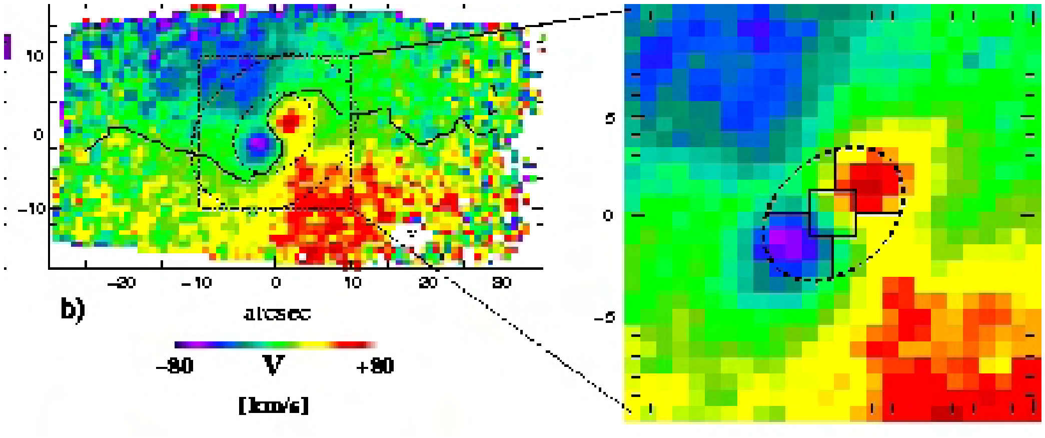

Fig. 1.5.— Kinematically decoupled core found in NGC 4365 (Davies et al. 2001). The different color levels represent different core rotation velocities, derived from spectral lines (Bender 1990). The bold line in the left panel marks the zero velocity loci.

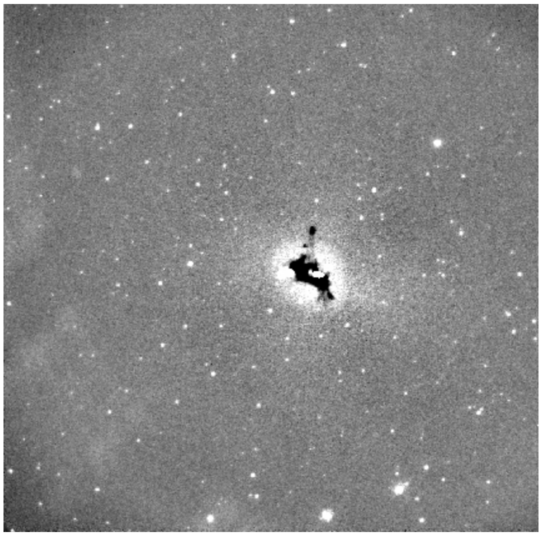

Fig. 1.6.— The central region of NGC 3311 observed with HST/WFPC2 using the F814W broad band filter. The image covers $\sim 20''$. To show the prominent dust lane in the center of NGC 3311 the diffuse galaxy light has been subtracted. The numerous point sources are mostly globular clusters. The image was retrieved from the HST archive.

1.2.2 Age determination of Stellar Populations

In the recent past, various methods have been developed to derive the ages of stellar populations, using either photometric or spectroscopic data sets. In the following different methods will be introduced, classified by the distance range in which they are applied.

1.2.2.1 At Our Doorstep

Since this thesis deals with extragalactic globular cluster objects we will only briefly mention three methods of age determination for objects which are close enough to be resolved into single stars, e.g. in the Milky Way, the Large Magellanic Cloud and the Small Magellanic Cloud. Hereby the color-magnitude diagram, similar to the one shown in Figure 1.7 is used. The *isochrone fitting* is based on the simultaneous fit of the Main Sequence Turn Off (MSTO) and the Sub-Giant Branch (SGB) by model isochrones. Major error sources in this approach are uncertainties in the distance estimate and the exact position of the MSTO. Distance independent methods work with the difference in magnitude (ΔV-method, Binney & Merrifield 1998 and references therein) or color ($\Delta(B-V)$ method, Sarajedini & Demarque 1990).

As a last example the *Luminosity function* method should be mentioned. Since stars are fading as they age (due to Main Sequence temperature decrease) the observed mass distribution within a stellar population, e.g. a globular cluster, depends also on its age. Jimenez & Padona (e.g. Jimenez & Padoan 1996; Padoan & Jimenez 1997) use this correlation to derive ages of globular

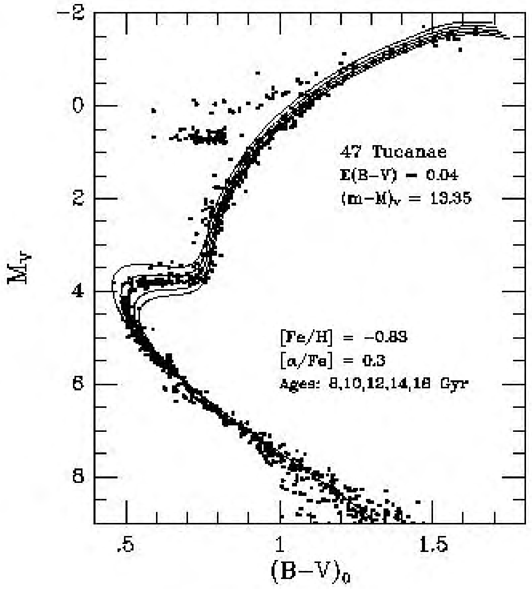

Fig. 1.7.— Color-magnitude diagram for the Milky Way globular cluster 47 Tucanea (Payne-Gaposchkin & Haramundanis 1970). The solid lines mark different model isochrones fitted to the data.

clusters in the Milky Way from the Globular Cluster Luminosity Function (see Section 1.2.3.2) (see also Jimenez & Padoan 1998).

1.2.2.2 In our Neighborhood and Beyond

More important for the work presented here are methods for age determination which can be applied to unresolved stellar population, e.g. galaxies and extragalactic globular clusters. Although working with the integrated light of such populations allows objects beyond the Local Group to be investigated, it bears a severe risk too. As shown by various authors (e.g. Goudfrooij et al. 2001a; Larsen et al. 2003) it is relatively easy to hide different stellar populations within the diffuse light of a galaxy. Additionally one has to consider that younger stellar populations are brighter and the contribution of each population to the integrated light is therefore luminosity weighted. At this point the importance of globular cluster systems becomes obvious. Stars in a single globular cluster share the same age and metallicity and the integrated light of a globular cluster is therefore quite suitable for age determination. Assuming that the integrated light can be used, information about the colors (photometry) as well as spectral features allow age estimates with an accuracy $\lesssim$1 Gyr.

The basic tool for the age estimate is the comparison of well defined features, e.g. colors or element abundances with model predictions (see Section 1.2.2.3). The definition of colors is in gen-

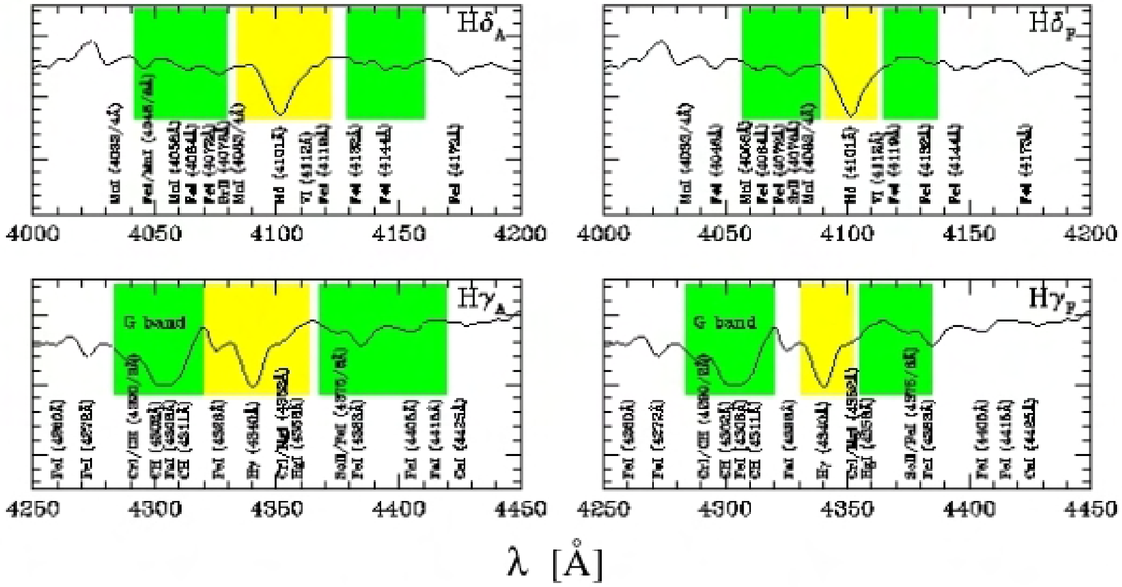

Fig. 1.8.— Definition of different line indices in the Lick Index System. The central yellow box sets the wavelength range for the chosen line, whereas the two green boxes mark the continuum. The continuum flux in the spectral line region is calculated as linear interpolation over both continuum's intervals (Puzia et al. 2004).

eral unified by the magnitude system and the used filter (Binney & Merrifield 1998), but comparing element abundances requires an accurate specification of how to calculate them. With the definition of the "Lick Index System" this obstacle has been overcome. Based on the early work by Burstein et al. (1984), continuously updated by Worthey et al. (1994), Worthey & Ottaviani (1997) and Trager et al. (1998), the Lick Index System allows for a calculation of element abundances on the basis of well defined spectral features (see Figure 1.8). As for the colors, those element abundances are than compared with model values, derived for a given age and chemical composition (see Figure 1.9). In order to overcome degeneracy effects (Worthey 1994) various colors or Lick indices have to be combined. Hereby a different sensitivity to age and metallicity is required. Using photometric data this is given if we combine optical and near-infrared colors, such as $(V-I)$ and $(V-K_s)$ (e.g. Kissler-Patig, Brodie & Minniti 2002). In spectroscopy, age sensitive spectral indices like the Balmer lines (e.g. H_β, H_γ or H_δ), are combined with metallicity sensitive indices like Mg_b or $\langle Fe \rangle$ are combined (Trager et al. 1998; Gorgas, Efstathiou & Aragon-Salamanca 1990). Throughout this thesis we will follow the color approach for age determination.

To obtain spectra of extragalactic globular cluster or distant galaxies with a high enough quality to calculate accurate Lick indices is not an easy task, thus one would like to rely on the

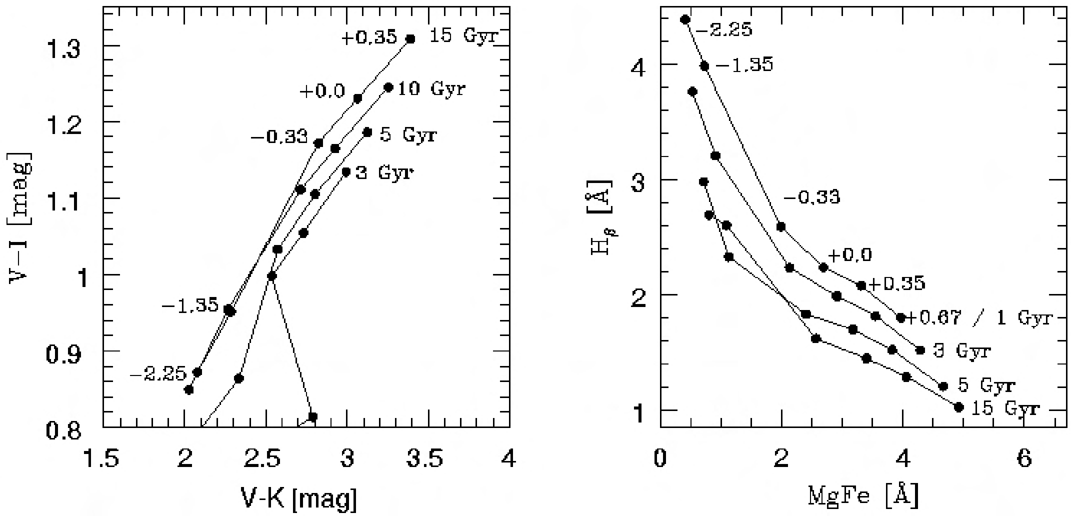

Fig. 1.9.— Based on SSP models (see Section 1.2.2.3), colors or Lick indices for a given age and metallicity are calculated and compared to observations.

strongest features only. These are the Balmer lines ($H_\beta, H_\gamma, H_\delta$), which are, due to the ubiquitous presence of hydrogen, among the strongest spectral features and mostly metallicity independent. The time dependency of the Balmer line strength (see Figure 1.10) has been used to age date compact star clusters in galaxies with recent star formation (e.g. Brodie et al. 1998; Schweizer & Seitzer 1998; Gallagher & Smith 1999; Delgado, Leitherer & Heckman 1999).

The fundamental plane (e.g. Djorgovski & Davis 1987; Dressler et al. 1987) and its validity up to high redshifts provides another mean of age determination. Hereby we use the correlation between age (t) and metallicity ($Z/Z_\odot$) with the Mg_b line index, shown in Figure 1.11 and parametrised in Equation 1.1. In the comparison between distant, thus young, galaxies and nearby ones, any difference in the Mg_b line strength can mostly be attributed to age effects, assuming passive evolution of those galaxies. With the age of nearby galaxies accessible we are therefore able to derive the ages of distant objects.

$$logMg_b = 0.20logt + 0.31logZ/Z_\odot + 0.37 \qquad \text{(Ziegler 2000)} \tag{1.1}$$

1.2.2.3 Single Stellar Population Models

Observables, such as photometric and spectroscopic properties, are the only information source on distant stellar object, e.g. galaxies, star clusters and of course individual stars, and provide snapshots of an evolution which might have lasted for ∼13 Gyr, i.e. almost the lifetime of the Universe (e.g. Bennett et al. 2003). If we are to use these snapshots to derive a detailed evolutionary history of galaxies or star clusters, we need either direct measures of their basic characteristics (like their age, chemical composition, mass) or alternatively, since those are hard to come by, the physical

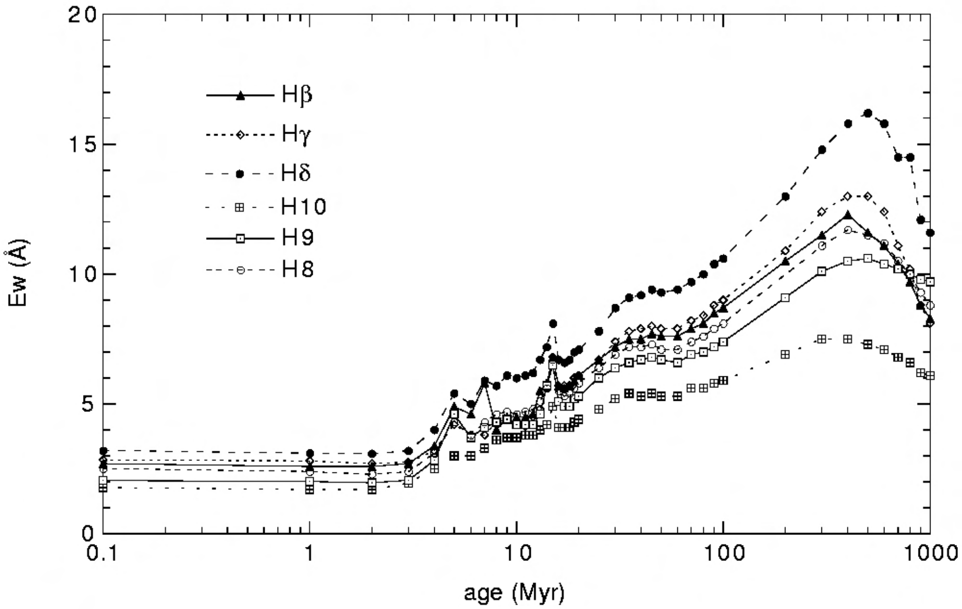

Fig. 1.10.— Equivalent width of various Balmer lines as a function of stellar age (Delgado, Leitherer & Heckman 1999) after an instantaneous burst of star formation.

knowledge to model the evolution of stars with a given mass and chemical composition over time and to derive the observational features. The comparison between observations and various stellar

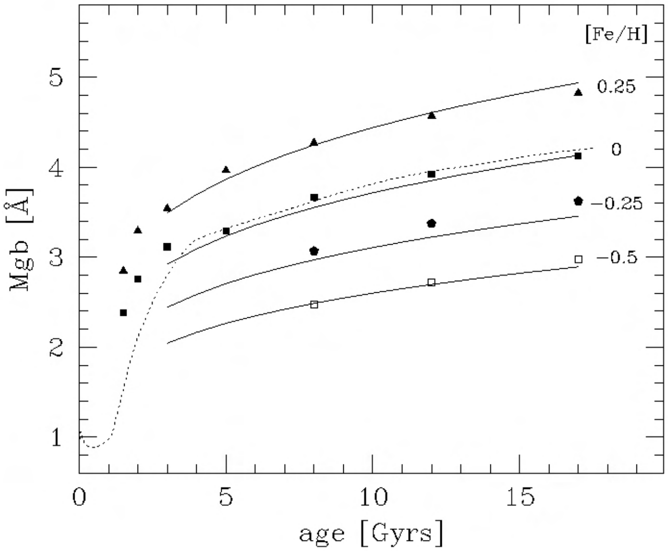

Fig. 1.11.— Dependency of the Mg_b index on metallicity and age. The degeneracy given by Worthey (1994) is shown by the symbols, whereas the dashed line corresponds to Bruzual & Charlot (1997), solid lines follow Equation 1.1 (Ziegler & Bender 1997).

population models will allow us to derive the age and element abundances in the observed targets and eventually to draw conclusions about the underlying formation process. The basic requirement for this model approach, introduced in the 60's by Crampin and Hoyle (1961) and Tinsley (1968), is the decomposition of the stellar object into Single Stellar Populations, short SSP's, built by coeval stars, sharing the same chemical composition and also called Simple Stellar Populations. In the context of this thesis we can see the advantage of working with SSP's instantly- they are perfectly matched by globular clusters. As globular clusters trace the major star formation event during the evolution of their host galaxy (see section 1.2.3) the determination of globular cluster ages can be used to describe the history of the galaxy.
Closing the loop: galactic globular clusters, observed in great detail and with independently determined ages and element abundances (e.g. Renzini & Fusi Pecci 1988), can be used to calibrate the stellar population models, that is to fit parameters such as convection, mass and mixing length to the models in correspondence to the observations. Convolving various SSP modes can then be used to model stellar systems which are more complex, built by several stellar populations (e.g. Arimoto & Yoshis 1986; Vazdekis 1996; Barbaro et al. 1997).

The basic components of stellar population models are the stellar evolutionary tracks and the stellar atmosphere models. The evolution of a star with a given mass and chemical composition is described by the evolutionary tracks and provides the basic stellar parameters, such as the bolometric luminosity L_*, effective temperature T_{eff} and surface gravity, as a function of time. Over the last decades various sets of stellar tracks have been developed, which can be split into two fundamental families, depending on whether convective overshooting is considered in the models. Examples of models taking convective overshooting into account are the “Padova” tracks (e.g. Fagotto et al. 1994), the “Geneva”-tracks (Maeder & Meyet 1989) as well as the “Yale” (e.g.Yi & Demarque 2001) -tracks. “Overshooting”-free stellar tracks are provided by VandenBerg et al. (2000) and Cassisi et al. (1998). The second ingredient, stellar model atmospheres, describes the emergent flux of a star assuming the above mentioned effective temperature, luminosity and surface gravity. Different SSP models, e.g. by Bruzual & Charlot (2000, 2003), Vazdekis (1999) and Maraston (2001) are based on a large set of stellar atmospheres, either empirical stellar libraries or modeled atmospheres. Into the first category we count the Library by Jones (1997), whereas Kurucz (1992) and Bessel et al. (1989) provide model atmospheres. A major step towards a uniform set of stellar model atmospheres, including a comparison to the empirical ones, are the stellar libraries by the BaSel- group (Basel Stellar Libraries, e.g. Lejeune, Cuisinier & Buser 1997; Westera et al. 2002).

Given that we know how stars of a given mass and chemical composition evolve in time (evolutionary tracks) and how they appear (model atmospheres)- how can we derive the ages and element abundances of stellar populations, built by stars of different masses? The missing ingredient is the Initial Mass Function (IMF), which describes the mass distribution $\zeta(M)$ within the stellar structure. The most common used IMF is the one by Salpeter (Salpeter 1955, $\zeta \propto M^{-2.35}$), followed by Miller & Scalo (1979), Kroupa, Tout & Gilmore (1993) and the Chabrier (2003).

By integrating the contribution of the individual stars within a plausible mass range (e.g. between 0.1 and 100 solar masses) the luminosity and color of a stellar population can be calculated. In the literature two integration methods are distinguished, the isochrone synthesis method (e.g. Charlot & Bruzual 1991; Bruzual & Charlot 1993) and the fuel consumption theorem (Renzini & Buzzoni 1986). Both methods are discussed in detail in Renzini (1994). Since during the course of this work different SSP models will be compared it is worth noticing that the Bruzual & Charlot models (2000, 2003) as well as the one by Vazdekis (1999) and Worthey (1994) rely on the isochrone synthesis method. Fuel consumption on the other hand is used by Maraston (see e.g. Maraston 1998). In Chapter 1.2.4 of this thesis the SSP model isochrones for three different models (Bruzual & Charlot, Vazdekis, Maraston) can be found.

1.2.3 Globular Cluster Systems

> *"Perhaps the most wonderful of all star clusters are those in which hundreds upon hundreds of faint stars are all gathered together in the shape of a globe."* Reverend James Baikie (1911)

Globular clusters are well established as tracers of their host galaxy's evolution for many reasons. Most importantly- globular clusters are found in almost any type of galaxy, in dwarf irregulars, spirals as well as in giant ellipticals and they can be observed at distance as far as ∼100 Mpc. With respect to galaxy formation and evolution studies globular cluster are close to ideal probes- they represent single stellar populations almost perfectly. Their stars share the same age and chemical composition, only differing in their evolutionary state, which is defined by their mass. Due to their large distances, galaxies other than our own and its nearest neighbours (e.g. LMC, SMC, M31) cannot be resolved into single stars, and as shown e.g. by Larsen et al. (2003) several age populations can be hidden in the diffuse light of a galaxy. Deriving ages from the diffuse galaxy light therefore leads to a large age uncertainty. As opposed to their host galaxy globular clusters are thus remarkably simple objects. In the discussion about major star formation events in early-type galaxies the age structure in globular cluster systems is of great importance, e.g. the existence of young/intermediate age and metal-rich globular clusters are striking evidence for a globular cluster formation scenario based on the interaction or mergers of galaxies (e.g. Ashman & Zepf 1992). The tight link between globular cluster formation and major star formation events in galaxies makes globular clusters prime probes of the evolution of their parent galaxies. The determination of globular cluster ages is therefore crucial for our understanding of the formation and evolution of early-type galaxies. As the globular cluster systems in early-type galaxies are the subject of this thesis we will discuss them in more detail in the following.

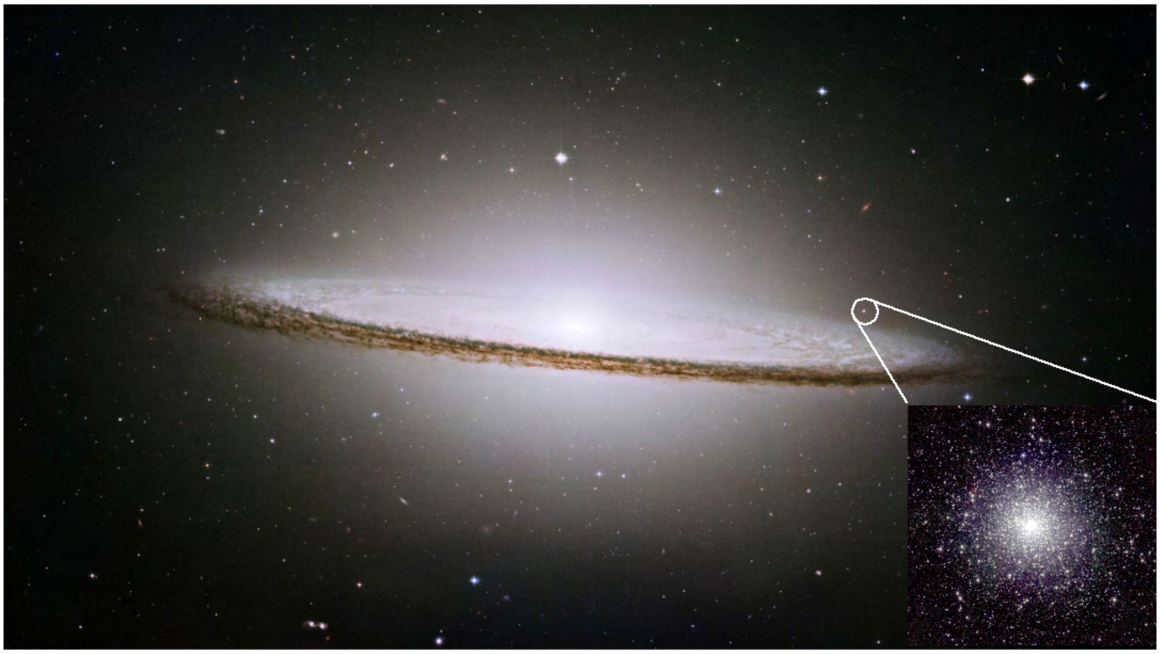

Fig. 1.12.— Almost all galaxies host a globular cluster system. Since globular clusters in more distant galaxies, such as the Sombrero galaxy (M104) cannot be resolved, the Milky Way globular cluster 47 Tucanea serves as an example in this figure (enlarged section). Credit: NASA/ESA, The Hubble Heritage Team (STScI/AURA) and Jarrett et al. (2003).

1.2.3.1 Formation of Globular Clusters

If we are to use globular cluster systems to probe the formation and evolution of their host galaxies we first have to understand how globular clusters form themselves. Until recently globular clusters were assumed to be exclusively old objects and even used to set constraints on the age of the Universe. Consequently, formation scenarios for globular clusters were based on what was known about the early Universe. In the work by Peebles & Dicke (1968) globular clusters are described to form from gaseous clouds, even before the host galaxy appears as such. The existence of metal-rich globular clusters in giant elliptical galaxies invalidates this scenario. Nevertheless, the basic idea of globular clusters being formed in giant molecular clouds remains (e.g. Gunn 1980; Fall & Rees 1985; Larson 1996; Elmegreen & Efremov 1997; Cen 2001), although the nature of what ignites the collapse of the cloud is still a matter of debate. The interesting consequence of the variety of catalysts is, that globular clusters can form wherever gas clouds can collapse. Trigger mechanisms are for instance gravitational stress (Elmegreen & Efremov 1997; Bekki et

Fig. 1.13.— M80 (NGC 6093) is one of the densest globular clusters found in the Milky Way. Located at a distance of ~ 28000 light years, the cluster contains several hundreds of thousands of stars rather than just the "hundreds upon hundreds" claimed by Baikie (1911). The bright red giants, which are stars similar to the Sun in mass are close to the ends of their lives. Credit: The Hubble Heritage Team (AURA/STScI/NASA/ESA)

al. 2002) and radiation fields (Cen 2001). The often discussed merger scenario for globular cluster formation (e.g. Ashman & Zepf 1992; Ashman & Bird 1993; Whitmore et al. 1993; Schweizer et al. 1996; Kissler-Patig 2000); and the accretion scenario (Côté, Marzke & West 1998; Hilker, Infante & Richtler 1999; Côté, West & Marzke 2002) both rely on the gravitational stress argument.

1.2.3.2 Globular Cluster Systems

Various parameters are nowadays used to describe and to compare globular cluster systems. In the discussion about the formation scenario wereckon that these parameters have to be predicted by the adapted scenario. In the following some of the mostly used characteristics of globular cluster systems will be introduced.

- *Luminosity Distribution*

  There are different ways to quantify the number of globular clusters δN per unit luminosity δL (see Eq. 1.2) or, correspondingly, per unit mass. Working with luminosities or masses the distribution follows a power law, which seems to be rather independent of galactocentric distance, globular cluster metallicity, galaxy type and others more (Harris 1998).

$$\delta N/\delta L \sim L^{-1.8\pm0.2} \qquad \text{for} L \gtrsim 10^5 M_\odot \tag{1.2}$$

  For masses below 10^5 $M_\odot$ the luminosity shows a changeover in its slope. Working with the cluster magnitude (logarithmic luminosity) the distribution, also called the globular cluster luminosity function (GCLF), is well fit by a Gaussian with a turnover magnitude $Mv = -7.4 \pm 0.2$ (e.g. Harris 1991; Ashman & Zepf 1998). This turnover magnitude seems to be rather stable for different galaxies (Ajhar, Blakeslee & Tonry 1994; Blakeslee 1996) with a deviation of ∼0.2 mag. As shown by Harris (2001), the dispersion σ of the GCLF is derived with σ=1.2 and 1.4 for spiral and elliptical galaxies, respectively. Due to the stable turnover magnitude globular clusters also serve as standard candles for distance estimates (e.g. Kavelaars et al. 2000; Kissler-Patig 2000). Although the completeness of the GCLF is usually hampered by the detection limit in the observations, the turnover magnitude is still accessible, and its value was confirmed by HST observations.

- *Numerical Size*
  The comparison between early and late type galaxies in the size of their globular cluster systems, described by the specific frequency S_N (Harris & van den Bergh 1981; Harris 1991), shows that especially giant ellipticals host surprisingly large globular cluster systems (West et al. 1995 and references therein). This has often been used as an argument against early-type galaxies being formed during galaxy mergers (e.g. van den Bergh 1995), assuming globular clusters and stars formed with the same efficiency. The resulting specific frequency should therefore be not too different to the one in the progenitors. Recent observations lead to a different conclusion. It seems that star formation in starburst regions occurs preferentially in clusters (e.g. Meurer et al. 1995; Schweizer et al. 1996). If early-type galaxies are formed by galaxy mergers, with a large number of new globular clusters, then the resulting specific frequency will exceed the S_N of the progenitors .

- *Spatial Distribution*
  The spatial distribution of globular cluster sub-populations will be discussed in detail in later chapters of this thesis, thus at this point only some general remarks will be made. Previous studies on globular cluster systems in nearby galaxies as well as in more distant giant elliptical galaxies are hampered by the limited size of the field of view in the observations. Wide field surveys are available on only a few galaxies, e.g. for NGC 1399, the central elliptical in the Fornax galaxy cluster (e.g. Dirsch et al. 2003). Also much attention has to be paid to reducing data on objects which are very faint compared to the underlying galaxy light. For elliptical galaxies the following radial globular cluster density profile Σ_{GCS} has been found (see Eq. 1.3), with the exponent α in the range between 1 and 2.5.

$$\Sigma_{GCS} \propto r^{-\alpha} \tag{1.3}$$

  The exponent is hereby assumed to correlate with the absolute magnitude of the galaxy (Harris 1991), with α increasing with the galaxy luminosity.

An alternative, and commonly used radial distribution function is described by the "de Vaucouleur" profile (see Eq. 1.4). Hereby the effective radius r_e is found roughly in the range between 10 to 50 h^{-1} kpc (Ashman & Zepf 1998).

$$\Sigma_{GCS} \propto \exp[(r/r_e)^{1/4} - 1] \tag{1.4}$$

Both functions match the observations reasonably well, except for the innermost regions, which can be accounted for by background and/or foreground contamination. Rather surprisingly it has been found that globular cluster systems are more spatially extended than the diffuse galaxy light, although no physical reason for that has been found yet.

- *Color Distribution*
  High quality photometric data on extragalactic globular clusters allow us to construct the color distribution in the optical wavelength range as well as in the infrared. Especially the later is of high importance in this thesis. One of the most striking results in globular cluster research in the recent past is the discovery of the bimodality of the color distributions in early-type galaxies (Zepf & Ashman 1993), as shown in Figure 1.14. Various studies, e.g. by Gebhardt & Kissler-Patig (1999) and Kundu & Whitmore (2001a,b) have shown that this multi-modality is in fact a common feature in color distributions. In the context of globular cluster and galaxy formation this multi-modality plays an important role, as it is for instance predicted by the merger scenario. The work presented here is based on the combination of optical and near-infrared colors and takes advantage of the different sensitivity of both colors to age and metallicity. As shown in Puzia et al. (2002), the direct comparison in sensitivity of $(V-I)$ and $(V-K)$ color differs by a factor of $\approx$2 and $\lesssim$4 for age and metallicity. These values represent a mean for different SSP models (see Chapter 1.2.2.3). The multi color approach has been successfully applied to various globular cluster systems (Kissler-Patig, Brodie & Minniti 2002; Puzia et al. 2002; Hempel et al. 2003 -corresponds to Chapter 3 in this thesis).

1.2.4 Scientific Goals

The goal of this thesis is to detect multiple star formation epochs in early-type galaxies. Globular clusters are used as star formation tracers, thus our immediate goal is the determination of the age structure in globular cluster systems in early-type galaxies. To do so we seek to detect globular cluster sub-populations with different ages, supposedly formed in several burst of star formation. In addition we want to quantify the importance of these different star formation events for the host galaxy by determining the relative size of the age sub-populations. Thus a large globular cluster sample is required for each galaxy, which can only be achieved using photometric data sets. As younger globular clusters are expected to be metal-rich ([Fe/H]>-1 dex), only the metal-rich globular cluster population is used in our analysis. The basic tool for this selection, as well as for

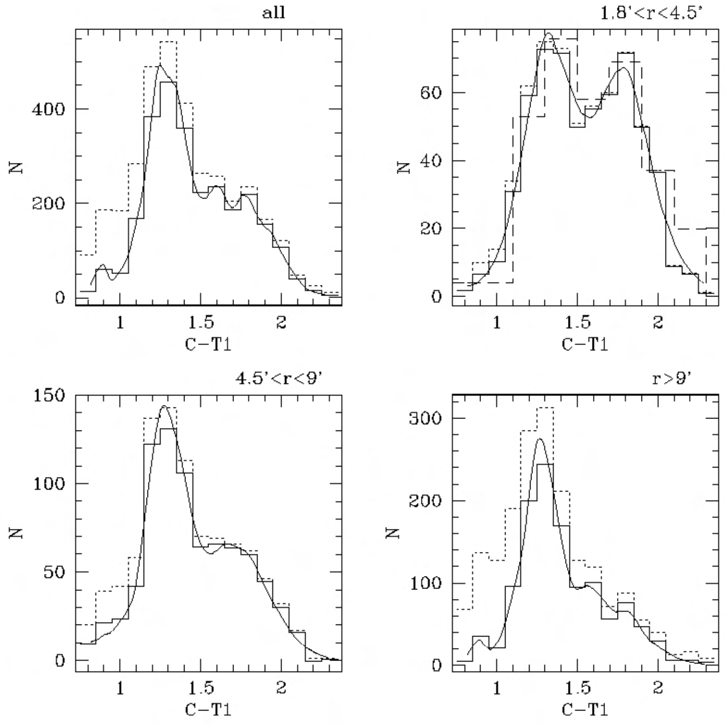

Fig. 1.14.— $(C-T1)$ color distribution in NGC 1399 (Dirsch et al. 2003) in the complete sample as well as in various radial intervals. The dotted and solid histograms represent the color distribution before and after correction for background contamination. In the top right panel the distribution is compared to the result by Ostrov et al. (1998, dashed histogram). The smoothed distribution (solid line) was obtained by filtering with an Epanechikov kernel.

the age determination, is the combination of optical and near-infrared observations. Monte-Carlo simulations of color-color distributions in globular cluster systems of a given age structure and the comparison to observed systems will be used to set constraints on the age and relative size of globular cluster sub-populations of different age. Hereby the size ratio is assumed to give clues about the importance of the various star formation events for the evolution of the galaxy. The intension is to apply this analysis to a large sample of galaxies in order to find systematical dependencies between the age structure in the globular cluster systems and the galaxy properties.

The thesis is a composite of papers, which have recently been published or submitted and is organized as follows. Details on the Monte-Carlo simulations and the derivation of age distributions from color-color diagrams are given in Chapter 2 together with a discussion about the strength and the caveats of this approach. First examples on cumulative age distributions in different early-type galaxies are presented in Chapter 3. During the course of the work it became obvious that the usual combination of optical and near-infrared observations, i.e. V, I- data in the optical and K_s

filter in the near-infrared allow for the detection of age sub-populations but are limited in the age accuracy. Therefore the observations have been extended to shorter wavelengths, now including U-band data. The results are presented in Chapter 4.

In the discussion about how and when early-type galaxies form the majority of their stars it becomes more and more clear that there is no general formation scenario, but rather correlations can be found between external and internal galaxy parameters (e.g. galaxy environment, size) and the evolutionary history of the galaxy. As an example for high luminosity galaxies NGC 3311, the central galaxy in the Hydra I galaxy cluster and IC 4051, a massive elliptical in the Coma cluster are investigated, the results are presented in Chapter 5. In Chapter 2 and 3 the influence of the applied SSP models is briefly discussed. The results presented in Chapters 3 to 5 are based on the application of the Bruzual & Charlot SSP models (2000) alone and we will include a comparison to the models by Vazdekis (1999) and Maraston (2001) in Chapter 5.5 for completeness.

Chapter 7 represents a compilation of all galaxies investigated so far. The conclusions of this thesis are given in Chapter 8 along with a short summary and an outlook to future work.

References

Ajhar, E.A., Blakeslee, J.P. & Tonry, J.L. 1994, AJ, 108, 2087

Arimoto, N. & Yoshis, Y. 1986, A&A, 164, 260

Arp, H.C. & Madore, B. 1987, “A Catalog of Southern Peculiar Galaxies and Associations”, Cambridge University Press

Ashman, K.M. & Zepf, S.E. 1992, ApJ, 384, 50

Ashman, K.M. & Bird, C.M. 1993, AJ, 106, 2281

Ashman, D. & Zepf, S.E. 1998, “Globular Cluster Systems”, Cambridge University Press

Baikie, J. 1911, in: ”Peebs at the Heavens”, Adam and Charles Black, London

Barbaro, G., Poggianti, B.M. 1997, A&A, 324, 490

Baugh, C.M., Cole, S. & Frenk, C.S. 1996, MNRAS, 283, 1361

Baugh, C.M., Cole, S. & Frenk, C.S. 1998, ApJ, 498, 504

Bekki, K., Forbes, D.A., Beasley, M.A. et al. 2002, MNRAS, 335, 1176

Bender, R. 1990, A&A, 229, 441

Bender, R., Burstein, D., Faber, S.M. 1992, ApJ, 399, 462

Bender,R., Burstein, D., Faber, S.M. 1993, ApJ, 411, 153

Bender, R., Ziegler, B.L. & Bruzual, G. 1996, ApJ, 463, L51

Bennett, C.L., Halpern, M., Hinshaw, G. et al. 2003, ApJ, accepted

Bessel, M.S., Brett, J.M., Scholz, M. et al. 1989, A&A, 213, 209

Binney, J. & Tremaine, S. 1994, “Galactic Dynamics’, Princeton University Press

Binney, j. & Merrifield, M. 1998, “Galactic Astronomy”, Princeton University Press

Blakeslee, J.P. 1996, PhD Thesis

Bower, R.G., Lucey, J.R., Ellis, R.S. 1992, MNRAS, 254, 601

Brodie, J.P., Schroder, L.L., Huchra, J.P. et al. 1998, AJ, 116, 691

Bruzual, G. & Charlot, S. 2000, private communication

Bruzual, A. & Charlot, S. 1993, ApJ, 405, 538

Bruzual, G. & Charlot, A. 2003, MNRAS, 344, 1000

Burstein, D., Bender, R., Faber, S.M. et al. 1997, AJ, 114, 1365

Carroll, B.W. & Ostlie, D.A. 1996, "Introduction to Modern Astrophysics, Addison-Wesley Publishing Company

Cassisi, S., Castellani, V., Degl'Innoceti, S. et al. 1998, A&AS, 129, 267

Cen, R. 2001, ApJ, 560, 592

Chabrier, G. 2003, PASP, 115, 763

Charlot, S. & Bruzual, G. 1991, ApJ, 367, 126

Chiosi, C. & Carraro, G. 2002, MNRAS, 335, 335

Cole, S., Lacey, C.G., Baugh, C.M. et al. 2000, MNRAS, 319, 1668

Colless, M., Burstein, D., Davies, R.L. et al. 1999, MNRAS, 303, 813

Côté, P., Marzke, R.O. & West, M.J. 1998, ApJ, 113, 1652

Côté, P., West, M.J. & Marzke, R.O. 2002, ApJ, 567, 853

Crampin, & Hoyle 1961, MNRAS, 122, 28

Davies, R.L., Sadler, E.M, Peletier, R.F. 1993, MNRAS, 262, 650

Davies, R.L., Kuntschner, H., Emsellem, E. et al. 2001, ApJ, 548, L33

Gonzáles Delgado, R., Leitherer, C. & Heckman, T.M. 1999, ApJS, 125, 489

Dirsch, B., Richtler, T., Geisler, D. et al. 2003, 125, 1908

Djorgovski, S. & Davis, M. 1987, ApJ, 313, 59

Djorgovski, S.G., Pahre, M.A., de Carvalho, R.R. 1996, ASP Conference Series, 86, 129

D'Odorico, V. & Molaro, P. 2004, A&A, 415, 879

Dressler, A., Lynden-Bell, D., Burstein, D. et al. 1987, ApJ, 313, 42

Eggen, O.J., Lynden-Bell, D., Sandage, A.R. 1962, ApJ, 136, 748

Elmegreen, B.G.,& Efremov, Y.N. 1997, ApJ, 480, 235

Faber, S.M. 1973, ApJ, 179, 731

Faber, S.M. & Jackson, R. 1976, AJ, 204, 668

Fagotto, F., Bressan, A., Bertelli, G. et al. 1994, A&AS, 105, 29

Fall, S.M. & Rees, M.J. 1985, ApJ, 298, 18

Forbes, D.A. 1996, AJ, 112, 954

Gallagher, J.S. & Smith L.J. 1999, MNRAS, 304, 540

Gebhartd, K. & Kissler-Patig, M. 1999, AJ, 118, 1526

Gorgas, J., Efstathiou, G & Salamanca, A.A. 1990, MNRAS, 245, 217

Goudfrooij, P. & Trichnieri, G. 1998, A&A, 330, 123

Goudfrooij, P., Kissler-Patig, M., Meylan, G. et al. 2000, AAS, 197, 3713

Goudfrooij, P., Alonso, M.V., Maraston, C. et al. 2001, MNRAS, 328, 237

Goudfrooij, P., Mack, J., Kissler-Patig, M. et al. 2001, MNRAS, 322, 643

Grillmair, Carl J.; Faber, S. M.; Lauer, Tod R. et al. 1994, AJ, 108, 102

Gunn, J.E. 1980, in: "Globular Clusters", eds. D. Hanes & M. Madore, Cambridge University Press

Harris, W.E. & van den Bergh, S. 1981, AJ, 86, 1627

Harris, W.E. 1991, ARA&A, 29, 543

Harris, W.E. 1998, in "Star Clusters", by B.W. Carney & W.E. Harris, Saas- Fee Advanced Course, 28

Hempel, M., Hilker, M., Kissler-Patig, M. et al. 2003, A&A, 405, 487, see Chapter 3

Hilker, M., Infante, L. & Richtler, T. 1999, A&AS, 138, 55

Hubble, E.P. 1929, ApJ, 29, 103

Hubble, Edwin P. 1936, "The Realm of the Nebulae", New Haven, Conn.: Yale University Press

Ibata, R.A., Gilmore, G. & Irwin, M.J. 1995, MNRAS, 277, 781

Jarrett, T.H., Chester, T., Cutri, R. et al. 2003, AJ, 125, 525

Jimenez, R. & Padoan, P. 1996, ApJ, 463, L17

Jimenez, R. & Padoan, P. 1998, ApJ, 498, 704

Jones, L.A. 1997, PhD thesis, Univ. North Carolina, Chapel Hill

Kant, I. 1755, “General Natural History and Theory of Heavens”

Kauffmann, G., White, S.D.M., Guiderdoni, B. 1993, MNRAS, 264, 201

Kavelaars, J.J., Harris, W.E., Hanes, D.A. et al. 2000, ApJ, 533, 125

Kissler-Patig, M. 2000, Rev. Mod. Astronomy, ed. Schielicke, 13, 13

Kissler-Patig, M., Brodie, J.P. & Minniti, D. 2002, A&A, 391, 441

Kroupa, P., Tout, C.A., Gilmore, G. 1993, MNRAS, 262, 76

Kundu, A. & Whitmore, B.C. 2001, 121,2950

Kundu, A. & Whitmore, B.C. 2001, 122, 1251

Kuntschner, H., Lucey, J.R., Smith, R.J. et al 2001, MNRAS, 323, 615

Kurucz, R.L. 1992, in: IAU Symp. 149, 225

Larsen, S., Brodie, J.P., Beasley, M.A. et al. 2003, ApJ, 585, 767

Larson, R.B. 1974, MNRAS, 169, 229

Larson, R.B. 1976, Saas-Fee Advanced Course 6, Galaxies, 69

Larson, R.B. 1996, ASP Conf.Ser.,92 (“Formation of the Galactic Halo...Inside Out”), 241

Lejeune, Th., Cuisinier, F., Buser, R. 1997, A&AS, 125, 229

Maeder, A. & Meyet, G. 1989, A&A, 210, 155

Maraston, C. 1998, MNRAS, 300, 872

Maraston, C., Kissler-Patig, M., Brodie, J.P. et al. 2001, A&A, 370, 176

Mehlert, D., Saglia, R.P., Bender, R. et al. 1998, A&A, 332, 33

Meurer, G. R., Heckman, T. M., Leitherer, C. et al. 1995, AJ, 110, 2665

Miller, G. & Scalo, J. 1979, ApJS, 41, 513

Ostrov, P.G., Forte, J.C. & Geisler, D. 1998, AJ, 116, 2854

Padoan, P. & Jimenez, R. 1997, ApJ, 475, 580

Payne-Gaposchkin, C.H. & Haramundanis, K. 1970, in:”Introduction to Astronomy”, ed. Prentice-Hall

Peebles, P. J. E.& Dicke, R. H. 1968, ApJ, 154, 891

Puzia, T.H., Zepf, S.E., Kissler-Patig, M. et al. 2002, A&A, 391, 453

Puzia. T.H., Kissler-Patig, M., Thomas, D. et al. 2004, in prep.

Renzini, A. & Buzzoni, A. 1985, in “Spectral Evolution of Galaxies”, eds. C.Chiosi, A.Renzini, J. Dyson, (Dordrecht), 195

Renzini, A. & Fusi Pecci, F. 1988, ARA&A, 6,199

Renzini, A. & Ciotti, L. 1993, ApJ, 416, L49

Renzini, A. 1994, in: “Galaxy Formation”, eds. J.Silk, N.Vittorio (Amsterdam, Holland), 303

Renzini, A. & Cimatti, A. 1999, ASP Conf. Proc., 193, 312

Salpeter, E.E. 1955, ApJ, 121, 161

Sandage, A. & Bedke, J. 1994, “The Carnegie Atlas of Galaxies”, 2, The Carnegie Institution of Washington

Sarajedini, A. & Demarque, P. 1990, ApJ, 365, 219

Shapley, A.E., Steidel, C.C., Pettini, M. et al. 2003, ApJ, 588, 65

Schweizer, F. 1990, in:”Dynamics of Galaxies”, ed. R. Wielen, Springer (Berlin)

Schweizer, F., Miller, B.W., Whitmore, B.C. et al. 1996, AJ, 112, 1839

Schweizer, F. & Seitzer, P. 1998, AJ, 116, 2206

Steidel, C. C., Giavalisco, M., Pettini, M. et al. 1996, ApJ, 462, L17

Surma, P.& Bender, R. 1995, A&A, 298, 405

Tinsley, B.M. 1968, ApJ, 151, 575

Toomre, A.& Toomre, J. 1972, ApJ, 178, 623

Trager, S.C., Worthey, G., Faber, S.M. et al. 1998, ApJS, 116, 1

van den Bergh, S. 1995, ApJ, 450, 27

VandenBerg, D., Swenson, F.J., Rogers, F.J. et al. 2000, ApJ, 532, 430

Västerberg, A. R., Lindblad, P. O., Jorsater, S. 1991, A&A, 247, 335

Vazdekis, A. et al. 1996, ApJS, 111, 203

Vazdekis, A. 1999, ApJ, 513, 224

West, M.J., Côté, P., Jones, Ch. et al. 1995, ApJ, 453, 77

Westera, P., Lejeune, Th., Buser, R. et al. 2002, A&A, 381, 324

Whitmore, B.C., Schweizer, F., Leitherer, C. et al. 1993, AJ, 106, 1354

Worthey, G. 1994, ApJS, 95, 107

Worthey, G. 1997, AIP Conf.Ser., 393,527

Worthey, G. & Ottaviani, D.L. 1997, ApJS, 111,377

Wright, A.E. 1972, MNRAS, 157, 309

Yi, S. & Demarque, P. 2001, ApJS, 136, 417

Zepf, S.E. & Ashman, K.M. 1993, MNRAS, 264, 611

Ziegler, B. L. & Bender, R. 1997, MNRAS, 291, 527

Ziegler, B.L. 2000, ASP Conf. Ser. 13, 211

2 Extragalactic Globular Clusters in the Near Infrared: IV. Quantifying the Age Structure using Monte-Carlo Simulations

Astronomy & Astrophysics, 2004, 419, 863

Maren Hempel & Markus Kissler-Patig

Abstract

In previous papers of the series, we used a combination of optical and near-infrared colors to derive constraints on the relative age structure in globular cluster systems. Here, we present the details, strength and limitations of our method based on Monte-Carlo simulations of color-color diagrams and cumulative age distributions. The simulations are based on general informations about the globular cluster systems (e.g. color-ranges, the number ratios between sub-populations) and the different single stellar population models (SSP's) which are used to derive relative ages. For both the modeled systems and the observed globular cluster systems we derive the cumulative age distribution and introduce two parameters to define it, the so-called 50% age and the result of the reduced χ^2test of the comparison between models and observations. The method was tested successfully on several systems and allowed to reveal significant intermediate age populations in two of them.

Keywords: Monte-Carlo simulation: color distribution, globular cluster: general, cumulative age distribution

2.1 Introduction

Globular cluster systems have been extensively used in the last decade to interpret the formation and evolution histories of early-type galaxies (see for example Geisler, Grebel & Minniti (2002) and Kissler-Patig (2003). A key question remains the origin of the multiple globular cluster sub-populations observed within most (if not all) individual galaxies. The metal-poor, halo sub-populations appear very uniform and are most probably linked to star cluster formation in the early structures of the universe (e.g. Ashman et al. 1994; Burgarella et al. 2001). However, the metal-rich sub-populations are less likely to be homogeneous in age and/or metallicity, as nicely seen e.g. in the sample of Kundu et al. (2001a,b) and might contain information on the more recent epochs of star formation in the galaxies. While certainly a large fraction of metal-rich globular clusters investigated so far is old (e.g. Puzia et al. 1999), the existence of large intermediate-age globular cluster populations has not been excluded yet and was actually shown to exist in at least some galaxies (e.g. Goudfrooij 2001; Puzia et al. 2002; Hempel et al. 2003).

This latter fact is closely related to one of the most important open questions in galaxy formation and evolution, namely whether galaxies formed the vast majority of their stars at early epochs, or whether a significant fraction of the stars originated from more recent events, such as dissipational mergers (e.g. Kennicutt 1998; Renzini 1999; Renzini & Cimatti 1999; Schweizer 2000 and references therein).

The study of globular clusters in order to determine the major star formation epochs presents several advantages over the study of the diffuse galaxy light. Indeed- several age populations can be hidden in the diffuse light of the host galaxy (e.g. Larsen et al. 2003). Globular clusters on the other side represent single stellar populations, their stars sharing the same metallicity and the same age. The existence of sub-populations of globular clusters gives henceforth a stronger indication for different star formation epochs. Since the prediction and first discovery of multiple globular cluster sub-populations in early-type galaxies by Ashman & Zepf (1992, see also Zepf & Ashman (1993)) their color distributions have been investigated extensively. Various studies, e.g. by Gebhardt & Kissler-Patig (1999) and Kundu & Whitmore (2001a,b) have shown that bimodal color distributions in elliptical galaxies are common. The exact interpretation, however, is hindered by the age-metallicity degeneracy of broad band colors (Worthey 1994).

Our group uses combined optical- and near infrared photometry (Kissler-Patig et al. 2002; Puzia et al. 2002; Hempel et al. 2003, hereafter cited as Paper I, II, III) to overcome this obstacle and partly lift this degeneracy. In Paper III, we showed how, using Single Stellar Population (SSP) models and the corresponding model isochrones (e.g. by Bruzual & Charlot 2000; Vazdekis 1999 and Maraston 2001), photometric studies of globular cluster systems can be used to derive their age distributions.

In this paper we present the details of our method, investigate the capability of photometric studies to detect globular cluster sub-populations of different ages within the metal-rich sub-population and the accuracy with which we can derive their relative ages.

The paper is organized as follows: in Section 2.2 we will describe our method of simulating color-color diagrams for globular cluster systems. Section 2.3 shows how these artificial distributions are compared to the observed data via their cumulative age distributions. Caveats and uncertainties of the method are presented in Sect. 2.4, first results and our conclusions are given in Sect. 2.5 and 2.6.

2.2 Modeling of color distributions

2.2.1 Overview of the method

The basic idea of our approach is best described by a question: How would a color-color diagram of a globular cluster system look like if it was indeed *formed in two or more distinguishable star formation events*? We decided to model different cases and compare these to our data (Fig. 2.1, see also Paper III).

Originally, our ambition was a direct detection of the different globular cluster sub-populations in a given galaxy in our data (color- color diagrams) by comparing observed color distributions with simulations following SSP models. This, however, turned out to be too difficult with non-converging solutions. Indeed for the direct comparison of observed and simulated color-color diagrams we applied a two-dimensional Kolmogorov-Smirnov test (Press et al. 1992). However we had to consider a number of parameters which are included in our observations but difficult to include in the simulations, e.g. completeness limits, photometric error, with high enough accuracy to still disentangle in 2 dimensions the parameters of interest (age, number ratios of the different populations). In Sect.2.3 we describe our alternative, 1- dimensional approach via the cumulative age distribution.

At this stage we do not address the question of what actually ignited the cluster formation and are working with the final observed color distribution only. Also, at this point, we stay with the assumption of two major star formation events and a first generation age of 15 Gyr out of convenience. The latter does not play a major role since we are interested in relative ages only. Further, if we take into account the age uncertainty of the model isochrone in the age range between 10 and 15 Gyr our assumption is still reasonable with respect to the new WMAP results giving a maximum age of the universe of 13.7 Gyr ± 0.2 Gyr (e.g. Bennett et al. 2003). We will also present results for NGC 5846 assuming the old population of age 10 Gyr in Sect. 2.5.1.

The basic principle is thus to input a number of properties for the two sub-populations to model (see next section), use a Monte-Carlo approach to model the distribution of the first color,

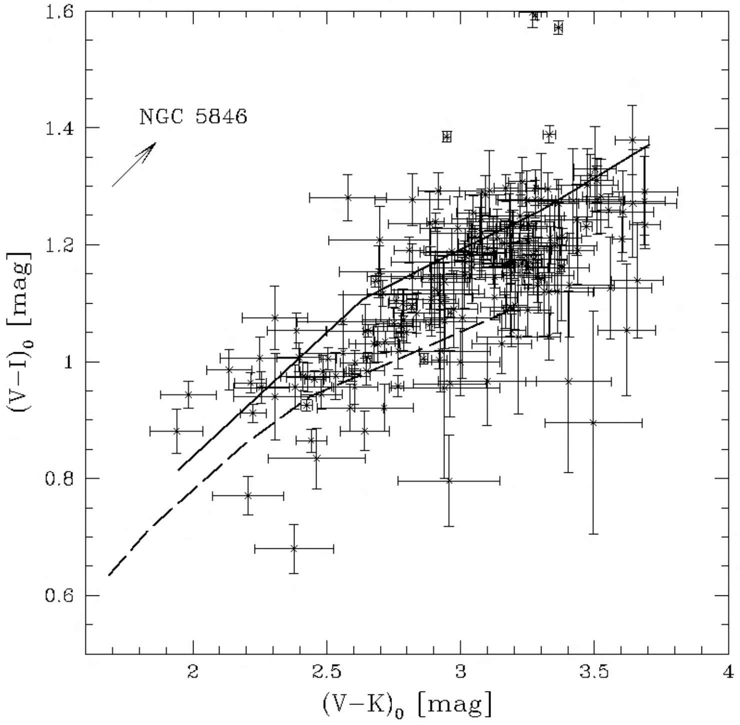

Fig. 2.1.— Color–color diagram for the NGC 5846 globular cluster system. The solid and dashed line mark the 15 Gyr and 2 Gyr isochrone respectively, following the Bruzual & Charlot SSP model (Bruzual & Charlot 2000).

determine the second color with the help of SSP's, construct a cumulative age distribution from this artificial two-color diagram and compare the latter to its observed counter-part. These steps are repeated for various input variables that scan the two parameter space (size of the second populations, age of the second population).

To illustrate the method, we use data presented in Paper III: we model color–color diagrams, $(V-I)$ *vs.* $(V-K)$, for a template globular cluster system corresponding to the one of NGC 5846. This is a favorable example given the relatively large number of objects with VIK colors (188 globular clusters for the complete sample, when no limits for photometric errors, color or limiting magnitudes are applied). In Sect. 2.4, we will also illustrate the caveats for smaller samples and the possibility of contamination.

An important note is that we are interested in the age structure of the metal-rich population only. We assume the *blue* ($2.0 \leq (V-K) \leq 2.7$) population to consist of *old* objects only (in NGC 5846 43 cluster were assigned to the metal-poor population), and model exclusively the red ($2.7 \leq (V-K) \leq 3.8$) color range. We generate for our example case in total 120 metal- rich objects, split into an *old* and *intermediate age* population.

2.2.2 Input parameters to the simulation

Several input parameters get fixed with respect to the observed distribution.

- **the total number of metal-rich objects**, in our example we have 120 metal-rich globular cluster candidates and simulate individual color distributions with that number of objects

- **the primary color range to be modeled**, in our template $(V-K)$ is used as primary color in the range $2.7 < (V-K) < 3.8$. The lower limit is driven by the observed gap between blue and red sub-populations, the upper limit encloses metallicities of up to twice solar at the highest ages, but excludes redder contaminating galaxies

- **the SSP model** to be used in order to associate, for a given age, the secondary color (in our case $(V-I)$) to each primary color point

- **the observed error distribution in the primary color** which is used to randomly "smear" the primary color after calculating the secondary color

- **the observed error distribution in the secondary color** which is used to randomly "smear" the secondary color

For each study of a particular data set these fixed parameters can be chosen such as to mimic closely the observed data. In addition to these fixed parameters two variable input parameters are of interest: how many young clusters are present, and what is their age?

2.2.3 Variables of the simulation

Our scientific goal is to investigate *i)* whether a second, intermediate-age population is present in the metal-rich sub-population; and if so *ii)* what is the most likely age of the population and *iii)* what is its importance in number of clusters relative to the old metal-rich population. Thus, we explore the parameter space span by the two latter properties. To do so, each set of simulations is performed for a pair of these variables:

- **The relative number ratio of the old with respect to the intermediate age sub-population**. We vary the ratio of both populations between a populations composed of 100% 15 Gyr old clusters (no younger sub-population present) to 100% young objects, in 10% increments.

- **The age of the second population** for which we modeled the cases of 1, 2, 3, 5, 7, and 10 Gyr.

Thus, simulations are preformed for each of the 66 possible pairs of variables. This leads to 66 master models which get compared to the observed data.

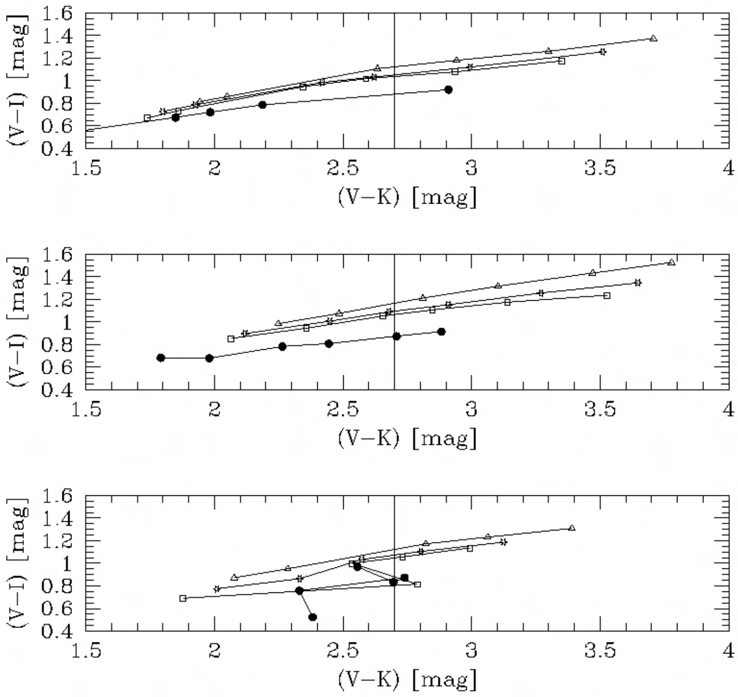

Fig. 2.2.— Comparison between the SSP model isochrones given by Bruzual & Charlot (2000) (upper panel), by Vazdekis (1999) (middle panel) and Maraston (2001) (lower panel). Different symbols mark the 1 Gyr (solid circles), 3 Gyr (open squares), 5 Gyr (open stars) and 15 Gyr (open triangles) isochrones. The solid line at $(V-K)$=2.7 marks the boundary between **blue** and **red** objects (see section 2.2.4).

2.2.4 Monte-Carlo simulation to get a set of primary colors

For each individual simulation, we start by creating an artificial globular cluster sample in our primary color. We populated the two $(V-K)$ color intervals assigned to a **"blue"** and a **"red"** sub-population with an fixed number of objects. Hereby we assume a random distribution within this range. A second run of simulations using a Gaussian color distribution in both populations did not lead to significantly different results than the once obtained for random distributed objects. Given the lack of physical support for Gaussian color distributions, we stay with the simplest case: a pure random distribution.

2.2.5 Determination of the second color and observational errors

The importance of using different SSP models, e.g. by Bruzual & Charlot (2000, hereafter named BC00), Vazdekis (1999, hereafter named VA99) or Maraston et al. (2001, hereafter named MA01) for our modeling becomes clear, if we compare the corresponding isochrones. In Fig. 2.2 the isochrones for a 1, 3, 5, 10 and 15 Gyr old SSP are shown following the model by Bruzual & Charlot (2000), Vazdekis (1999) and Maraston (2001). Especially in the red $(V-K)$ color range we find a significant discrepancy for the corresponding $(V-I)$, resulting in a model dependency of the derived ages. Therefore we will apply different models in the age dating.

The next step in the simulation is the parametrisation of the model isochrones. A least square fit of $(V-I)$ as a logarithmic function of $(V-K)$ in the form $(V-I)$=A$\cdot$ln$(V-K)$+B, as shown in Fig. 2.3, gives us a set of parameter A and B for all SSP models. Unfortunately the Maraston isochrones for SSP's in the lower age range (less than 5 Gyr) allow no simple parametrisation. We therefore decided to postpone the work with this specific model. The relations were used to calculate the **secondary** color $(V-I)$ for each assumed age population. We generated color-color diagrams for globular cluster systems consisting of an old (15 Gyr) population and a second one, as explained in Sect. 2.2.3. Each simulation will therefore create the $(V-I)$ $vs.(V-K)$ color-color diagram for a mixed population of globular clusters. Finally both colors $(V-K)$ and $(V-I)$ were smeared with up to 3σ photometric error, taken from the NGC 5846 observed error catalog. In a last step, an artificial catalog with the two colors and their 1σ error is created. The final outcome of this process is the color-color distribution $(V-I)\pm\,\Delta(V-I)$ $vs.(V-K)\pm\,\Delta(V-K)$ for six age combinations and eleven number ratios. We generated 1000 models for each set of model parameters. The final product, the cumulative age distribution (see section 2.3.1) to be compared with the observations, was determined as the statistical mean of the distribution of these 1000 models.

As we can see in Fig. 2.3, the isochrones for various SSP models (e.g. Bruzual & Charlot, Vazdekis and Maraston) differ strongly. Nevertheless there is no quality argument (Vazdekis et al. 1996) behind our choice of BC00 and VA99. Since Bruzual & Charlot provide models for the largest variety of ages and metallicities we started our modeling program using parametrised BC00 isochrones (Fig. 2.3, left panel). VA99 has been added later to test our method for model dependence. The latter will be discussed in section 2.5. Both models assume a Salpeter IMF.

2.3 Quantifying the age structure

2.3.1 Cumulative age distribution

Photometric errors, which might become rather substantial in combined optical and near-infrared photometry, contribute largely to the uncertainty in age determination. Comparing our

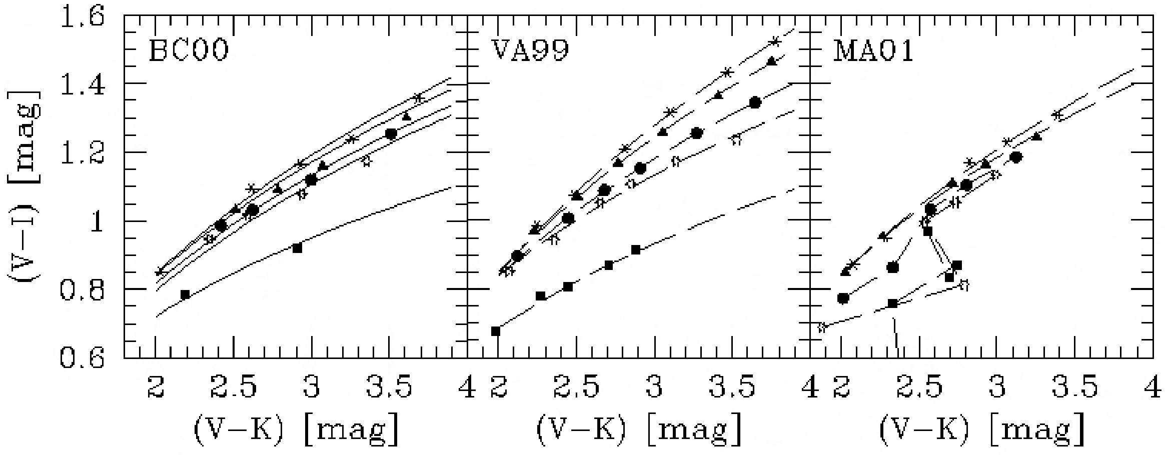

Fig. 2.3.— Least square fit of model isochrones given by Bruzual & Charlot (2000)(left), Vazdekis (1999) (center) and Maraston (2001) (right). Various isochrones are marked with solid squares (1Gyr), open stars (3 Gyr), solid circles (5 Gyr), solid triangles (10 Gyr) and asterisks (15 Gyr).

limiting photometric error of 0.15 mag and the color difference in $(V-I)$ for SSP's which differ in age by at least 1 Gyr (see Fig. 2.3), we conclude that not only absolute ages are out of reach but also age resolution more accurate than several Gyr. Nevertheless- our major goal is the detection of cluster sub-populations in order to give evidence for various major star formation events during the evolution of the galaxy. Since we assume this events to be caused by merging or accretion, likely but not very frequent events, age differences larger than 5 Gyr are to be expected. The cumulative age distribution (see Fig. 2.4) which we derive is only based on the object density in the color-color diagram with respect to the isochrones and is less sensitive to photometric errors compared to a direct age determination. Since the result will refer to the globular cluster system the size of the sample becomes important, as we will show in a later section (see Sect. 2.4.2).

The derivation of the cumulative age distribution is a straight forward procedure and is identical for observed and simulated samples. Each object was assigned to an age older than X if its $(V-I)$ color was found to be redder than for the isochrone of that age. The model isochrones for different ages at low $(V-K)$ values are hard to distinguish and the $(V-I)$ color of a specific isochrone depends only weakly on $(V-K)$ in the red- color regime. Therefore we set a lower color limit (see also Chapter 2.6) for $(V-K)$ of $\geq$2.6, corresponding roughly to a metallicity of [Fe/H]$\sim$-0.7dex, slightly above the split between metal poor and metal rich clusters in galaxies.

The upper limit was set to $(V-K) \leq 3.6$, which agrees with the upper $(V-K)$ limit in our NGC 5846 sample. The age distributions are normalised with respect to the total number of objects within $2.6\leq(V-K)\leq3.6$. The notation 0 Gyr in the cumulative age distribution refers to the total number of objects (per definition all objects are 'older' than 0 Gyr).

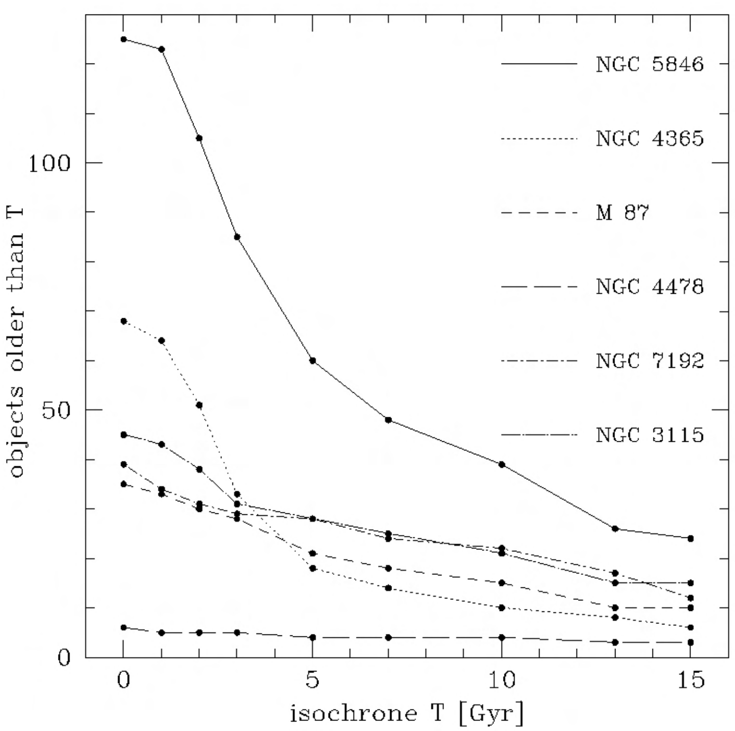

Fig. 2.4.— Cumulative age distribution in the globular cluster systems of NGC 5846, NGC 4365, NGC 7192, NGC 3115, NGC 4478 and M87.

2.3.2 The comparison with observed data: χ^2-test

The relative size of globular cluster sub-populations provides some constraints for the galaxy formation scenario. In Ashman and Zepf (1992) the efficiencies of the globular cluster formation in dependency of the environment (cluster galaxies or 'normal' elliptical galaxies) and the amount of available gas are compared and found to differ significantly. Therefore we are interested in the ratio between possible globular cluster sub-populations. Since the globular cluster samples are limited to the inner most region of the globular cluster systems this result will only answer the question whether there is a second population and to which extend we can constrain its age and relative size compared to an old population.

To quantify the age structure we compare the cumulative age distributions of the observed and modeled data sets. By using a reduced χ^2-test we find the best fitting model for the observed system.

Due to the age uncertainty of the models, the 3σ scatter in color allowed in the model, and to the photometric error in the observations, we expect a certain degeneracy in the age/ratio combinations. Nevertheless we are able to constrain the age as well as the ratio between the two

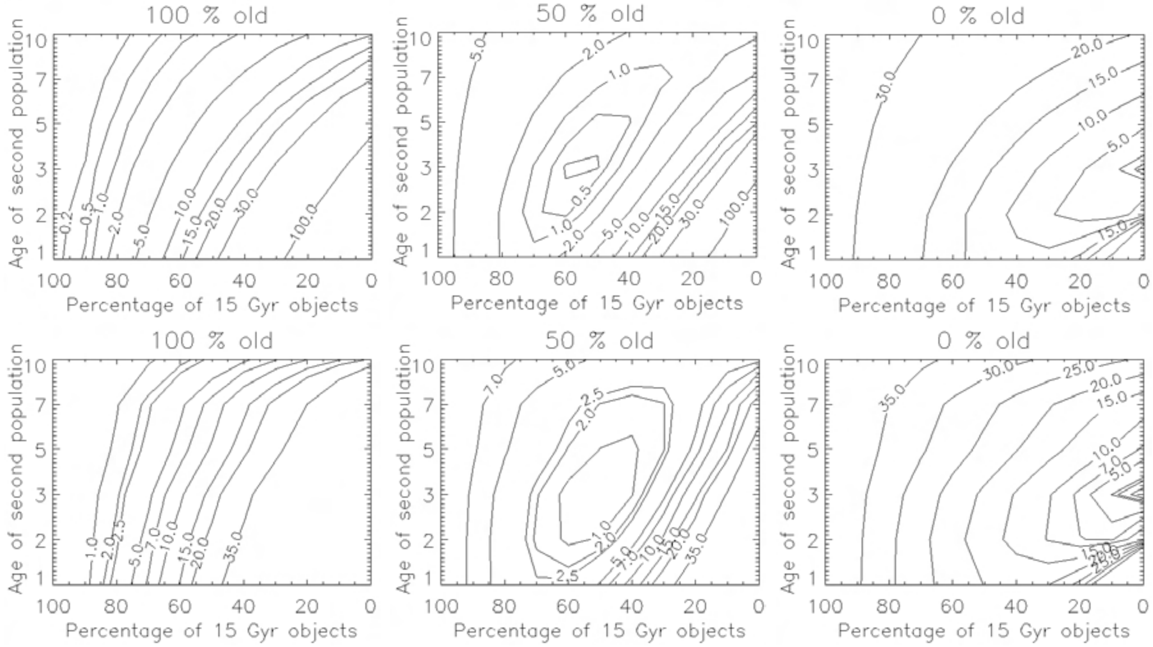

Fig. 2.5.— Self-consistency test: age distributions of individual model systems compared to the complete model set. The result of the χ^2-test are shown as χ^2- contours. For this test we use the model of a purely 15 Gyr old population (left), a 15 Gyr + 3 Gyr mixture (middle) and a purely 3 Gyr old population (right). As expected the result for the purely old population is much more uncertain than for the other two, allowing as best fitting model also mixed populations. The upper plots show the result for the BC00 model and the lower plots the VA99 models. The different spread of the isochrones (see Fig. 2.2) results in different uncertainties.

populations. This was tested by comparing the age distribution for three selected models with the complete model set. The χ^2-test should pinpoint the model which was chosen in the first place. In Fig. 2.5 we show the result for the χ^2-test for models of a 100% 15 Gyr, a 50% 15 Gyr + 50% 3 Gyr and a 100 % 3 Gyr population respectively. As we can see in the plots the χ^2-tests return the model parameters we chose as the best fit, including an uncertainty in age and number ratio. Due to the different $(V-I)$ color range for BC00 (upper panel) and VA99 (lower panel) SSP isochrones the result of the χ^2-test differ slightly.

2.3.3 Comparison of different SSP models

Before we start comparing our results based on the SSP models by Bruzual & Charlot (Charlot & Bruzual 1991; Bruzual & Charlot 1993) and by Vazdekis (Vazdekis et al. 1996) we want to make the point that our choice is by no means to interpret as judgment on the various models. As Vazdekis et al. (1996) pointed out there is, despite the different modeling procedure, little difference in the quality of the various models, which mostly differ in the covered range of metallicity and age and in accuracy of the physical input parameter. The SSP models by Bruzual & Charlot are based on the Padova library from 1994. The newer version, based on the Padova 2000 library, is used in the latest SSP model by Bruzual & Charlot, but not recommended by the authors (see Bruzual & Charlot 2003). Details can be found in Bruzual & Charlot (2003). For more information about the VA99 model we refer to Vazdekis et al. (1996). The essential difference to the BC00 models being the application of empirical stellar libraries whereas Bruzual and Charlot make use of the libraries by Lejeune (e.g.Lejeune et al. 1997). The later are based on the stellar atmospheres derived by Kurucz (e.g.Kurucz 1992). We would like to stress again that we do NOT attempt to judge the quality of different models but use them to discuss our method with respect to model uncertainties. Our choice of the BC00 and VA99 model is therefore highly subjective and mostly driven by the typical error is introduced by parametrising the model isochrones for calculating the secondary color (as explained in 2.2.4). In the future, we intend to replace the parametrised by linear interpolated secondary colors in order to reduce this error. In the discussion of our results (see Sect. 5.1, Fig. 2.18) we will present first results based on this modification.

The smaller spread in $(V-I)$ for BC00 results in a finer scanning of the color-color diagram and gives therefore better results in the χ^2-test. For larger sample sizes (observed and simulated systems) this effect will become more and more negligible. We expect the strongest effect for the comparison of small observed systems (e.g. NGC 4478) with the relatively large (120 clusters) model systems (see Sect. 2.5).

2.4 Potential caveats

2.4.1 Contamination with background objects

Using color distributions with respect to model isochrones is strongly affected not only by photometric errors but also by false identification of objects. Within the red color range, as it has been defined in section 2.3.1, the contamination of our globular cluster sample by background galaxies and/or foreground stars has to be considered. In the red $(V-K)$ color range these objects are most likely unresolved background galaxies. Assuming their random distribution on the sky we use the Hubble-Deep-Field South, available from the archive of ST-ECF[1] as a representative background sample. We are well aware that a random distribution of background objects is only the case in a first approximation (Roche et al. 1993; Infante & Pritchet 1995; Maller et al. 2003).

In Figure 2.6 we compare the color-color diagrams for observed systems, taken from Paper I, II and III, with the background sample, to which the same selection criteria as to the cluster sample have been applied, i.e. limits for the photometric error, the limiting K- magnitude and

---

[1] www.stecf.org/hstprogrammes/ISAAC

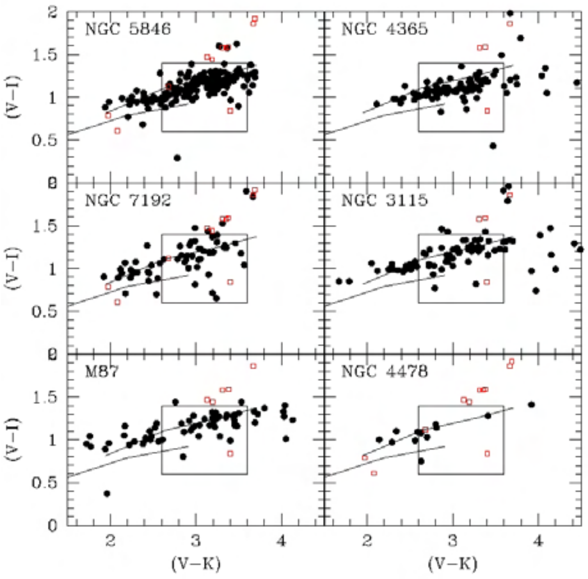

Fig. 2.6.— Comparison of color -color diagrams for the globular cluster systems and the HDF-S. Globular clusters are marked by filled circles and HDF-S objects by open squares. The solid lines mark the 1 Gyr and 15 Gyr isochrone respectively, as given by Bruzual & Charlot (2000). The box marks the color range used for determining the cumulative age distribution.

the color cuts for $(V-K)$ and $(V-I)$ (marked by the box). Additionally the HDF objects have been selected using the SExtractor star/galaxy classifier as shape parameter. For comparison, the color-color diagram for the HDF-S sample is given in Fig. 2.7 using only error cuts and limiting magnitude (symbol: $\triangle$) or including ellipticity (left panel) and classifier (right panel) as well. The latter was applied to our observed data sets.

To account for the background contamination we applied different correction procedures. For all of them we determined the age distribution for the HDF-S objects (Fig. 2.8), using the procedure given in Sect. 2.3.1. Due to the different limiting K-band magnitude in the observed systems the age distribution of the HDF was determined for each globular cluster system separately.

In the first trial (see Chapter 2.6) we corrected age distribution for the observed systems following a worst case scenario. Hereby we subtracted the number of HDF-S objects in each age interval (older than **'X'**) from the number of objects found in the observed systems. This works only in cluster samples much larger than the HDF-S sample, but will fail in less numerous systems, e.g. NGC 3115, NGC 7192 and NGC 4478.

In a second run the correction was applied to the color-color distribution in the observational data. Before counting objects with respect to a given model isochrone we rejected all objects in the observed sample if a HDF-S object was found with a difference in $(V-K)$ and $(V-I)$ <0.1 mag. This links each contaminating object directly to an observed object. Differences in the color distribution are therefore included. Observed systems with a large number of objects are handicapped in this procedure if a background object is found in the vicinity of several objects in the observed cluster system. Additionally no informations about the shape of the background objects are included yet. The globular cluster samples are selected for point sources whether the HDF objects include as well (even mostly) extended objects.

The final most realistic correction for background objects was therefore done by setting limits for the photometric error in all bands (0.15 mag) and the parameter "classifier" given by SExtractor. Due to the extraordinary depth of the HDF images the classifier has been set to a limit of 0.8, which should be sufficient to reject most of the extended objects. As an example the correction effect in the cumulative age distribution for NGC 5846 is shown in Fig. 2.9. In the left panel the absolute number of objects per age bin [0 Gyr, T] before and after correction is shown. The right panel gives the relative age distribution for both sets. In case of NGC 5846 we find only 7 HDF-S objects within the selected color range, which results in an insignificant correction. Nevertheless - this changes drastically for smaller cluster samples or in case of deeper imaging of the globular cluster systems.

In our comparison of cumulative age distributions we work with globular cluster systems of very different sizes, NGC 5846 and NGC 4365 being the largest with a total number of about 190 clusters, and on the other side NGC 4478 with only 21 GCs, most of them excluded from the age distribution by the color cuts. As described in Sect. 2.2 we used NGC 5846 as template system

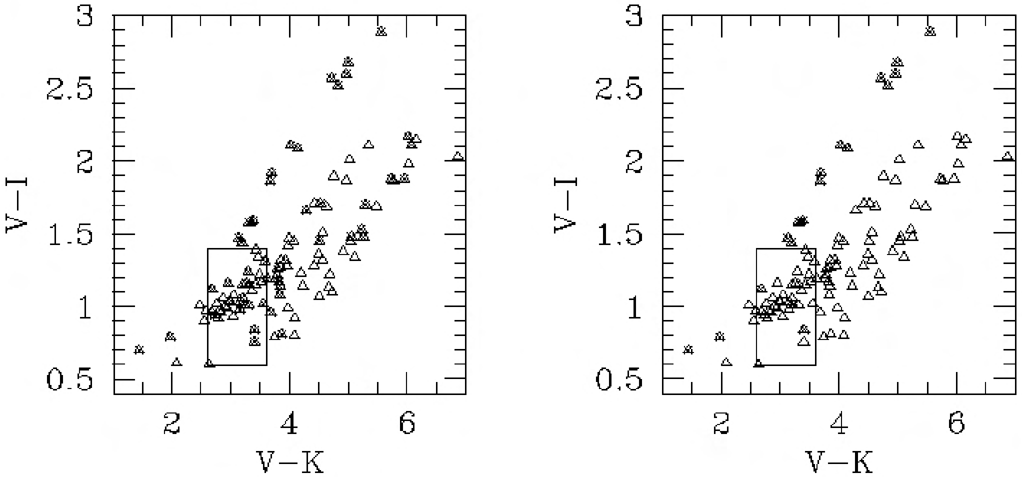

Fig. 2.7.— Color- color diagram for the HDF-S sample (K>21.5) before (triangles) and after (cross) applying shape parameter for selection. For selection the ellipticity (< 0.2, left panel) and the star/galaxy classifier (> 0.8, right panel) have been used. For final correction we choose a combination of photometric error, limiting magnitude and classifier. As in Fig.6 the box indicates the color limits.

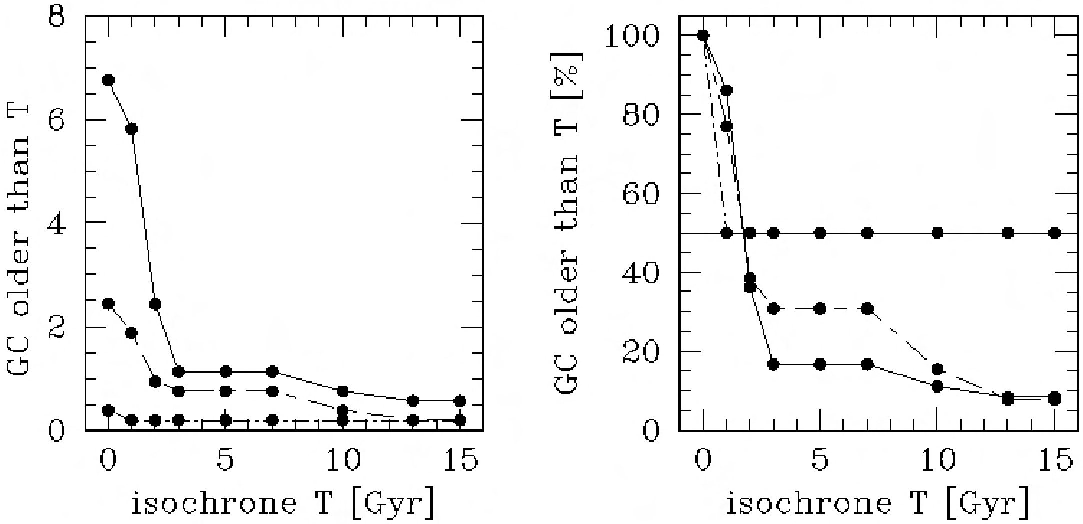

Fig. 2.8.— Cumulative age distribution in the HDF-S sample (BC00) normalised to 1 arcmin^2 (left: absolute, right: relative). The solid line marks the result if only a error cut of 0.15 mag for all filters is applied. Applying an additional ellipticity limit (<0.2) results in a age distribution indicated by the dashed line. Using a combination of error cut and star/galaxy classifier (>0.8) given by SExtractor (Bertin & Arnout 1996) most background galaxies can be rejected from the data set (dotted-dashed line).

and have therefore to check whether the age distribution and the resulting χ^2-test depend on the size of the observed globular cluster systems. In Fig. 2.10 we show the cumulative age distribution for all observed globular cluster systems before and after correcting for background contamination. Due to the selection criteria for background objects the correction effect is rather small, except for NGC 4478, where the remaining cluster set might not allow statistical stable results (see next section).

2.4.2 Stability of contamination correction

In the previous section we opened the discussion to which extend the sample size affects the final result. In the competition between spectroscopy and photometry toward relative age dating this becomes even more important, the sample size being the advantage of photometry. But what is the minimum size of the cluster system, for which the scattering in the data (e.g. due to photometric errors) becomes negligible in the age distribution? To answer this question we modeled the color-color diagram of a mixed cluster population (50% 15 Gyr old objects and 50% 3 Gyr old objects). The age distributions for systems between 10 and 200 objects are shown in Fig. 2.11. We find that in systems with less than 60 objects the age distribution varies significantly. With respect

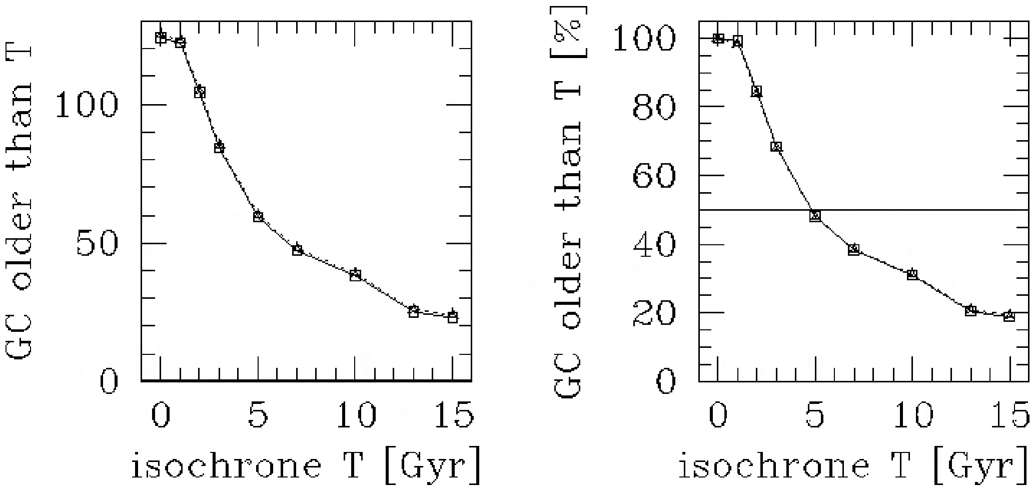

Fig. 2.9.— Cumulative age distribution in NGC 5846. The left panel shows the cumulative age distribution before (triangles, dotted line) and after (open squares, solid line) correction for contamination applying an error cut as well as a selection by star/galaxy classifier. In the right panel the distribution has been normalised to the total number of objects in the sample after correction (125 objects within the color limits). The age dating was done following the SSP models by Bruzual & Charlot.

to section 2.3 we find this effect being even stronger if the VA99 model isochrones are used.

In order to minimise the scattering effect in the simulated cluster system we generated 1000 models and work with the statistical mean of the age distribution (see Sect. 2.2.4). Still the sample size for the models has to be considered. In Fig. 2.12 we compare the age distribution for models consisting of either 100% old objects or a 50%: 50% mix of 15 Gyr and 3 Gyr old globular clusters in a set of only 10, 60 or 120 clusters. The error bars give the standard deviation of the object counts in the 1000 models. In systems with only 10 objects the age distribution for a mixed population and a purely old system are, within the error limits, indistinguishable. In slightly larger samples (e.g. 60 objects) the age distributions of a purely old and a mixed population overlap in the older age bins. The result would be multiple findings of best fitting models (see Sect. 2.4.3). As a last point we want to mention that our primary assumption of a random distribution in $(V-K)$ becomes critical for small samples.

2.4.3 Is there a significant intermediate age cluster population?

In Figure 2.13 we show the result of the reduced χ^2-test for finding a specific input model within our complete set of 66 models of varying sample sizes for the BC00 model. In contrast to the simulations the age distribution in the observed globular cluster systems represents a single sample

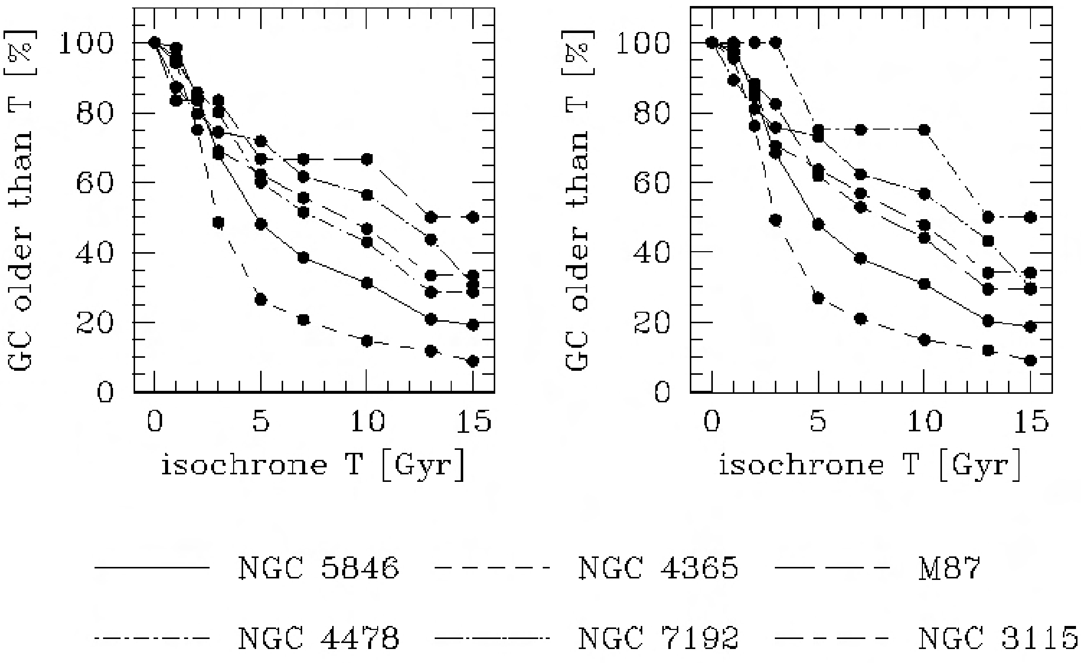

Fig. 2.10.— Cumulative age distribution (using BC00) in the globular cluster systems observed so far. The left panel shows the relative distribution without background correction. The correction applied in the right panel follows the procedure given in the previous section.

still subject to stochastic effects. In order to test the stability of our derived ages/number ratios for various sample sizes we compare the age distribution for six individual simulations (assuming the same model parameters but different sample sizes). The example shown here are based on the BC00 model. As we can see, we should be able to detect sub-populations, if their ages differ by several Gyr. Nevertheless, for small sample sets the results become quite unstable, i.e. the age of the young sub-population and the size ratio between both populations are more uncertain. Again- this is more important for the VA99 model, due to the steeper $(V-I)$ gradient of the isochrones. We also have to keep in mind that all the models were created based on our largest globular cluster system- NGC 5846 and we therefore expect the most reliable results for sample sets which are in size and color range similar to NGC 5846. Special attention has to be paid to NGC 4478, where the majority of objects is found in the blue color range. In order to draw stricter conclusions about the red sub-populations the modeling parameters (size, $(V-K)$ color range) have to be chosen with respect to the observed cluster system.

Although we have discussed the effect that unresolved background objects can have on the results, we are aware that we are at this point not able to offer a quantitative correction for each of the observed systems. Even if our final selection criteria (error cut and classifier) for background objects (see Sect. 2.4.1) are too strict - we do not expect contamination to play a major role in

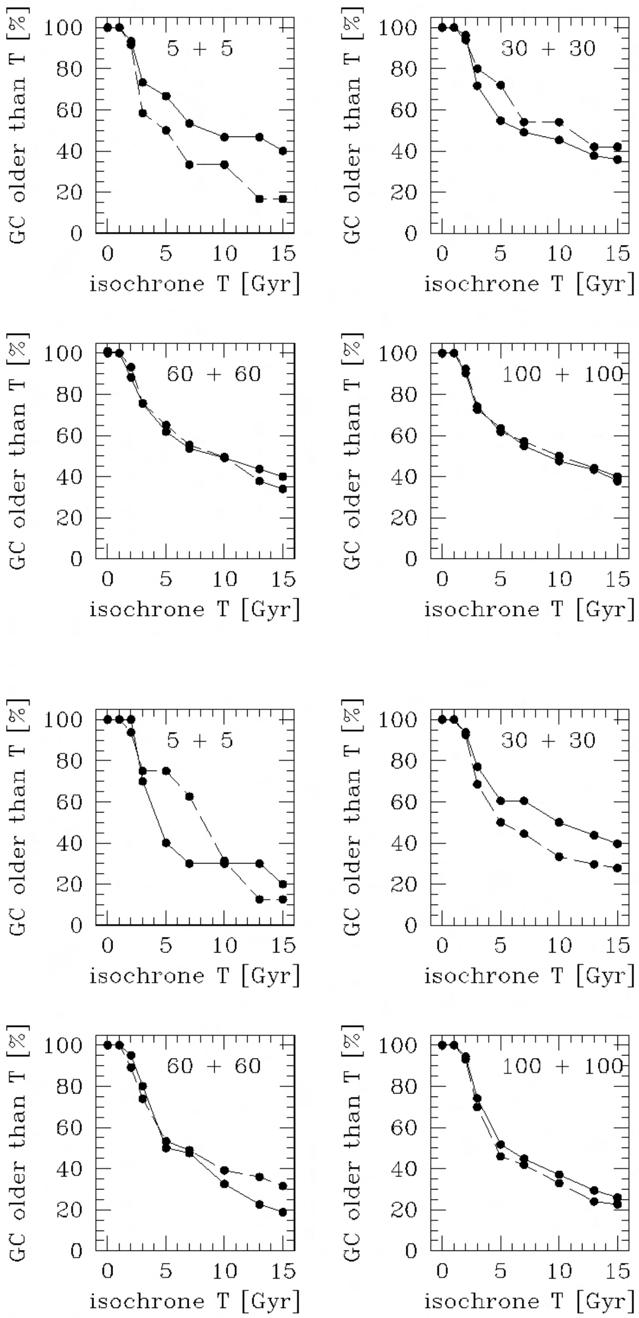

Fig. 2.11.— Cumulative age distribution for modeled samples, consisting of a different number of objects but assuming a constant mixture of old and intermediate age objects (50% : 50%). The results are shown for the BC00 (rows 1 and 2) and VA99 (rows 3 and 4) SSP models respectively. Each panel shows the age distribution for two out of six different runs of modeling.

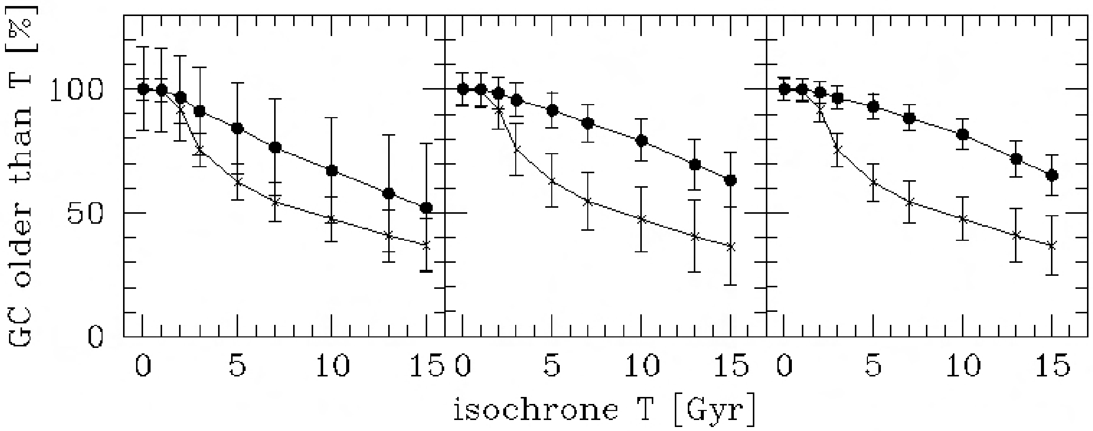

Fig. 2.12.— Cumulative age distribution (using BC00) derived for models of 10, 60 and 120 objects respectively. To show the importance of large number of objects we show the standard deviation of the counting rate. The models were created for a purely 15 Gyr old population (solid circles) and a 50%: 50% mix (×) of 15 and 3 Gyr old objects.

large globular cluster systems. Only the NGC 4478 (21 cluster in total) sample falls into the low number region where the stability of the χ^2-test is questionable.

2.5 Results for observed systems

The goal of relative age dating via the cumulative age distribution is to find evidence for various major star formation events in elliptical galaxies and to constrain those in their age difference and importance for the galaxy evolution. To do so we compare two features of the age distribution, the so-called 50%-age and the result of an χ^2-test between simulated and observed globular cluster systems. The 50%-age is defined as the age at which the cumulative age distribution intersects with the 50% level. Figure 2.14 shows the cumulative age distribution for all globular cluster systems observed so far, using the SSP model by Bruzual & Charlot and Vazdekis, respectively.

If we compare this 50%-level age derived for the observed systems with the models (see Fig. 2.15) we find a significant model dependence. We will include this parameter in our discussion.

For NGC 5846 and NGC 4365 with large globular cluster systems we obtain consistent results, independently on the SSP model. The 50%-age of both systems agrees with the 50%-age derived for a mixed population, hosting a second cluster population at an age up to 5 Gyr. In M87 the 50%- age gives as well evidence for a second population with an age of ~7 Gyr. For NGC 7192, NGC 3115, NGC 4478 the results for the 50%-age are inconsistent and depend on the used SSP models. NGC 4478 is a exceptional case for this study. The observed globular cluster system is very small and consists of mostly metal-poor objects. Within the $(V-K)$ color range we find only

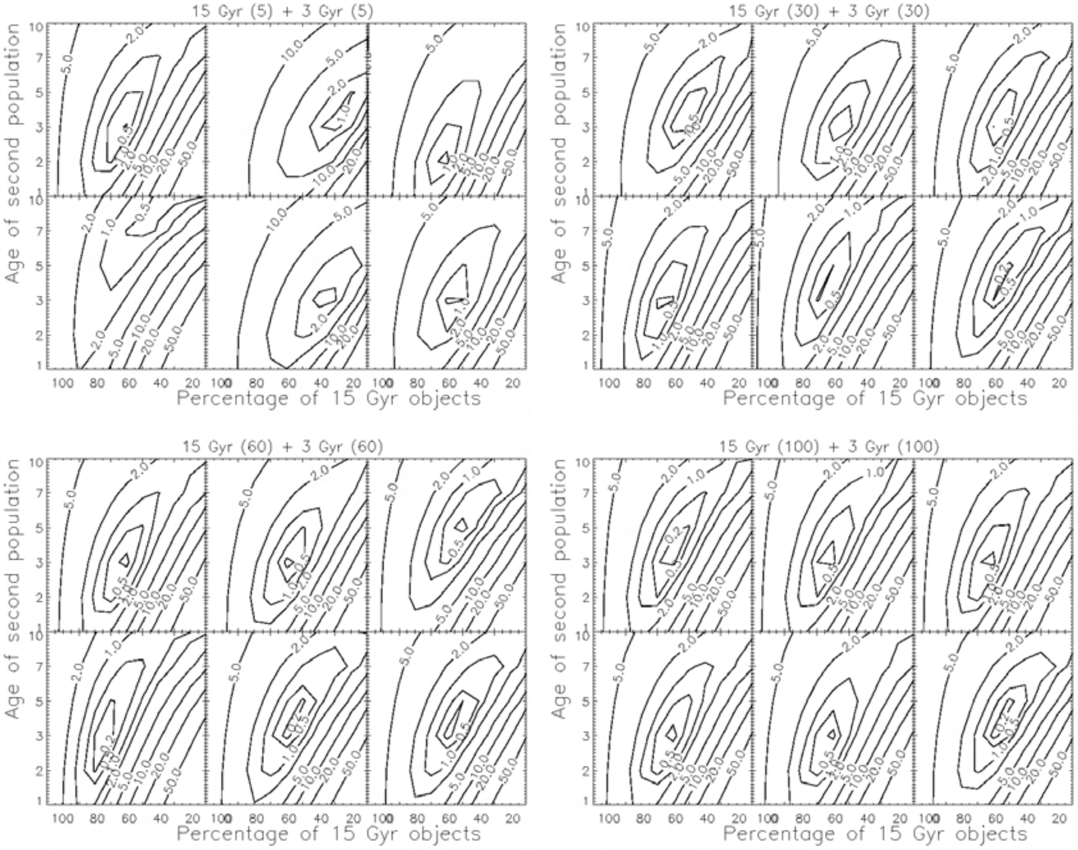

Fig. 2.13.— Examples of the reduced χ^2-test (see section 2.4.2) results for different sample sizes (10, 60, 120 and 200 objects). The age distribution for a mixture of 50% 15 Gyr and 50% 3 Gyr old clusters (see Fig.2.11) with the complete set of models are compared. On top of each plot the number of old and intermediate objects within the "red" population is given. We compare the results for six separate runs of modeling.

3 clusters, which is not sufficient for our analysis.

As mentioned in Paper III our intention regarding the modeling was the possibility to make quantitative statements about the star formation history in various galaxies. In the next section we present the result of the comparison between of the observed globular cluster systems and the Monte-Carlo simulations. We provide some limits on the age structure for 4 of the observed systems. As introduced in section 4.3 we discuss the results in the light of their SSP model dependence, which seems to be predictable in a way that applying VA99 models results in slightly younger ages and requires a larger sample size.

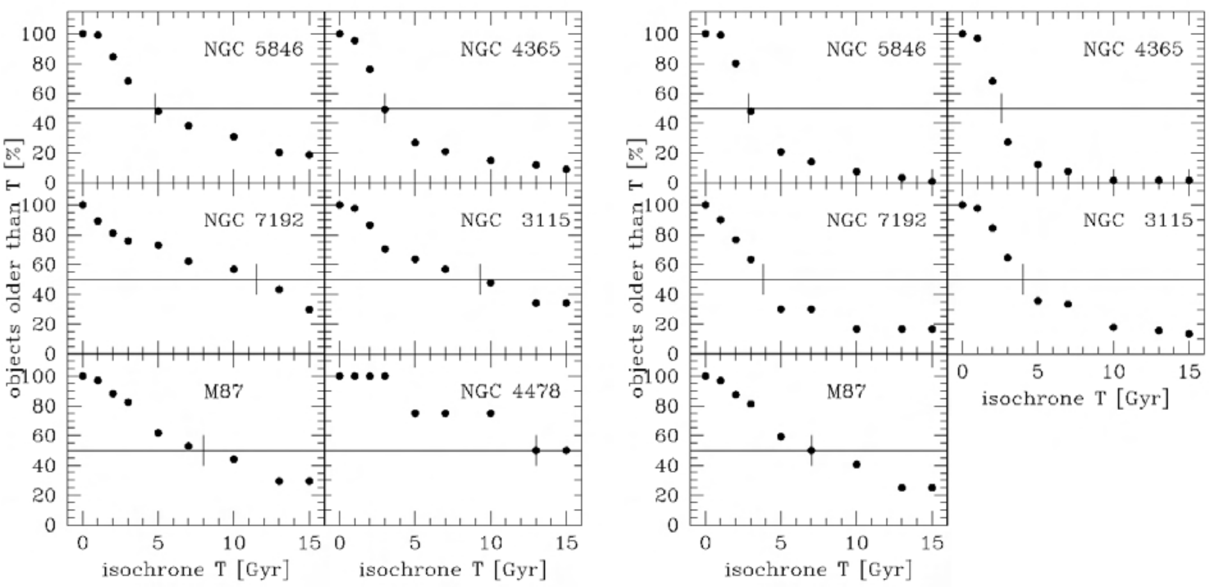

Fig. 2.14.— Cumulative age distribution in the globular cluster systems using BC00 (first and second row) and VA99 (third and fourth row) SSP model isochrones. The samples are corrected for background contamination following the procedure given in section 2.4.1. The horizontal line marks the 50% level and the vertical line its intersection with the derived age distribution.

2.5.1 NGC 5846 and NGC 4365

Spectroscopic (Larsen et al. 2003) and photometric (Paper II and III) results for NGC 5846 and NGC 4365 have shown that both globular cluster systems host an intermediate age population indicating a second star formation period. In Fig.2.16 we present the photometric and spectroscopic data for the globular clusters in NGC 4365, NGC 5846, NGC 7192 and NGC 3115 for which optical/ near-infrared photometric and spectroscopic data are available (33 objects). The left panel shows the $(V-I) vs. (V-K)$ color-color distribution of all clusters compared to the MA01 model isochrones. In the right panel the index measurements for H_β and MgFe are compared with the SSP model by Thomas et al. (Thomas et al. 2003) and confirm the photometric age dating. The globular clusters assigned to an intermediate age are those found in NGC 4365 and NGC 5846.

Consequently we expect the 50%-age to show the best agreement with the value calculated for mixed populations as well as the best fitting model being a mixture 'old' and 'intermediate' age globular cluster. For both SSP models we obtain 50%-ages belowe 5 Gyr the Vazdekis model giving slightly younger ages. Still the results are in good agreement with the value derived for models mixing an old population with globular clusters with ages up to 3 Gyr. The upper panels of Fig. 2.17 show the results of the χ^2 test for NGC 5846 and gives the highest agreement between the cluster sample and the models assuming a mixture of and old (15 Gyr) population and roughly up to 90% 3-5 Gyr old clusters. We will discuss this extremely large value, which we find for most of

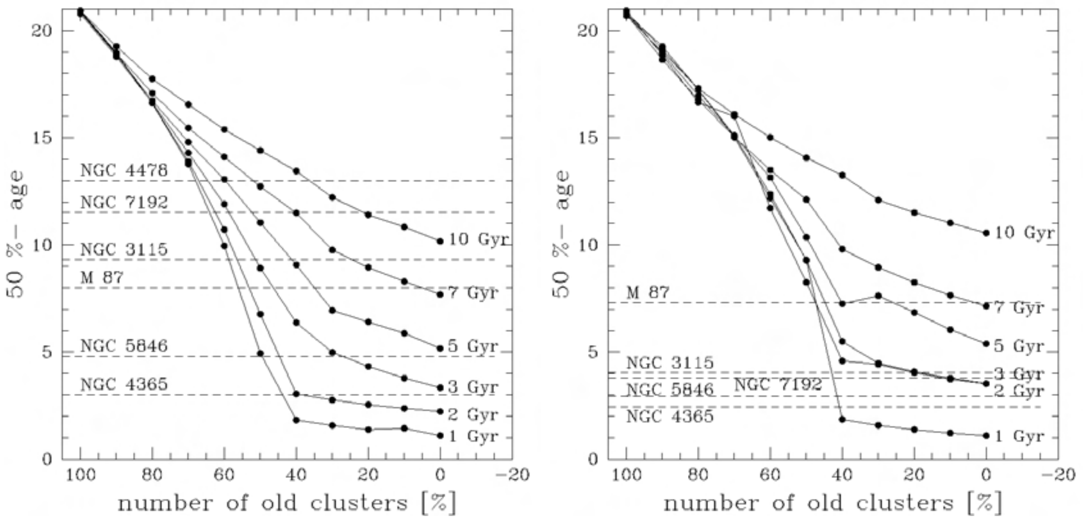

Fig. 2.15.— We compare the 50%-age calculated by a best fit of the cumulative age distribution for observed and simulated systems using BC00 (left) and VA99 (right) SSP model isochrones. The x-axis gives the amount of 15 Gyr old objects within the model and the label on the right hand side the age of the intermediate age sub-population. The larger spread in $(V-I)$ for VA99 isochrones results in a less reliable result for smaller samples. All systems have been corrected for background contamination.

our target systems in section 2.6. For NGC 4365 (Fig. 2.17, lower panels) we derive a mixture of 15 Gyr and 1-3 Gyr old objects with a higher content of intermediate age objects. The age range is in agreement with the spectroscopic results given by Larsen et al.(2003). Both observed cluster samples are relatively rich ($N_{NGC\ 5846}$ and $N_{NGC\ 4365}$ are in the range of 190) and the correction effect is relatively weak and, taking the stability tests into account as well (see section2.4.2), stable.

As mentioned in Sect. 2.1 the simulations are based on the assumption of the old population which is 15 Gyr old. We present one example to illustrate how the results will change in case of a 10 Gyr *old* population (see Fig. 2.18). Although the relative size of both populations change considerably, as we would expect, the detection of a intermediate age population is confirmed and the relative ages of both populations does not change significantly. Moving from 15 to 10 Gyr, besides being driven by real physical arguments, also illustrates how our results would change if the SSP models are not perfectly calibrated.

2.5.2 M87 and NGC 7192

With respect to the formation scenario for early-type galaxies we are interested in the environmental effect. Therefore our galaxy sample includes also cD galaxies (M87) and rather isolated

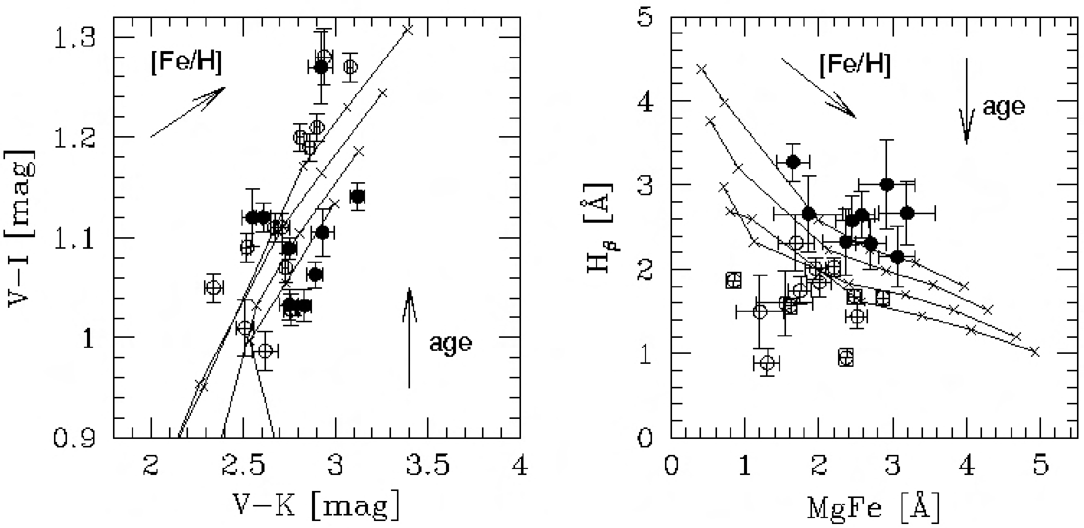

Fig. 2.16.— Left panel: Color-color diagram for globular clusters in 4 different galaxies. The model grid follows the Maraston (2001) SSP model isochrones (ages between 3 and 15 Gyr following the age- arrow). The metallicity ([Fe/H] between -2.25 and +0.35) increases in direction of the metallicity arrow. Right panel: Comparison of index measurements with the models by Thomas et al.2003 (age range: 3- 15 Gyr, metallicity range: -2.25- +0.67). Objects with spectroscopic ages below 5 Gyr are shown by solid circles.

galaxies (NGC 7192). In both types of globular cluster systems one wouldn't expect a second, younger globular cluster population (for M87 see Jordán et al. 2002). This expectation is only met by the 50%-age derived for M87. Using the Bruzual & Charlot model we estimate a 50%- age of 8 Gyr and for VA99 ~7 Gyr, both values being more consistent with models containing only a small population of somewhat younger objects. The fact that this result could not be confirmed by the χ^2-test (see Fig. 2.19) led us back to the problem of small sample sizes. As soon as we include the size of both globular cluster systems, 35 found for M87 and 39 for NGC 7192 respectively, this inconsistency can be explained. Both systems are still not numerous enough to allow a meaningful analysis.

2.6 Discussion and conclusions

In this paper we described our method of relative age dating in globular cluster systems using integrated photometry and constrain its suitability. The main emphasis is not the determination of ages with only small uncertainties, as it has been done in various papers by using spectroscopy for integrated light or globular clusters (e.g. Trager et al. 1998; Kuntschner 2000; Poggianti et al. 2001; Moore et al. 2002; Puzia et al. 2003), but to introduce a method to identify different age populations in large systems and to evaluate the importance of the underlying star formation

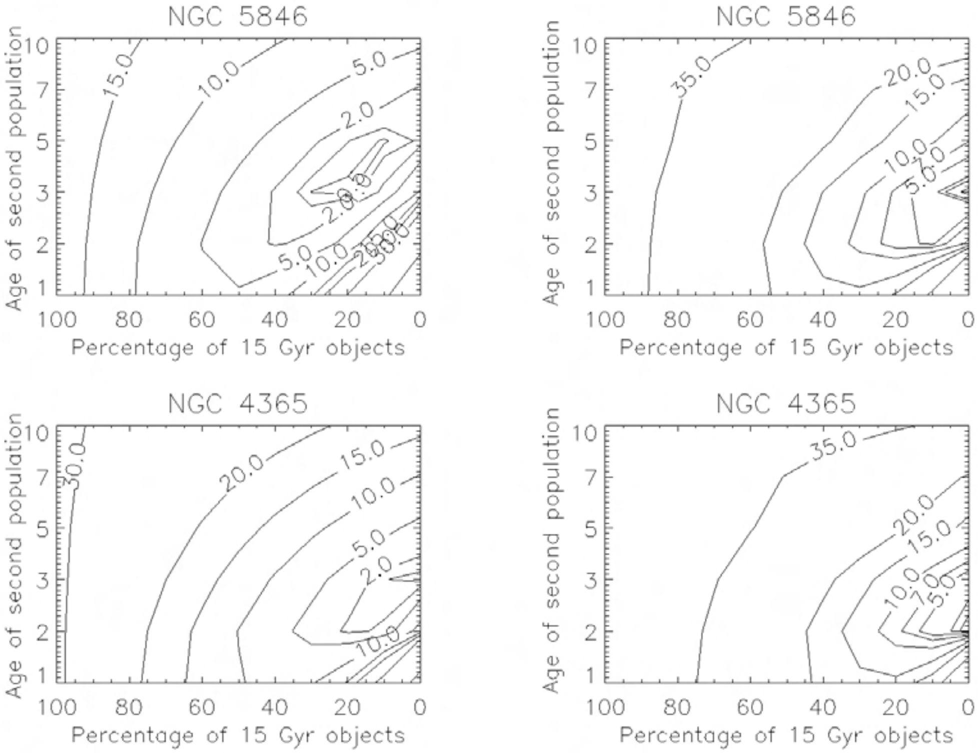

Fig. 2.17.— χ^2-test result for NGC 5846 (upper) and NGC 4365 (lower). The different levels represent the reduced χ^2 of the comparison between the age distribution in the observed systems and the various models. The correction for contamination following the procedure given in section 2.4.1 has been applied.The left panels give the result following the BC00 models and the right panels following the VA99 models.

events. From the results presented here we conclude that for large globular cluster sets integrated photometry is a suitable tool to search for sub-populations of globular clusters. The size of the young population appears excessively large when compared to the maximum allowed young population in the integrated light of these galaxies. Based on the fact that we study all globular cluster systems in the center of galaxies and assuming that intermediate clusters, formed during merger, settle down in the new center of gravity, our data will be biased toward these intermediate age objects. More observations, covering regions more distant to the center of the host galaxies are necessary to overcome this bias effect. Yet, the bias alone is unlikely to explain the fraction >80% found in NGC 5846 and NGC 4365. Our example in Sect. 2.5.1, using an age of 10 Gyr for the old population, resulting in fractions close to 40% of young clusters, illustrates how the method is sensitive to this choice and/or proper SSP calibration. We conclude that our idealized SSP models probably still host uncertainties, especially do not take into account anything but age and metallicity, e.g. α/Fe varying abundance ratios etc. might play a role and introduce additional scatter or systematic error in the old population, driving our results to an interpretation of overly large young populations.

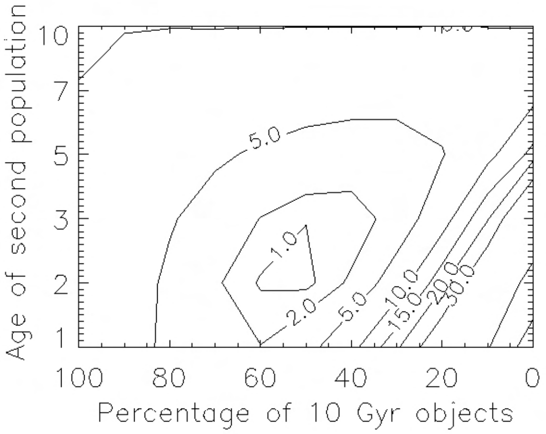

Fig. 2.18.— Result of the χ^2-test comparing the age distribution in NGC 5846 with simulated systems assuming the *old* population being 10 Gyr old. As clearly seen the best fitting model still contains a much smaller, but still significant number of intermediate age objects.

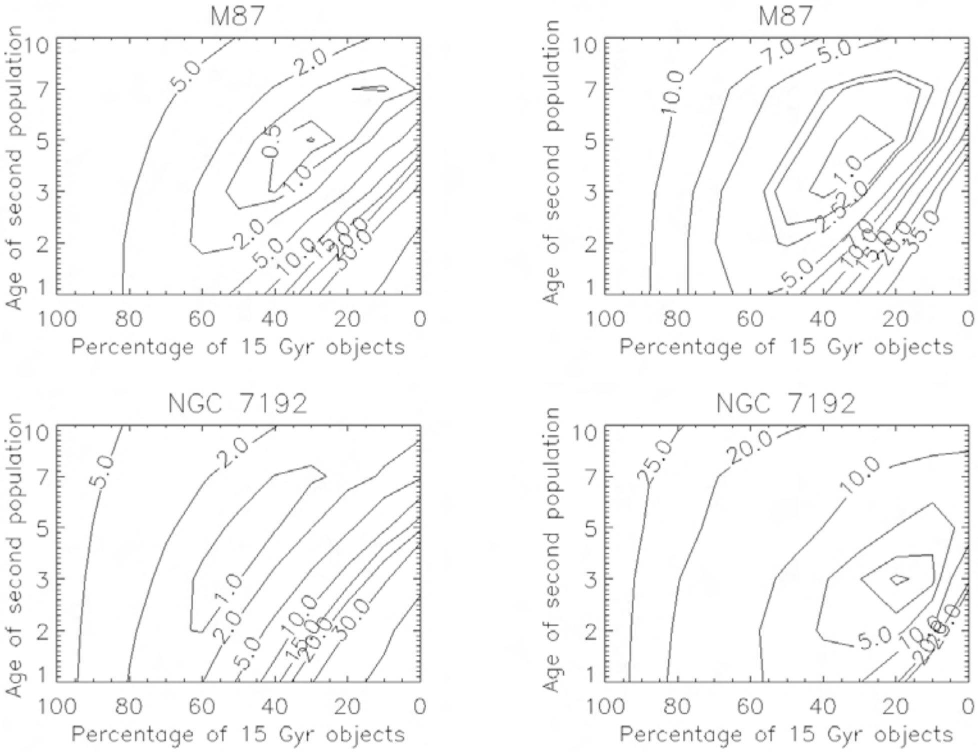

Fig. 2.19.— χ^2-test result for M87 (upper) and NGC 7192 (lower). As in Fig. 2.17 the results for BC00 (left panels) and VA99 (right panels) are shown.

These effects will be investigated in the future together with modelers. In particular the effect of α/Fe enhancement, as now incorporated into the models by C. Maraston & D. Thomas (Thomas et al. 2003; Maraston et al. 2003). Together with a modified calculation of the secondary color (see Sect.2.2.5) these are the next step for improving our approach. For now the method is able to detect intermediate age populations, roughly constrain their age but most probably overestimates their importance. To lower the age uncertainty in the color-color distributions the observations will be extended into the blue wavelength region, e.g. by including the U-band. As shown in Fig. 2.20 $(U-I)$ $vs.(V-K)$ color-color diagrams will result in a considerably larger age resolution.

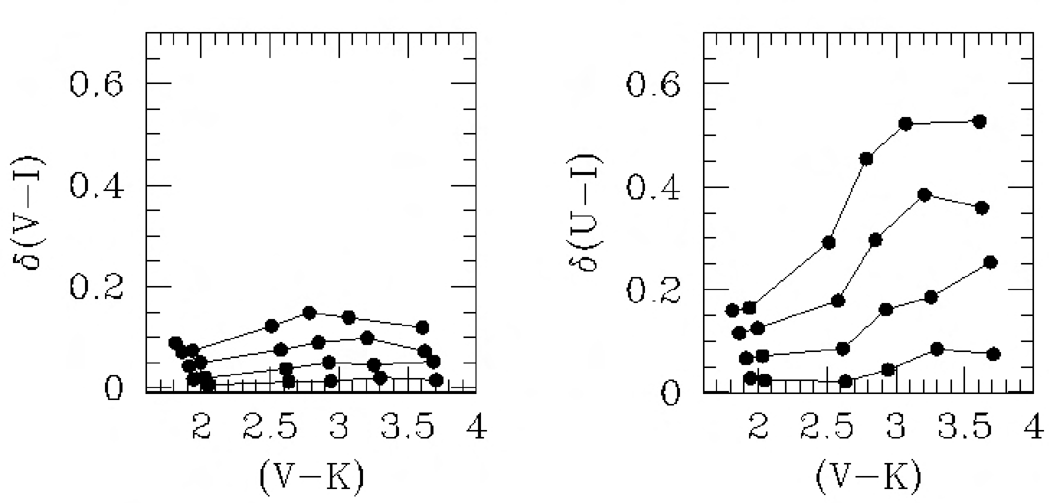

Fig. 2.20.— Age resolution for SSP model isochrones by Bruzual & Charlot (Bruzual & Charlot 2000) in $(V-I)vs.(V-K)$ (left panel) and $(U-I)vs.(V-K)$ (right panel) color-color diagrams. The age splitting in $(U-I)vs.(V-K)$ plots is increased by a factor of 2 and will therefore result in a better age resolution. For direct comparison we chose an uniform scaling for both plots. The difference in $(V-I)$ and $(U-I)$, respectively, between a 15 Gyr model isochrone and the one for 13, 10, 7, and 5 Gyr (from bottom to top) is shown here.

Acknowledgments The authors would like to thank the referee, A. Vazdekis for a careful review and many helpful remarks.

References

Ashman, K.M., Zepf, S.E. 1992, ApJ, 384, 50

Ashman, K.M., Bird, C.M., Zepf, S.E. 1994, AJ, 108, 2348

Bennett, C.L., Halpern, M., Hinshaw, G. et al. 2003, ApJ, accepted

Bertin, E., Arnout, S. 1996, A&AS, 117, 393B

Brodie, J.P. 2002, IAU Symposium Series, 207, 218

Bruzual, G.A. & Charlot, S. 1993, ApJ, 405, 538

Bruzual, G.A. & Charlot, S. 2000, private communication

Bruzual, G.A. & Charlot, S. 2003, MNRAS, 344, 1000

Burgarella, D., Kissler-Patig, M., Buat, V. 2001, AJ, 121,2647

Charlot, S., Bruzual, G.A. 1991, ApJ, 367, 126

Charlot, S., Worthey, G., Bressan, A. 1996, AJ, 457, 625

de Grijs, R., Bastian, N., & Lamers, H.J.G.L.M. 2003, ApJ, 583, L17

Elmegreen, B.G., Efremov, Y.N. 1997, ApJ, 480, 235

Forbes, D.A., Brodie, J.P., Grillmair, C.J. 1997, AJ, 113, 1652

Forbes, D.A., Forte, J.C. 2001, MNRAS, 322,257

Gebhardt, K.& Kissler-Patig, M. 1999, AJ, 118, 1526

Geisler, D., Grebel, E.K., Minniti, D. (eds.) 2002, "Extragalactic Star Clusters", IAU Symposium, 207

Goudfrooij, P., Alonso, M.V., Maraston, C. et al. 2001, MNRAS, 328, 237

Harris, W.E. 1991, ARAA, 29, 543

Harris, W.E. 2003, "Extragalactic Globular Cluster Systems", Springer Verlag, ed. Kissler-Patig, M, ESO Astrophysics Symposia, 317

Hempel, M., Hilker, M., Kissler-Patig et al. 2003, A&A, 405, 487 (Paper III)

Infante, L. & Pritchet, C.J. 1995, AJ, 439, 565

Jordán, A., Côté, P., West, M.J. et al. 2002, ApJ, 576, L113

Kennicutt, R.C. 1998, in "Galaxies:Interactions and Induced Star Formation", eds. Friedli, Martinet, Pfenniger, Springer Verlag

Kissler-Patig, M. 2000, RvMA,13,13

Kissler-Patig, M., Brodie, P. B., & Minniti, D. 2002, A&A, 391, 441 (Paper I)

Kissler-Patig, M.(ed.) 2003, "Extragalactic Globular Cluster Systems", Springer Verlag Berlin

Kundu, A., Whitmore, B.C. 2001, AJ, 121,2950

Kundu, A., Whitmore, B.C. 2001, AJ, 122,1251

Kuntschner, H. 2000, MNRAS, 315,184

Kurucz, R.L. 1992, IAU Symp.149, 225

Larsen, S. 2001, IAU Symposium Series, 207

Larsen, S., Brodie, J.P., Beasley, M.A. et al. 2003, ApJ, 585, 767)

Lejeune, Th.; Cuisinier, F.; Buser, R. 1997, A&AS, 125, 229L

Maller, A.H., McIntosh, D.H., Katz, N. et al., 2003, ApJ, submitted (astro-ph/0304005)

Maratson, C., Greggio, L., Thomas, D. 2001, Ap&SS, 276, 893

Maraston, C., Greggio, L., Renzini, A. et al., 2003, A&A, 400, 823

Moore, S.A.W., Lucey, J.R., Kuntschner, H. et al. 2002,MNRAS, 336, 382

Poggianti, B.M, Bridges, T., Carter, D. et al. 2001, AJ, 563,118

Press, W.E., Teukolsky, S.A., Vetterling, W.T. et al. 1992, "Numerical Recipes in Fortran", Cambridge University Press

Puzia, T.H.,Kissler-Patig, M., Brodie, J.P. et al. 1999, AJ, 118, 2743

Puzia, T. H., Zepf, S. E., Kissler-Patig et al. 2002, A&A, 391, 453 (Paper II)

Puzia, T.H., Kissler-Patig, M., Thomas, D. et al. A&A, in prep.

Renzini, A. 1999, in "The formation of galactic Bulges", eds. Carollo, Ferguson & Wyne, Cambridge University Press

Renzini, A., Cimatti, A. 1999, ASP Conference Proceedings, 193, 312

Roche, N., Shanks, T., Metcalf, N. et al., 1993, MNRAS, 263, 360

Schweizer, F., Miller, B.W., Whitmore, B.C. et al. 1996, AJ, 112, 1839

Schweizer, F. 2000, Phil. Trans. R. Soc. Lond., Ser. A, 358,2063

Thomas, D., Maraston, C.,& Bender, R., 2003, MNRAS, 339, 897

Tinsley, B.M. 1972, ApJ, 179, 319

Toomre, A., in The Evolution of Galaxies and Stellar Populations, ed. V.Trimble and R.B.Larson, 1977, 401

Trager, S.C., Worthey, G., Faber, S.M. 1998, ApJS, 116,1

Trager, S.C., in Carnegie Observatories Astrophysics Series, 2003, 4, Cambridge University Press

Vazdekis, A., Casuso, E., Peletier, R.F. et al., 1996, ApJS, 106, 307

Vazdekis, A. 1999, ApJ, 513, 224

Worthey, G. 1994, ApJS, 95, 107

3 Extragalactic Globular Clusters in the Near Infrared: III. NGC 5846 and NGC 7192 Quantifying the age distribution of sub-populations

Astronomy & Astrophysics, 2003, 405, 487

Maren Hempel, Michael Hilker, Markus Kissler-Patig, Thomas H. Puzia, Dante Minniti,
Paul Goudfrooij

Abstract

In this third paper of our series on near-IR and optical photometry of globular cluster systems in early-type galaxies we concentrate on the photometric results for NGC 5846 and NGC 7192, two group ellipticals, and on a first comparison between the globular cluster systems investigated so far. In NGC 5846 the color-color diagram shows clear bi-modality in $(V-K)$, which is confirmed by a KMM test. The mean color of both peaks were estimated to be $(V-K)_{\mathrm{blue}}=2.57\pm0.06$ and $(V-K)_{\mathrm{red}}=3.18\pm0.06$. The situation in NGC 7192 is different, in that the color-color diagram gives no evidence for a distinct second population of globular clusters. Using simulated color distributions of globular cluster systems, we make a first step in quantifying the cumulative age distribution in globular cluster systems. Also here the result for NGC 5846 leads us to the conclusion that its metal-rich globular cluster population contains two globular cluster populations which differ in age by several Gyr. The age structure for NGC 7192 shows instead strong similarity with a single-age population.

Keywords: Galaxies: star clusters, Galaxies: individual (NGC 5846, NGC 7192)

3.1 Introduction

As shown by many studies during the last decade (Zepf & Ashman 1993; Ashman & Zepf 1998; Kundu & Whitmore 2001a; b; Larsen et al. 2001; Kissler-Patig et al. 2002) globular cluster systems are a very powerful tool in galaxy formation and evolution studies. Although there is a wide agreement about the existence of sub-populations in cluster systems regarding their metallicity and their age, the discussion about the origin of those populations is still ongoing. Starting with Peebles & Dicke (1968) who assumed globular clusters to be the first objects formed in the early universe, the number of possible formation scenarios increased drastically since then. One of the main issues is to explain the multi-modality found in color-color diagrams of globular cluster systems. In general it is agreed that different globular cluster populations are produced during strong star formation events, but the nature of these events remains under debate. Besides the merger scenario, favoured by Ashman & Zepf (1993) (see also Ashman & Zepf 1992; Whitmore et al. 1993; Whitmore & Schweizer 1995; Schweizer et al. 1996; Kissler-Patig 2000), there is a number of alternatives, i.e. the accretion scenario (Côté et al. 1998; Côté et al. 2002; Hilker et al. 1999) or the monolithic collapse (Forbes et al. 1997a; Kissler-Patig et al. 1998, and references therein). From the photometric point of view it has been shown that the multi-modality of the color distribution is a common feature of globular cluster systems (Gebhardt & Kissler-Patig 1999). In particular, the existence of a blue, old and metal-poor cluster population (Ashman & Bird 1993; Burgarella et al. 2001) is a general feature. Regarding the red sub-population the almost only consensus which has been reached so far, is about the large varieties between different cluster systems. This includes the possible existence of sub-populations within the red population which is interpreted as a sign of different star formation events in later stages of the galaxy evolution.

The main problem in specifying and dating different star formation events arises from the age-metallicity degeneracy of the most commonly used optical colors. So far the bulk of high-quality photometric investigations have been performed using *Hubble Space Telescope (HST)* in the optical wavelength regime (Forbes et al. 1998; Kundu & Whitmore 1998; Gebhardt & Kissler-Patig 1999; Larsen et al. 2001). It has been shown (Minniti et al. 1996; Kissler-Patig 2000; Kissler-Patig et al. 2002 (hereafter cited as Paper I), Puzia et al. 2002 (hereafter Paper II)) that combining optical and near-infrared data is a more promising method to separate age and metallicity effects and to access the relative ages of the globular cluster populations. The method relies on a sampling effect, where the V-band is dominated by stars near the turn-off (TO) region, whereas the main contribution to the K-band is from giant branch stars (Yi et al. 2001). Whereas the TO is dominated by age effects, the giant branch shows a high sensitivity to metallicity (Saviane et al. 2000). This results in a similar dependence of $(V-I)$ and $(V-K)$ on the age of the clusters, but a higher sensitivity of $(V-K)$ to the metallicity.

In the previous two papers of this series (Papers I and II), a systematic survey of globular cluster systems of E and S0 galaxies in the combined optical and near-infrared wavelength range (using the V, I, and K_s bands) has been started. In Paper I, we compared the globular cluster systems of two ellipticals in the Virgo cluster, namely the giant central galaxy M87 and an intermediate-luminosity galaxy NGC 4478. We found that in those cases, the $(V-K)$ color distribution yielded roughly consistent conclusions relative to those derived from the $(V-I)$ colors measured by *HST*. In Paper II however, the $(V-K)$ colors of globular clusters in NGC 4365 led us to postulate the existence of a significant population of intermediate-age (∼ 2-6 Gyr old), metal-rich globular clusters, which was not revealed by the $(V-I)$ colors. This important result has recently been confirmed by deep spectroscopy (Larsen et al. 2003), adding credibility to the results derived from our optical + near-infrared imaging program.

One of the aims of this series is to study the the globular cluster systems of galaxies in different environments, e.g. giant ellipticals in centers of clusters as well as rather isolated and less luminous galaxies. The present work will focus on NGC 5846, a giant E0 galaxy in the center of the Virgo-Libra Cloud, and on NGC 7192, an isolated elliptical with only one companion. Basic informations on both galaxies are provided in Table 1.

Both systems have already been studied in the optical (Forbes et al. 1997b; Gebhardt & Kissler-Patig 1999), and show a very broad $(V-I)$ color distribution. This work aims at the detection of different globular cluster sub-populations, the determination of their age structure and a first comparison of various globular cluster systems. The present paper is organised as follows. In §2 the observations and the data reduction procedures are described. Chapter 3 contains the main results of the observations and §4 describes our approach towards quantifying the age structure in globular cluster systems and the results for both systems. In chapter 5 we will give an outlook on the upcoming work.

Table 3.1: General information about the host galaxies NGC 5846 and NGC 7192. The references are (1): de Vaucouleurs et al. 1991, (2): Schlegel et al. 1998, (3): Buta & Williams 1995, (4): Frogel et al. 1978, (5): Tonry et al. 2001

Property	NGC5846	NGC 7192	Reference
RA(J2000)	15h 06m 29s	22h 06m 50s	(1)
DEC(J2000)	+01° 36' 25"	−64° 18' 57"	(1)
$B_{\mathrm{T},0}$	10.87	12.19	(1)
E_{B-V}	0.055	0.034	(2)
$(B-V)_{\mathrm{o}}$	0.96	0.92	(1)
$(V-I)_{\mathrm{eff,o}}$	1.28±0.01	1.24±0.01	(3)
$(V-K)_{\mathrm{eff,o}}$	3.51±0.01		(4)
$(m-M)_V$	31.98±0.20	32.89±0.32	(5)
M_V	-22.07 ± 0.20	-21.62 ± 0.35	(1),(5)

3.2 Observations and Data Reduction

3.2.1 VLT/ISAAC Near–Infrared Data

The $K_{\rm s}$ band exposures for both galaxies have been taken in service mode (ESO program 63.N–0287) with the Near-Infrared Spectrometer And Array Camera (ISAAC) attached to the Unit Telescope 1 (Antu) of the European Southern Observatory's Very Large Telescope (VLT). The field-of-view of ISAAC's Rockwell infrared array is $2.5' \times 2.5'$, with a pixel scale of $0.147''$/pixel. All data were obtained in April and June 1999 in different nights under varying photometric and seeing conditions. Standard star observations revealed that the conditions were not photometric during all nights and an adjustment (described below) was necessary to align all nights onto a photometric system. As in Papers I and II we will always refer to the K_s filter as K.

The NGC 5846 data were obtained during the nights of April 6th, 8th, and 9th 1999 while the NGC 7192 data were taken during the nights of June 1st, 2nd, 21st, and 22nd. The observing strategy for NGC 5846 data was the following: 10×10sec object + 5x(2x10sec) sky + 10x10sec object. The one for NGC 7192: 10×10sec object + 2x(6x10sec) sky + 10x10sec object. The monitoring of the seeing, magnitude variations, sky level and geometric correction was done by measuring the parameters of four isolated stars in each single frame for both galaxies. A detailed description of the sky subtraction and combination procedure of the K band data is given in Puzia et al. (2002).

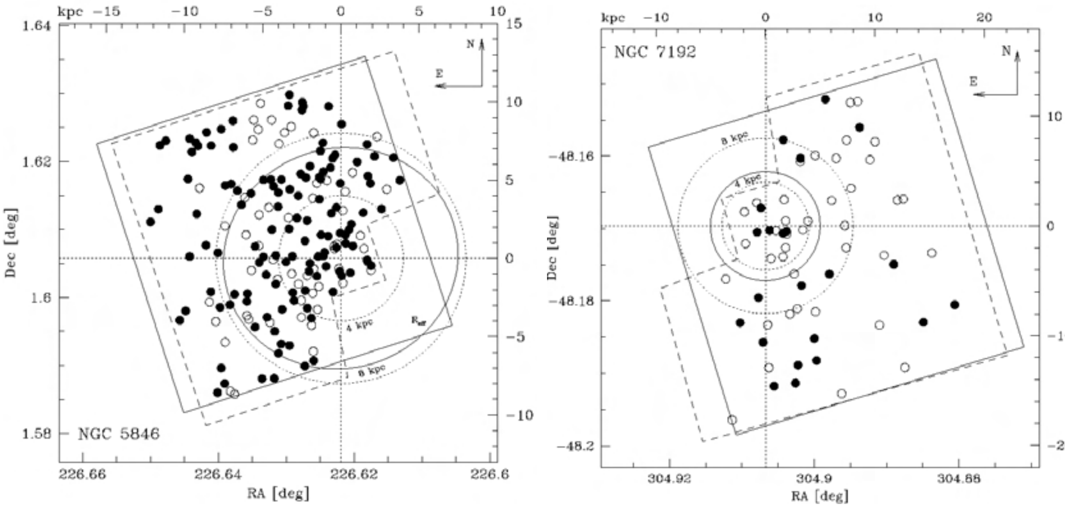

Fig. 3.1.— Field of view of NGC 5846 (left) and NGC 7192 (right). The ISAAC field was chosen to fit the available archive data taken with WFPC2 on board the HST. The dashed lines in both frames indicate the HST field and the solid one the corresponding ISAAC image. Dotted circles show the 4 and 8 kpc distance to the galactic centers, the solid circles the half light radii of the galaxy's light. The globular cluster samples were divided in two color sub-populations. Dots mark objects with $0.8 \leq (V-I) \leq 1.2$ and open circles represent clusters in the range $1.2 < (V-I) \leq 1.5$.

The FWHM of the stellar PSF in the final K-band image is $\sim 0.4''$ for NGC 5846 and $\sim 0.5''$ for NGC 7192. The total exposure times for NGC 5846 and NGC 7192 are 10000 sec, and 12000 sec, respectively.

3.2.1.1 Photometry

The photometric calibration of the NGC 5846 and NGC 7192 data set was based on the photometry of 3 and 4 near-IR standard stars, respectively (Persson et al. 1998).

Measuring the instrumental magnitudes in an aperture of 6 pixel diameter and applying the same analysis as described in Puzia et al. (2002), the following calibration relations for the photometric nights have been derived

$$\begin{aligned} K_{5846} &= k_{\mathrm{inst}} + 23.81(\pm 0.018) - 0.05(\pm 0.009)\chi \qquad (3.5) \\ K_{7192} &= k_{\mathrm{inst}} + 23.83(\pm 0.010) - 0.05(\pm 0.007)\chi \qquad (3.6) \end{aligned}$$

where K_{galaxy} is the calibrated magnitude, k_{inst} is the instrumental magnitude, and χ the effective airmass (= 1.23 for NGC 5846 and 1.34 for NGC 7192). The error of the zero points (second term in eq.(1) and (2)) includes photometric errors of each single standard star measurement and the errors of the aperture correction analysis. The error of the airmass term is an estimate from the variations in airmass of all single exposures.

The zero point shifts of the non-photometric nights to photometric conditions has been derived by tracing the magnitudes of four isolated stars over all nights. The final photometry was performed on the overall combined image. For NGC 7192 it was first done on two combined images separately. One for the photometric nights (June 1st and 2nd), and one for the non-photometric nights (June 21st and 22nd). The magnitudes of both images have been averaged after a zero point correction of the latter. The true photometric uncertainty, measured by the scatter of the single measurements is of the order of ≤ 0.04 mag, mainly due to the strongly varying sky background.

Finally, all magnitudes were corrected for Galactic foreground reddening using the reddening values of Table 1 and the extinction curves of Cardelli et al. (1989). The corrections for NGC 5846 and NGC 7192 are $A_K = 0.020$ mag and $A_K = 0.012$ mag.

3.2.2 HST/WFPC2 Optical Data

The HST data were taken from the public HST archive. NGC 5846 was observed with HST + WFPC2 under program GO.5920. The total exposure times of the combined images are 6600 sec in F555W, and 6900 sec in F814W. NGC 7192 has been imaged with WFPC2 under program GO.5943 in F555W and F814W filters with 1300 sec and 1000 sec of total exposure time, respectively. The HST images were reduced and calibrated following the procedure as described in Puzia et al. (1999, 2002). All magnitudes were measured with the SExtractor tool using a 8 and 4-pixel-diameter aperture for the PC and WF chip and corrected with respect to the Holtzman $0.5''$ standard aperture (Holtzman et al. 1995). Instrumental magnitudes were then transformed to the Johnson V and I magnitudes according to the prescription given by Holtzman et al. (1995). All magnitudes were reddening corrected using the following values: $A_V = 0.182$ and $A_I = 0.107$ for NGC 5846 and $A_V = 0.113$ and $A_I = 0.066$ for NGC 7192 (see E_{B-V} in Table 1).

3.2.3 Selection criteria

After combining the optical and near-infrared data using the GEOMAP task within IRAF, the globular cluster sample includes 184 and 61 objects for NGC 5846 and NGC 7192, respectively. Figure 3.1 shows the field of view for both galaxies and the spatial distribution of the cluster candidates. In order to limit the contamination of the sample by background galaxies or foreground stars and to set a limit onto the photometric error, general selection criteria have been applied. In our discussion only objects with an photometric error $\Delta(V-I) \leq 0.1$ mag and $\Delta(V-K) \leq 0.1$ mag and a FWHM of the PSF below $0.25''$ in the V and I-band are considered.

3.3 Color-color diagrams for NGC 5846 and NGC 7192

Color-color diagrams together with various SSP models (e.g. in this paper by Bruzual & Charlot 2000) are the basis for age and metallicity estimates. Different models, at identical colors, can show differences in *absolute* age of about 3 Gyr. Thus, the SSP approach can only lead to approximate *absolute* ages for the sub-populations. However, *relative* ages can be estimated accurately enough to separate sub-populations built up during major star formation events.

As shown in Puzia et al.(2002), the various models differ mainly in the metal-rich range (approx. [Fe/H]> -0.8). A detailed comparison between the different models in an absolute sense can be found in Maraston et al. (2001a). The metal-rich regime, however, is exactly the one we intend to probe, given that the intermediate-age populations are expected to be enriched in metals.

As opposed to the situation for absolute ages, the *relative* age predictions for given colors are relatively similar from model to model. Since we focus on the *relative* age dating of globular cluster systems the choice of a specific model is not crucial and we use the model of Bruzual & Charlot (2000) throughout the following analysis.

As we will show in the following two subsections the results of the KMM test (McLachlan & Basford 1988, updated version 2001) and the derived metallicities are found to differ significantly from expected values and even seem to be in contradiction to what visual inspection of the color-color diagrams tells us. Considering the relatively small sample size, the photometric errors in $(V-K)$ and the limited depth of the observations (shifting the peak position toward red colors) the results of the KMM test, as described by McLachlan & Basford (1988), have to be discussed with much caution. Since this work concentrates on relative ages at this stage we will only mention the results of the KMM and leave the discussion for later.

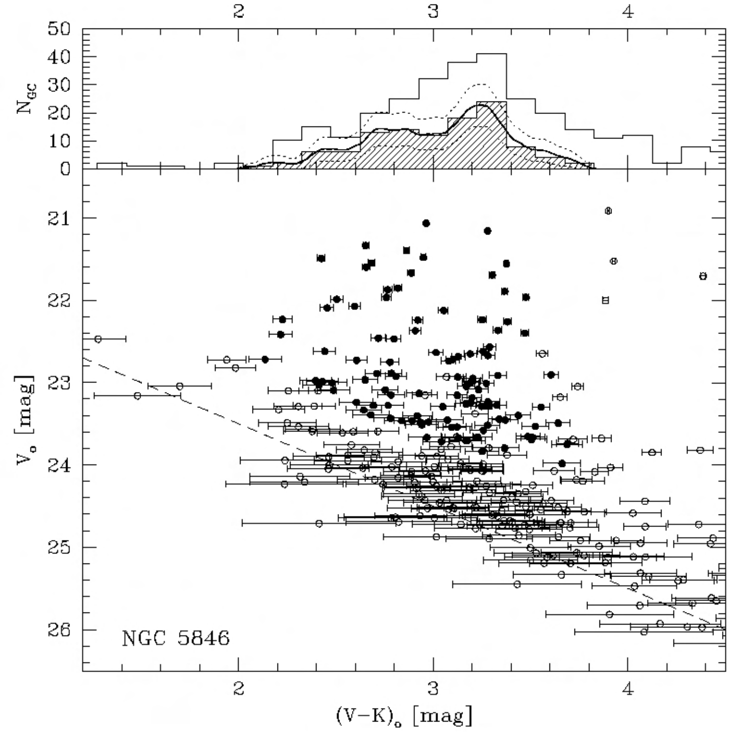

Fig. 3.2.— V vs. $(V-K)$ color-magnitude diagram for NGC 5846. The top sub-panel shows the color distribution of all (open histogram) and selected (hashed histogram) objects. The solid line marks the probability density distribution together with its 1σ uncertainty (dotted line). The lower sub-panel shows the CMD. Here the filled symbols mark the selected clusters while open circles indicate rejected objects (see Section 3.2.3). Since the photometric errors are dominated by the K-band, only the $(V-K)$ errors are shown. The dashed line marks the limiting magnitude in the K-band ($K = 21.5$ mag).

3.3.1 NGC 5846

The color-magnitude diagram (hereafter CMD) and the color-color diagrams for NGC 5846 are given in Figures 3.2 and 3.3. The histogram in the upper part of the CMD shows the complete set of clusters as a solid histogram whereas the selected objects, following the selection criteria given in Section 3.2.3, are shown by the hatched histogram. As expected the selection criteria affect mostly the objects in the very red color range, since the photometric errors are larger and background galaxies possibly contaminate the sample.

The CMD (Fig. 3.2) reveals evidence for the a bimodal color distribution. The KMM test as described by Ashman et al. (1994) confirms this result with a confidence level of ∼90% for a bimodal color distribution. We obtain peak positions of $(V-K)_{\rm blue} = 2.57\pm0.06$ and $(V-K)_{\rm red} = 3.18\pm0.06$ for both color populations with an estimate of correct allocation value (confidence level) of 0.79 and 0.94 for the blue and the red peak, respectively. Hereby about 30% of the globular clusters were assigned to the blue population and 70% to the red. Using the calibration by Kissler-Patig (Paper I) for old populations, this corresponds to a metallicity of $[\rm Fe/H]=-0.54\pm0.6$ dex and 0.27 ± 0.4 dex for the metal-poor and the metal-rich populations, respectively.

Note that our completeness limit is dominated by the K-band, and that we are biased in favour of red clusters (Paper II, see Fig. 3.2). Thus, both the ratio of the numbers of red to blue clusters and the metallicity of the blue peak are overestimates.

It is interesting to mention that no multi-modality could be found in the $V-I$ color distribution. This is similar to the situation in NGC 4365 where the intermediate-age population,

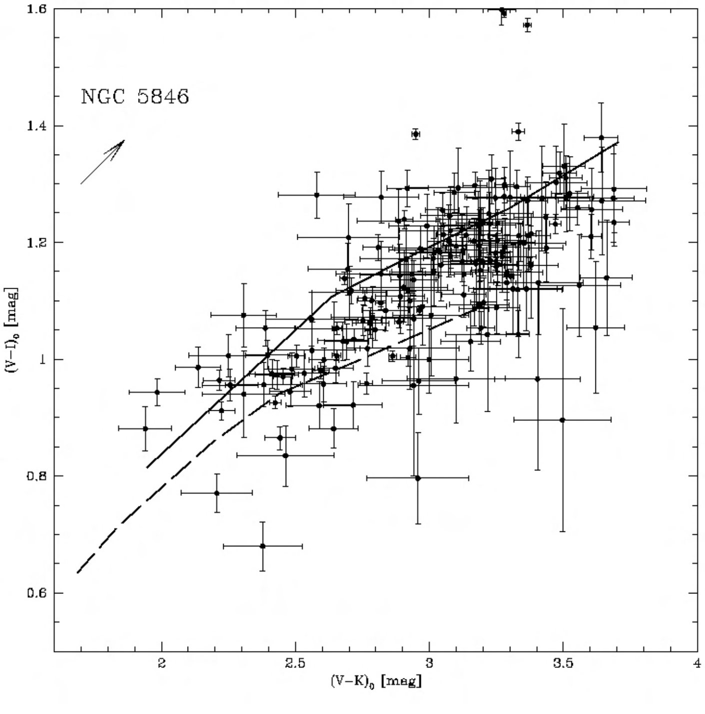

Fig. 3.3.— $(V-I)$ vs. $(V-K)$ color-color diagram for NGC 5846. All data are corrected for Galactic foreground reddening. The reddening vector is marked by the arrow. As example the 15 Gyr and 2 Gyr isochrones (Bruzual & Charlot 2000) are marked by a solid and dashed line, respectively. As for NGC 4365 (Puzia et al. 2002) we find a second population of objects which are red in $(V-K)$ but intermediate in $(V-I)$ with $(V-I)\in[1.0,1.2]$, and thus are clearly not compatible with old SSPs.

when projected on the $V-I$ axis, fills the gap between the two old (metal-rich and metal-poor) sub-populations. When forced to bimodality, the $(V-I)$ peak positions determined by the KMM test are $(V-I)_{\rm blue} = 1.11$ and $(V-I)_{\rm red} = 1.13 \pm 0.02$. This is in agreement with the results by Gebhardt & Kissler-Patig (1999).

3.3.2 NGC 7192

Referring to the CMD and the color-color diagram for NGC 7192 given in Figure 3.4 and Figure 3.5, the difference to the globular cluster system of NGC 5846 can be seen: while NGC 5846 exhibits a strong spread perpendicular to the isochrones, NGC 7192 is more homogeneously populated along the isochrone.

The small number of objects do not allow one to draw strong conclusions from the KMM test in terms of the existence of color bimodality. The color-color plot for NGC 7192 does suggest the existence of two populations of different metallicity (i.e., a 'metal-poor' population with $(V-I) < 1.1$ and $(V-K) < 2.8$ and a 'metal-rich' population with $(V-I) > 1.0$ and $(V-K) > 2.8$) but the small number statistics do not allow one to support this firmly statistically.

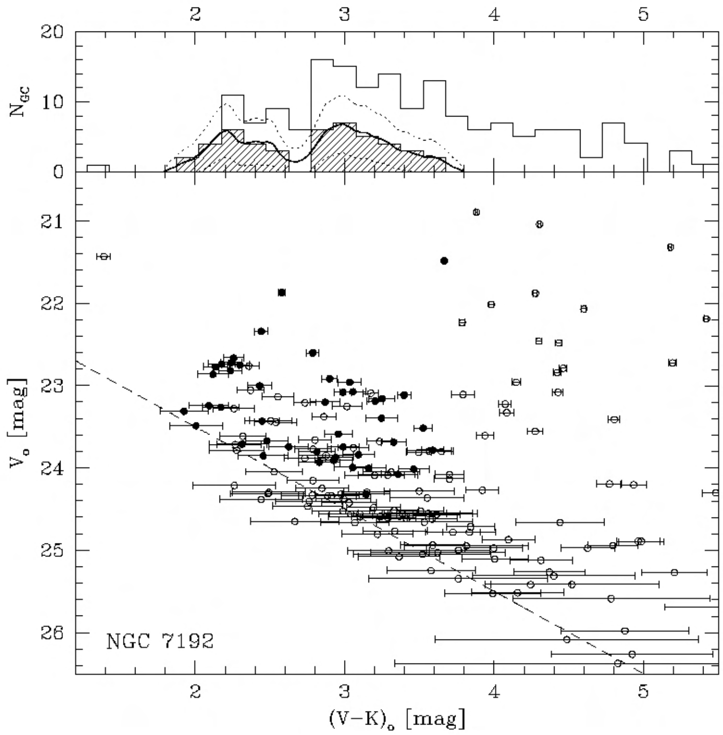

Fig. 3.4.— V vs. $(V-K)$ color magnitude diagram for NGC 7192. (panels and symbols as in Fig. 3.2).

Formally, the color for the two peaks of the distribution projected on the $V-K$ axis is returned by KMM to be $(V-K)=2.83$ and 2.89 (with 90% of the objects assigned to the first peak), if a bimodal distribution is assumed. Since the difference in color between the two peaks is well below the photometric error it seems far-fetched to assume the existence of two distinct globular cluster sub-populations.

Therefore we assume that the NGC 7192 globular cluster system consists only of one dominant population. Following the calibration values by Kissler-Patig (Paper I) we derive a peak metallicity of $[\mathrm{Fe/H}]=-0.57\pm0.37$.

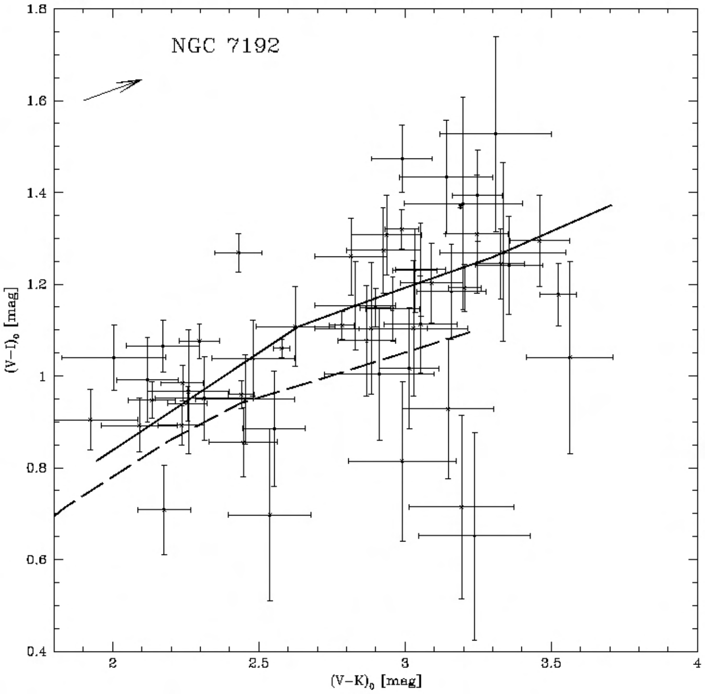

Fig. 3.5.— Color-color diagram for NGC 7192. No clear indication for a second red sub-population can be found (isochrones as in Fig.3.3).

3.4 Determining the age structure from color-color diagrams

3.4.1 Color distributions

The basic idea in using optical and near-infrared photometry in globular cluster studies is to lift the age – metallicity degeneracy and to resolve possible age sub-populations of globular clusters. The minor drawback with respect to using optical colors alone is an increased photometric error mainly caused by the infrared observations, i.e., in the K-band. This, however, is more than compensated for by the larger diagnostic power of the optical – near-infrared combination (see Papers I and II). A separation in the color-color plot of sub-populations with different metallicities becomes easier, and a separation in age at a given metallicity becomes feasible.

Table 3.2: Fit parameter for model isochrones (Bruzual & Charlot 2000) for a logarithmic fit $(V-I)=$ A$\cdot$log$(V-K)$+B.

Isochrone [Gyr]	1	2	3	5	7	10	13	15
A	0.5645	0.7136	0.7674	0.7795	0.7922	0.8134	0.8423	0.8573
B	0.3296	0.2809	0.2633	0.2765	0.2826	0.2766	0.2596	0.2502

We investigate below what the diagnostic power of the method is in terms of separating sub-populations of different ages. To do so, we investigated artificial color-color distributions of composite populations based on the Bruzual & Charlot (2000) isochrones. These artificial systems were built as follows:

• **In a first step** we create an artificial $V-K$ distribution of metal-rich globular clusters. We populate the red $(V-K)$ color range $(2.7 \leq (V-K) \leq 3.8)$, assuming that it is occupied by **"old"** and **"intermediate"** age objects. We do not consider bluer clusters $(2.0 \leq (V-K) \leq 2.7)$, assuming that these are only **"old"** objects.

For now, we assume cases similar to NGC 5846 (see Figure 3.3) in terms of sample size and photometric errors. For a first exemplary case, we assume 50% of the red population to be 15 Gyr old and 50% to be 3 Gyr old. These numbers are not assumed to reflect the 'true' situation, but rather serve to demonstrate the method at this point. We will probe models with different ratios in the future (see Section 3.5.2). Further, it will become clear below that we are not directly comparing observed and simulated color-color diagrams but rather their cumulative age distributions, i.e., properties of the distributions still need to be "calibrated".

The final modeled systems contain 43 old, blue objects (not considered further) and 120 red objects homogeneously distributed within the $V-K$ range [2]. The red population was divided into an old (15 Gyr) and young (3 Gyr) population with 60 objects each.

• **In a second step** we attach to each $V-K$ data point a (1σ) error drawn randomly from our observed list of $\Delta(V-K)$ errors for NGC 5846, and then smear in a Monte-Carlo approach each $V-K$ point with up to ±3 times its associated error (i.e. allowing up to 3σ errors in very rare cases). These new $V-K$ values are stored with their $1\ \sigma$ error and used for the further process.

• **The third step** consists of associating a $V-I$ color to each new $V-K$ color. To do this, we perform a least-square fit to the SSP model isochrones (in this case from Bruzual & Charlot

---

[2] We experimented also with Gaussian distributions within this color range, but the final results of the experiment did not differ significantly and we have no better physical justification for a Gaussian than for a homogeneous color distribution.

2000) by a logarithmic function (($V-I$)=A·log($V-K$)+B). The particular fit parameters A and B are given in Table 2. Figure 3.6 shows the isochrones as given by Bruzual & Charlot 2000 and our fits to the isochrones (solid lines).

The fits are then used to compute for each $V-K$ point the corresponding $V-I$ point, once the age was chosen. In our case, we used the 15 Gyr fit for the 60 old artificial clusters, and the 3 Gyr fit for the other 60 (young) artificial clusters.

- *Finally, in* **the fourth step** we associate a measurement error $\Delta(V-I)$ to each $(V-I)$ data point in a similar way as for $(V-K)$. We now have a set of 120 objects (60 old, 60 young) with associated $(V-K)$ and $(V-I)$ colors and errors.

As an example of such artificial color-color distributions, we show in Figure 3.7 the modeled color-color diagram of a purely 15 Gyr old population and a composite **old** (15 Gyr) and **young** (3 Gyr) clusters as well as the resulting age distribution (lower panels). This distributions should be compared to the observed data for NGC 5846 in Fig. 3.3.

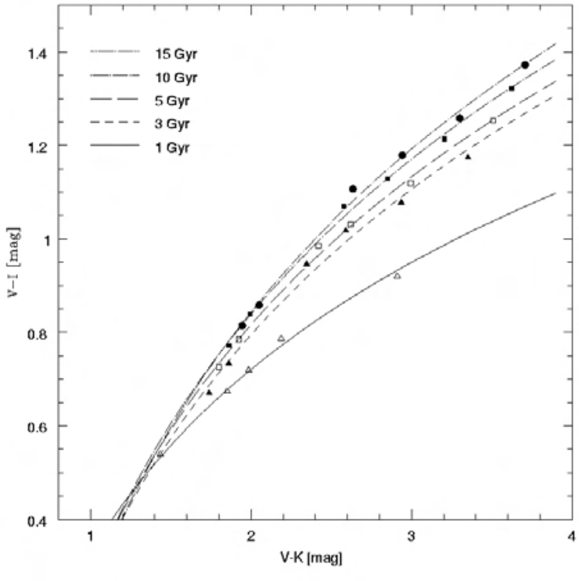

Fig. 3.6.— SSP isochrone fit for $(V-I)$ vs.$(V-K)$ color-color diagrams. The symbols are colors given by the SSP models (Bruzual & Charlot 2000) for 1 Gyr (open triangle), 3 Gyr (solid triangle), 5 Gyr (open square), 10 Gyr (solid square) and 15 Gyr (dots). The lines represent the result of a logarithmic fit to the isochrones with $(V-I)=$ A·log$(V-K)+B$. The fit parameters A and B are given in Table 2.

3.4.2 Cumulative age structure

The separation of the isochrones in Fig. 3.6 and the difference between the distributions in Fig. 3.7 (upper panels) motivated us to use the optical-near infrared photometry in order to try to separate globular cluster populations of different ages. This appears from the above plots to be at least possible to age differences of 10 Gyr or more (with respect to 15 Gyr for the oldest clusters). Therefore we decided to take the analysis one step further and to make a first attempt towards determining the age structure of the globular cluster systems.

We first attempted to compare directly the observed and the artificial color-color distributions, but this turned out to be too complicated. Two dimensional statistical tests are required in that case and the typical number of data points is not leading to any statistically significant results. We experimented with 2-dimensional f-test, 2-dimensional Kolmogorov-Smirnov tests, but in order to constrain the tests somewhat, one needs to put rather artificial constraints and the physical meaning of the final results is dubious.

We therefore decided to focus on 1-dimensional representations of the age structure. The dimension was chosen to maximize the age gradient along it, i.e., "perpendicular" to the isochrones.

Briefly, we associate to every cluster in our observed or artificial distribution an "age greater than X" when it lies above the isochrone of that age X in the color-color diagram. We start with the youngest isochrone (0 or 3 Gyr, see below) for which most cluster will lie above, and then

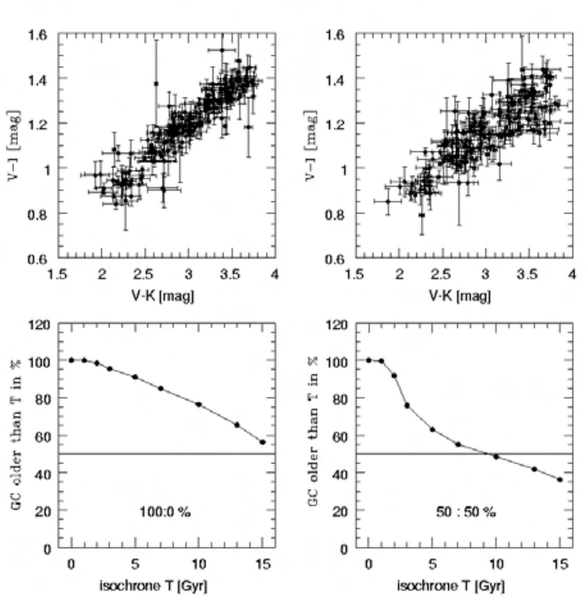

Fig. 3.7.— The upper two panels show the $(V - I)$ vs. $(V - K)$ color-color diagram for a single age population (left panel) and a composite 50% old (15 Gyr) and 50% young (3 Gyr) cluster population (right panel). In the lower panels, the cumulative age structure (see §3.4.2) for both cases is given as the mean of 1000 such simulations. The 50%-level is marked as a solid line.

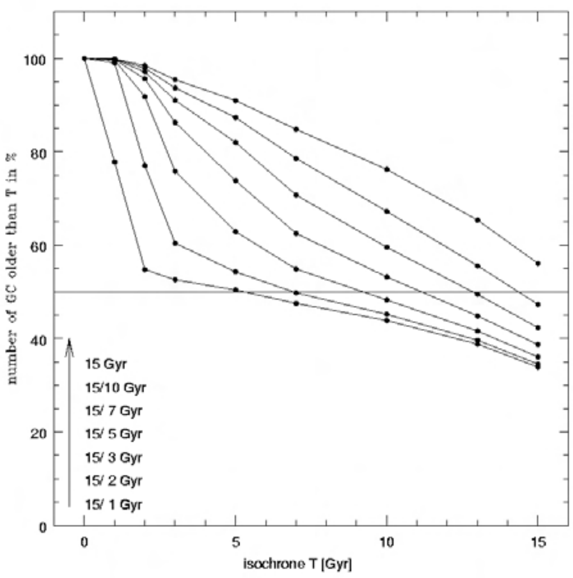

Fig. 3.8.— Age distribution for mixed cluster populations assuming half of the objects being 15 Gyr old and half of them being respectively 1, 2, 3, 5, 7 or 10 Gyr old. The 50% level is marked by a solid line.

move up isochrone by isochrone (in the steps 1,2,3,5,7,10,13,15 Gyr). Hereby the notation "0 Gyr" refers to objects below the 1 Gyr isochrone. The result is an inverted cumulative distributions as shown in Fig. 3.8 for artificial distributions and in Fig. 3.9 for the observed distributions of all our galaxies analyzed so far. The cumulative age distribution can be represented in absolute numbers (left panel) or normalized to the total number of objects (at an arbitrary bin, right panel).

3.4.2.1 Artificial data sets

As described above, the first set of simulations was done for combinations of a 15 Gyr old sub-population and an equal number of intermediate-age objects (1,2,3,5,7,10 Gyr). The results are shown in Figure 3.8. Each curve shows the mean age structure as evaluated from 1000 models for that given age composition.

The realistic photometric errors create a spread in the color-color diagram such that even a pure 15 Gyr system does not show 100% of the clusters to be older than 15 Gyr. Instead, the spread in the $(V-I)$ vs. $(V-K)$ diagram leads to a gentle fall-off with isochrone age.

However, this fall-off clearly changes when a second, younger sub-population gets mixed in. By the time one mixes a 1,2,3 Gyr population in the system, the fall-off becomes very steep around 2,3,4 Gyr, and the curves cross the 50% level well before the 10 Gyr mark.

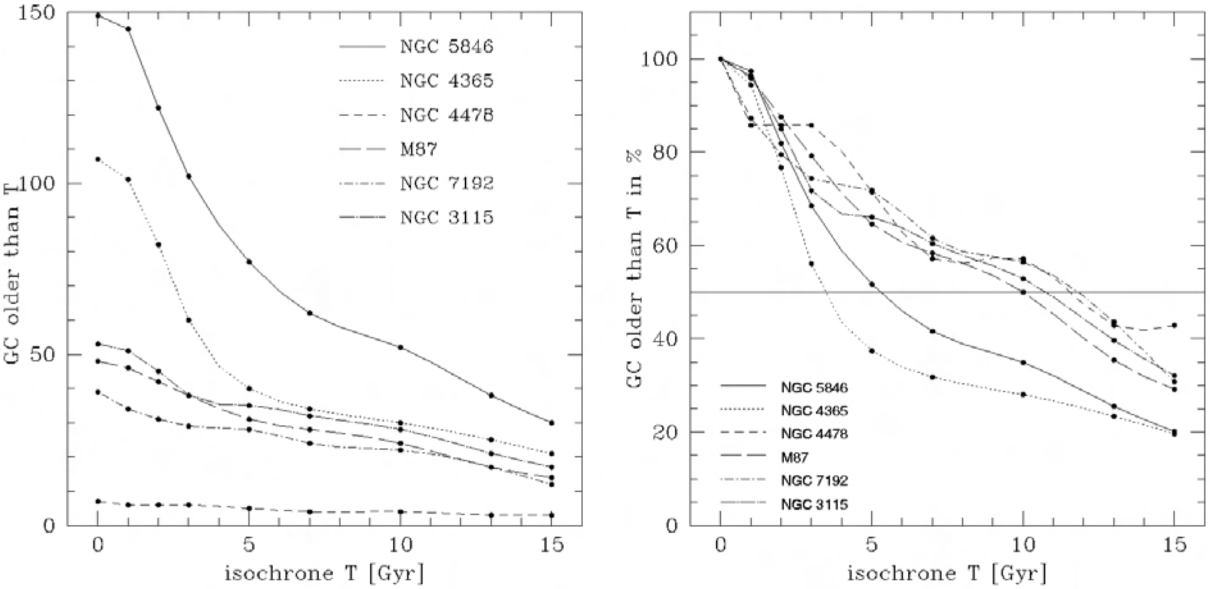

Fig. 3.9.— Age distribution for different galaxies (see text). The absolute number counts (left panel) are normalised to the total numbers of clusters in the sample (right panel). It is clearly seen that two systems (NGC 5846, NGC 4365) are significantly different from NGC 4478, M 87, NGC 7192 and NGC 3115. This is interpreted as NGC 5846 and NGC 4365 hosting intermediate-age sub-population (which was confirmed spectroscopically for NGC 4365). The 50% level is marked by a solid line.

3.4.2.2 Observed data sets

The result for the artificial distributions can be compared with the observed age distributions of the globular cluster systems (see Figure 3.9) in galaxies analyzed so far (M 87, NGC 4478, NGC 4365, NGC 3115, NGC 5846 and NGC 7192).

Taking first the observed data alone, we notice a clear similarity between NGC 5846 and NGC 4365, as opposed to the 4 other systems (see right panel of Fig. 3.9. Both galaxies fall-off steeply at early isochrone age and cross the 50% line well before 10 Gyr.

When compared to the results of artificial distributions, this leads immediately to the interpretation that both must host a significant fraction of intermediate-age clusters within their red sub-population. For NGC 4365, this was suspected already in Paper II and has since then been confirmed spectroscopically (Larsen et al. 2002).

In contrast, the age distribution of NGC 7192, NGC 3115, NGC 4478 and M 87 seems to be more consistent with what we would expect for a single age and old ($\geq$10 Gyr) population.

3.4.3 Contamination of background objects

Contamination of background objects is a potential problem in our analysis and we briefly investigate its impact below.

As above for the artificial distributions, we adopt a situation similar to the observations of NGC 5846. We used the Hubble Deep Field South (available at: www.stecf.org/hstprogrammes/ISAAC), which presents two advantages: it covers exactly the same (WFPC2) field of view as our observation, and it has a deep enough K-band observation to match our ISAAC observations of the globular cluster systems ($K < 21.5$ mag). The HDF-S sample was further selected in colors as for our samples. However, we could *not* apply a FWHM selection (having only the list of objects) so that the contamination is expected to be an overestimate. Even in that case, however, we show below that the effect is negligible for cases such as NGC 5846.

Figure 3.10 shows the color-color diagram of the HDF-S. Depending on magnitude selection, we have between 25 and 40 background objects in our color selection box. The resulting cumulative age distribution for the HDF-S sample is shown in Figure 3.11 and assigns about 50% of the objects to a population younger than 3 Gyr. Further, from the color-color plots, it becomes clear that the majority of these objects actually lie below the 2 Gyr line, being bluer in $(V-K)$ and $(V-I)$ than the intermediate-age, metal-rich globular clusters in NGC 5846. It is most probably dominated by a star-forming galaxy population that would be rejected by our FWHM criteria.

The effect of contamination on NGC 5846 is shown in Figure 3.12. There, we plot the uncorrected (absolute and relative) age distributions, as well as the ones corrected for background contamination using the HDF-S source counts. Clearly, the effect is marginal. The contaminating objects tend to drag the age distribution towards younger ages, mimicking a slightly younger sub-population, e.g. the intersection with the 50%-level occurs at a larger age. Thus, “old” distribution such as for M 87, NGC 3115 etc would appear even older when corrected for contamination. In the cases of NGC 4365 and NGC 5846 (large numbers of clusters) the effect of this (overestimated) contamination is small and does not influence the conclusion that these systems host a significant intermediate-age population.

3.5 Conclusions and future work

3.5.1 Conclusions

In this paper, we presented results of our optical − near-infrared study of the globular cluster systems of NGC 5846 and NGC 7192. While the latter does not show any significant anomaly, the former shows a case very similar to that of NGC 4365 (see Paper II) with good evidence for a significant metal-rich, intermediate-age population in addition to an old, metal-rich one.

We developed a new method to quantify the age structure of the globular cluster systems studied so far, based on a comparison of the cumulative age distributions of the observed and

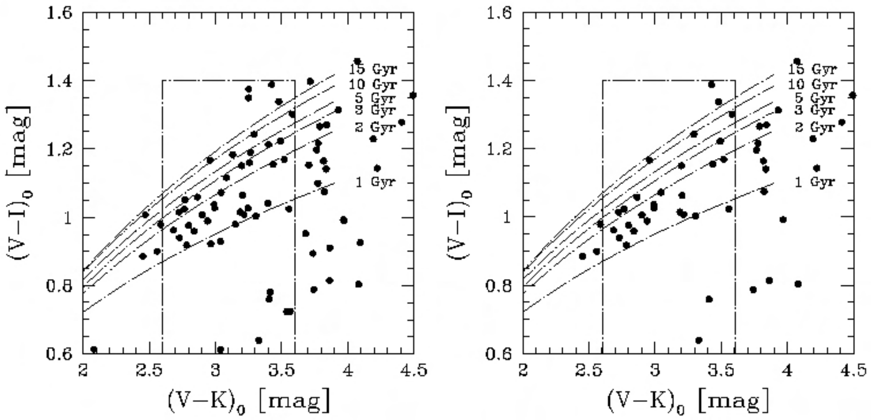

Fig. 3.10.— $(V-I)$ vs. $(V-K)$ color-color diagram for the Hubble Deep Field-South using different K completeness limits: left, all objects with $K < 21.5$, right all objects with $K < 21.0$ (bracketing our completeness limit for NC 5846). The box marks the color range in $(V-I)$ and $(V-K)$ used for the determination of the globular cluster age structure as described in section 3.4.2. Both diagrams show that the highest contamination of our sample is expected below the 2 Gyr isochrone. The isochrones superimposed are from Bruzual & Charlot SSP models (2000).

modeled optical – near-infrared color-color diagrams. This method appears powerful enough to detect intermediate-age sub-population within globular cluster systems.

Our first conclusions for the galaxies studied so far are that both NGC 4365 and NGC 5846 have a cumulative age distribution of the metal-rich globular clusters that is different from those

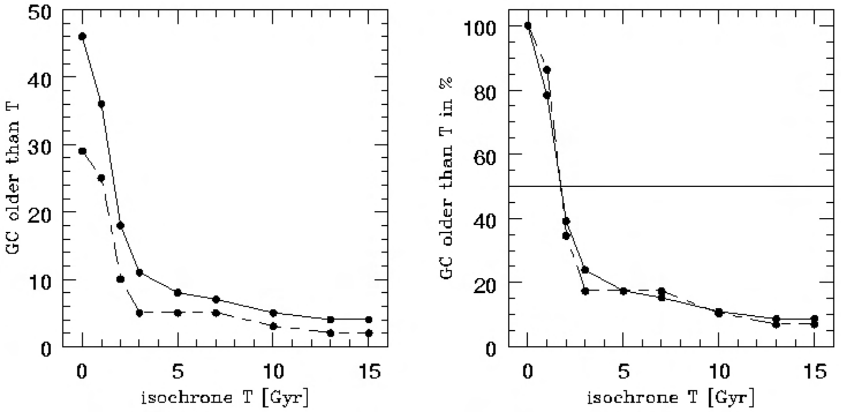

Fig. 3.11.— Age structure of the HDF-South objects using the procedure given in Section 3.4.2. Left and right panels show the absolute and relative age distributions respectively. The color selected samples with $K < 21.5$ and $K < 21.0$ are shown as solid and dashed curves, respectively. The 50% level is marked by a solid line.

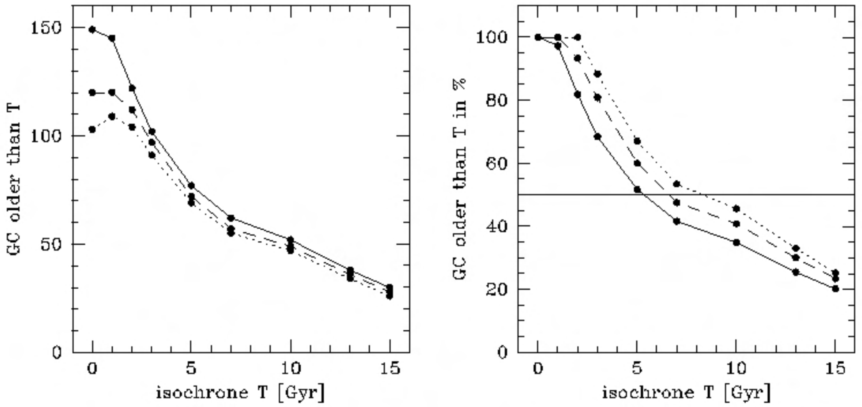

Fig. 3.12.— Influence of background contamination on the age structure of the system in NGC 5846. The left and right panels show the absolute and relative cumulative age distributions, respectively. The uncorrected distribution is shown as a solid curve. The distribution corrected for background contamination of $K < 21.5$ and $K < 21.0$ are shown as long dashed and short dashed lines, respectively.

of the 4 other galaxies (NGC 3115, NGC 4478, NGC 7192 and M 87). The former are better modeled by by a composite metal-rich population including an old (15 Gyr) as well as a significant young (1-5 Gyr) population. The others, in contrast, are very similar to the model for pure old populations and are thus best explained by being dominated by old objects.

NGC 7192 suffers from small number statistics, but the current dataset is, with respect to the color-color diagram and the age structure, more consistent with only one sub-population. Compared to the globular cluster systems investigated so far, NGC 7192 most closely resembles NGC 3115.

For M 87 and NGC 4478 the results given in Paper I were not fully conclusive. NGC 4478 also suffers from small number statistics. M 87 appears now more clearly dominated by two sub-populations differing in metallicity, but with a metal-rich population dominated by old objects (see also Jordán et al. 2002).

We need to emphasize again that the method cannot, currently, produce reliable **absolute** numbers, neither in terms of ages, nor in terms of ratios between the different populations. The results in this paper should therefore be considered as qualitative for now, and will be better quantified in the future.

3.5.2 Future work on age dating

The upcoming papers will analyze the remaining galaxies in our dataset (in total 11 galaxies). This will allow us to discuss the results in the light of galaxy properties. In particular, we will look at trends with galaxy size and environment. The local density (Tully 1988) covered by our galaxy sample spans from 0.08 Mpc^{-3} (NGC 3115) to 4.17 Mpc^{-3} (M87) and environmental effects appear to be an important ingredient to galaxy formation and evolution.

On the modeling side, our goal is to improve the quantitative information of our method. We are developing a χ^2-test to find the best solution in the two parameter space of the models: ratio old/young and age of the young population, which are slightly degenerate. We also plan, with the help of spectroscopy and wide field photometry, to be able to better calibrate the models in terms of absolute age.

Also, we are exploring the dependence of the results on a particular SSP model and we will repeat the determination of the age structure using SSP models by Maraston (2000) and Vazdekis (1999). Further, we will investigate in more detail the effect of background contamination. This latter aspects will be the subject of a separate paper.

The authors would like to thank the ESO user support group and the ESO science operations for having carried out the program in service mode. We are also grateful to Stephane Charlot for providing his population synthesis models prior to publication. M. Hilker acknowledges support through Proyecto Fondecyt 3980032. THP gratefully acknowledges the support by the German *Deutsche Forschungsgemeinschaft, DFG* project number Be 1091/10–2. DM is supported by FONDAP 15010003 Center for Astrophysics.

References

Ashman, K. M., Zepf, S. E. 1992, ApJ, 384, 50

Ashman, K.M., Bird, C.M. 1993, AJ, 106, 2281

Ashman, K.M., Bird, C.M., Zepf, S.E. 1994, AJ, 108, 2348

Ashman, K. M., Zepf, S. E. 1998, "Globular Cluster Systems", Cambridge, University Press

Ashman, K.M., Zepf, S.E. 2001, AJ, 122, 1888

Bruzual, G.A. & Charlot, S., 1993, AJ, 405, 538

Bruzual, G.A. & Charlot, S. 2000, private communication

Burgarella, D., Kissler-Patig, M., & Buat, V. 2001, AJ, 121, 2647

Buta, R. & Williams, K. L. 1995, AJ, 109, 543

Cardelli, J. A., Clayton, G. C., & Mathis, J. S. 1989, ApJ, 345, 245

Côté, P., Marzke, R.O., West, M.J., 1998, ApJ, 501, 554

Côté, P., West, M.J., Marzke, R.O. 2002, ApJ, 567, 853

de Vaucouleurs, G., de Vaucouleurs, A., Corwin, H. G., et al. 1991, Third Ref. Catalogue of Bright Galaxies, New York: Springer

Forbes D.A., Brodie J.P., & Grillmair C.J. 1997, AJ, 113, 1652

Forbes, D.A., Brodie, J.P., Huchra, J. 1997, AJ, 113, 887

Forbes D.A., Grillmair, C.J., Williger, G.M.et al. 1998, MNRAS, 293, 325

Frogel, J. A., Persson, S. E., Matthews, K. et al. 1978, ApJ, 220, 75

Gebhardt, K. & Kissler-Patig, M. 1999, AJ, 118, 1526

Hilker, M., Infante, L., Richtler, T. 1999, A &AS, 138, 55

Holtzman J., et al. 1995, PASP, 107, 1065

Jordán, A., Côte, P., West, M.J., et al. 2002, ApJL, 576, 113

Kissler-Patig, M., Forbes, D.A., Minniti, D. 1998, MNRAS, 298, 1123

Kissler-Patig, M. 2000, "Reviews in Modern Astronomy", ed.Schielicke, 13, 13

Kissler-Patig, M., Brodie, J.P., & Minniti, D. 2002, A&A, 391, 441 (Paper I)

Kundu, A., Whitmore, B. C. 1998, AJ, 116, 2841

Kundu, A., Whitmore, B. C. 2001, AJ, 121, 2950

Kundu, A., & Whitmore, B. C. 2001, AJ, 122, 1251

Larsen, S.S., Brodie, J.P., Huchra, J.P. et al. 2001, AJ, 121, 2974

Larsen, S., Brodie, J.P., Beasley, M.A. et al. 2003, ApJ, 585, 767

Maraston, C. 1998, MNRAS, 300, 872

Maraston, C., 2000, priv.communication

Maraston, C., Greggio, L., Thomas, D. 2001, Ap&SS, 276, 893

McLachlan, G.J. & Basford, K.E. 1988, "Mixture Models", Marcel Dekker Inc.

Minniti,D., Alonso, M.V., Goudfrooij, et al. 1996, ApJ, 467, 221

Peebles, P.J.E., Dicke, R.H. 1968, ApJ, 154,891

Persson, S. E., Murphy, D. C., Krzeminski, W. et al. 1998, AJ, 116, 2475

Puzia, T. H., Kissler-Patig, M., Brodie, J. P. et al. 1999, AJ, 118, 2734

Puzia, T. H., Kissler-Patig, M., Brodie, J. et al. 2001, in IAU Symposium 207, *Extragalactic Star Clusters*, eds. D. Geisler, E. K. Grebel, & D. Minniti, p. 294

Puzia, T. H., Zepf, S. E., Kissler-Patig et al. 2002, A&A, 391, 453 (Paper II)

Saviane, I., Rosenberg, A., Piotto, G., Aparicio, A. 2000, A&A, 355, 966

Schlegel, D. A., Finkbeiner, D. P., Davis, M. 1998, ApJ, 500, 525

Schweizer, F., Miller, B.W., Whitmore, B.C. et al. 1996, AJ, 112, 1839

Tonry, J. L., Dressler, A., Blakeslee, J. P., et al. 2001, ApJ, 546,681

Tully, R.B. 1988, "Nearby Galaxies Catalog", Cambridge, University Press

Vazdekis, A. 1999, ApJ, 513, 224

Whitmore, B. C., Schweizer, F., Leitherer, C., et al. 1993, 106, 1354

Whitmore, B.C.& Schweizer, F. 1995, AJ, 109, 960

Yi, S., Demarque, P., Kim, Y., et al. 2001, ApJS, 136, 417

Zepf, S. E., Ashman, K. M. 1993, MNRAS, 264, 611

4 Intermediate-age Globular Clusters in early-type Galaxies

Better age determinations by adding U-band observations to the V,I,K datasets

Astronomy & Astrophysics, accepted

Maren Hempel & Markus Kissler-Patig

Abstract

This paper represents an extension to a series of publications on combined optical and near-infrared photometry of globular cluster systems in early-type galaxies. Based on color-color diagrams the cumulative age distributions of their globular cluster systems have been derived and revealed intermediate age clusters in two galaxies, namely NGC 4365 and NGC 5846. The extension of this observations towards the blue wavelength range was performed in order to increase the age resolution of photometric studies. In this paper we present the results of U-band observations of NGC 4365 and NGC 5846 and their combination with previously obtained V, I and K_s- band photometry. $(U-I)\ vs.(V-K_s)$ color-color diagrams are used to derive the cumulative age distribution. The later is compared to simulated globular cluster systems of known age and size composition in order to set constrains on relative ages and size of the sub-populations.

Keywords: globular clusters: general, galaxies: star clusters, galaxies: individual (NGC 4365, NGC 5846)

4.1 Introduction

Photometric studies on globular cluster systems are of growing interest for our understanding of how and when galaxies form and how they evolve. Being less expensive in observing time than spectroscopy, they are the first step in surveys on the age structure of globular cluster systems. Due to the age-metallicity degeneracy (e.g. Worthey 1994) photometry alone can, in terms of accuracy in the age determination, not compete with spectroscopic data. Nevertheless, single stellar population (SSP) models (e.g. by Maraston 2000; Bruzual & Charlot 1993; 2003, and Vazdekis 1999) allow the detection based on color distributions of globular cluster sub-populations differing in age by several Gyr. With the introduction of near-infrared photometry (Kissler-Patig et al. 2002; Puzia et al. 2002; Hempel et al. 2003; Hempel & Kissler-Patig 2004, hereafter cited as Paper I, II, III and IV) the age resolution improved significantly and relative ages of globular cluster sub-populations in a galaxy could be derived.

An advantage of photometry for these type of work is that it surpasses spectroscopic investigations with regard to the observing time required to obtain data for a statistical relevant sample. As we demonstrated in Paper IV, the sample size is a key issue in our method to derive the relative age and size of globular cluster sub-populations. The latter is, as first considered by Ashman & Zepf (1992), linked to the formation scenario of a given galaxy. The accuracy to which the age and metallicity as well as extinction and mass can be determined depends strongly on wavelength coverage of the observations, as shown in a recent work by Anders et al. (2003). With the partly lifted age -metallicity degeneracy in combined optical/near-infrared photometry, the age resolution within an intermediate age population can be further improved by the coverage of the short wavelength range, sensitive to age of integrated stellar populations.

Thus, a more accurate age dating by including U- and/or B-band observations become possible. Also, because a hidden disadvantage of the infrared observations was the limiting magnitude and associated higher photometric errors that needs to be conceded. The latter translates directly into a finite age accuracy which prevents us from taking full advantage of the $(V-I)$ $vs.$ $(V-K_s)$ color-color diagram. As shown in Figure 4.1, $(U-I)$ improves the age resolution by a factor of ~ 3 with respect to $(V-I)$ when matched with $(V-K)$ colors. As an example we compare the color difference between a 15 Gyr and a 5 Gyr old cluster population. Hereby we stay in the red color range $((V-K_s)\geq 2.6)$, where we expect to find a second generation of metal-rich globular clusters (Paper III). The $(U-I)$ color between both age populations differ by $\gtrsim 0.4$ mag. This is well above the error limit of 0.15 mag for both colors which we typically apply to select reliable photometry for globular clusters.

In the following, we present the results of our U- band observations of two galaxies, NGC 4365 and NGC 5846, combined with previously obtained V, I, and K_s- band data. In both galaxies intermediate age globular clusters have been found. In line with the work presented in Paper III and IV the $(U - I)$ $vs.$ $(V - K_s)$ color-color distribution will be used to derive the cumulative age distribution and to set stronger constraints on relative age and size of the second generation of globular clusters. To show the effect of the extended wavelength range on the age distribution we will compare the results for both color combinations (i.e. $UVIK_s$ $vs.VIK_s$).

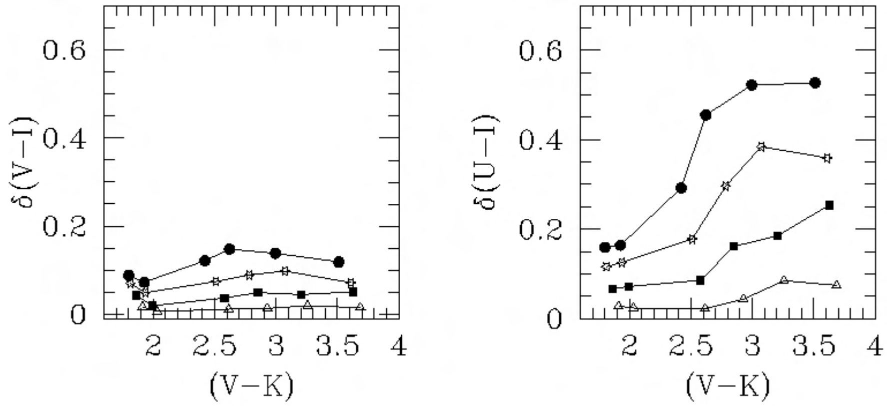

Fig. 4.1.— Both panels show the difference in the secondary color ($(V - I)$, left or $(U - I)$, right) for a 5 (solid circles), 7 (open stars), 10 (solid squares) and 13 Gyr (open triangles) isochrone compared to a 15 Gyr old population (following the Bruzual & Charlot 2000 SSP model). The metallicity increases with $(V - K_s)$ from 0.005 $Z_\odot$ up to 2.5 $Z_\odot$.

4.2 VLT/FORS1 U-band Photometry

4.2.1 Observations

We have complemented our V, I and K_s- band observations of two galaxies, NGC 4365 and NGC 5846 with U-band data. The U-band exposures for both galaxies have been taken in visitor mode (ESO program 71.B–0596) with the FOcal Reducer/low dispersion Spectrograph 1 (FORS1) in imaging mode, attached to the Unit Telescope 1 (Antu) of the European Southern Observatory's Very Large Telescope (VLT). The field-of-view of FORS1's Tektronix CCD is $6\farcm8 \times 6\farcm8$, with a pixel scale of $0\farcs2$ /pixel.

The data were obtained during the nights of May 6th, 7th, and 8th, and June 23th and 24th 2003. The total exposure times are 43800 sec for NGC 5846 and 38400 sec for NGC 4365. Our goal was to obtain a S/N=15 for objects with U=25 mag, expecting a $(U - K)$ color range ($\leq$3.5 mag) for an old (15 Gyr) stellar population at a limiting K_s= 21.5 mag. The total exposures were split into 1800 sec observations to avoid saturation of the galaxy. Exposures, taken under photometric conditions, were used to calibrate the total exposure. The photometric zero point ZP= 25.199±0.021 mag (derived using 8 standard stars) was provided by the FORS 1 quality control group.

4.2.2 Photometry

For both galaxies the V, I and K_s- band data have been obtained in previous observing runs and the reductions was described in detail in Paper II and III. Therefore we will restrict ourselves on detailing the U-band photometry. Measuring the instrumental magnitudes with an aperture radius of 10.″0 (as used for the standard star photometry), the calibration of the short time exposure (photometric) follows the equations given below.

$$\mathrm{U}_{galaxy} = \mathrm{u}_{inst} + 25.199(\pm 0.021) - 0.505\chi$$

where U_{galaxy} is the calibrated magnitude, u_{inst} is the instrumental magnitude , and χ the airmass (1.13 for NGC 5846 and 1.52 for NGC 4365). The error of the zero points (second term in the equation) includes photometric errors of each single standard star measurement and the errors of the aperture correction analysis.

The final images for both targets were obtained by averaging the 25 (NGC 5846) and 22 (NGC 4365) single exposures. Their alignment and stacking was done using the IRAF tasks *imalign* and *imcombine*. Before combining the images have been processed individually. The images were divided by a normalised masterskyflat, created from the twilight flat field exposures for each night. The photometry was carried out using SExtractor v2.1.6 (Bertin & Arnouts 1996). To calibrate the total exposure we used a single exposure taken under photometric conditions and calculated the difference in instrumental magnitude of 33 (NGC 5846) and 19 (NGC 4365) objects to the one obtained in the total exposure. This photometric offset was calculated to be 23.98(±0.021) mag in NGC 5946 and 24.01 (±0.055) mag in NGC 4365 and added to the instrumental magnitude of all detected sources. To avoid crowding effects the instrumental magnitudes were determined for a

Table 4.1: General information about the host galaxies NGC 5846 and NGC 4365. The references are (1): de Vaucouleurs et al. 1991, (2): Schlegel et al. 1998, (3): Buta & Williams 1995, (4): Frogel et al. 1978, (5): Tonry et al. 2001

Property	NGC5846	NGC 4365	Reference
RA(J2000)	15h 06m 29s	12h 24m 28s	(1)
DEC(J2000)	+01° 36’ 25”	+07° 19’ 03”	(1)
$B_{\mathrm{T,0}}$	10.87	10.49	(1)
E_{B-V}	0.055	0.021	(2)
$(B-V)_{\mathrm{o}}$	0.96	0.95	(1)
$(V-I)_{\mathrm{eff,o}}$	1.28±0.01	1.25±0.01	(3)
$(V-K)_{\mathrm{eff,o}}$	3.51±0.01	3.29±0.1	(4)
$(m-M)_V$	31.98±0.20	31.55±0.17	(5)
M_V	−22.07	−22.01	(1),(5)

$1\farcs0$ aperture (radius) and corrected for the $10\farcs0$ radius used for the zero point determination.

Finally, all magnitudes were corrected for Galactic foreground reddening using the reddening values of Table 1 and the extinction curves of Schlegel et al. (1998). The corrections for NGC 5846 and NGC 4365 are $A_U = 0.299$ mag and $A_U = 0.115$ mag.

We detected 514 objects in NGC 4365 and 1201 objects in NGC 5846 on the final U-band images using SExtractor (Bertin & Arnouts 1996). For later analysis we selected only objects for which a photometric error of ΔU$\leq$0.1 mag had been determined. For both targets this limit is only exceeded close to the detection limit of our observations. The remaining samples contained 498 and 1198 objects in NGC 4365 and NGC 5846, respectively.

4.3 Combined U,V,I,K photometry

Given the depth of the V-and I-band exposures (obtained with WFPC2 on board the Hubble Space Telescope) the detection limit in the combined photometry will be driven by the U- and K$_s$-band observations. From previous work we recall the detection limits for the K$_s$-band to be 21.5 mag for NGC 5856 and 20.25 mag for NGC 4365. Typical $(U-K)$ colors as derived from the SSP model isochrones (e.g. Bruzual & Charlot 1993) for stellar populations with ages between 1 and 15 Gyr range between ($1\leq U-K_s\leq 4$). Thus, U-band data as deep as $U = 25.5$ mag and $U = 24.25$ mag would be required for NGC 4365 and NGC 5846 respectively, in order not to introduce a additional limitation due to the U-band.

Using the *addstar* task within IRAF we test the reliability of the Sextractor detection within this magnitude range. As shown in Figure 4.2 (left panel) the U-band magnitude for artificial objects is recovered by Sextractor up to U$_{lim}$=25 mag and 25.5 mag for NGC 4365 and NGC 5846. In both cases the best fit deviates from an "input magnitude = output magnitude" relation by an amount smaller than the photometric error. The difference between such an ideal detection and real measurements is shown in the central panels of Figure 4.2. The dotted line represents the best fit to the magnitude difference for all input particles, whereas for objects with U$\leq$U$_{lim}$ the best fit follows the solid line. Objects brighter than 25.0 and 25.5 mag (correct detection) are detected with a 70% probability as seen in the right panels of Figure 4.2. If we apply additionally the above mentioned error cut for the U-band (0.1 mag) detections we find that objects fainter than $U = 24.2$ mag and $U = 25.0$ mag will not be detected in NGC 4365 and NGC 5846, respectively.

4.3.1 NGC 4365

The color- magnitude diagram (CMD) and the color- color diagrams of NGC 4365 are given in Figures 4.3 and 4.4. The histogram on top of the CMD shows the complete sample as an open histogram whereas the hatched regions mark the selected sample ($\delta(U-K)\leq$ 0.15 mag). As in

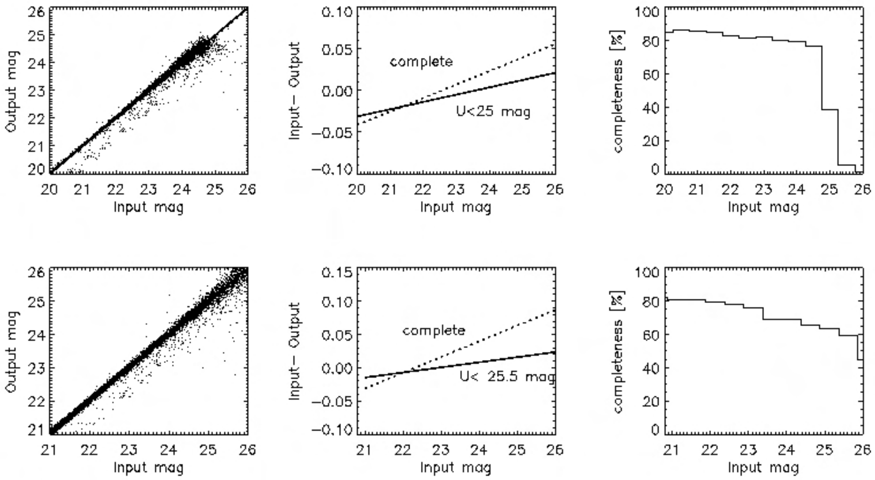

Fig. 4.2.— Left: Comparison between input and measured U-band magnitude of artificial objects (1000 objects per 0.5 mag). The dotted line represents the best fit to the complete data set whereas the solid line includes only objects with U<25 mag (top: NGC 4365) and U< 25.5mag (bottom: NGC 5846). Central: Difference between an ideal detection (input=output magnitude) and the best fit. Right: Detection rate for NGC 4365 and NGC 5846. Objects brighter than 25 mag (NGC 4365), respectively 25.5 mag (NGC 5846) are detected to at least 70 %.

the $(V - K_s)$ color distribution (Paper II) we find two distinct populations in the $(U - K_s)$ color distribution, although the sample is too small to allow a well defined double Gaussian fit to the data, in order to determine the mean color of both sub-populations. We compare the color-color diagrams using V, I and K_s band observations (top panel) or U, V, I and K_s -band data (bottom panel) in Figure 4.4, which demonstrates the age resolution as a function of different color combinations. The remaining cluster in the sample are more widely spread in the color space and their ages can be defined more reliably by model isochrones if U-band observations are included.

4.3.2 NGC 5846

Taken from Paper III (see Figure 3 therein), and later confirmed by spectroscopy, NGC 5846 contains as well as NGC 4365, a significant fraction of *intermediate age* globular clusters, for which we now aim at a more precise age estimate. Shown in Figure 4.5 and Figure 4.6 are the color-magnitude diagram for NGC 5846 and the color-color distribution. As in NGC 4365 the number of very red (in $U - K$) objects is cut down, but the bimodal color distribution can still be seen in Figure 4.5 although a fit to the color distribution suffers from the low number statistics. Nevertheless, at this stage we are interested in the age resolution and will settle with the fact that our derived size ratios between the globular cluster sub-populations refer to a strongly biased fraction

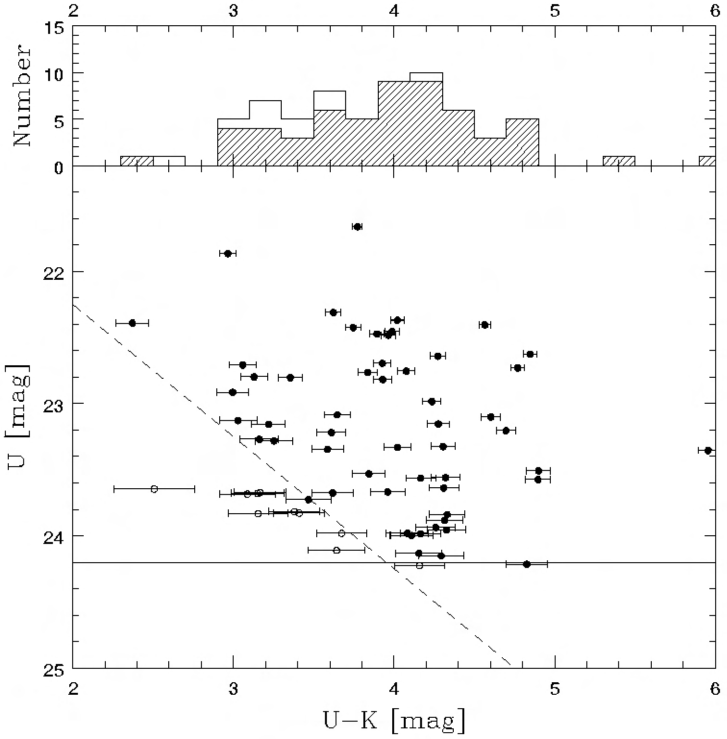

Fig. 4.3.— U vs. $(U-K)$ color-magnitude diagram for NGC 4365. The top panel shows the color distribution of all (open histogram) and selected (shaded histogram). As selection criterion we applied a error cut for $(U-K)$ with $\delta(U-K) \leq 0.15$ mag. The lower sub-panel shows the CMD. Here the filled circles mark the selected clusters while open circles indicate rejected objects. The dashed line marks the limiting magnitude in the K_s-band (K=20.25 mag) and the solid line the U-band limit for $\Delta U \leq 0.1$ mag.

of the total globular cluster system (see below).

4.3.3 Color-color diagrams for NGC 4365 and NGC 5846

In Paper II and III of this series color-color diagrams of combined optical and near-infrared photometry were used to detect globular cluster sub-populations with different ages. In both galaxies up to 80% of the objects included in the calculation were assigned to an intermediate age population, although see Paper III and Paper IV for caveats on this estimates. Using the higher resolution power of $(U-I)$ *vs.* $(V-K)$ color-color diagrams compared to $(V-I)$ *vs.* $(V-K)$ (see Figure 4.1) we aim at a more accurate age determination for the second generation of globular clusters. This is achieved as sown in Figures 4.4 and 4.6 (right panels), where we find the globular cluster colors much closer linked to a specific isochrone, resulting in only a small age uncertainty for a given SSP model.

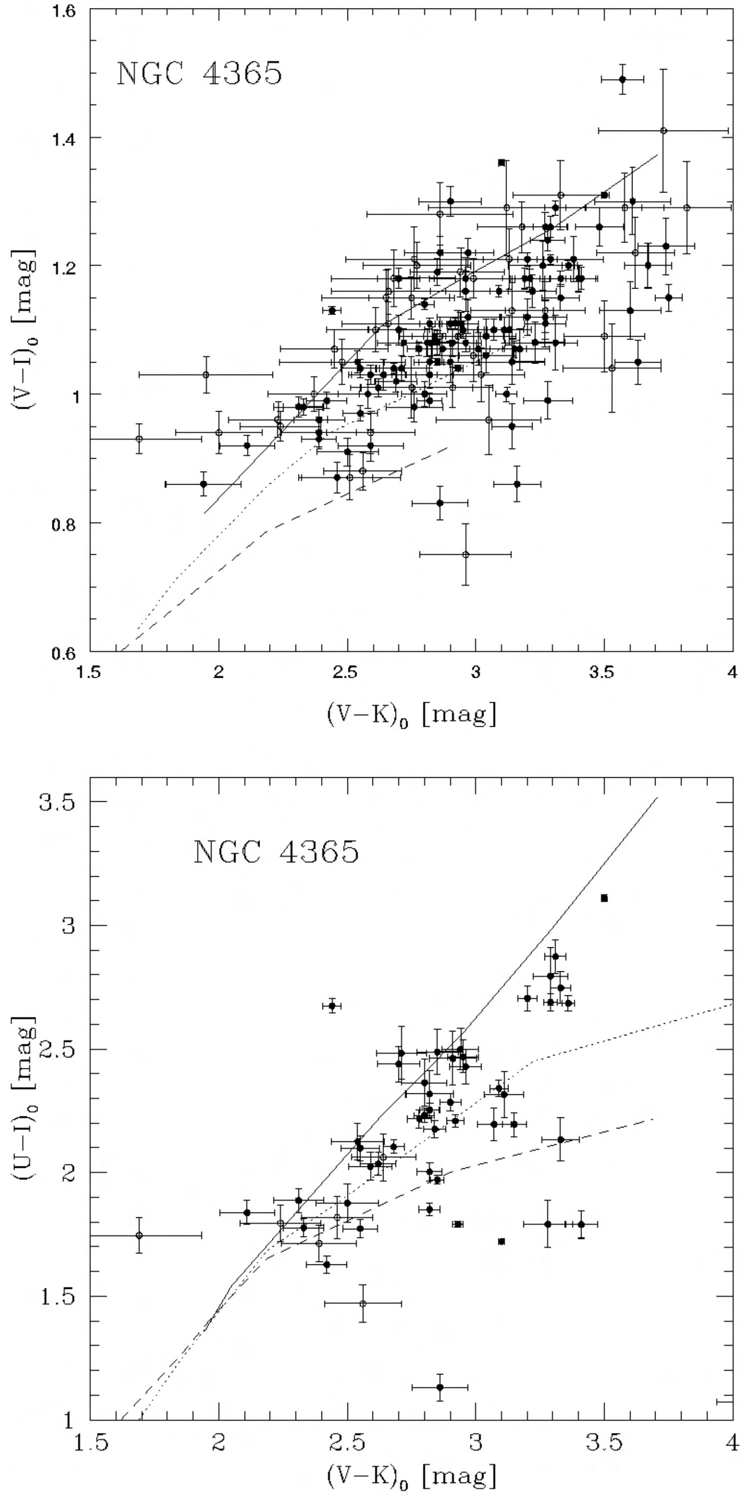

Fig. 4.4.— $(V - I)$ vs. $(V - K)$ and $(U - I)$ vs. $(V - K)$ color-color diagram for NGC 4365. All data are corrected for galactic foreground reddening (Table 4.1). As example the 1 (dashed), 5 (dotted), and 15 (solid) Gyr isochrones (Bruzual & Charlot 1993) are marked.

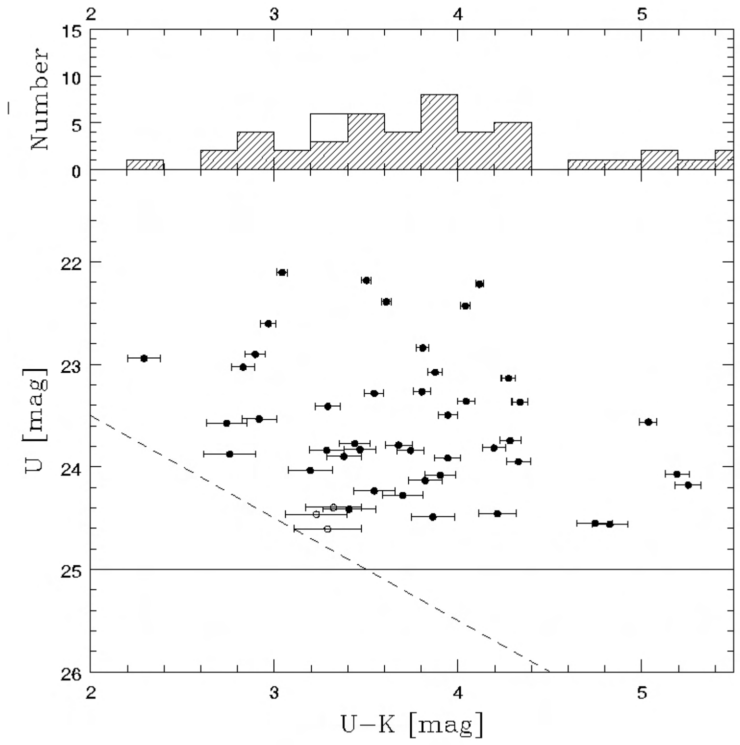

Fig. 4.5.— U vs. $(U-K)$ color-magnitude diagram for NGC 5846 (dereddened, Schlegel et al. 1998). The limiting K$_s$- band magnitude is K$_s$=21.5 mag, panels and symbols are indicated as in Fig. 4.3).The horizontal line at U=25.0 mag marks the U-band limit for detections with ΔU$\leq$0.1 mag.

After matching the U,V,I, and K_s band observations and applying the error selection criterion the globular cluster sample contains 62 objects in NGC 4365 and 51 objects in NGC 5846. In the discussion of the results, the relative size and age of cluster sub-populations, we have to weight the effects of an improved age resolution against the diminished globular cluster samples. The limiting bands are U and K$_s$. The first will favor detections at low $(V-I)$, the second at high $(V-K_s)$. Thus, our detection probability decreases in the color-color diagram from the bottom right to top left. In other word, **young and metal-rich** globular clusters are now favored and both samples biased towards these.

The $(U-I)$ and $(V-K_s)$ color ranges in which globular cluster are found is defined by the age and metallicity range. Following the SSP model isochrones (Bruzual & Charlot 2000), globular clusters with an age of 1 Gyr and a metallicity of up to 2.5×Z$_\odot$ will show a $(V-K_s) \leq 2.9$. The upper limit $(V-K_s) \leq 3.6$, which we apply for the determination of the age distributions, refers to a 15 Gyr isochrone. The latter sets also an upper limit to $(U-I)$ of 3.6 mag.

A major issue in our analysis are various bias effects. Any quantitative statement about the size of globular cluster sub-populations requires careful considerations of selection effects, either

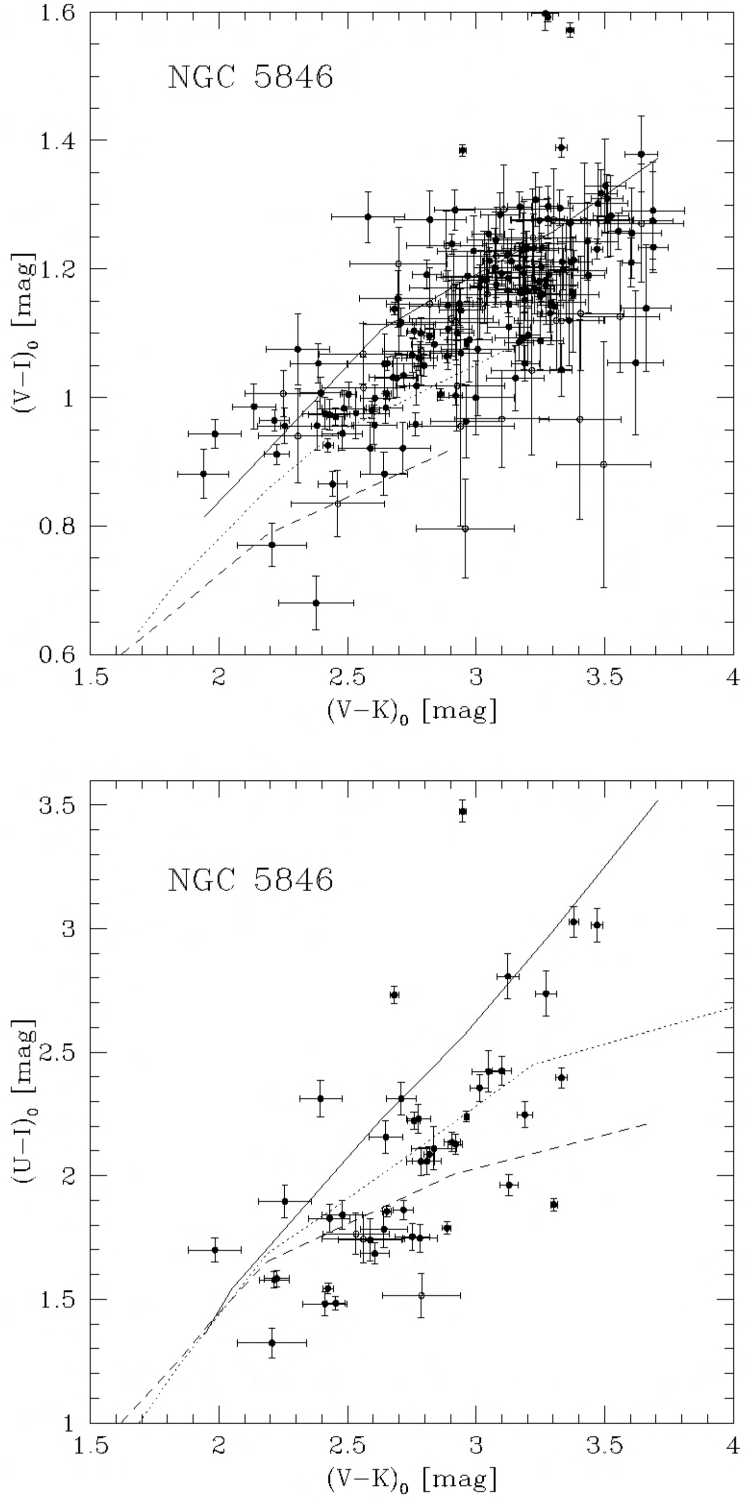

Fig. 4.6.— Color-color diagrams (top $(V-I) vs. (V-K)$, bottom:$(U-I) vs.$ $(V-K)$) for NGC 5846. Solid and open symbols mark data with photometric errors below, respectively above 0.15 mag. The model isochrones (Bruzual & Charlot 2000) for a 15 Gyr (solid), a 2 Gyr (dotted) and a 1 Gyr (dashed) SSP are shown.

related to the spatial distribution or to the completeness in the observations. As shown in Figure 4.7 the observations were carried out with the fields of view centered on the galaxy. So far data in all 4 filter bands are only available for objects within ≤ 1.5 R$_{eff}$ of both galaxies, i.e. their innermost regions. Simulations of merger processes (e.g. Hibbars & Mihos 1995) and observations of recent merger remnants (e.g. NGC 7252, Schweizer & Seitzer 1998) have shown that the gas, from which globular clusters will form during a galaxy-galaxy merger, funnels towards the center of the merger, within a few 100 Myr. A much higher fraction of intermediate age globular clusters is expected in the center than in the outskirts of the globular cluster system. Therefore we expect our sample to contain a high fraction of intermediate/young age globular clusters. We have also to consider that only globular clusters with a high bolometric magnitude will be detectable in all four filter bands and this selection will create an additional bias in favor of the most massive and youngest objects as it can be seen in Figure 4.8. There we compare the U-band luminosity function for NGC 4365 and NGC 5846 within the ISAAC field of view. The open histogram includes all U-band detections, whereas the shaded histogram refers only to objects which could also be detected in the near-infrared. Finally, as mentioned above the combination of the limiting magnitudes in both U and K band biased the sample in favor of the young and metal-rich globular clusters, discriminating against the old metal-poor, as well as against the old, metal-rich globular clusters.

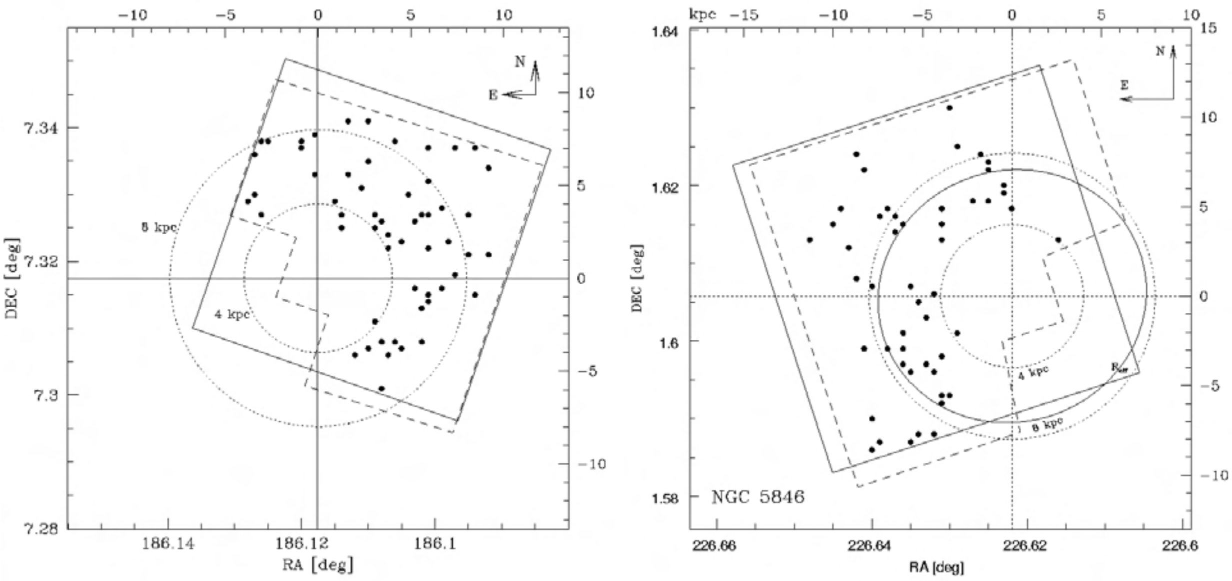

Fig. 4.7.— Field of view for the NGG 4365 (top panel) and NGC 5846 (bottom panel) data on the sky. The data (solid circles) show all objects for which data in all 4 bands, U,V,I, and K$_s$ are available. Due to the small field of view covered by ISAAC our complete data set is limited by the K$_s$-band observations (solid line) and the larger HST/WFPC2 images (dashed line) and we abandon from superimposing the much larger FORS1 field of the U-band observations.

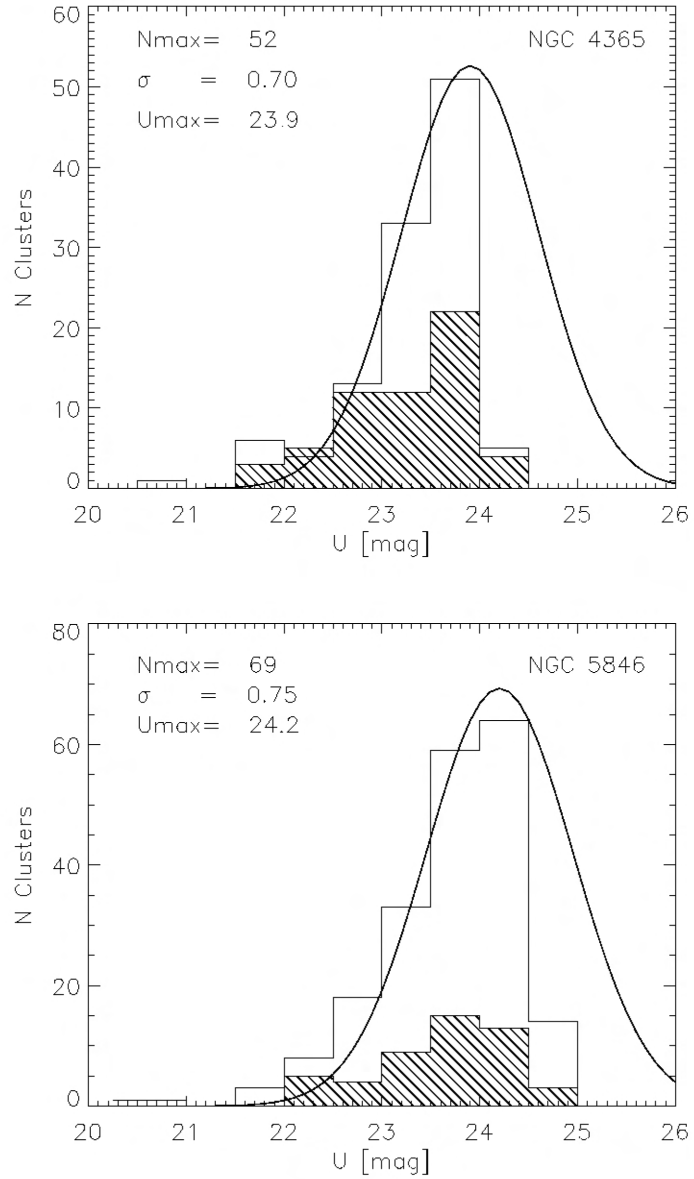

Fig. 4.8.— Luminosity distributions for NGC 4365 (top) and NGC 5846 (bottom). The open histograms represent the total sample of objects found within an □ 2′.5 field of view (VLT/ISAAC). The shaded histogram contains objects for which counterparts in V, I and K_s could be found. An error cut was set to δU$\leq$0.1 mag.

As a conclusion, we can state that the addition of the U-band greatly improves the age resolution, and thus allows to better quantify the ages of sub-populations. It does so, however, at the cost of introducing strong biases with respect to the numbers of clusters detected in each age/metallicity sub-population, so that the current U,V,I,K dataset is not appropriate to derive relative sizes of the different sub-populations.

4.4 Age sub-populations

4.4.1 Cumulative Age Distribution

Following the procedure described in Paper III and IV the cumulative age distributions were derived for NGC 4365 and NGC 5846, and are shown in Figure 4.9. The contamination with background objects is considered to be not significant, based on the selected color range and the corresponding HDF-South data.

The cumulative age distribution gives a first indication for age sub-populations but the comparison with simulated cluster systems (Paper IV) allows to set constraints on their relative age and size. In our previous simulations (Paper III and IV) we assumed the first generation of globular clusters to be 15 Gyr old (see Figure 17 in Paper IV). In agreement with the latest WMAP results (e.g. Bennet et al. 2003, Spergel et al. 2003) we are now working with an age of 13 Gyr for the **old** cluster population. Thus we expect a small change in the ratio between the sub-populations and the age of the intermediate age population.

The age difference between both populations stays more or less constant at ∼10 Gyr. On the other side the results are in different way affected by the extended color range as we will discuss in Section 4.4.2 (see also Section 4.3).

4.4.2 Impact of the sample size

In Figure 4.10 we present the results for the comparison between the cumulative age distribution of simulated globular cluster samples with varying sample size. By combining the previous V,I and K_s band data with U-band observations, we increase the age resolution on one side, but the number of clusters drops significantly. In the simulations we work with 120 objects within the red color range, where we expect the majority of the second generation clusters. Due to the different size of observed and simulated globular cluster systems we need to test the stability of our χ^2 test, as we did in Paper IV for V,I and K_s - band photometry. To do so we compare the cumulative age distribution of simulated globular cluster systems (hereafter called *original*) consisting of 10, 20, 60, 120, and 240 red globular clusters, with the complete model set. For our *originals* we assume a 50%- mix of 13 Gyr and 3 Gyr old objects. The χ^2 -test between *original* and model set should return the correct age and size combination of the former. The models are built as combinations of a 13 Gyr old first generation and a second population with an age of 1, 1.5, 2, 3, 5, 7, or 10 Gyr. As described in Paper III and Paper IV the size ratio changed between a 100 % old population and and a pure young/intermediate population in 10% increments. We note that for each parameter set we derive the age distribution as the statistical mean of 1000 separate simulations per age and size composition.

In Paper IV the stability test for the comparison between age distributions of samples of different sizes and our model database based on $(V-I)$ $vs.(V-K_s)$ color-color diagrams shows that $\gtrsim$100 object are needed in this approach. Using $(U-I)$ $vs.(V-K_s)$ color-color diagrams leads to stable result for a smaller sample as an increased age resolution compensates for the reduced sample size. As we can see in Figure 4.10 for samples of $\geq$60 objects in total age and size are recovered. The model which fits best to the "original" data set is found to consist of two equal size sub-populations with ages of 3 Gyr and 13 Gyr, i.e. the input model parameters. A sample size of 62 and 51 in NGC 4365 and NGC 5846 is therefore sufficient to allow a χ^2-test which will not be affected significantly by number statistics.

4.4.3 Age structures in NGC 4365 and NGC 5846

Given the high age resolution of the $(U-I)--(V-K)$ combination, a few conclusions about the age structure in NGC 4365 and NGC 5846 can already been drawn from the color-color diagrams for both targets.

In NGC 4365 (Figure 4.4, bottom panel) the majority of the globular clusters has a $(V-I)$ color which corresponds to an age $\gtrsim$2 Gyr, whereas only a few objects are found to be even bluer than the 1 Gyr model isochrone.

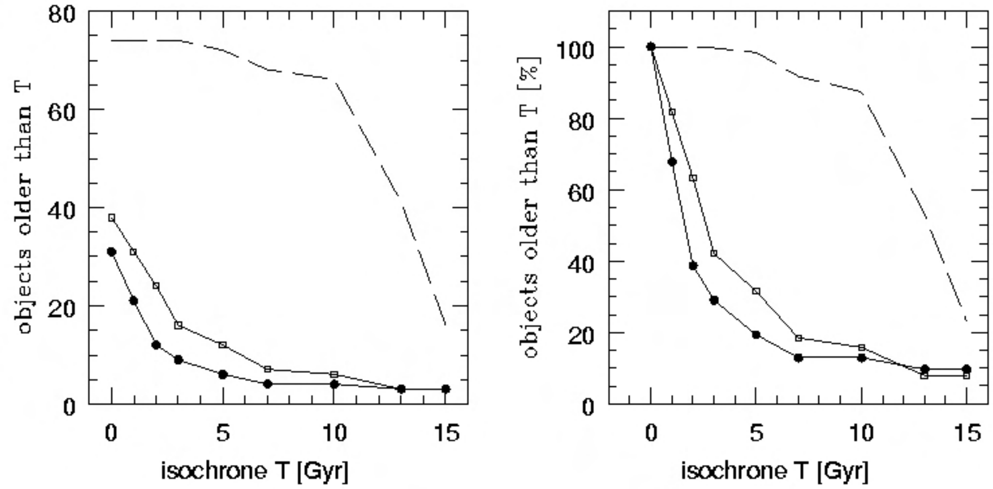

Fig. 4.9.— Cumulative age distribution in the globular cluster systems of NGC 4365 and NGC 5846. For the age dating we applied the SSP model by Bruzual & Charlot (2000).The left panel shows the number of objects being older than a specific isochrone and the right panel the relative distribution (normalised to the total number of objects).Open symbols represent NGC 4365 globular clusters and closed symbols NGC 5846 objects, respectively. As an example the age distribution for a simulated cluster systems (13 Gyr old objects only) is marked by the dashed line.

In NGC 5846 the situation is different. In Figure 4.6 (bottom panel) we find the majority of objects to be younger than 2 Gyr and only a very small fraction of old objects (i.e. $\geq$ 5 Gyr).

The results of the χ^2-tests for the comparison between the cumulative age distribution of observed and simulated globular cluster systems are shown in Figure 4.11. Results from U,V,I,K datasets and the V,I,K datasets alone are compared (top vs. bottom panel). We confirm the existence of an intermediate age population of globular clusters in both galaxies, being $\sim$ 10 Gyr younger than the first generation of clusters (assumed age: 13 Gyr). This age difference agrees well with the results assuming a first generation age of 15 Gyr in the models used in Paper IV and finding the best fitting model to contain a second population at age 3-5 Gyr. As expected for the extended wavelength range the relative age and size of the globular cluster populations are

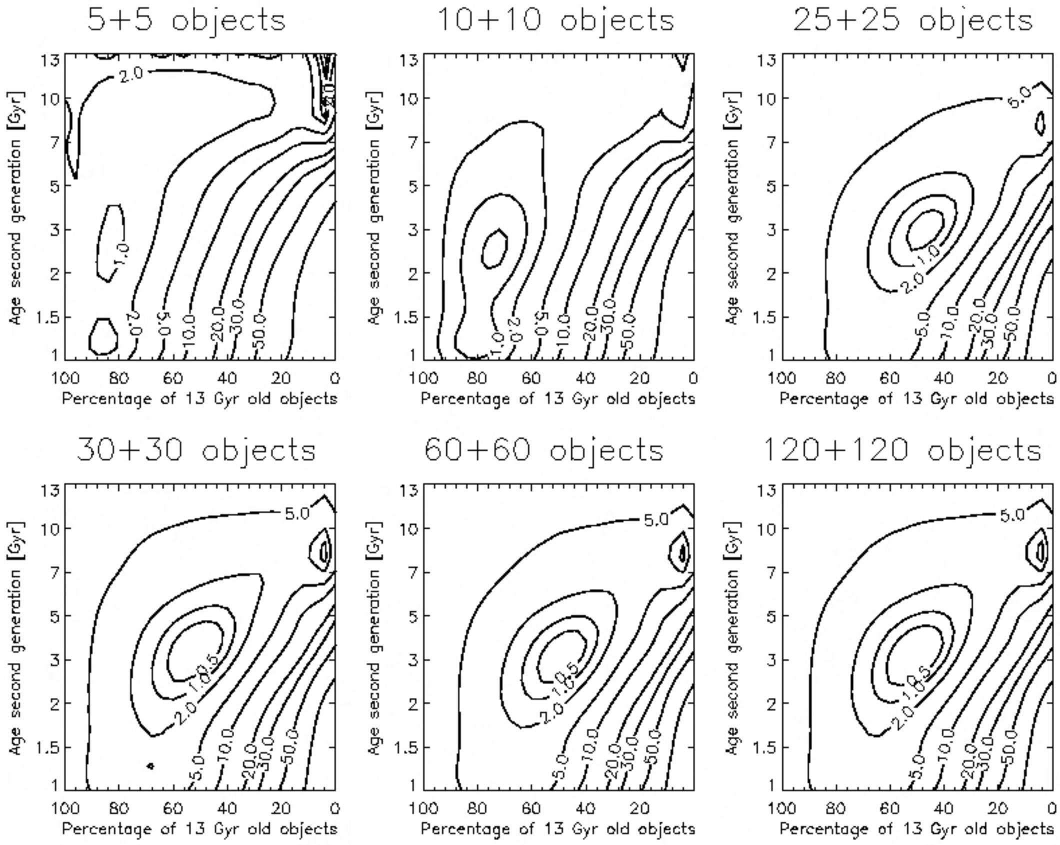

Fig. 4.10.— Result of the χ^2-test comparing the cumulative age distribution of simulated systems consisting of 10, 20, 60, 120 and 240 red objects, respectively. The red populations is split into 50% old (13 Gyr) and 50% young (3 Gyr) objects. The age distribution is compared to the complete set of simulations, as used for comparison to the observed globular cluster systems. The number of objects in both age populations is given on top of each panel. The different models were picked randomly out of a set of 1000 simulations.

now much better defined, as shown by the χ^2- contours (Figure 4.11, lower panel). Nevertheless- working with globular clusters detected in U, V, I and K_s introduces selection effects (see Sect 4.3): the method now favors young population. In case of NGC 4365 the cumulative age distribution is best fitted by a model containing ~ 40% of 13 Gyr old objects and ~ 60% clusters which are 2 Gyr old. In NGC 5846 the age of the second generation globular clusters is derived with 1-1.5 Gyr. The size ratio between both age populations is similar to that in NGC 4365.

4.5 Discussion and Summary

In this study we extend previously obtained optical and near-infrared observations towards the shorter wavelength range (U-band) in order to increase the age resolution in color-color distributions. This goal has been achieved, the distribution of the globular clusters in $(U-I)vs.(V-K_s)$ color plots allows a much better age determination than in $(V-I)vs.(V-K_s)$ plot. If we apply

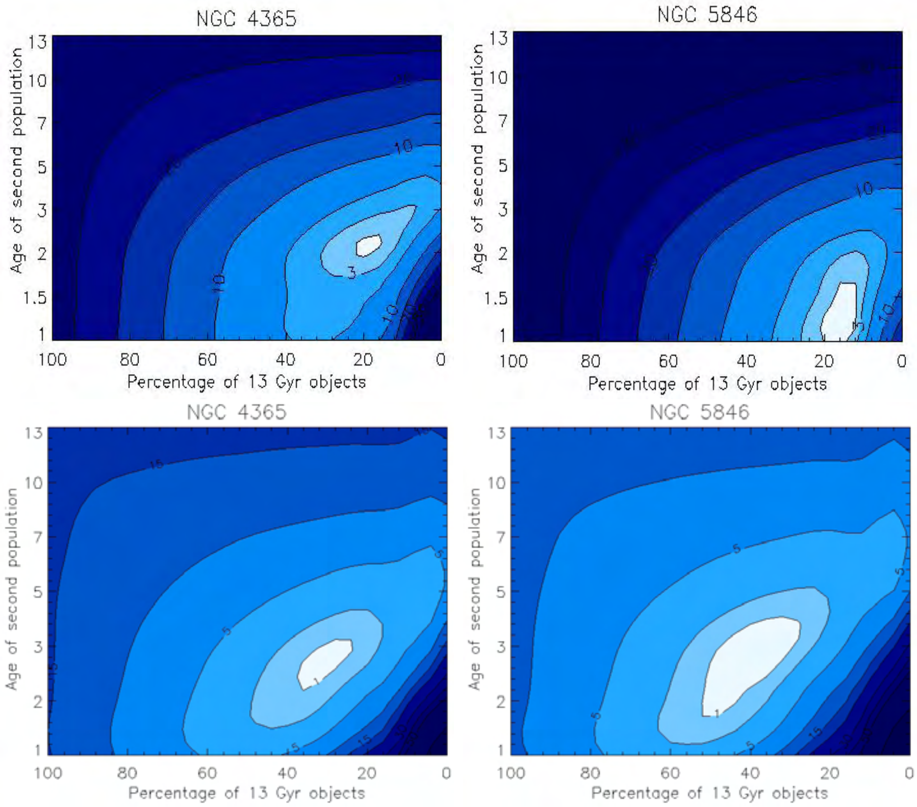

Fig. 4.11.— Results of the comparison between the observed globular cluster systems of NGC 4365 (left) and NGC 5846 (right) and simulated systems. The top panel represent the χ^2 test results using age distributions derived from $(U-I)$ $vs.(V-K_s)$ color- color diagrams compared to the $(V-I)$ $vs.(V-K_s)$ results shown in the lower panels.

a semi-numerical approach to derive the age structure in globular cluster systems the higher age resolution for the remaining globular cluster samples is confirmed.

In Section 4.3.3 we discussed the various new bias effects introduced by the U-band in the method. These hamper a correct interpretation of the derived size ratios between the cluster sub-populations. The spatial bias can be reduced by spatial extended surveys, which include as well globular clusters at larger galactocentric distances. The selection effect introduced by the limiting magnitudes in the U and K bands could be removed by even deeper observations but this is currently the limiting aspect of the method. We summerise that the derived size of the young/intermediate age globular cluster population in both galaxies has to be considered as an upper limit, even more so, since the diffuse galaxy light does not show evidence for a dominant 1-5 Gyr old stellar population. Nevertheless, our conclusion of a second star formation event during the galaxies evolutions is supported by morphological features. In NGC 4365 a counter-rotating core has been detected (e.g. Wagner, Bender & Möllenhof 1988; Bender, Saglia & Gerhard 1994; Davies et al. 2001), wheras in the center of NGC 5846 prominent dust filaments have been found (Goudfrooij & Trichnieri 1998).

Our original intension to use the size of the sub-populations to draw conclusions on the formation scenario for a given early-type galaxy would require very deep, wide-field data, e.g. as can be hoped for by the advent HAWK-I on the VLT which will provide an near-infrared counterpart to the typical field-of-view of optical instruments on 8 to 10m-class telescopes.

For now, the addition of the U-band 'only' improves the age resolution by a significant amount. From this, we determine very young average ages for the young metal-rich globular cluster sub-populations in NGC 4365 and NGC 5846 of ~ 2 and $1 - -1.5$ Gyr, respectively. Both early-type galaxies must have experienced a significant star formation episode very recently, forcing us to re-think the global star formation histories of at least some early-type galaxies. How representative these two galaxies are will be discussed in a sub-sequent paper discussing a larger sample of galaxies.

References

Anders, P., Bissantz, N., Fritze-v.Alvensleben, U. et al. 2004, MNRAS, 347, 196

Ashman, K.M. & Zepf, S.E. 1992, ApJ, 384, 50

Ashman, K.M., Bird, C.M., Zepf, S.E. 1994, AJ, 108, 2348

Bender, R., Saglia, R.P. & Gerhard, O. E. 1994, MNRAS, 269, 785

Bennett, C.L., Halpern, M., Hinshaw, G. et al. 2003, ApJS, 148, 1

Bertin, E. & Arnouts, S. 1996, A&AS, 117,393

Bruzual, A.G., Charlot, S., 1993, AJ, 405, 538

Bruzual, A.G. & Charlot, S. 2000, private communications

Bruzual, A.G., Charlot,S. 2003, MNRAS, 344, 1000

Buta, R. & Williams, K. L. 1995, AJ, 109, 543

Davies, R.L., Kuntschner, H., Emsellem, E. et al. 2001, ApJ, 548, L36

de Vaucouleurs, G., de Vaucouleurs, A., Corwin, H. G., et al. 1991, Third Ref. Catalogue of Bright Galaxies, New York: Springer

Frogel, J. A., Persson, S. E., Matthews, K. et al. 1978, ApJ, 220, 75

Goudfrooij, P., Trinchieri, G. 1998, A&A, 330, 123

Hempel, M., Hilker, M., Kissler-Patig, M. et al., 2003, A&A, 405, 487, Paper III

Hempel, M., & Kissler-Patig, M. 2004, A&A, 419, 863, Paper IV

Hibbard,J.E. & Mihos, J.C. 1995, AJ, 110,140

Kissler-Patig, M., Brodie, P. B., & Minniti, D. 2002, A&A, 391, 441 (Paper I)

Maraston, C., 2000, priv.communication

Puzia, T. H., Zepf, S. E., Kissler-Patig et al. 2002, A&A, 391, 453 (Paper II)

Schlegel, D. A., Finkbeiner, D. P., Davis, M. 1998, ApJ, 500, 525

Schweizer, F. & Seitzer, P. 1998, AJ, 116, 2206

Spergel, D.N., Verde, L., Peiris, H.V. et al. 2003, ApJS, 148, 175

Tonry, J. L., Dressler, A., Blakeslee, J. P., et al. 2001, ApJ, 546,681

Vazdekis, A. 1999, ApJ, 513, 224

Wagner, S.J., Bender, R., & Möllenhoff, C. 1988, A&A, 195, L5

Worthey, G. 1994, ApJS, 95, 107

5 Extragalactic Globular Clusters in the Near Infrared V.: IC 4051 and NGC 3311

Astronomy & Astrophysics, submitted

Maren Hempel, Doug Geisler, D. W. Hoard, W. E. Harris

Abstract

We present the results of combined optical and near-infrared photometry for the globular cluster systems of the giant ellipticals IC 4051 and NGC 3311. We use the reduced age-metallicity degeneracy in $(V-I)$ *vs.* $(V-H)$ color-color diagrams to derive the cumulative age distribution within the red sub-population of globular clusters and to search for age sub-populations. The age distribution is then compared to the one determined for simulated globular cluster systems in order to set constraints on the relative age and size of these globular cluster sub-populations. In both galaxies we find a significant fraction of globular clusters with ages between 1- 3 Gyr. We also investigate the metallicity distribution in both systems. Small number statistics prevent us from making any definite statements concerning NGC 3311, but we find that the derived metallicity distribution of the IC 4051 clusters strongly depends on the assumed age distribution. Based on our most likely result that finds roughly equal numbers of old (13 Gyr) and young/intermediate age clusters (∼2 Gyr), we find metallicity peaks at ∼ -0.8 and -0.1 for the old clusters and +0.5 for the young clusters.

Keywords: globular clusters: general — globular clusters: individual (NGC 3311, IC 4051), sub-populations, age distribution, Monte-Carlo simulations

5.1 Introduction

Globular cluster systems (GCSs) have long been widely used to probe the formation and evolution of their host galaxies (e.g. Searle & Zinn 1978; Zepf & Ashman 1993; Ashman & Zepf 1998; Kissler-Patig et al. 2002) although they represent only a small fraction of the galaxy's total luminosity. Hosting an almost perfect single stellar population (SSP), globular clusters allow the investigation of galaxies which, due to their large distances, cannot be resolved into single stars. The investigation of early-type galaxies, not found in the neighborhood of the Milky Way, in particular suffers from the large distance drawback. The diffuse light of a galaxy is a composite of all underlying stellar populations which cannot be disentangled, and populations of several ages and/or metallicities might indeed be hidden in the integrated light (e.g. Larsen et al. 2003). Detailed information on the age structure of the galaxy is therefore very difficult to obtain from the diffuse integrated light. Globular clusters, on the other hand, are luminous enough to be observed even at distances of ∼100 Mpc. Their stars share the same age and metallicity, and especially early-type galaxies can host quite numerous GCs (Ashman & Zepf 1998). The availability of SSP models (e.g. Bruzual 2000; Bruzual & Charlot 2003; Vazdekis 1999; Vazdekis et al. 2003; Thomas, Maraston, & Bender 2003; Thomas & Maraston 2003) for a wide range of ages and metallicities, applied to deep photometric or spectroscopic data of GCSs, allows us to set constraints on their age and chemical composition (e.g. Goudfrooij et al. 2001a; Puzia et al. 2002; Puzia et al. 2004b).

This basic tool allows extragalactic GCS research to probe a variety of important questions. Since the discovery of the bimodal color distributions in globular cluster systems, their origin has been a source of ongoing debate, although there is general agreement that distinct globular cluster populations of different age and/or metallicity are the origin of this bimodality. When and how these populations were formed and what can be inferred for the evolution of the host galaxy are some of the most outstanding questions addressed today, with crucial implications for galaxy formation theories. Consequently, much effort has been put into the observation of GCSs in early-type galaxies, which were classically assumed to have formed early on and to have evolved passively since then. From previous surveys, it is known that early-type galaxies are, on the one hand, well represented by the fundamental plane, indicating basic similarities, but their GCSs also show significant differences; for example with regards to metallicity (e.g. Geisler, Lee & Kim 1996), color distribution (Gebhardt & Kissler-Patig 1999), and specific frequency (Harris & van den Bergh 1981; Harris 1991; Harris 2001). Therefore, much caution has to be paid before claiming a universal formation scenario for early-type galaxies. In fact it seems more and more likely that we have to abandon the idea of a single formation theory and find external parameters which might be decisive for the particular formation and evolution of a given galaxy. Factors involving the galaxy environment, such as its position within the host galaxy cluster/group or its isolation from other galaxies, is likely to be one of the most important external parameters. Galaxy interactions (e.g. mergers and accretion events) seem to be an important, if not the dominant process, governing galaxy formation and evolution (see contributions in Wielen 1990). Consequently, the GCSs hosted by galaxies which were likely involved in such interactions need to be investigated. First results on the investigation of early-type galaxies in low-density environments were published by Kuntschner et al. (2002), who used integrated-light spectroscopy to derive ages and metallicities of 40 E and S0 galaxies and conclude that early-type galaxies in a low density environment show a broad distribution of luminosity-weighted ages and are on average younger than cluster ellipticals. Unfortunately no early-type galaxies in a high galaxy density environment exist in the local Universe. The determination of globular cluster ages by integrated-light spectroscopy is therefore quite challenging due to the faintness of the targets. The capability of high signal-to-noise spectroscopy with respect to age and metallicity determination has been demonstrated by various studies (e.g. Puzia et al. 2004a; Puzia et al. 2004b) and spectroscopy will doubtless be the method of choice when precise age estimates of a subsample of bright clusters are required. However, as long as the objective is to detect different broad age subpopulations in GCSs and to set coarse age limits on the GCS as a whole, then photometric studies (e.g. Kundu & Whitmore 2001a; Kundu & Whitmore 2001b; Gebhardt & Kissler-Patig 1999) are the most efficient alternative.

Until recently, the major drawback for the use of photometric studies to investigate the age distribution in GCSs was the age-metallicity degeneracy (Worthey 1994). With the introduction of combined optical and near-infrared photometry (e.g. Minniti et al. 1996; Goudfrooij et al. 2001b; Kissler-Patig et al. 2002) it is now possible to at least partially overcome this obstacle and derive the relative ages of globular cluster sub-populations, as well as their metallicities. The extended wavelength range allows one to recognize intermediate age globular clusters (e.g. those formed in a recent merger) from the bulk of first generation objects. In addition, V-H provides a sensitive metallicity index. The integrated IR colors for Galactic globular clusters of Cohen & Matthews (1994) show that the $V-H$ index has three times the metallicity sensitivity of $V-I$, making it a good index for investigating the reality of any multiple metallicity populations.

In this study we investigate the GCS of two important early-type galaxies, viz. NGC 3311, representing a giant cD galaxy at the center of a high density environment (the Hydra I galaxy cluster) and IC 4051, a giant E2 in the Coma galaxy cluster with no luminous neighbor, located several cluster core radii from the center. This will provide a range of environmental densities in order to begin to probe their effect on the GCS. The GCS of NGC 3311 has been investigated in the optical by many different groups (e.g. Grillmair et al. 1994; McLaughlin et al. 1995; Brodie, Larsen, & Kissler-Patig 2000; Secker et al. 1995). They found a populous GCS which appears to show the general color bimodality of such systems. Due to its central position in a high density environment, several wide field surveys have been carried out (e.g. Harris, Smith, & Myra 1983; Hilker 2003a; Hilker 2003b) to investigate spatial features in the GCS. NGC 3311 is of special interest in globular cluster studies, since it is not only the third closest cD galaxy, following in distance M 87 in Virgo and NGC 1399 in Fornax, but also hosts one of the richest GCSs (e.g. Harris, Smith, & Myra 1983;

McLaughlin et al. 1995). The GCS of IC 4051 has only been attainable until now from HST imaging and was the subject of papers by Baum et al. (1997) and Woodworth and Harris (2000). The latter work used V, I photometry and found tentative evidence of bimodality, with metal-intermediate ([Fe/H]~ -0.7) and metal-rich ($\sim$ solar) peaks and a near-complete lack of metal-poor clusters. The lack of metal-poor clusters and the very high specific frequency ($S_N = 11 \pm 2$) that they found makes the GCS of IC 4051 very unique and worthy of further study. General information concerning these 2 galaxies can be found in Table 1.

In this paper, we combine optical and near-infrared photometry to derive the cumulative age distribution (e.g. Hempel & Kissler-Patig 2004) which we will compare to simulated GCSs of known age structure (size and age of sub-populations). In this particular case the model isochrones by Bruzual & Charlot (2000) have been applied (see Bruzual & Charlot 1993; Bruzual 2000). The results enable us to set constraints on the age structure in both systems and to infer clues to the evolutionary history of their host galaxies (Hempel & Kissler-Patig 2004). The paper is organized as follows. In Section 5.2 we describe the observations as well as the data reduction. The derivation of the cumulative age distribution within the observed samples is described briefly in Sect.5.3.2. For a detailed description we refer to Hempel et al. (2003) and Hempel & Kissler-Patig (2004). In Section 5.4 we discuss the metallicity distribution. We summarize our results in Section 5.5.

5.2 Observations and Data Reduction

The optical and the near-infrared data for both galaxies were reduced by different groups, using different software. Therefore we will give a brief description for each data set.

5.2.1 Optical data: HST/WFPC2

Both targets were observed with HST + WFPC2 in two optical pass bands, NGC 3311 in F814W and F555W, and IC 4051 in F814W and F606W, respectively. NGC 3311 observations are part of a large survey on extragalactic GCSs, carried out under program number GO.6554. The

Table 5.1: General information about the host galaxy.

Property	NGC 3311	IC 4051	Reference
RA(J2000)	10h 36m 43s	13h 00m 55s	deVaucouleur et al. 1991
DEC(J2000)	−27° 31’ 42”	+28° 00’ 27”	deVaucouleur et al. 1991
$B_{\mathrm{T},0}$	12.65	14.17	deVaucouleur et al. 1991
E_{B-V}	0.079	0.011	Schlegel, Finkbeiner & Davis 1998
A_V	0.263	0.035	Schlegel, Finkbeiner & Davis 1998
A_I	0.154	0.02	Schlegel, Finkbeiner & Davis 1998
A_H	0.046	0.006	Schlegel, Finkbeiner & Davis 1998
$(B-V)_{eff}$	1.04	1.01	deVaucouleur et al. 1991
$(m-M)_V$	33.70 ± 0.08	34.82 ± 0.13	Jensen, Tonry & Thomson (2001)
M_V	-22.07 ± 0.20	-21.62 ± 0.35	deVaucouleur et al. 1991

observations of IC 4051 were carried out under program GO.6283, dedicated to stellar populations in elliptical galaxies. The total exposure times in the various pass bands are given in Table 5.2 for both targets.

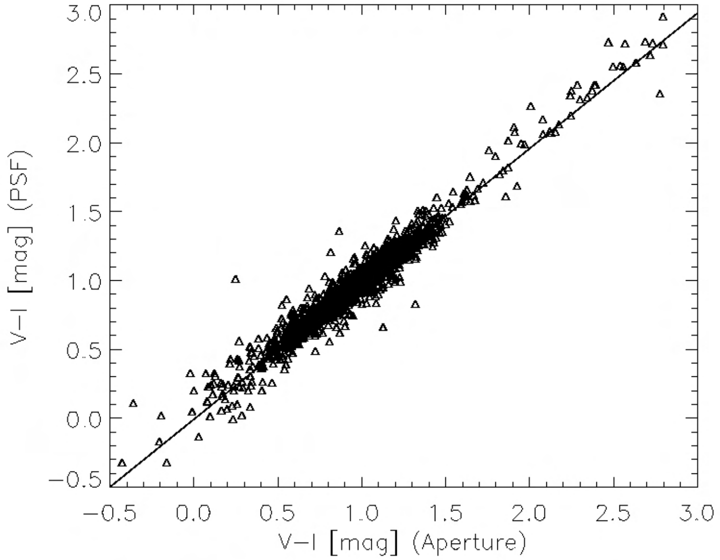

Fig. 5.1.— Comparison between $(V-I)$ colors based on *aperture* and *psf* photometry. The solid line represents the least-squares fit to $(V-I)$ based on aperture photometry. The objects in this plot contain the $(V-I)$ colors for the PC1 chip as well as for all three wide field chips. As mentioned in Sect. 5.2 the latter could not be included in our age analysis, due to the smaller spatial coverage of the near-infrared observations.

For IC 4051 we took the photometry directly from Woodworth & Harris (2000). The reduction of the optical data for NGC 3311 is described in the following.
The photometry on NGC 3311 clusters was done using the DAOPHOT package for *aperture*- and alternatively for *psf* photometry as well as using SExtractor (Bertin & Arnout 1996) *aperture* photometry. In Figure 5.1 we show the comparison between $(V-I)$, calculated from instrumental V and I band magnitudes, using DAOPHOT *psf*-photometry and SExtractor *aperture*-photometry. The results of a least square fit between the $(V-I)$ results are:

Table 5.2: Exposure times for NGC 3311 and IC 4051

Filter (Instrument)	NGC 3311	IC 4051
F814W (WFPC2)	3800 sec	5200 sec
F555W (WFPC2)	3700 sec	–
F606W (WFPC2)	–	20500 sec
F160W (NICMOS2)	2560 sec	2560 sec

$$(V-I)_{aperture} = 0.982(V-I)_{psf} - 0.007 \tag{5.7}$$

There is no difference between the results, the color offset being smaller than the photometric error, except for very red objects ($(V-I) > 2.0$ mag). The NGC 3311 results presented in this Paper are based on SExtractor photometry.

The instrumental magnitudes were transformed to the Johnson V and I magnitudes according to the procedure given by Holtzman et al. (1995) and reddening corrected using the values given in Table 5.1. The aperture corrections for both filter bands were determined as the mean difference (21 objects) between a 6 pixel instrumental magnitude and the $0\farcs5$ aperture used by Holtzman et al. (1995). The calculated corrections, 0.229 mag and 0.265 mag for the V and I band, respectively, were than applied to all of the V- and I-band detected objects. The small aperture was necessary because of crowding.

5.2.2 Near-Infrared Data: HST/NICMOS2

Both galaxies were observed with NICMOS Camera 2 (fov: $19\farcs2 \times 19\farcs2$, $0\farcs075$ pix^{-1}) through the F160W filter (approximately H band) in a slightly overlapping (~10-20 pixels) four-point mosaic pattern, centered on the galaxy. The combined mosaic image covers approximately the same area and galaxy field as the WFPC2 PC1 chip. Each of the four quadrants is a combination of 5 sub-images. The exposure time for each sub-image is 512 sec, the total exposure time sums up to 2560 sec (see Table 5.2). As for the optical filter bands, we give the details for data reduction separately for each target.

5.2.2.1 IC 4051

In IC 4051 the SExtractor routine (Bertin & Arnout 1996) was used to identify all targets in the four quadrant images of the galaxy-subtracted NICMOS2 image. This resulted in the detection of a total of 642 targets. The aperture photometry was then carried out using the non-standard IRAF task CCDCAP (Mighell & Rich 1995), which is optimized for aperture photometry of undersampled images. Hereafter, the photometry procedure recommended in the NICMOS Data Handbook [3] (Dickinson et al. 2002) was applied. The instrumental magnitudes were measured with an aperture of $0\farcs5$ (radius, corresponding to 6.6 pixel) and corrected to "infinite" aperture radius by adding -0.1517 mag, calibrated by adding 23.566 mag (which is the magnitude of a star with count rate of 1 electron per second in the NICMOS F160W filter), and corrected for the total quadrant image exposure time. Finally, we performed a transformation from the NICMOS F160W filter magnitudes to standard H magnitudes (Stephens et al. 2000). Based on the mean metallicity of IC 4051 globular clusters of $\langle \mathrm{Fe/H} \rangle \sim$-0.1 (Woodworth & Harris 2000), combined with observations of Galactic and M31 globular clusters (Barmby et al. 2000), leads to the following transformation:

---

[3] See http:www.stsci.edu/hst/nicmos/

$$H = F160W - 0.115\ (\pm 0.048)\ mag \tag{5.8}$$

After all calibration corrections were applied to the instrumental magnitudes, a number of targets were rejected: all targets within 12 pixels of any edge of a quadrant image, all targets for which CCDCAP failed to measure a magnitude, all targets with SExtractor star/galaxy indices less than 0.5 (indicating they are likely galaxies), targets located near the the center of the subtracted galaxy (within ∼2.″0, where photometric errors are very large due to the background galaxy light), and for identical targets located within the overlapping regions of two quadrant images, the one with the larger uncertainty. A total of 348 objects remained. After transforming the WFPC2 pixel coordinates to the NICMOS coordinates, and allowing an offset of up to 2 pixels in both x and y coordinates, the optical and near-infrared data were matched. The final sample now includes 256 objects.

5.2.2.2 NGC 3311

As in the optical filter bands the source detection on the NICMOS images was done using DAOPHOT/PHOT as well as SExtractor. To be as consistent in the data reduction as possible, we will stay with the SExtractor results. The transformation of the F160W data to the Johnson H band followed the procedure described in Section 5.2.2.1 and results in the following correction:

$$H = F160W - 0.110\ (\pm 0.024)\ mag \tag{5.9}$$

The differences in the transformation between F160W and H-band magnitudes between NGC 3311 and IC 4051 originates in the difference of the mean metallicity, derived from the $(V - I)$ distribution, where we have adopted a mean metallicity of [Fe/H]=-0.75 (Brodie, Larsen, & Kissler-Patig 2000). Besides the F160W- H band transformation, the instrumental magnitudes were aperture corrected, the photometric zero point for NICMOS2 applied and finally corrected for galactic reddening (see Table 5.1). After combining optical and near-infrared data the globular cluster sample includes 148 objects.

In this series of papers we concentrate on the age structure in globular cluster systems, which we derive from color-color diagrams. The basic tool in this approach (see Section 5.3.2 and Hempel & Kissler-Patig 2004) is the color distribution of the observed globular clusters with respect to SSP model isochrones. Therefore we have to consider the contamination of the globular cluster samples. Considering the color range, the contaminants are most likely background galaxies. Although we apply selection criteria, e.g. shape parameters and color limits, we are aware that contamination is still an issue. Nevertheless, the final globular cluster samples, combining optical and near-infrared data, contain only objects in the very central region of the GCS, where we find the highest globular cluster density. In combination with the small sample size (≈100 objects), as discussed in Section 5.3.2, we estimate that unresolved background galaxies make only a minor contribution to our sample and should have a minimal effect on the age distribution.

5.3 Results

5.3.1 Color-Color Distributions

Our basic tools to derive ages and metallicities of stellar populations from photometric data are color-color diagrams together with various SSP models; for example by Bruzual & Charlot (2000), Vazdekis (1999), or Maraston (2001). In this paper we will use the Bruzual & Charlot models (Bruzual & Charlot 1993). In our further analysis we select only clusters which satisfy an error limit of $\sigma_{(V-I)}$ and $\sigma_{(V-H)} < 0.15$ mag. The error selected globular cluster samples for NGC 3311 and IC 4051 contain 105 and 149 objects, respectively. In our further analysis of the age structure additional color cuts will be applied to avoid contamination with unresolved background objects and to select objects within a restricted color range that allows the best age resolution (see Section 5.3.2).

5.3.1.1 IC 4051

In Figures 5.2 and 5.3 we show the CMD and the $(V-I)$ *vs.* $(V-H)$ color-color diagram for IC 4051. Clearly, the data below the 50% completness limit of the H photometry is unreliable and will be excluded from further analysis, as will all objects with color errors above our error cut. In Woodworth & Harris (2000) it was tentatively suggested that the $(V-I)$ distribution of the IC 4051 globular clusters is bimodal and, therefore, we attempted to fit a double Gaussian function to the $(V-H)$-color distribution, which is three times more sensitive to metallicity than $(V-I)$. If the complete sample set is included in this analysis, then comparably good fits are obtained for variable amplitudes for both sub-populations or (forced) equal amplitude, equal width settings. In the latter case the Gaussian centers are at $(V-H)$=2.70 and 3.18. The mean of these two Gaussian centers is 2.94, which is approximately equal to both the mean of the color and the center of the single Gaussian fit. Thus, this fit essentially devolves to merely reproducing the single Gaussian case. However, since uni- and bimodal fits give similarly good results (see Figure 5.4), we will stay with the assumption of a unimodal $(V-H)$ color distribution and a corresponding mean color of $\langle V-H\rangle = 2.92$. We note that the situation changes drastically if we apply the selection by error limit. As we can see in Figure 5.2, the blue population ($V-H$ <2.4) is significantly diminished by the error limit, which makes it difficult to draw strong conclusions from the color distribution. The metallicity distribution is further investigated in Section 5.4.

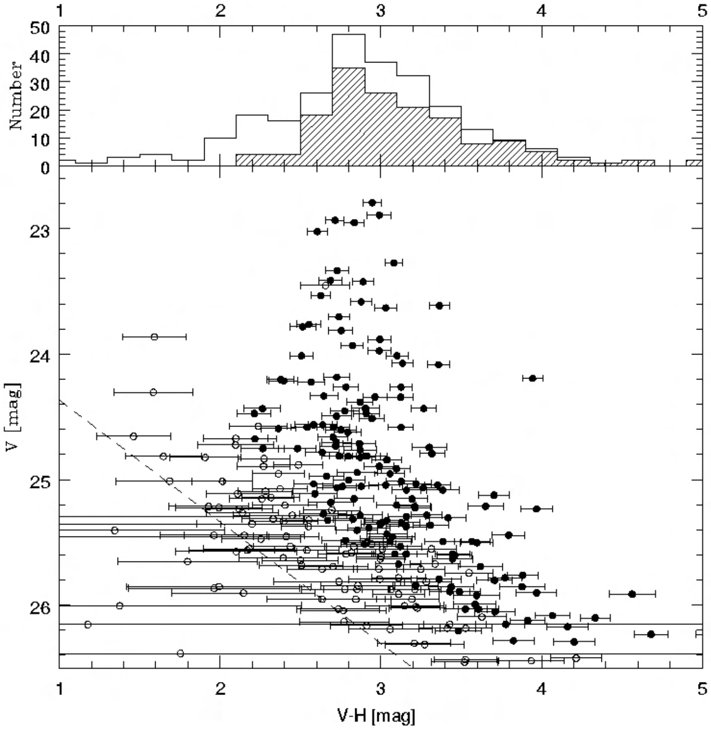

Fig. 5.2.— V *vs.* $(V-H)$ color-magnitude diagram for IC 4051. The top sub-panel shows the color distribution of all (open histogram) and error-selected (hashed histogram) objects. The lower sub-panel shows the color-magnitude diagram. Herein the filled symbols mark the selected clusters, while the open circles mark rejected objects. The dashed line marks the 50% completeness limit for the H-band.

With the discovery of bimodal color distributions in globular cluster systems (e.g. Whitmore & Schweizer 1995; Geisler, Lee & Kim 1996; Kundu & Whitmore 2001a; Gebhardt & Kissler-Patig 1999) the interest in the GCSs of early-type galaxies, which were supposedly old and uniform, grew immensely. The spatial distribution of GCs adds an extra clue to their origin. E.g., in the Galaxy, metal rich GCs are found to be more confined to the Galactic disk out to distances up to ∼10 kpc from the Galactic center (Searle & Zinn 1978), and metal-poor clusters are found at even larger distance but spherically distributed in the Galactic halo (Ashman & Zepf 1998). Although the near-infrared data for IC 4051 cover only the innermost region of IC 4051 (maximum distance ∼9 kpc) it is still worth investigating the radial distribution of the globular clusters mean colors. Figure 5.5 shows the distribution of globular cluster colors as a function of galactocentric angular distance R; we have listed the mean colors in $2''\!.5$ wide bins in Table 5.3. We note that there is no obvious trend in the mean colors. $V-H$ is primarily sensitive to metallicity, so this indicates the lack of any strong metallicity gradient in the IC 4051 GCS, for radial distances R$\leq 22''\!.5$.

Comparing the combined optical and near-infrared colors with SSP model isochrones (see

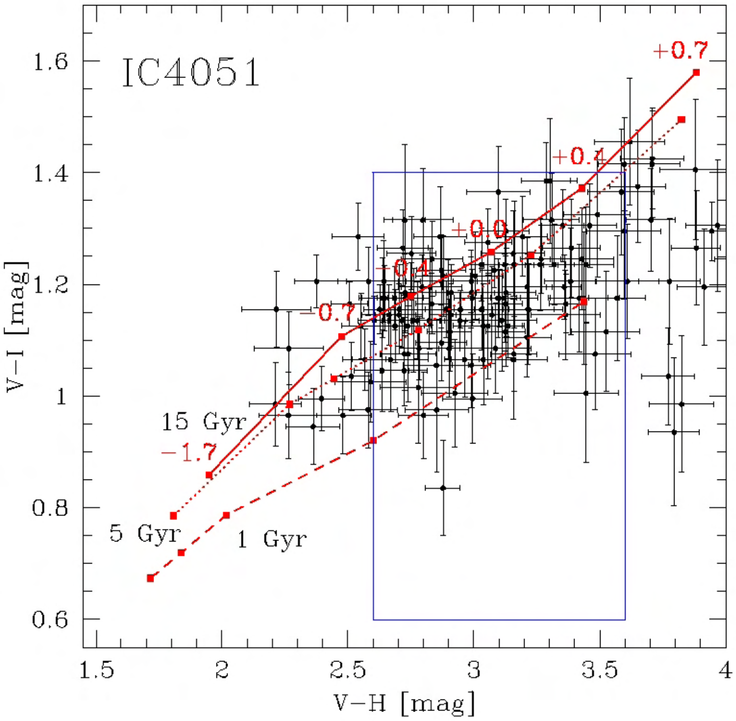

Fig. 5.3.— $(V-I)$ *vs.* $(V-H)$ color-color diagram for IC 4051. All data are corrected for foreground reddening (see Table 5.1). The 15 Gyr, 5 Gyr and 1 Gyr isochrones are based on the Bruzual & Charlot SSP models (Bruzual 2000). The solid squares mark the metallicity in [Fe/H], increasing with $(V-H)$ from -2.3 up to +0.7. The box marks the color range selected for the determination of the cumulative age distribution.

Figure 5.3) reveals that only a fraction of the red cluster population is consistent with an old (>10 Gyr) population. We find a large fraction of objects whose $(V-I)$ color at a given $(V-H)$ is too blue to fit into an "old" globular cluster scenario. Their color is much better matched by an intermediate age population (i.e. with an age between ∼1 and 7 Gyr). Such a large intermediate/young population of globular clusters seems suspicious, since the integrated galaxy light does not show any hint of a recent major star formation event and it is a relatively isolated galaxy. Although we will discuss the relative size of age sub-populations in the next section, we want to emphasize that only within the red sub-population is it possible to distinguish the age of globular clusters whereas the blue population should represent only the first generation, but deriving even crude age estimates for such clusters in very difficult. In Section 5.1 we mentioned a gas rich merger as a possible scenario to form a second generation of globular clusters, which requires a certain minimum galaxy density. IC 4051 is found somewhat outside the core of the Coma galaxy cluster, surrounded by numerous other galaxies, but not in the center of the gravitational potential of the galaxy cluster. However, additional evidence for a less passive evolution of this galaxy is the existence of a co-rotating galaxy

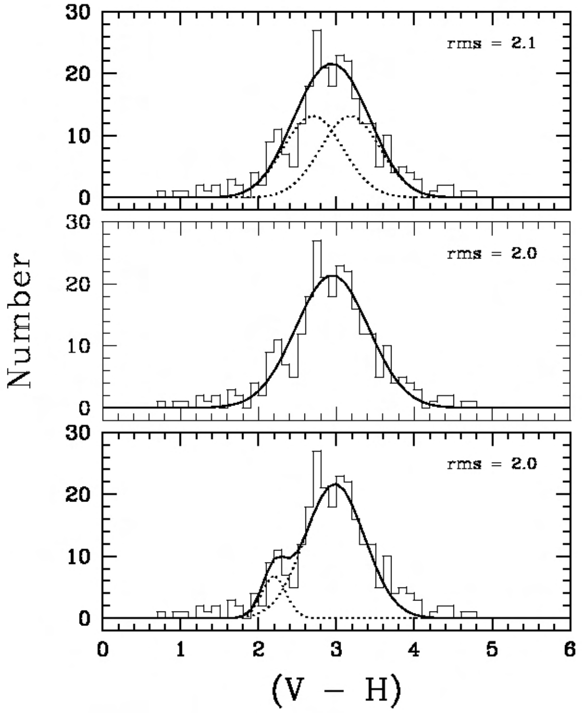

Fig. 5.4.— $(V-H)$ color distribution in the complete IC 4051 sample showing a single Gaussian fit (middle) and two different double Gaussian fits (top: equal amplitude/equal width, bottom: variable amplitude/variable width). The dotted lines mark the contribution of each individual component, solid lines are their sum.

core, which rotates at a different velocity from the main galaxy body. It is not known yet whether it is dynamically decoupled or not(Mehlert et al. 1998).

5.3.1.2 NGC 3311

The V *vs.* $(V-H)$ color-magnitude diagram (CMD) and $(V-I)$ *vs.* $(V-H)$ color-color diagram for NGC 3311 are presented in Figures 5.6 and 5.7. The histogram in the upper part of the CMD shows the color distribution of the complete sample as an open diagram, whereas the error selected sample is shown by the hatched histogram.

The color-color distribution in Figure 5.7 shows, that in addition to many old GCs, a large fraction of red globular clusters ($V-H > 2.4$) have a $(V-I)$ color which is too blue to be consistent with an old cluster population. A direct comparison to the SSP isochrones assigns those objects an age $\lesssim$5 Gyr. The possibility of a young/intermediate population of globular clusters formed in a merger was already discussed by Hilker (2002). Our near-infrared observations do not favor the second possibility, viz. an old and metal poor population. Interestingly, NGC 3311 contains a

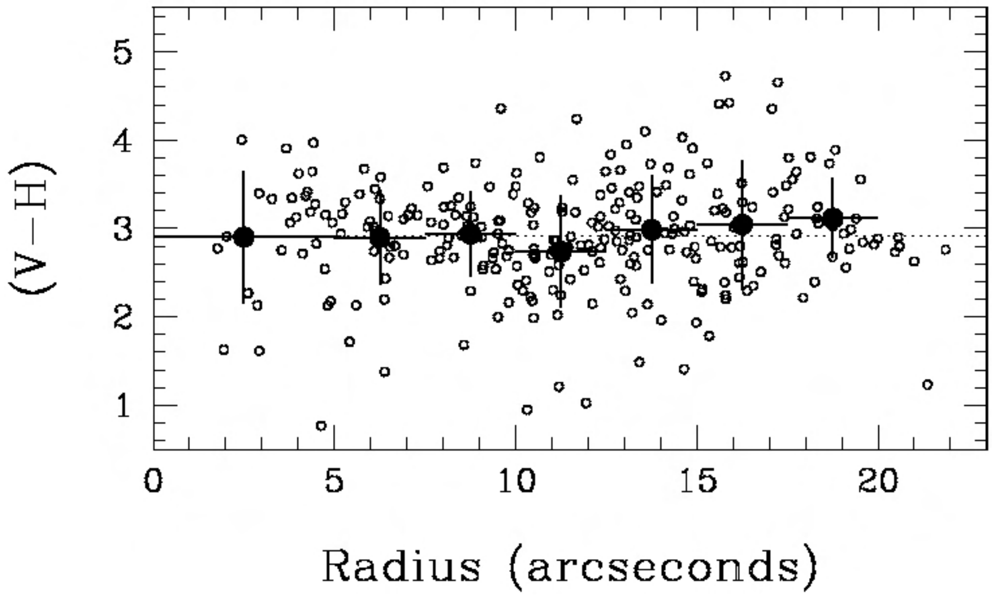

Fig. 5.5.— Distribution of globular cluster colors for IC 4051 as a function of radius from the center of the galaxy (open circles). The dashed line marks the mean value of the entire data set, ⟨V-H⟩=2.922 mag. The solid circles show the mean colors in increasing radius bins, as listed in Table 5.3.

prominent dust lane in its center (e.g. Västerberg, Jörsäter & Lindblad 1991; Grillmair et al. 1994), which adds further evidence to support a recent merging or accretion event. The dust content in the core of NGC 3311 was estimated as $10^{3.5}$ $M_\odot$ (Ferrari et al. 1999) based on V and R-band photometry. Grillmair et al. (1994) derived a lower limit of 4.6×10^4 $M_\odot$ for the total dust mass. Assuming a similar gas-to-dust ratio as found in the Galaxy, m_{gas}/m_{dust}~100 (Jura 1986; McNamara, Bregman & O'Connell 1990), the total gas and dust mass will reach at least $4.6\times10^6 M_\odot$. The globular cluster sample included in our analysis, however, refers only to the innermost region in NGC 3311. Additional near-infrared observations covering larger galactocentric radius will be necessary before any conclusion can be inferred from comparing our small central sample to the entire blue globular cluster population found by Hilker (2002).

5.3.2 Cumulative Age Distribution

Our technique to derive cumulative age distributions, as described in Hempel et al. (2003) and Hempel & Kissler-Patig (2004), is to help lift the age-metallicity degeneracy (Worthey 1994) via the combination of optical and near-infrared broad band colors. Hereby the higher sensitivity of infrared colors to metallicity as compared to age is utilized. An example of the comparison of the age and metallicity dependency of $(V-I)$ and $(V-K)$ ($\sim(V-H)$) can be found in Puzia

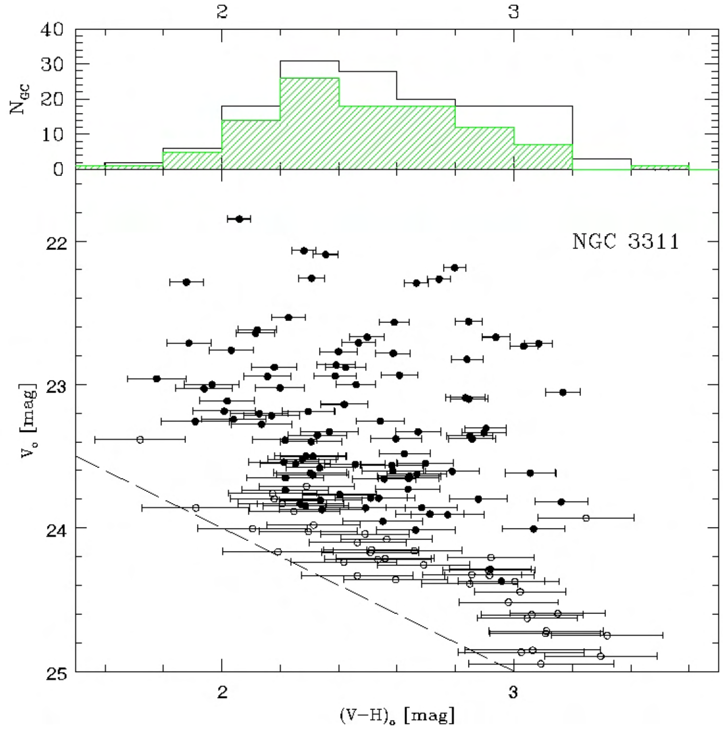

Fig. 5.6.— V $vs.(V-H)$ color-magnitude diagram for NGC 3311. The top sub-panel shows the color distribution of all (open histogram) and error-selected (hashed histogram) objects. The lower sub-panel shows the color-magnitude diagram. Herein the filled symbols mark the selected clusters, while the open circles mark rejected objects (by error cut). The dashed line marks the 50% completeness limit for the H-band, derived from the detection rate in artificial data sets using the Addstar routine in the IRAF package.

et al. (2002) and references therein. The cumulative age distribution is then defined as the percentage of objects **older than T Gyr**, and is derived by comparing their $(V-I)$ color with the SSP model prediction for a population that is **T Gyr** old. The lowest age bin is assigned to 0

Table 5.3. Mean Color versus Radius for IC 4051

Radius ($''$)	N	$\langle V-H \rangle$	σ_{V-H}
<5.0	30	2.901	0.745
5.0–7.5	28	2.897	0.530
7.5–10.0	41	2.938	0.478
10.0–12.5	51	2.737	0.635
12.5–15.0	51	2.984	0.612
15.0–17.5	38	3.044	0.724
17.5–20.0	25	3.114	0.451

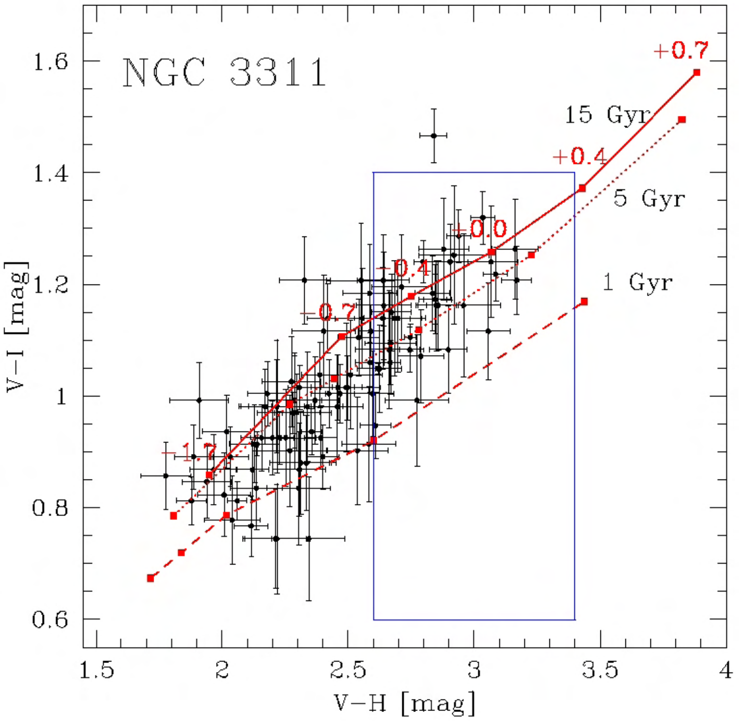

Fig. 5.7.— $(V-I)$ *vs.* $(V-H)$ color-color diagram for NGC 3311. The data obey the selection by photometric error cut (<0.15 mag) and are corrected for foreground reddening (see Table 5.1). As examples the 15 Gyr, 5 Gyr, and 1 Gyr isochrones, corresponding to the Bruzual & Charlot model isochrones (Bruzual & Charlot 1993; Bruzual 2000) are marked. The metallicity, rising from [Fe/H]=-2.3 to [Fe/H]=+0.7, is marked by solid squares. The color range selected for the determination of the cumulative age distribution is marked by the box. Compared to IC 4051 the $(V-H)$ color range is slightly shorter to fit the observed data.

Gyr since all globular clusters are older than 0 Gyr. With respect to a possible formation scenario of the GCSs and their host galaxies, we want to go one step further and set constraints on the age and the relative size of the cluster sub-populations. The method is based on the comparison between observed and simulated GCSs (Hempel et al. 2003; Hempel & Kissler-Patig 2004) via a χ^2 -test. To simulate the color distribution in GCSs and to derive the age distribution in simulated and observed systems, the SSP model isochrones of Bruzual & Charlot (2000) were again used. Examples for the simulated color-color diagrams and the resulting cumulative age distributions are shown in Figure 5.8. Instead of a step-function-like age distribution we find a much more gradual slope in the age distribution, which is mostly due to the fact that the $(V-I)$ colors in our simulations are not strictly independent from metallicity effects and, therefore, show a certain dependency on $(V-H)$. The final consequence is that even with a much improved age resolution of combined optical and near-infrared colors, the determination of accurate absolute ages for single globular clusters is still out of reach. Our intention is now to detect age sub-populations, to set constraints on their age and to find systematic effects of external parameters on the age structure. In nearby galaxies more precise age determinations can be derived from spectroscopic spot checks. For our simulations we assume a composition of two age sub-populations with ages ranging from 1, 2, 3, 5, 7, 10 and 13 Gyr. Hereby we vary the amount of young/intermediate age globular clusters between 100% and 0%. The χ^2- test finds the best fitting model with a given age and size ratio.

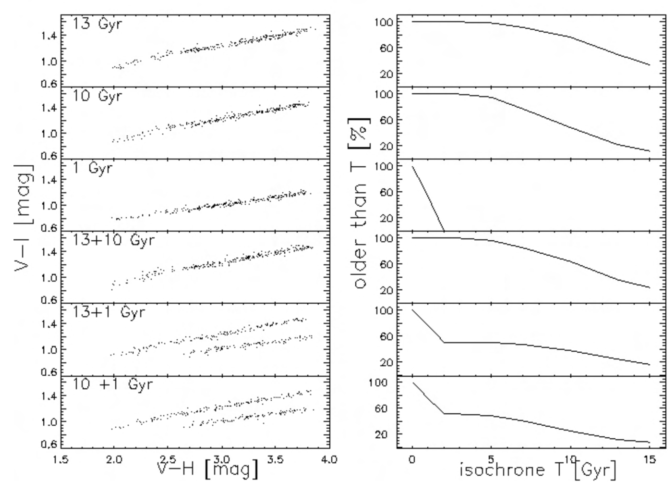

Fig. 5.8.— Simulated color-color diagrams (left) and the resulting cumulative age distribution (right) for various age combinations. The two populations are equally mixed between the old and intermediate age populations. The ideal colors, following the Bruzual & Charlot (2000) SSP models, were smeared randomly with an up to 3σ photometric error.

As shown in Sect. 5.3.1.2 and 5.3.1.1 the color-color diagrams give us a first indication for the existence of multiple age sub-populations in the GCSs of both NGC 3311 and IC 4051. If we compare the cumulative age distributions (Figure 5.9) with the simulation of a purely old system (see Figure 5.8, upper, right panel) the differences are obvious.

From Figure 5.9, the age distribution of the IC 4051 sample assigns ∼55% of the globular clusters to an age younger than 5 Gyr. In NGC 3311 this fraction is slightly smaller, ∼40%. Recall that this refers only to GCs with $V - H > 2.6$. Although the combination of optical and near-infrared colors helps lift the age-metallicity degeneracy, $(V - I)$ is still mildly affected by the metallicity. Combined with the scatter in both colors, induced by the photometric errors, and the relatively small sample size (IC 4051: 102 GCs, NGC 3311: 37 GCs), this results in an uncertainty with respect to the size estimate of the sub-populations. To overcome this obstacle we will not use the cumulative age distribution as a direct measure for the age structure in the GCSs, but rather compare the observations with the simulated systems via a χ^2- test. In this test we determine the difference between the cumulative age distribution in observed and simulated systems.

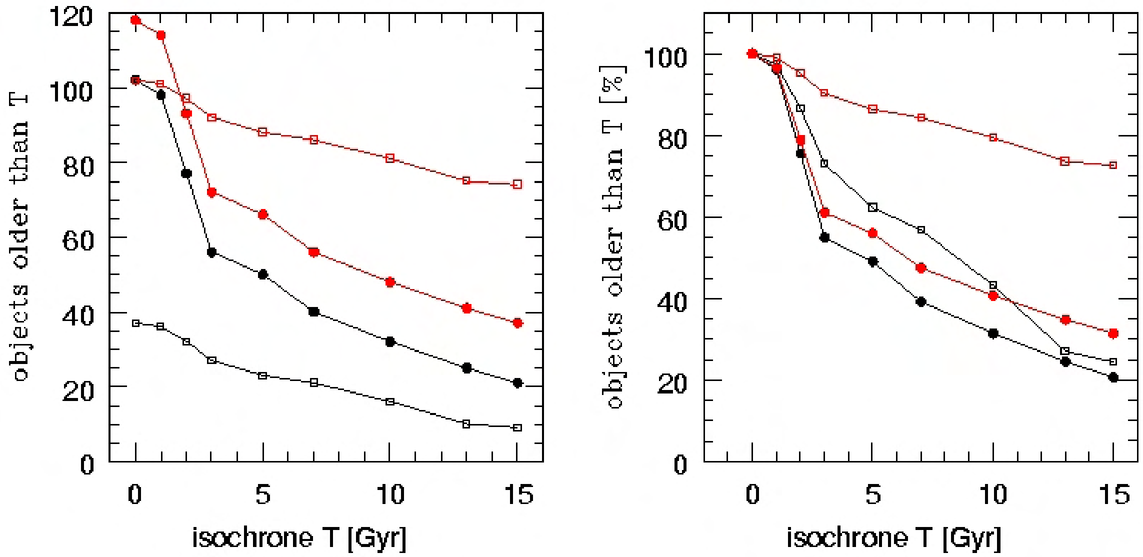

Fig. 5.9.— Cumulative age distribution (black line) in NGC 3311 (open squares) and IC 4051 (solid circles) derived following the procedure given in Section 5.3.2. The left panel shows the absolute numbers of globular clusters older than a given age. In the right panel the distribution was normalised with respect to the total number of objects found. If we assume the blue population of globular clusters ($(V-H)<2.6$) to consist of only 13 Gyr old objects the cumulative age distribution would change as shown by the red patterns.

Nevertheless, we still have to accept a certain degeneracy between age and size of sub-populations, which results in a finite accuracy with respect to the best fitting model. Since the major goal of this project is to detect age sub-populations and set some constraints on their age, it is of no importance here (and impossible for us to detect) whether the second generation of globular clusters is 2 or 3 Gyr old and contains 30 or 40 % of the globular cluster sample. Especially in the case of NGC 3311 with its small number of selected globular clusters, the size estimates of the sub-populations will be very uncertain, mostly due to stability problems in the χ^2- test.

The results of these χ^2 tests are presented in Figures 5.10 and 5.11. The χ^2 test results find the best fitting model to the age distribution in both GCSs to be a composite of an old population and a second population which is ∼10 Gyr younger. In both galaxies, the best fitting model to the age distribution suggests approximately 40% to 60% intermediate age clusters, with a larger fraction of younger clusters in IC 4051 than in NGC 3311. Such a surprisingly large fraction of young/intermediate globular clusters, also found in NGC 4365 and NGC 5846 (Hempel & Kissler-Patig 2004), needs confirmation and careful investigation, especially since such large fractions of young stars should be visible in the integrated light, but are not detected yet.

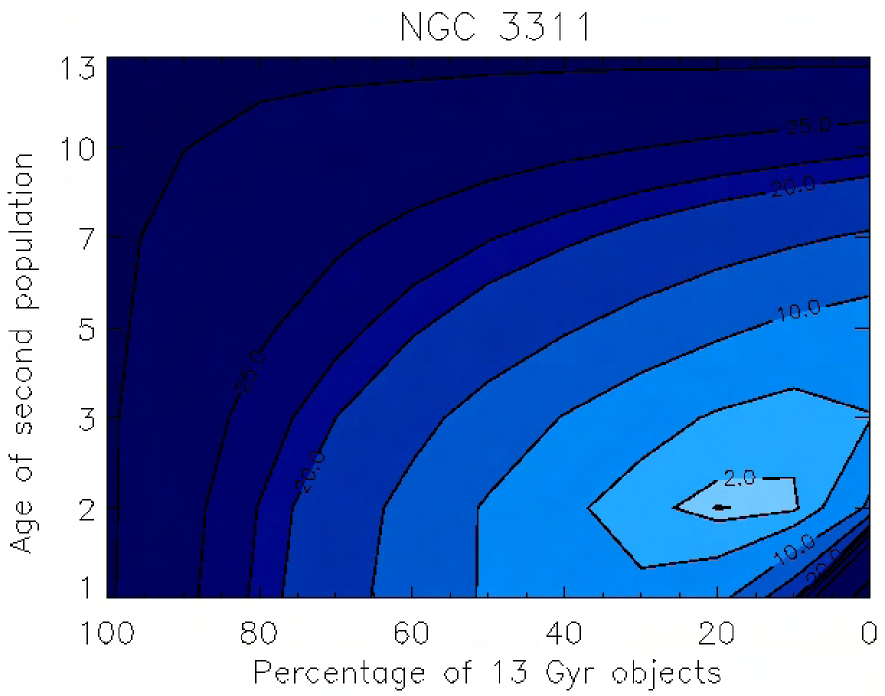

Fig. 5.10.— χ^2- test result for NGC 3311. Different levels represent the reduced χ^2 of the comparison between the cumulative age distribution in NGC 3311 and various models. The best fitting model consists of $\sim$ 40% intermediate age globular clusters and ~60% of 13 Gyr old objects. The large size of this young population is surprising and is discussed in Section 5.5.

Factors which affect the results include:

- **Firstly**, we have to consider that the sample used in our analysis is color-selected, so only objects with $2.6 \leq (V - H) \leq 3.6$ and $0.6 \leq (V - I) \leq 1.4$ are used. The lower limit to $(V - H)$ is set due to the small color differences in the SSP models. The blue, metal-poor population of globular clusters will mostly contribute to the old sub-population and change the size ratio between old and young population in favor of the first generation objects. The upper limit, as well as the $(V - I)$ interval, is set to avoid significant contamination of our sample with background galaxies (Puzia et al. 2002). Especially the $(V - H)$ blue fraction, supposedly old globular clusters, will affect this result and shift the ratio between old and young/intermediate age globular clusters to higher values. However, as shown in Figure 5.9, even in the extreme case where all GCs bluer than $(V - H)$=2.6 are old, 13 Gyr old clusters, the mean GC age, at least in IC 4051, only changes from ~6.5 to~8.5 Gyr and there remains a substantial fraction of young/intermediate age clusters.

- **Secondly**, we have to be aware of spatial bias effects. Due to the small NICMOS field of

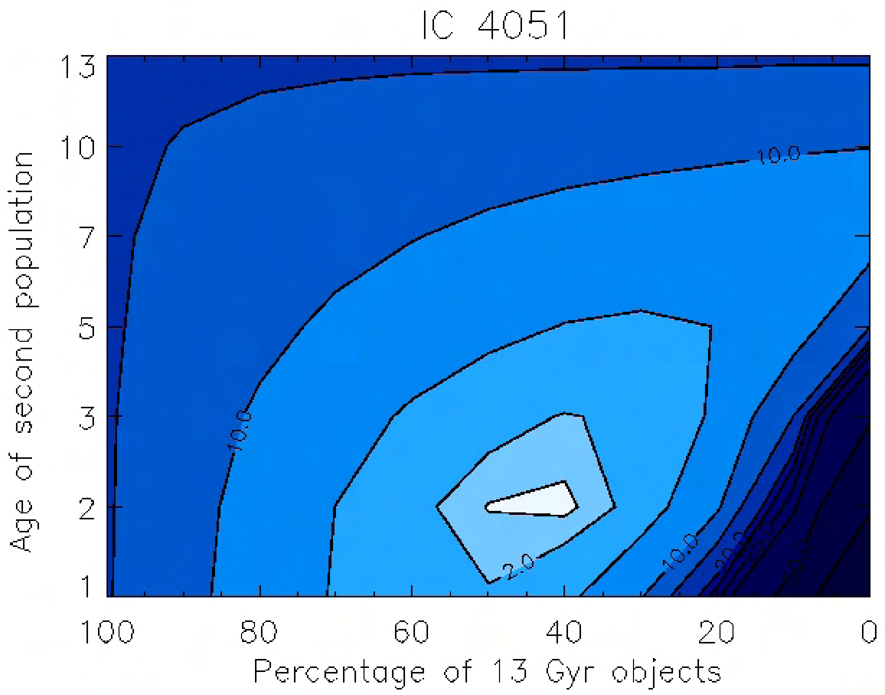

Fig. 5.11.— The comparison between the age distribution in IC 4051 and the simulated systems again (as in Figure 5.10) reveals a large fraction of young/intermediate age objects (>∼50), with the population of second generation globular clusters slightly larger than in NGC 3311.

view, centered on the galaxy, it covers only the innermost region of NGC 3311 and IC 4051. As observed by Schweizer & Seitzer (1998) and simulated by Hibbard & Mihos (1995) for the merger remnant NGC 7252, the central region of a galaxy is where one would expect to find the second generation of globular clusters, if they are indeed formed during a merger or accretion event. Although mostly born in the tidal tails (Li, Mac Low & Klessen 2004) of a merger, these star clusters will funnel toward the center of the merger remnant within several 100 Myr up to 1 Gyr (Hibbard & Mihos 1995). Our samples are therefore spatially biased and the fraction of young/intermediate age globulars should be overestimated, compared to the global fraction over the entire galaxy.

- **Thirdly**, small number statistics will affect the χ^2- test. As shown in Hempel & Kissler-Patig (2004) the results of this test become unstable (i.e. show multiple best fitting age/size combinations) for small data sets. Previous tests have shown that $\gtrsim$100 objects are needed to obtain reliable results. Strictly speaking this condition is only (barely) achieved in the IC 4051 sample. Recall that the total sample of IC 4051 and NGC 3311 contain 256 and 148 objects, respectively, but after applying the selection criteria (photometric error and color cuts) only 102 (IC 4051) and 37 (NGC 3311) objects contribute to the age distributions.

Although the presence of a significant population of young/intermediate age globular clusters in NGC 3311 agrees with various other features of the galaxy (e.g. central dust lane) more data are required for a solid argument.

5.4 Metallicity Distribution

In the framework of galaxy formation and evolution studies the age structure of the galaxy and its GCS plays a major role hence our main interest is focused on the age structure. Nevertheless, since the latter is determined by using SSP model isochrones, which combine age and metallicity predictions, it is necessary to test to what degree age and metallicity effects are still entangled. In the following we present the results of rough metallicity estimates based on the derived age structure.

A 2 Gyr old stellar population, with a $(V-H)$ color between $2.6 \leq (V-H) \leq 3.6$, i.e. consistent with the color limits set for the determination of the age distribution, contains objects with metallicities between [Fe/H]=+0.09 and [Fe/H]=+0.56, respectively. Assuming a mean color of $(V-H)$=3.1 we obtain [Fe/H]=+0.44, using the Bruzual & Charlot models (Bruzual 2000). Although, as shown in Figure 5.11, the best fitting model consists of a 2 Gyr old second globular cluster population, the age uncertainty allows as well a slightly higher age, i.e. ∼5 Gyr. In this case the metallicity of objects in the same color range lies between [Fe/H]=-0.21 and +0.59, with a mean value of [Fe/H]=+0.28 for $(V-H)$=3.1. As we will show, this corresponds closely to the mean metallicities determined for the young/intermediate GCs in IC 4051. Since the metallicity depends quite strongly on the derived age (more than the other way around) and although we can detect age sub-populations and set constraints on the age, the age uncertainty allows a large variety of metallicities. The following discussion about the metallicity distribution has to be seen in the light of this persistent degeneracy between age and metallicity.

With the introduction of combined optical and near-infrared observations we are able to investigate the metallicity distribution approximately independently from the age structure, with the above caveats. In order to derive globular cluster metallicities we use the above-derived information about the age structure in the observed globular cluster sample (see Figures 5.10 and 5.11). The results in Section 5.3.2 tell us that the age structure in both systems is well matched by a mix of a 13 Gyr old population with globular clusters which are ∼10 Gyr younger. The determination of the metallicity distribution follows the procedure given below and applies the Bruzual & Charlot (2000) SSP model isochrones.

- We split the globular cluster sample (selected by photometric error) with respect to the $(V-H)$ color into a blue ($(V-H)< 2.6$) and presumably old population and a second, red ($2.6 < (V-H)$) sub-population, containing both old as well as young/intermediate globular clusters. In addition we set an upper limit of $(V-H)\leq 3.6$ to avoid strong contamination with background galaxies (Hempel & Kissler-Patig 2004).

- For globular clusters found in the blue sub-population, the metallicities (given as $Z/Z_\odot$) were calculated by interpolating the metallicity-$(V-H)$ correlation of the 13 Gyr model isochrone.

- Corresponding to the age structure, we found that the red sub-population is split into old and intermediate/young populations, and use the 5 Gyr model isochrone for the latter. All objects with $(V-I) \leq (V-I)_{5\ Gyr}$ are then assumed to form the second generation of globular clusters. Although the comparison of the cumulative age distributions to simulated GCSs assigns the intermediate/young objects to an age of ∼2 Gyr, we allow an age uncertainty of 3 Gyr, based on the χ^2 contours, and set the age split at 5 Gyr.

- The metallicity is then determined by interpolating $Z/Z_\odot$ at $(V-H)_{GC}$ using the 13 Gyr and 2 Gyr isochrones (Figures 5.12 and 5.13, left panels). For comparison we also derive the metallicity distributions assuming a purely old globular cluster population (Figures 5.12 and 5.13, middle panels) and for mixed GCSs containing 13 Gyr and 5 Gyr old objects (Figures 5.12 and 5.13, right panels). In both Figures the upper panels give the metallicities on a linear scale, whereas the lower panels refer to [Fe/H] values.

- The metallicity estimates depend strongly on the age structure and are therefore also hampered by bias effects (see Section 5.3.2). The case of NGC 3311 suffers from small-number statistics, which makes the results of the χ^2-test statistically unstable. Nevertheless, the comparison of the $(V-H)$ colors, seen in Figures 5.3 and 5.7, shows that NGC 3311 lacks the most metal rich globular clusters found in IC 4051. Due to the above uncertainty for NGC 3311 we will concentrate on the GCS in IC 4051.

In the discussion about the bimodality of metallicity distributions we want to emphasize the importance of the chosen scaling. It is interesting to note that the metallicity distribution for a purely old (13 Gyr) population seems to suggest a bimodality in the [Fe/H] distribution for the IC 4051 GC, which is NOT seen if we transform the GC metallicities into linear abundances. However, if we fit the [Fe/H] distribution by either a double or a single Gaussian, as shown in the middle panels in Figure 5.14, the resulting χ^2 of the fit is found to be χ^2=1.67 and 1.57 for the double and single Gaussian, respectively, virtually identical. Hence there is no strong evidence for bimodality in the metallicity distribution, which considers all clusters as old. Although a bimodal distribution is not favored over unimodality in the 13 Gyr old population, it becomes obvious in mixed globular cluster systems (see upper and lower panel in Figure 5.14).

Since we find objects within a wide range of metallicities applying a logarithmic scaling, as given in the distribution of the [Fe/H] values, increases the chances for detecting metallicity populations. In the linear Z space formerly clearly detected [Fe/H]-populations are much more spread and may not be detected anymore, i.e. in smaller samples or in globular cluster populations with a smaller age difference. The metallicity distribution given in $Z/Z_\odot$ for a 13 + 5 Gyr old population is widely spread, but not as clearly bimodal as in the case of a 13 + 2 Gyr old sample.

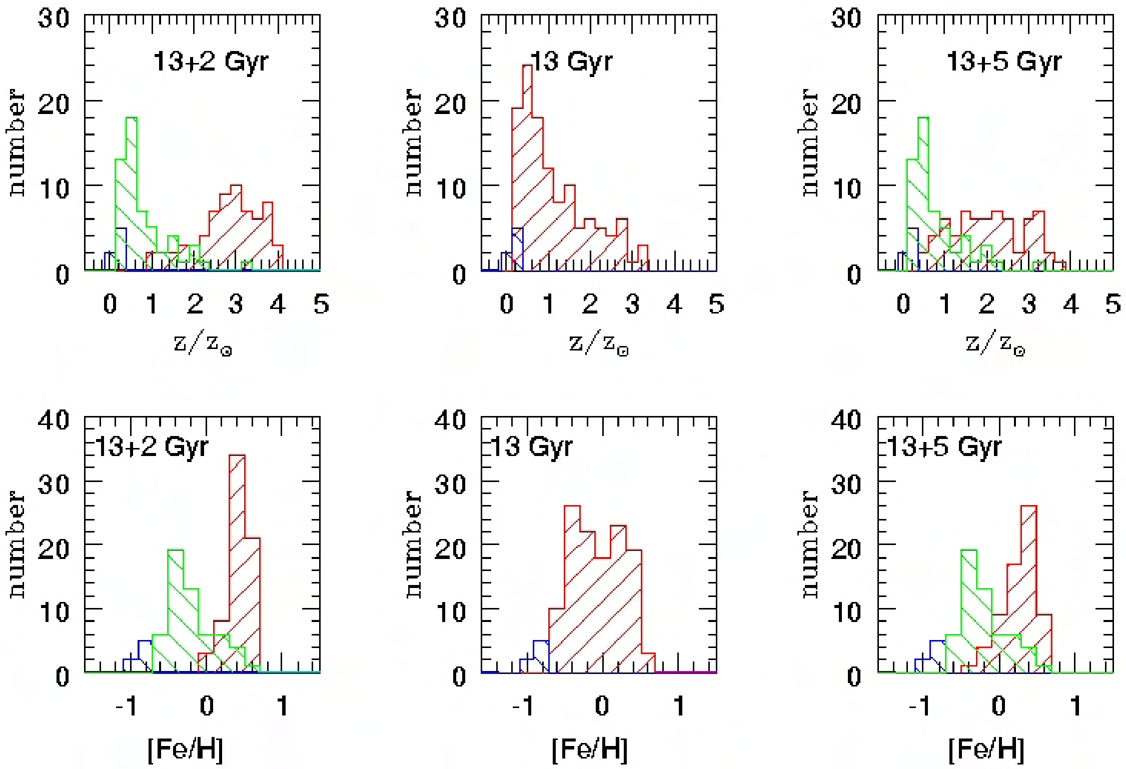

Fig. 5.12.— Metallicity distribution in IC 4051 assuming different GC distributions. We show the metallicity distribution both in terms of linear metal abundance (upper panel) as well as in logarithmic metallicity [Fe/H] (lower panels). In the left panels the metallicity distribution is based on the assumption of a 2 and 13 Gyr old population (following the best fit model from the age distribution), whereas the central panel assumes all clusters to be 13 Gyr old. We also show the metallicity distribution assuming the young/intermediate globular clusters to be 5 Gyr old (right panel). The color coding of the histograms is as follows; red: young and metal rich, green: old and metal rich, blue: old and metal-poor.

We caution that a bimodal color distribution does not necessarily translate into a clear bimodal metallicity or linear abundance distribution (see also Kissler-Patig 2002).

The mean metallicity based on the $(V-I)$ colors alone and a unimodal color distribution (Woodworth & Harris 2000) was determined to be $\langle$Fe/H$\rangle$=-0.1 or Z/Z$_\odot$=0.8. Based on the central panels of Figure 5.12, a 13 Gyr old population in IC 4051 would have a mean metallicity of $\langle$Fe/H$\rangle$$\sim$+0.06, working with the more metal sensitive $(V-H)$ color. For a composite GCS, the mean metallicity of the 2 Gyr old population is derived as $\langle$Fe/H$\rangle_{2Gyr}$=+0.48, with $\langle$Fe/H$\rangle_{13Gyr}$=-0.82 and -0.1 for the metal-poor and metal-rich old population. Assuming 5 Gyr as the age of the intermediate age population, the results change only marginally to $\langle$Fe/H$\rangle_{5Gyr}$=+0.30, with a larger metallicity spread. The metallicities derived for the metal-rich populations in either case are very high; compared to observed spectroscopic metallicities for other second generation GCs (e.g. Schweizer & Seitzer 1998, Goudfrooij et al. 2001a, Goudfrooij et al. 2001b) and must be regarded as very tentative. Several issues have to be discussed here, which all affect the derived metallicity distribution.

- Again, the basic requisite to derive globular cluster metallicities is an accurate age determination. Although the combined optical and near-infrared photometry allows us to derive the mean age of sub-populations, the age-metallicity degeneracy is not entirely broken. Even more important, for a given $(V-H)$-bin the derived metallicity depends on the SSP isochrone. Thus applying the mean age of sup-populations to calculate individual metallicities causes additional systematic errors.

- In our analysis we use the SSP model isochrones by Bruzual & Charlot (Bruzual & Charlot 1993; Bruzual 2000). If we compare the age predictions of these models with Vazdekis (1999) or Maraston (2001) then we find considerable differences, especially within the red populations. Following the Bruzual & Charlot models a 5 Gyr old object would by ~0.1 mag redder in $(V-I)$ compared to the Vazdekis models, given the same $(V-H)$. This discrepancy

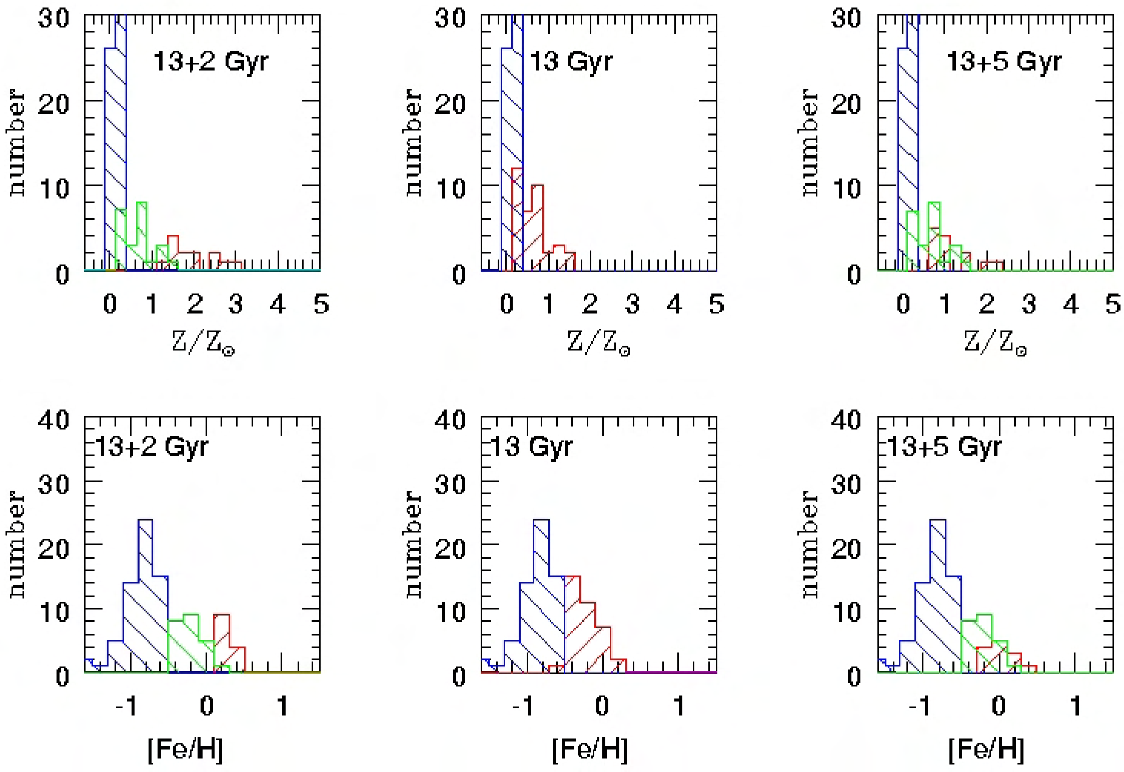

Fig. 5.13.— Metallicity distribution in NGC 3311 assuming different age distributions. We apply the same color coding and method for displaying the abundance distribution as in Figure 5.12.

has only little effect on the mean ages of globular cluster sub-populations as long as we apply identical SSP models for the age determination in observed and simulated samples and do not attempt to derive ages of individual clusters. Nevertheless, the metallicity is considerably affected. To quantify this effect we will repeat the analysis, i.e. the determination of the

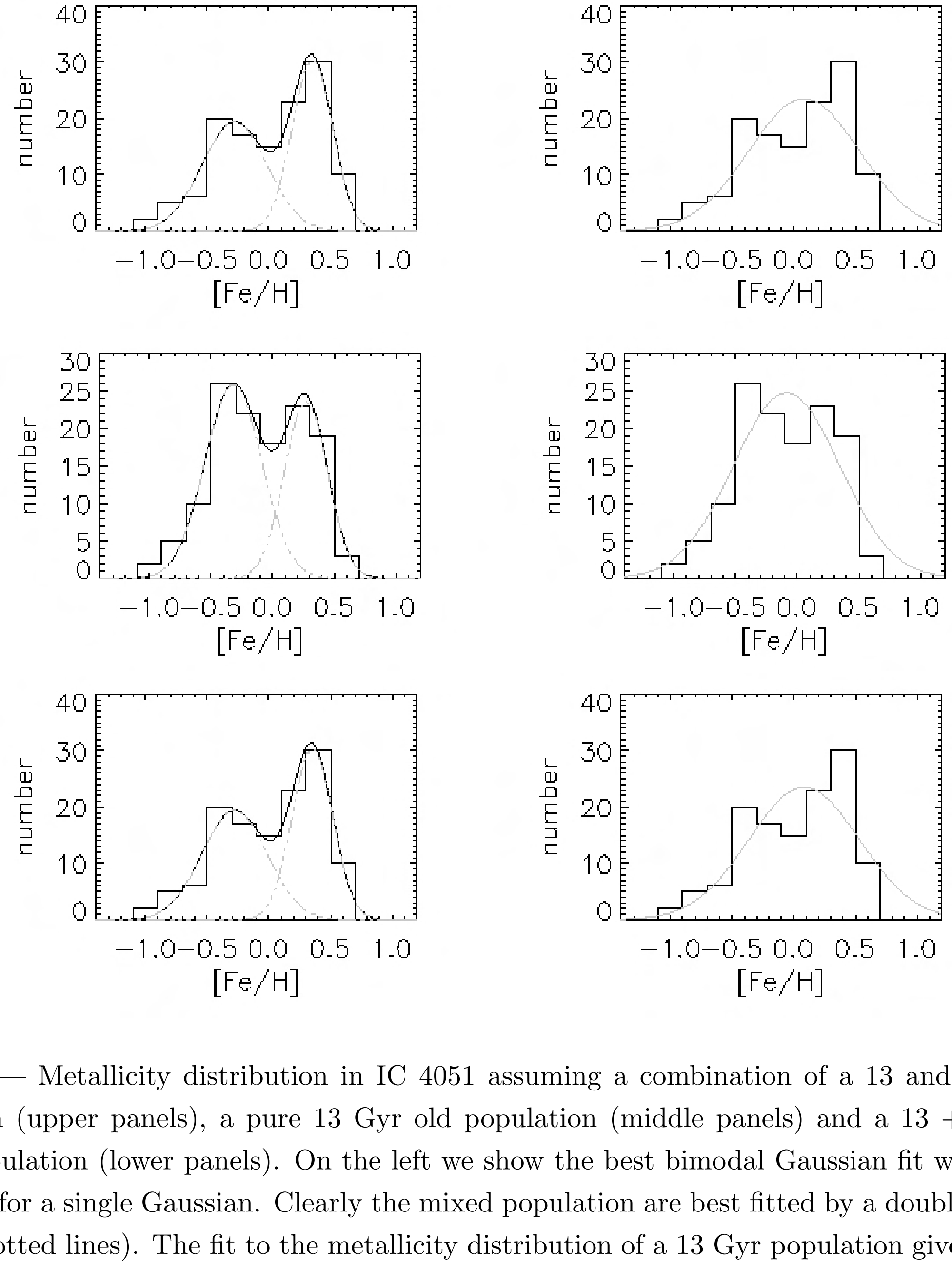

Fig. 5.14.— Metallicity distribution in IC 4051 assuming a combination of a 13 and 2 Gyr old population (upper panels), a pure 13 Gyr old population (middle panels) and a 13 +5 Gyr old mixed population (lower panels). On the left we show the best bimodal Gaussian fit while on the right that for a single Gaussian. Clearly the mixed population are best fitted by a double Gaussian (dashed-dotted lines). The fit to the metallicity distribution of a 13 Gyr population gives similarly good results for a single and a double Gaussian, although the χ^2 of the fit is slightly better for a single Gaussian. In the left panel the dashed-dotted lines shows the two Gaussian whereas the solid line shows their combination.

cumulative age distribution and the modeling procedure using the SSP model isochrones by Vazdekis. The results will be presented in a subsequent paper.

- In Paper IV of this series (Hempel & Kissler-Patig 2004) the contamination of the globular cluster sample with unresolved background galaxies has been discussed. Although we try to limit the contamination by setting upper limits on $(V-H)$ and $(V-I)$ we can not entirely exclude it. These color limits are derived from the SSP model isochrones, assuming a maximum GC age of 15 Gyr and a maximum metallicity of $2.5 \times Z_{\odot}$ for the younger generation of GCs..

5.5 Summary

We have investigated the age structure of GCs in two luminous early-type galaxies, IC 4051 and NGC 3311, each with large GC populations, using the combination of optical and near IR colors to help break the age-metallicity degeneracy. In both galaxies, we find evidence for a significant fraction of young/intermediate age clusters (≈2- 5 Gyr), in addition to their old counterparts, by comparing the observed color distribution with models. The comparison between the observed and simulated systems hints at a second major star formation event in the recent past of both galaxies. Further evidence for a less passive evolution of the galaxies is given by independent features (dust lanes, co-rotating core), but especially in NGC 3311, the effects of small number statistics make our results tentative. Based on the small number of objects in this sample, our detected fraction of 40– 50% of young globular clusters in the total GCS in NGC 3311 has a large uncertainty. The results for IC 4051 are more statistically reliable, suggesting more than half of the globular clusters are young/intermediate age objects. This fraction should be regarded as an upper limit, considering that most of the GCs excluded from the age analysis are probably mainly old, and that our observations are biased to the central regions, where younger objects should preferentially be found. Thus, at this stage the global importance of the star forming event leading to a second generation of globular clusters in NGC 3311 and IC 4051, cannot be firmly established. Nevertheless, the improved age resolution of combined optical and near-infrared photometry reveals age sub-populations, which could not be detected using optical data alone.

Acknowledgments

Support for this work was provided by NASA through grant number GO-07280 from the Space Telescope Science Institute, which is operated by the Association of Universities for Research in Astronomy, Inc., under NASA contract NAS5-26555. K.Mighell kindly provided advice concerning the CCDCAP package. D.G. would like to thank Nick Suntzeff and Malcolm Smith of the staff of Cerro Tololo Inter-American Observatory for their kind support of this project. D.G. gratefully acknowledges support from the Chilean *Centro de Astrofísica* FONDAP No. 15010003.

References

Ashman, D.M. & Zepf, S.E. 1998,”Globular Cluster Systems”, Cambridge University Press

Barmby, P., Huchra, J.P., Brodie, J.P., et al. 2000, AJ, 119, 727

Baum, W.A., Hammergren, M. Thomsen, B. et al. 1997, AJ, 113, 1483

Bertin, E., Arnout, S. 1996, A&AS, 117, 393B

Brodie, J.P., Larsen, S., Kissler-Patig, M. 2000, ApJ, 543, L19

Bruzual, G.A.& Charlot, S. 1993, AJ, 405,538

Bruzual, G.A. 2000, private communication

Bruzual, G.A.,& Charlot, S. 2003, MNRAS, 344, 1000

Cohen, J.G. & Matthew, K. 1994, AJ, 108, 128

deVaucoleurs, G., deVaucouleurs, A., Corwin, H.G.et al. 1991, “Third Ref.Catalogue of Bright Galaxies”, Springer New York

Dickinson, M., Sosey, M., Rieke, M. et al. 2002, ”NICMOS Photometric Calibration”, in the proceedings of the “2002 HST Calibration Workshop”, Space Telescope Science Institute, Baltimore, Maryland, 17./18.10. 2002, eds. Santiago Arribas, Anton Koekemoer, and Brad Whitmore, 233

Ferrari, F., Pastoriza, M.G., Macchetto, F. et al. 1999, A&ASS, 136, 269

Gebhardt, K., & Kissler-Patig, M. 1999, AJ, 118, 1526

Geisler, D., Lee, M.G., & Kim, E. 1996, AJ, 111, 1529

Goudfrooij, P., Mack, J., Kissler-Patig, M. et al. 2001, MNRAS, 322, 643

Goudfrooij, P., Alonso, M.V., Maraston, C. et al. 2001, MNRAS, 328, 237

Grillmair, C.J., Faber, S.M., Lauer, T.R. et al. (1994), AJ, 108, 102

Harris, W.E.,& van den Bergh, S. 1981, AJ, 85, 1627

Harris, W.E., Smith, M.G., Myra, E.S. 1983, ApJ, 272, 456

Harris, W.E. 1991, ARA&A, 29, 543

Harris, W.E. 2001, in Star Clusters, Saas-Fee Advanced Course 28, Swiss Society for Astrophysics and Astronomy, ed. L.Labhardt & B.Binggeli (Berlin: Springer-Verlag), 223

Hempel, M., Hilker, M., Kissler-Patig, M. et al. 2003, A&A, 405, 487, Paper III

Hempel, M. & Kissler-Patig, M. 2004, A&A, 419, 863, Paper IV

Hibbard, J.E. & Mihos, J.C. 1995, AJ, 110, 140

Hilker, M. 2002, Hilker, M. 2002, In: Proceedings of the IAU Symp. 207 "Extragalactic Star Clusters", eds. D. Geisler, E.K. Grebel, & D. Minniti; San Francisco: ASP, 281

Hilker, M. 2003, in "New Horizons in Globular Cluster Astronomy", eds. G. Piotto, G. Meylan, G. Djorgovski, & M. Riello, ASP Conf. Ser., 296, 583

Hilker, M. 2003, Hilker, M. 2003, in ESO Astrophysics Symposia, "Extragalactic Globular Cluster Systems", ed. M. Kissler-Patig, Springer, 173

Holtzman, J.A., Burrows, C.J., Casertano, S. et al. 1995, AJ, 107, 1065

Jensen, J.B., Tonry, J.L., Thomson, R.I. et al. 2001, ApJ, 550, 503

Jura, M. 1986, ApJ, 306, 483

Kissler-Patig, M. 2002, IAU Symp.207, 207

Kissler-Patig, M., Brodie, J.B., & Minniti, D. 2002, A&A, 391, 441, Paper I

Kundu, A.& Whitmore, B.C. 2001, AJ, 121,2950

Kundu, A.& Whitmore, B.C. 2001, AJ, 122, 1251

Kuntschner, H., Smith, R.J., Colless, M. et al. 2002, MNRAS, 337, 172

Larsen, S., Brodie, J.P., Beasley, M.A. et al. 2003, ApJ, 585, 767

Li, Y., Mac Low, M.-M., Klessen, R.S. 2004, ApJ, submitted, (astro-ph/0407248)

Malhotra, S. 2002, "NICMOS Instrument Handbook", Version 5.0 (Baltimore: STScI)

Maratson, C., Greggio, L., Thomas, D. 2001, Ap&SS, 276, 893

McLaughlin, D.E., Secker, J., Harris, W.E et al. 1995, AJ, 118, 1033

McNamara, B.R., Bregman, J.N.,& O'Connell, R.W. 1990, AJ, 360, 20

Mehlert, D., Saglia, R. P., Bender, R. et al. 1998, A&A, 332, 33

Mighell, K.J., Rich, R.M. 1995, AJ, 110, 1649

Minniti, D., Alonso, M.V., Goudfrooij, P. et al. 1996, ApJ, 467, 221

Puzia,T.H., Zepf, S.E., Kissler-Patig, M.et al. 2002, A&A, 391, 453, Paper II

Puzia, T.H., Kissler-Patig, M., Thomas, D. et al. 2004, A&A, 415, 123

Puzia, T.H., Kissler-Patig, M., Thomas, D. et al. 2004, A&A, submitted

Searle, L. & Zinn, R. ApJ, 225, 357

Secker, J., Geisler, D., McLaughlin, D.E. et al. 1995, AJ, 109, 1019

Schlegel, D.A., Finkbeiner, D.P., Davis, M. 1998, ApJ, 500,525

Schweizer, F. & Seitzer P. 1998, AJ, 116, 2206

Stephens, A.W., Frogel, J.A., Ortolani, S, et al. 2000,AJ, 119,419

Thomas, D., Maraston, C.,& Bender, R. 2003, MNRAS, 339, 897

Thomas, D., & Maratson, C. 2003, A&A, 401, 429

Tully, B. 1988, “Nearby galaxies catalog”, Cambridge University Press

Västerberg, A.R., Jörsäter, S., & Lindblad, P.O. 1991, A&A, 247, 335

Vazdekis, A. 1999, ApJ, 513, 224

Vazdekis, A., Cenarro, A.J., Gorgas, J. et al. 2003, MNRAS, 340, 1317

Whitmore, B.C. & Schweizer, F. 1995, AJ,

Wielen, R. (ed.) 1990, Dynamics and Interactions of Galaxies, Springer Verlag

Woodworth, S.C., Harris, W.E. 2000, AJ, 119, 2699

Worthey, G. 1994, ApJS, 95, 107

Zepf, S. & Ashman, D. 1993, MNRAS, 264, 611

6 Influence of the various Single Stellar Population models

6.1 Introduction

Besides high quality photometric data in optical and near-infrared passbands the basic tool in our approach towards the age structure in globular cluster systems are Single Stellar Population models. In the recent past various models have become available (see Chapter) and are now widely used to drive not only the ages but the metallicity and element abundances as well. In this chapter we investigate in how far our choice of a Single Stellar Population model affects the derived age distribution for globular cluster systems. As stated in Chapter 2.6 we find systematic differences in the color prediction for a stellar population of a given age mostly in the red cluster population, which we use to derive the age distribution. Therefore, in order to either exclude a model dependent age distribution or to evaluate the influence of the SSP model, we apply not only the Bruzual & Charlot SSP models (Bruzual & Charlot 1993Bruzual 2000,Bruzual & Charlot 2003) but also the SSP models by Vazdekis (1999) and Maraston (2001) to the photometric data of various globular cluster systems. As in Chapter 2.6 we want to emphasize that the comparion between the different models is by no means a quality judgement but rather a consistency test of our new method to evaluate the age structure in globular cluster systems.

6.2 Comparison Single Stellar Population Models

In Chapter 1.2.4 the model dependency has been tested on the SSP models by Bruzual and Charlot (Bruzual 2000) and Vazdekis (1999) assuming the first generation of globular clusters to be 15 Gyr old. Since we decided to set *old=13 Gyr* we will present the new χ^2-test results for the Vazdekis models and the Maraston (2001) model in addition to Bruzual & Charlot (2000) presented in the previous chapters. The cumulative age distributions calculated for the simulations can be found at the end of this chapter.

The SSP models by Maraston differ from the Bruzual & Charlot or Vazdekis model by implementing the fuel consumption theorem (see Section 1.2.2.3) and thus we want to include them in our comparison. Unfortunately the Maraston SSP model isochrones for ages below 3 Gyr intersect and for a given $(V-I)$-$(V-K)$ color combination there exist various age- metallicity combinations. Therefore we are unable to differentiate ages below 3 Gyr. Since the various SSP models differ in the secondary $(V-I)$ mostly for the metal-rich population, where we expect to find the intermediate/young globular cluster population, the cumulative age distribution for a given globular cluster system will vary, as clearly seen in Figures 3.9 and 6.1 for the Bruzual & Charlot, Vazdekis and Maraston models. The different age spread for a $(V-I)$ interval leads to serious consequences for the stability of the χ^2-test. With an decreasing number of globular clusters in the available sample the χ^2-test becomes less and less stable. The effect of number statistics on the χ^2-test has been demonstrated for the Bruzual & Charlot SSP model in chapter 1.2.4 and becomes

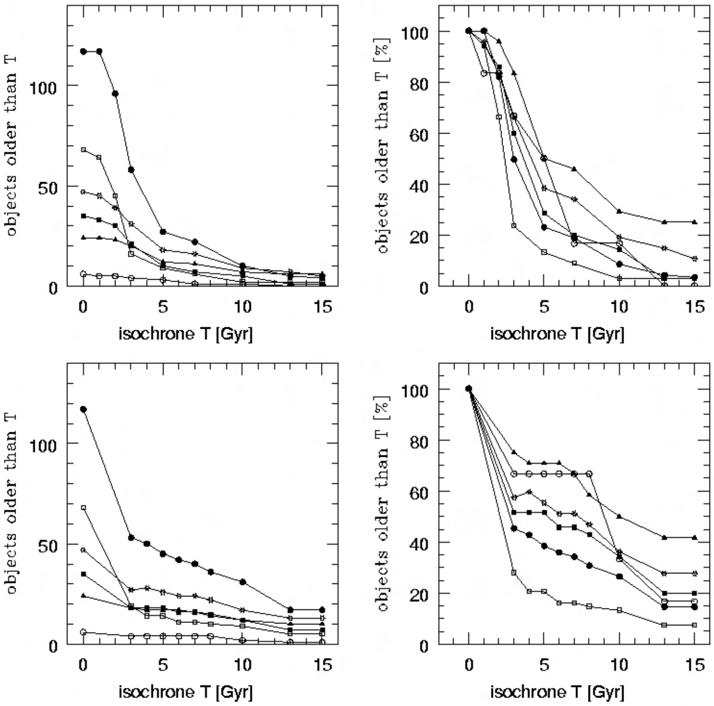

Fig. 6.1.— Cumulative age distribution for various galaxies using the SSP model isochrones by Vazdekis (upper panels) and Maraston (lower panels). The absolute (left) and relative (right) distribution for the galaxies are marked as follows: NGC 5846:solid circles, NGC 4365:open squares, NGC 3115:asterisk, NGC 7192:solid triangles, NGC 4478: open circles, M87: solid squares.

even more important for the Vazdekis and Maraston SSP models.

The SSP models by Vazdekis (1999) give in general a slightly redder $(V - I)$ color for a specific isochrone, compared to Bruzual & Charlot, although this difference depends on the age as well. Thus, any given object will therefore be assigned to a younger age and a better age resolution can be achieved. As a drawback we have to note that a larger globular cluster sample is required to obtain stable results in the χ^2-test. As we see in Figure 6.2 only the largest samples, NGC 5846 and NGC 4365 give reasonable good results in the χ^2 -test with χ^2 values which allow to claim a “fitting” model. For the four other tested globular cluster systems we can exclude the stellar population to be dominated by stars younger than 3 Gyr, but stronger conclusions would be far-fetched.

Since the SSP model isochrones given by Maraston (2001) do not show a unique $(V - I)$- age correlation for ages below 3 Gyr the cumulative age distributions of observed and simulated systems were compared only for ages above this limit. For the most numerous globular cluster samples we obtain consistent results, compared to the Bruzual & Charlot or Vazdekis models. The best fitting model to the cumulative age distribution contains a large fraction of objects younger than 3 Gyr. The NGC 5846 sample hosting less second generation (intermediate age) globular clusters than NGC 4365. A closer look at the model isochrones tells us why this consistency is only found

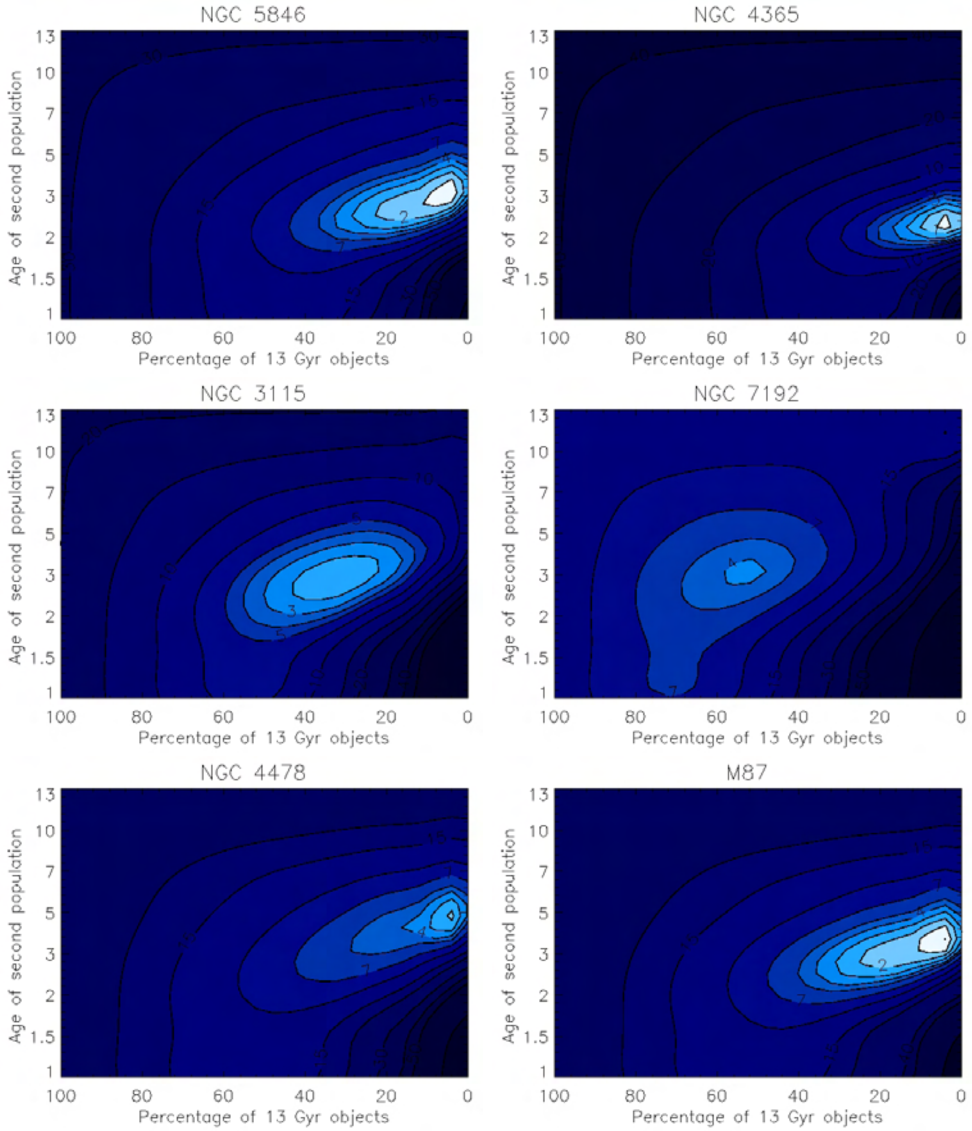

Fig. 6.2.— Results of the χ^2- test to find the best fitting to the observed globular cluster systems using the Vazdekis (1999) SSP model isochrones for age determination and modeling.

for NGC 5846 and NGC 4365 and why the χ^2-test fails in other globular cluster systems. Comparing the color-color distributions of the different globular cluster systems we find a very distinct over-density of objects in NGC 5846 and NGC 4365 supposedly younger than 5 Gyr, the resulting cumulative age distribution will therefore show a large fraction of the globular cluster sample in this age range and only a small percentage of the red cluster population will be assigned to an older age. The slope of the cumulative age distribution in the higher age region is thus very small, as we obtain it in the models for a cluster sample dominated by young objects. The nearly constant age distribution, as best seen in NGC 4365, is a very distinct feature of the age distribution and defines

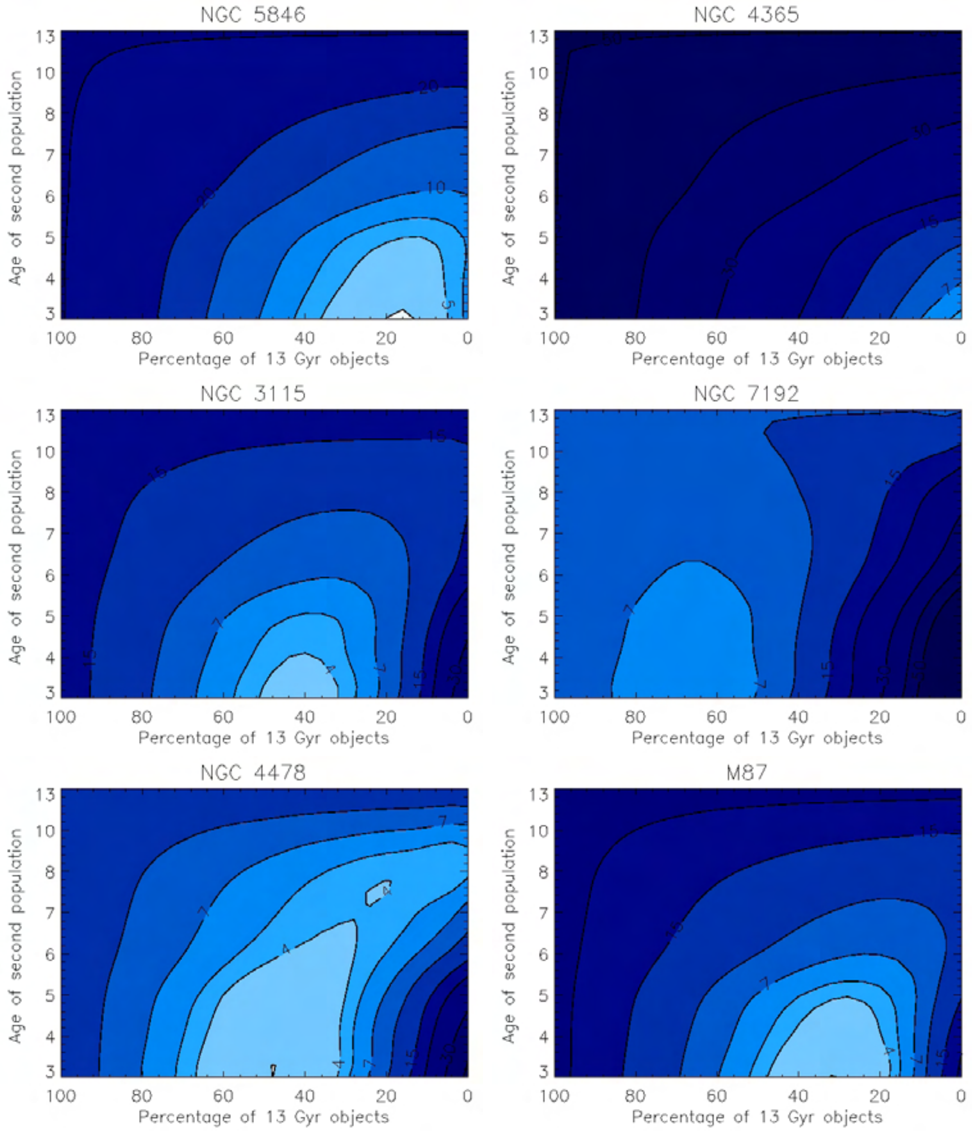

Fig. 6.3.— Results of the χ^2- test to find the best fitting model to the observed globular cluster systems on the basis of the Maraston (2001) SSP model isochrones.

mostly the result of the χ^2 -test. In the other four tested globular cluster systems such a well defined sub-population is not found and together with the remaining age-metallicity degeneracy effect the result of the χ^2-test is much more uncertain. Nevertheless, we want to emphasize here that this is by no means to be understood as criticism on the Maraston models, which in their latest version allow variations in the α-element abundances (Thomas & Maraston 2003, Thomas, Maraston & Bender 2003). Due to the photometric errors in our observations and the not completely broken age-metallicity degeneracy our observational data hamper a direct age determination (see Chapter 2.6), which is the base of our semi-numerical approach.

6.2.1 Model Settings: Size of the reference sample

In Chapter 1.2.4 and 2.6 the method of modeling color distributions by Monte-Carlo simulations was described, as well as the determination of the cumulative age distribution. With respect to the model parameters used previously it has been pointed out that the size of the simulated globular cluster sample was set with respect to the NGC 5846 sample, one of the most numerous globular cluster samples in our set of galaxies. From the stability tests (Section 2.4.2) we know that the sample size becomes important for the χ^2-test and we therefore want to know whether for small samples the test results improve if the simulated color distributions agree in their size with the different observed globular cluster systems. For NGC 7192, NGC 3115 and M87 we simulated globular cluster with the blue/red $(V-K)$ sub-population containing 21/40, 22/60 and 22/60 objects in NGC 7192, NGC 3115 and M87 respectively. The results of the comparison between the age distributions are shown in Figure 6.4. In the comparison with the corresponding plots in Figure 7.5 and 7.9 we do not find a significant improvement in the results. The age and size estimates for the small sample size are still much more uncertain than for NGC 5846 and NGC 4365. Thus we conclude that the minimum sample size, required for our semi-numerical method to describe the age structure in globular cluster systems, is mostly dependet on our choice of the applied SSP models in combination with the available broad band colors (see Chapter 3.5.2).

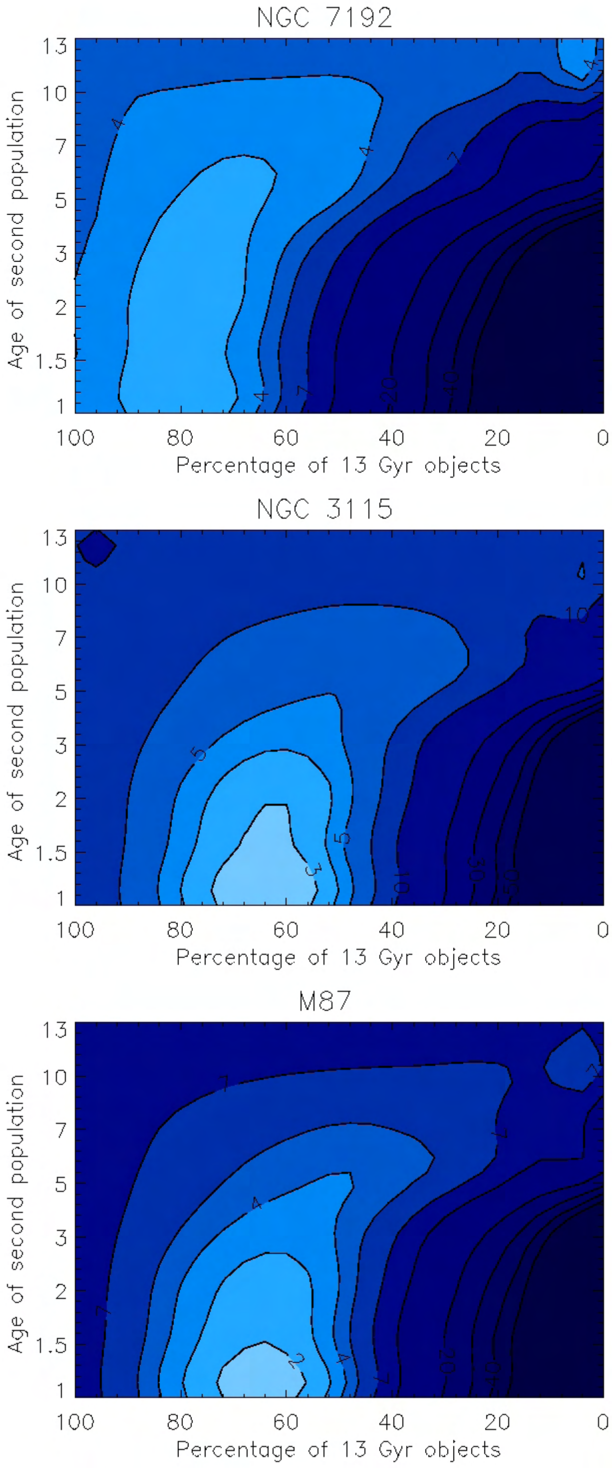

Fig. 6.4.— Results of the χ^2- test if the globular cluster sample in the simulations is set similar to the observed system (previous runs used the significantly larger models than NGC 7192, NGC 3115 and M87). We exclude NGC 4478 from this test due to its extremely small sample (6 objects only). The modeling as well as the determination of the cumulative age distributions was done using the Bruzual & Charlot SSP models (2003).

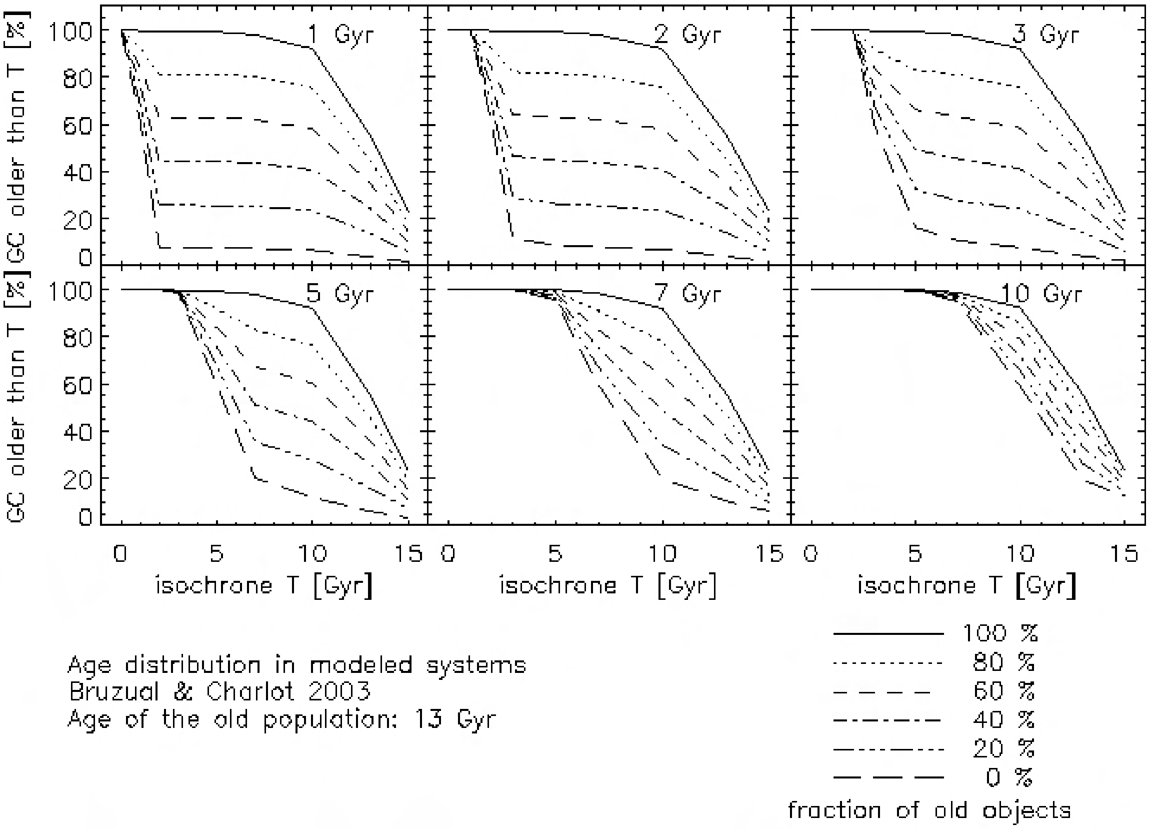

Fig. 6.5.— Cumulative age distributions derived for simulated globular cluster systems using the Bruzual & Charlot SSP model isochrones (2000).

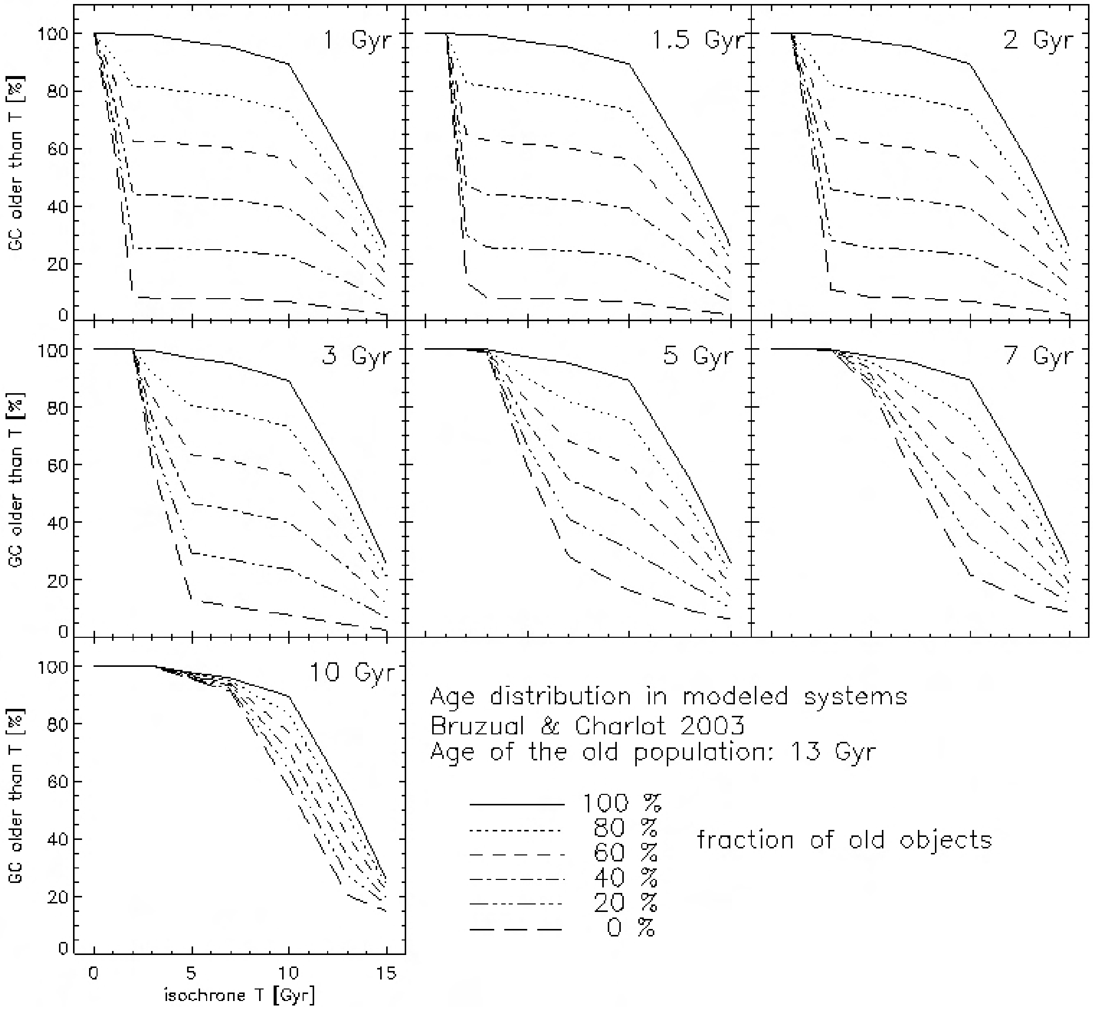

Fig. 6.6.— Cumulative age distributions derived for simulated globular cluster systems using the Bruzual & Charlot SSP model isochrones (2003).

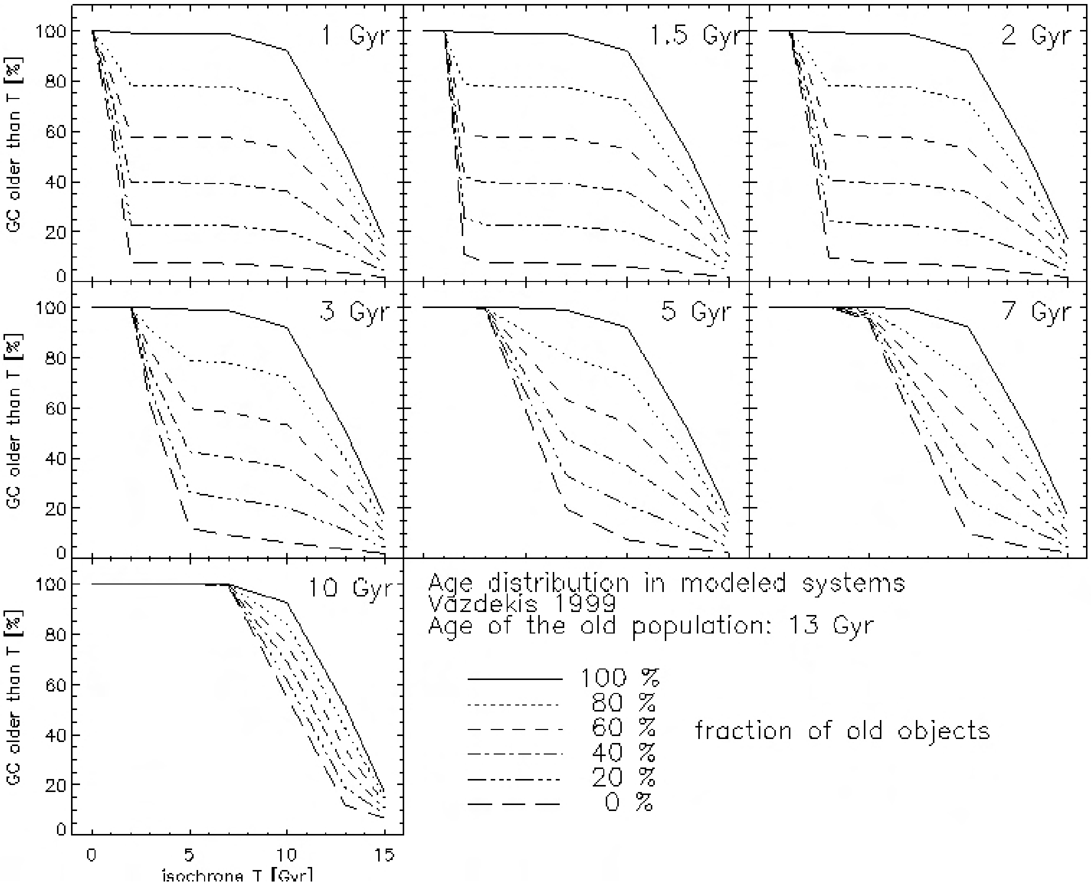

Fig. 6.7.— Cumulative age distributions derived for simulated globular cluster systems using the Vazdekis SSP model isochrones (1999).

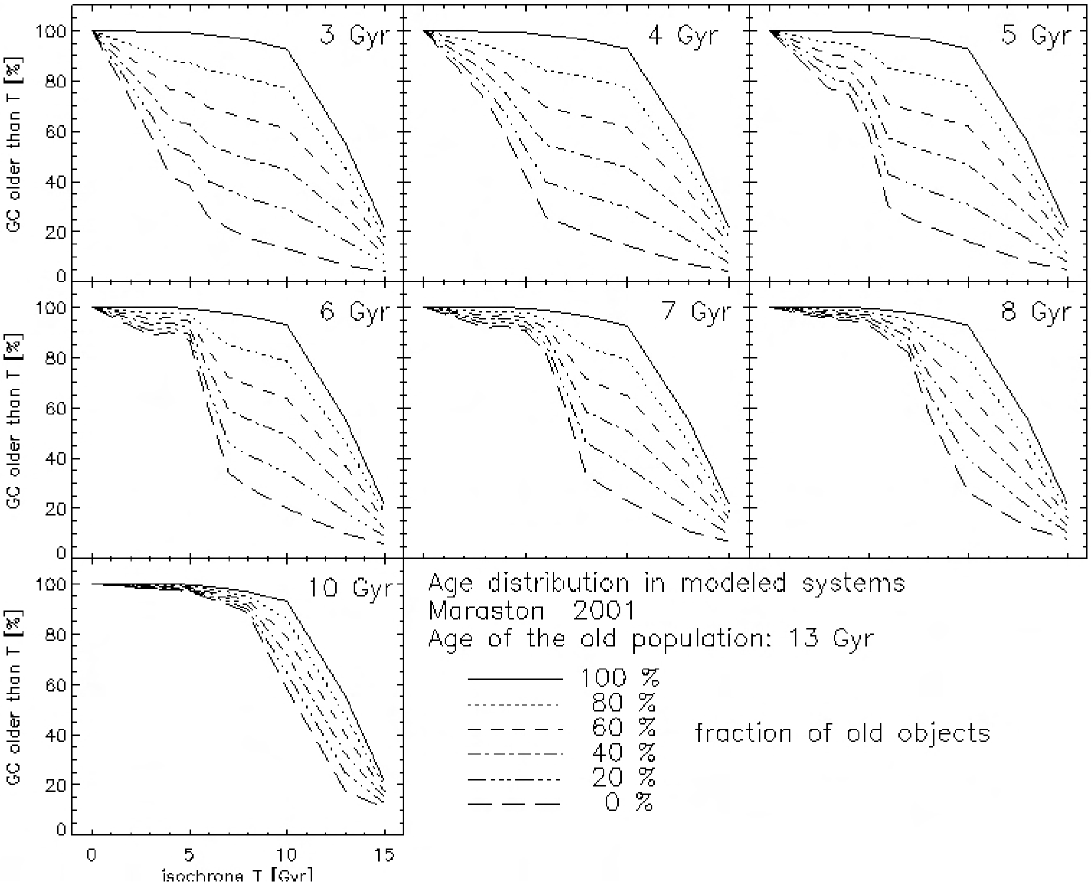

Fig. 6.8.— Cumulative age distributions derived for simulated globular cluster systems using the Maraston SSP model isochrones (2001).

References

Bruzual, G.A. & Charlot, S. 1993, ApJ, 405, 393B

Bruzual, G.A. 2000, private communication

Bruzual, G.A. & Charlot, S. 2003, MNRAS, 344, 1000

Maraston, C., Greggio, L. & Thomas, D. 2001, Ap&SS, 276, 893

Thomas, D.& Maraston, C. 2003, A&A, 401, 429

Thomas, D., Maraston, C. & Bender, R. 2003, MNRAS, 339, 897

Vazdekis, A. 1999, ApJ, 513, 224

7 Globular Cluster Systems *vs.* Globular Cluster Systems

Abstract

The age structure of globular cluster systems in early-type galaxies provides important clues about their formation and evolution. The semi-numerical method of detecting globular cluster sub-populations and deriving age and size limits for them, as introduced in chapter 1.2.4 and 2.6, has been applied to various globular cluster systems. In this chapter the galaxy sample will be extended and the results will be compared. In this comparison we use the galaxy environment as external parameter, in order to investigate to which degree the evolution of the galaxy depends on where the galaxy is found, e.g. in the center or the fringe of a massive galaxy clusters, in smaller groups or in rather isolated environment. In a sample of eight early-type galaxies four have been found with globular cluster sub-populations of different age, three of them in smaller groups or in the outskirts of the galaxy cluster center.

7.1 Introduction

In the last decades an immense wealth on observational data on globular clusters and globular cluster systems has become available and been mined fiercely. The tight link between globular cluster systems and their host galaxies on the one side, and the still ongoing discussion about "**the**" formation scenario valid for early-type galaxies on the other side created an ever growing interest in this objects. Fact is, that various features of a given early-type galaxy are best explained by any of the commonly accepted formation scenarios, whereas others are in complete contradiction to it. The fundamental plane, for example, is defined by correlations between photometric, kinematic and chemical properties (e.g. Djorgovski & Davies 1987, Dressler et al. 1987, Djorgovski, Pahre & de Carvalho 1996) and has been proven valid for a large range in redshift/look back time. The conclusion seemed to be that early-type galaxies form a very homogeneous population, consisting of an old stellar population and being similar in their basic features (e.g. Bower, Lucey & Ellis 1992, Renzini & Ciotti 1993, Ellis et al. 1997). Already before the observational and theoretical tools to derive the ages in extragalactic stellar populations with high accuracy became available, evidence was found that these correlations may hide more complicated and variable galaxy structures. In Chapter and 5 galaxies are discussed, which show kinematically de-coupled cores or prominent dust lanes. Obviously, galaxies with such peculiar features are prime targets to study the age structure in their globular cluster systems. Previous attempts to derive the age of stellar populations, either photometrically or spectroscopically, have been hampered by the age-metallicity degeneracy in broad band colors (Worthey 1994), luminosity weighted contributions of different age sub-populations to the diffuse galaxy light or, from a more technical point of view, the large distance of early-type galaxies. The introduction of combined optical and near-infrared photometry, the discovery of globular clusters representing single stellar populations and 8-10 m class ground based or space based telescopes made it possible to overcome those obstacles. Consequently, the next step towards an understanding of the formation of early-type galaxies is to investigate their age structure and find systematic correlations to external parameters, such as the luminosity/mass or the galaxy environment. Since high signal to noise spectra for globular clusters are still very time consuming photometric studies are a powerful tool to search for age sub-populations in globular cluster systems and to extend the galaxy sample, i.e. to cover a range of luminosities and different galaxy environments (cluster/group galaxies, field galaxies).

This thesis introduces a semi-numerical approach to detect age sub-populations in globular cluster systems on the basis of combined optical and near-infrared photometry. After the method has been describes and first results presented in the previous chapters, we now complement the galaxy sample and compare, respectively discuss the results.

7.2 Age Structure in Globular Cluster Systems

Based on the procedure described in Chapter 1.2.4 we derive the cumulative age distribution for the observed globular cluster systems and compare it to simulated systems via a reduced χ^2-test. In what follows we will discuss the results for individual galaxies with respect to their galaxy environment and draw a more general picture at the end of this chapter. Since the influence of the chosen SSP models, e.g. Bruzual & Charlot (2000, 2003), Vazdekis (1999) or Maraston (2001) will have been discussed in Chapter 5.5we will use for the comparison homogenous results using the Bruzual & Charlot models (Bruzual & Charlot 1993,Bruzual & Charlot 2000).

7.2.1 Modification in the Monte-Carlo Simulations

In contrast to Chapter 1.2.4 and Chapter 2.6 the models discussed here are based on the assumption of an old globular cluster population of age 13 Gyr, to be consistent with the WMAP results (e.g. Spergel et al. 2003). The most important modification in the determination of the cumulative age distribution as well as in the simulation process is that instead a least square fit to the model isochrones we are now working with linear interpolated secondary colors. Doing so we obtain a more accurate value for the secondary color $(V-I)$. As before the age distribution includes only objects with an near-infrared brightness $\geq$ the completeness limit and for which the photometric error (δ(V-I), δ(V-K), δ(V-H)) was found to be $\leq$0.15 mag. Additionally we note that in the comparison presented here no correction for background contamination with unresolved objects was applied (see Section 2.4.1). The approximation of the contamination rate by the Hubble-Deep-Field South works in general well in large globular cluster samples without showing a large effect, but a more accurate distribution of background objects is needed for smaller samples in order not to overestimate the contamination rate.

7.3 Galaxy Sample

Understanding the age structure in globular cluster systems of early-type galaxies as a function of the environment can provide further evidence to either of the basic formation scenarios, e.g. the monolithic collapse (e.g. Larson 1974, Forbes, Brodie & Grillmair 1997) or the hierarchical merging (e.g. Press & Schechter 1974, White & Frenk 1991, Ashman & Bird 1993). From the variety in early-type galaxies it becomes obvious that there exist external parameters, setting the conditions for a specific formation scenario to occur. The galaxy environment, e.g. the average density of galaxies as described by the Tully density parameters (Tully 1988), is a likely choice. Within the hierarchical merging scenario the impact of the galaxy density is easy to understand. Galaxies close to the gravitational center of a galaxy cluster, such as M87 or NGC 3311 in our galaxy sample and shown in Figure 7.1, are likely subject to galaxy -galaxy interactions at a very

early stage in the cluster formation. If merging played an important role for the evolution of the galaxy, it most likely happened early-on. Stellar populations, formed during such encounters might be younger than the bulk of the stellar component, but an age differences of $\lesssim 2$ Gyr will not be distiguishable in an age range between 10 and 15 Gyr. Due to the exposed position of cD galaxies we expect an increased probability of stripped globular clusters. Globular clusters found in the vicinity of cD galaxies might in fact not belong to this specific galaxy but to the galaxy cluster as such. Later we will discuss this scenario explicitly using the example of NGC 3311, the central galaxy of the Hydra I galaxy cluster (see Figure 7.1, right panel).
Although not very massive we would like to include NGC 4478 in this galaxy category, since it resides close to M87 (Figure 7.1, left panel, right edge) and thus close to the center of the Virgo galaxy cluster as well.

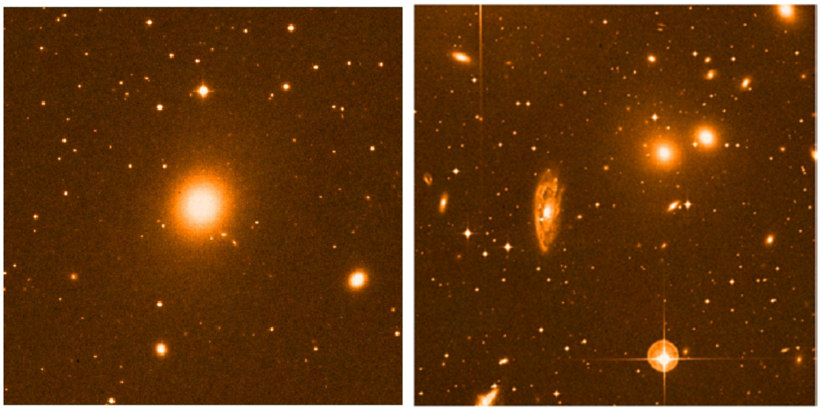

Fig. 7.1.— M87 (left) and NGC 3311 (right) two examples of central cluster galaxies (i.e. in the Virgo and Hydra I galaxy cluster). NGC 3311 is found close to another giant elliptical, NGC 3309 and NGC 3312, a spiral galaxy (left of NGC 3311). Credit Sloan Digitizes Sky Survey/ Sky Server. The image size is 20.′0 for M87 and 10.′0 for NGC 3311.

At the other end of the galaxy density spectrum we find isolated galaxies, e.g. NGC 7192 and NGC 3115 (Figure 7.2), with only few and distant neighbours. Galaxy interaction like mergers or accretion are not impossible though rather unlikely and two or more stellar populations may be found in special cases but are certainly not the norm.

More interesting for our search of intermediate age stellar populations are early-type galaxies in an environment where galaxy interactions are likely events, with long intervals between interactions, compared to the star formation time scale. Hence galaxies in groups or clusters, but off the cluster center, are where one would look first for globular cluster systems with different age components. Our galaxy sample contains three galaxies which fall in this category, namely NGC 5846, NGC 4365 and IC 4051 (Figure 7.3).

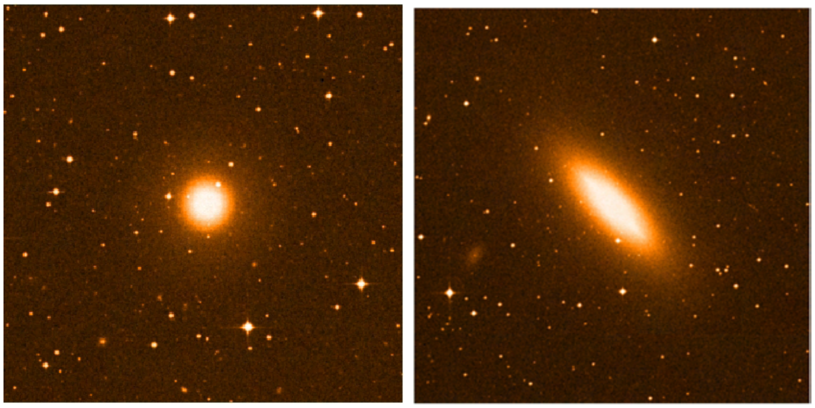

Fig. 7.2.— NGC 7192 (left) is a rather isolated elliptical galaxy with only one companion (NGC 7191). NGC 3115 (right), a S0 galaxy, on the other hand is situated at the very tip of the southern extension of the Leo group, as well with only one dwarf companion. The image scale is 10$'\!.0$ and 15$'\!.0$ for NGC 7192 and NGC 3115, respectively. North is up and East is to the left. Credit Sloan Digitized Sky Survey/Sky Server

7.3.1 Cluster Galaxies

The globular cluster systems discussed here are found within, or close to the gravitational center of galaxy clusters, which will certainly affect the galaxy and its globular cluster system. Due to their exposed position the timescale for the galaxy assembly will be rather short (e.g. Carretero et al. 2004) and any interaction has probably occurred early in the evolutionary history of the

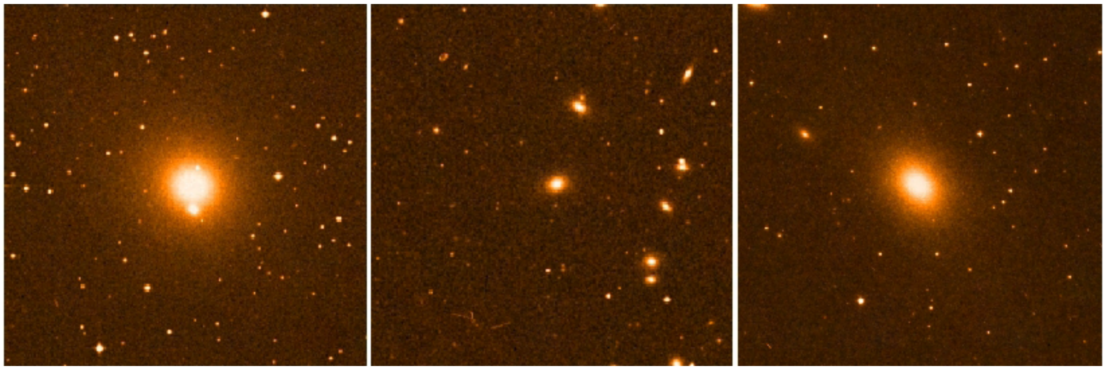

Fig. 7.3.— Examples for galaxies in group environment, or slightly off the galaxy cluster center. The image scaling for NGC 5846 (left) and IC 4051 (center) is 10$'\!.0$ and for NGC 4365 (right) 15$'\!.0$. The scaling for IC 4051 has been chosen to show the high density of galaxies within the Coma galaxy cluster. The observed galaxy is in all cases the one in the center of the image. North is up and East is to the left.

galaxy with no traceable signature, e.g. distinct second stellar population, left. However - one should also notice that there are exceptions like NGC 1316, the central cluster galaxy of the Fornax galaxy cluster. According to Goudfrooij et al. (2001) this galaxy host a population of ∼3 Gyr old globular cluster and is in fact a merger remnant. On the other hand the giant ellipticals, such as M87 (NGC 4486) and NGC 3311, have been found to host extremely numerous globular cluster systems. The specific frequency (Harris & van den Berggh 1981) is determined with 14±3 (Lee, Demarque & Zinn 1994, McLaughlin 1994) and 15±6 (Secker et al. 1995, McLaughlin 1995) for M87 and NGC 3311, respectively. This in mind one has to ask whether the globular clusters really formed in situ the galaxy or whether a significant fraction has been stripped away from close neighbours.

The Virgo galaxy cluster is the nearest big cluster of galaxies and dominates with its ∼2000 member galaxies our intergalactic neighbourhood. It also represents the physical center of our local super-cluster (Coma-Virgo Super-cluster) and influences all other galaxies and galaxy groups by its enormous mass (for more details see Binggeli 1999 and references therein). The peculiar velocities of the member galaxies for example, with respect to the cluster center, reach up to 1500km/sec.

M87 and its globular cluster system have been investigated extensively, e.g. for its extraordinary position in the galaxy cluster, the richness of the globular cluster system, its proximity of only 16.1 Mpc (e.g.Tonry et al. 2001) and not at least for its prominent jet, discovered by H.D. Curtis (1918). This giant elliptical is also identified with the strong radio source Virgo A (e.g. Owen, Eilek & Kassim 2000) as well as being a X-ray emitter. The formation and evolution of such a peculiar galaxy is therefore of large interest. Studies on the globular cluster system of M87 are manifold and led to controversial results. Based on Keck spectroscopy Cohen et al. (1998) find no sign of age differences between the globular clusters, neither did Jordán et al. (2002), using Strömgren photometry obtained with HST/WFPC2. On the other hand- globular cluster sub-populations with an age difference of 3-6 Gyr were claimed by Kundu et al. (1999).

The data we use to derive the age distribution were published and discussed by Kissler-Patig, Brodie & Minniti (2002). The combined optical and near-infrared colors of the globular cluster sample are mostly consistent with an old population (15 Gyr). Nevertheless, a very red ($(V-K)$>3.4) population is found with a $(V-I)$ color which is to blue for an old population. This leaves still room to discuss the possibility of coexisting globular cluster populations with slightly different ages.

One of the nearest neighbours of M87, the dwarf elliptical NGC 4478, was studied as well by Kissler-Patig, Brodie & Minniti (2002). The most interesting outcome of this work is that NGC 4478 don't seem to host metal rich clusters at all, similar to NGC 4874, one of the Coma galaxy cluster dominating ellipticals (e.g. Harris et al. 2000). In case of NGC 4478 the author's interpretation is that metal-rich globular clusters have probably never formed.

The third example for a galaxy in the center of a massive galaxy cluster is NGC 3311. Its globular cluster system is very populous and shows as a striking feature a large fraction of blue ($(V-I)\leq 0.9$) globular clusters, which can be found well beyond the tidal radius of the galaxy (Hilker 2003a, Hilker 2003b). Based only on optical data the color can be explained either by an old and very metal-poor or a young and metal-rich population. Wich ever explenation will found to be valid, the spatial distribution of this globular clusters is in anyway a matter of debate (Hilker 2003b). Early investigations, claiming that NGC 3311 host an extremely metal-rich globular cluster population, were disproved by Brodie, Larsen & Kissler-Patig (2000), who found the metallicity range in NGC 3311 to be very wide but not unreasonable.

Using the procedure described in Chapter 1.2.4, we derive the cumulative age distribution for M87, NGC 4478 and NGC 3311 as shown in Figure 7.4. In the absolute number distribution (left panel) we see immediately a significant difference between M87 and NGC 4478 on one side and NGC 3311. The later assigns $\sim\frac{2}{3}$ of the clusters to ages $\leq$3 Gyr, whereas the samples of M87 and NGC 4478 show a much less dominant fraction of intermediate/young globular clusters. To compare globular cluster samples of different sizes the relative age distribution is derived. Before applying any selection criteria the globular cluster systems of our "cluster"galaxies contained 93 (M87), 19 (NGC 4478) and 148 (NGC 3311) objects.

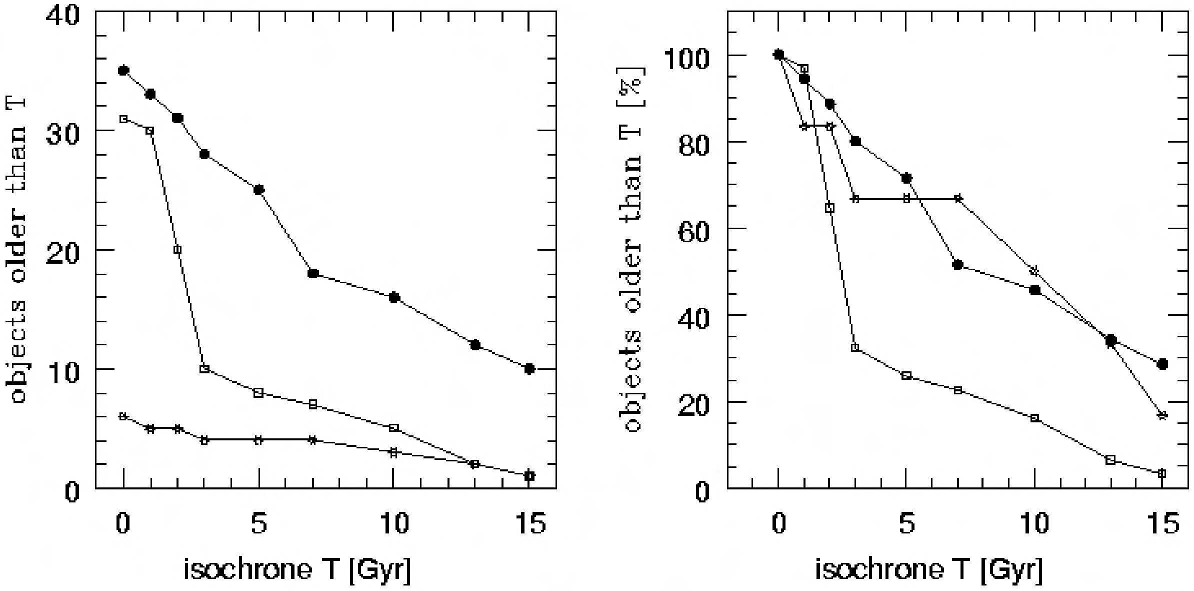

Fig. 7.4.— The cumulative age distribution for M87 (solid circles), NGC 3311 (open squares) and NGC 4478 (asterisk) in absolute values (left panel) and normalised to the total number of objects included (right panel).

From the relative age distribution we conclude that M87 and NGC 4478 seem to be very similar in their age structure. But much caution has to be paid in the argumentation about NGC 4478. After the application of all selection criteria, e.g. photometric error, near-infrared completeness and color limits (see Chapter 1.2.4 and 2.6) the globular cluster sample of NGC 4478 contains only 6 objects. As discussed in section 2.4.2 the comparison to simulated color distributions, i.e. the derived age distribution, bacome statistical unstable for such small samples. For M87 and NGC 3311 the cumulative age distribution derived for the observed samples has been compared to a set of simulated color distribution via a reduced χ^2 -test in order to confirm the intermediate/young globular cluster population and to set constraints on its relative age and size. For M87 the model for which the best agreement between the age distribution was found, contains about 70% old globular clusters and a small fraction of object younger than 2 Gyr. As we can see a good result for the χ^2- test can also be obtained assuming an exclusively old population of globular clusters with ages between 10 and 13 Gyr. This uncertainty is a result of the still existing, though lifted age degeneracy, combined with the sample size, only 35 globular clusters in M87 meet all selection criteria. Due to the relative small sample size the results are affected by the degeneration of the combination of age and size ratios between the different populations As already mentioned NGC 4478 is an extreme case for number statistics. For comparison reasons the result of the χ^2-test is presented in the middle panel of Figure 7.5, but drawing conclusions about the age structure and even the formation history of this galaxy is suspicious. According the selection criteria, mostly the color limits, only 6 globular cluster can be used for this analysis.

Although the infrared observations with NICMOS2 at the HST cut down the data set for NGC 3311 (field of view in total $40.''$), the usable sample still contains 31 objects. Comparing their age distribution with modeled systems reveals an intermediate/young age dominated globular cluster system, as already expected from the cumulative distribution. Our conclusion that the evolution of NGC 3311 does not follow the common “old + passive” scenario is also supported by the discovery of prominent dust shells around the central region of NGC 3311 (e.g. Västerberg, Lindblad & Jorsater 1991). Nevertheless, the question remains whether the blue $(V - I)$ and intermediate/young age globular clusters found in this sample are of the same origin as the once found at larger distances, and if so how they can sustain this position. If indeed a recent merger event led to the formation of this second generation of globular clusters, than one would expect them more concentrated in the center of the merger remnant, as shown for NGC 7252 by Hibbard & Mihos (1995). Since a more detailed discussion of the NGC 3311 results has already been given in Chapter 4.5 we will at this point stay with the fact of a second generation of globular clusters in a central cluster galaxy.

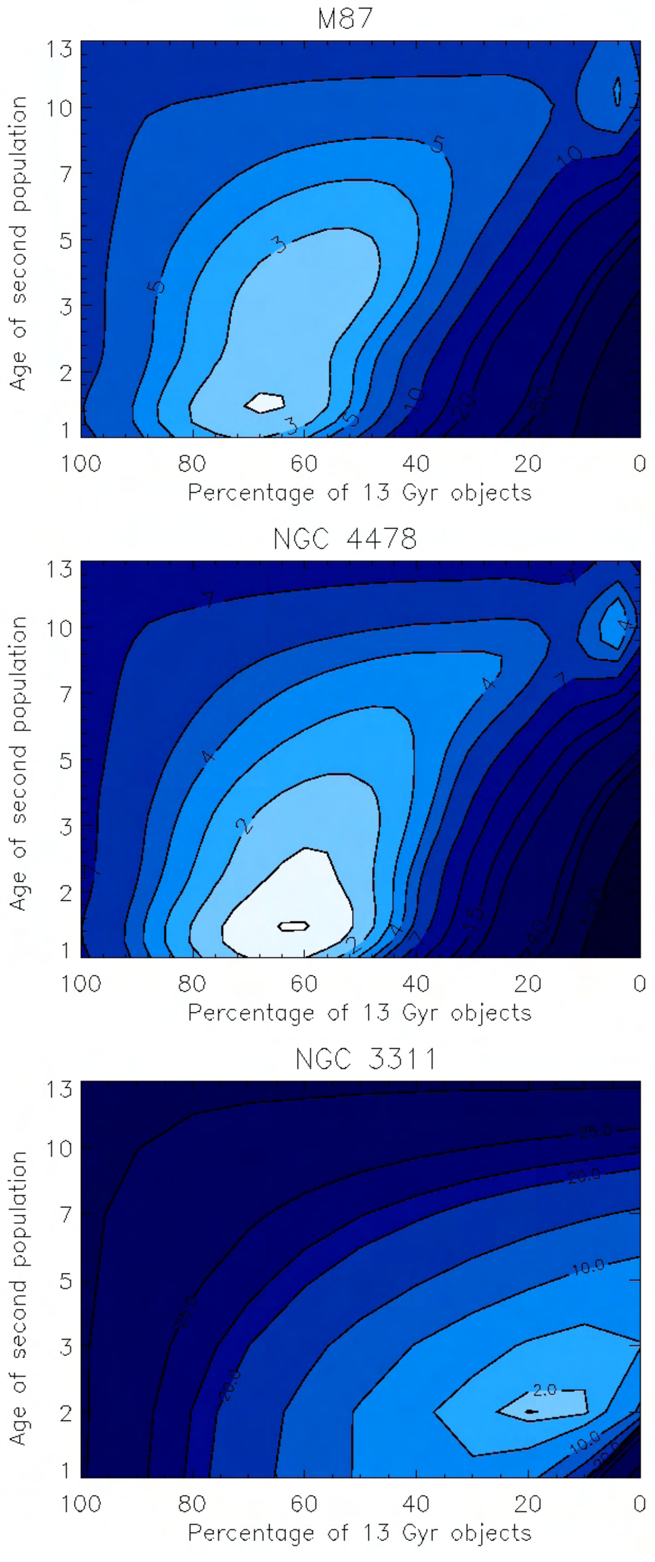

Fig. 7.5.— Results of the χ^2-test for M87, NGC 4478 and NGC 3311, galaxies close to the center of the host galaxy cluster. The contours represent the reduced χ^2 of the comparison between the cumulative age distribution in observed and modeled color distribution.

7.3.2 Group galaxies

Besides younger stellar populations one would expect more evidence for a galaxy interaction as trigger of star formation, e.g. dynamical peculiarities and morphological souvenirs. If we are to introduce our method of identifying age sub-populations in globular cluster systems our first choice of targets are galaxies with such special features, such as dynamical decoupled cores, dust shells, tidal tail like features or other hints to a more eventful past of the galaxy. In group or cluster environment (without being central cluster galaxies) galaxies have a probability for encounters with other group or cluster members. Compared to the center of galaxy clusters these interaction events are more distributed over a Hubble time.

Three galaxies in our sample, NGC 5846, NGC 4365 and IC 4051 belong either to a smaller group of galaxies or are found in the outskirts of their host galaxy cluster. With respect to above mentioned “peculiarities” we note that NGC 4365 and IC 4051 host dynamically decoupled cores (e.g. Surma & Bender 1995, Mehlert et al. 1998), whereas in the central region of NGC 5846 a prominent dust shell has been found (Goudfrooij & Trichnieri 1998).

One of the first globular cluster systems in early-type galaxies observed in the near-infrared is the one of NGC 4365 (Puzia et al. 2002). The $(V-I)$ *vs.* $(V-K)$ color distribution (see Figure U-band) reveal a distinct population of globular clusters, which belong to the red (in $(V-K)$) and metal-rich population, but have a $(V-I)$ color which is to blue for an old stellar population. NGC 5846 and IC 4051 show a similar color distribution, although the supposedly younger globular clusters in IC 4051 don’t show the same clustering in in infrared color as in NGC 5846 and NGC 4365. The cumulative age distributions for all three globular cluster systems, derived from the color-color diagrams is shown in Figure 7.6.

The comparison of the relative age distributions tells us that the age structure in all three observed globular cluster systems is very similar, with 50% of all clusters being younger than 5 Gyr which has also been found in NGC 3311. If we now compare the derived age distributions of observed and simulated systems (see Figure 7.7) we find the age structure in all three globular cluster systems to be best fit by a mix of two age populations, although there are differences between the individual systems. As already seen in the cumulative age distribution in NGC 5846 the second generation of globular clusters is not as well defined as it is the case for NGC 4365. Additionally in the best fitting model a larger fraction is assigned to the first generation of old (13 Gyr) globular clusters than in NGC 4365. The broader infrared color distribution found in IC 4051 for the younger globular clusters translates into a stronger degeneracy between age and metallicity effects as shown by the χ^2-contours.

With respect to our goal of finding systematic dependencies of the age structure in globular cluster systems we conclude that early-type galaxies in group environment are further evidence for a hierarchic star formation history. Since the selected galaxies are eye-catching by their dynamical

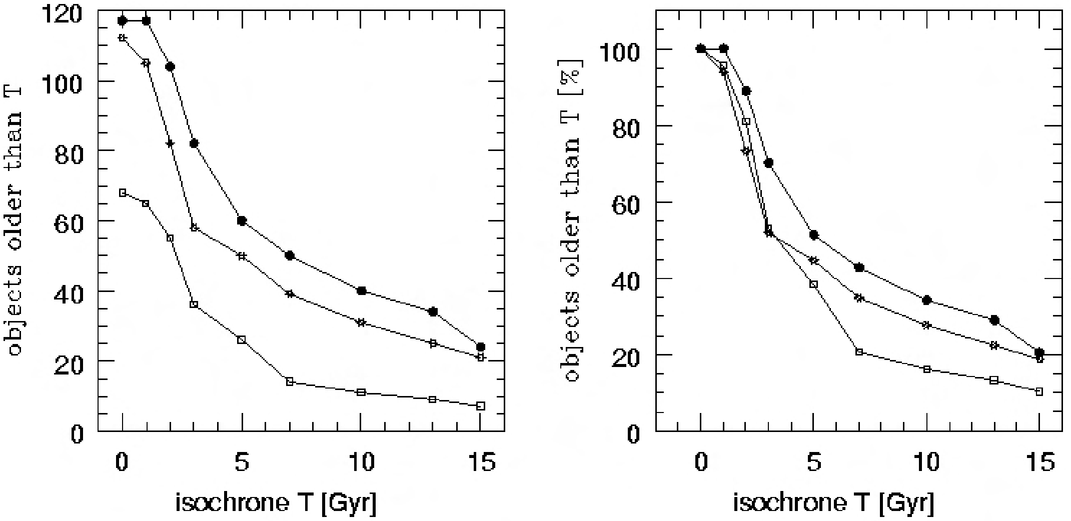

Fig. 7.6.— The cumulative age distribution for NGC 5846 (solid circles), NGC 4365 (open squares) and IC 4051 (asterisk) in absolute values (left panel) and normalised to the total number of objects included (right panel).

or morphological properties a larger and less biased galaxy sample has to be investigated to judge the significance of this result to the population of early-type galaxies.

7.3.3 Isolated Galaxies

In the previous two sections we found indeed differences between the age structure of globular cluster systems of early-type galaxies in the centerers of galaxy clusters and in the less exposed regions. Thus it is logical to to include rather isolated galaxies in the discussion as well and use their globular cluster systems as test examples for our method of age determination. Examples for rather isolated galaxies are NGC 7192 and NGC 3115. NGC 7192 and its color distribution has already been discussed in Chapter 2.6 and the photometric results for NGC 3115 can be found in Puzia et al. (2002). Compared to the other galaxies in our sample NGC 7192 and NGC 3115 correspond much better to the image of passively evolving galaxies. Accompanied only by dwarf galaxies (e.g.Puzia et al. 2000) both are unlikely to have been involved in galaxy interactions with a subsequently major star formation process. The cumulative age distribution, shown in Figure 7.8 and Figure 3.9 reflects this conclusion with a rather gentle slope and ∼50% of all globular clusters being older then 10 Gyr. Applying the selection by photometric error and K- band magnitude the globular cluster samples for NGC 7192 and NGC 3115 contain 47 and 24 objects, respectively.

In the comparison with age distribution in simulated globular cluster color distributions (see Appendix A) both globular cluster systems are more consistent with models containing either a large fraction (between 80% to 60 %) of 13 Gyr old objects, or even built by exclusively old objects, as seen best in the NGC 7192 contour plot. Nevertheless, we find the age structure in isolated galaxies to be similar to central cluster galaxies or galaxies close to the cluster center.

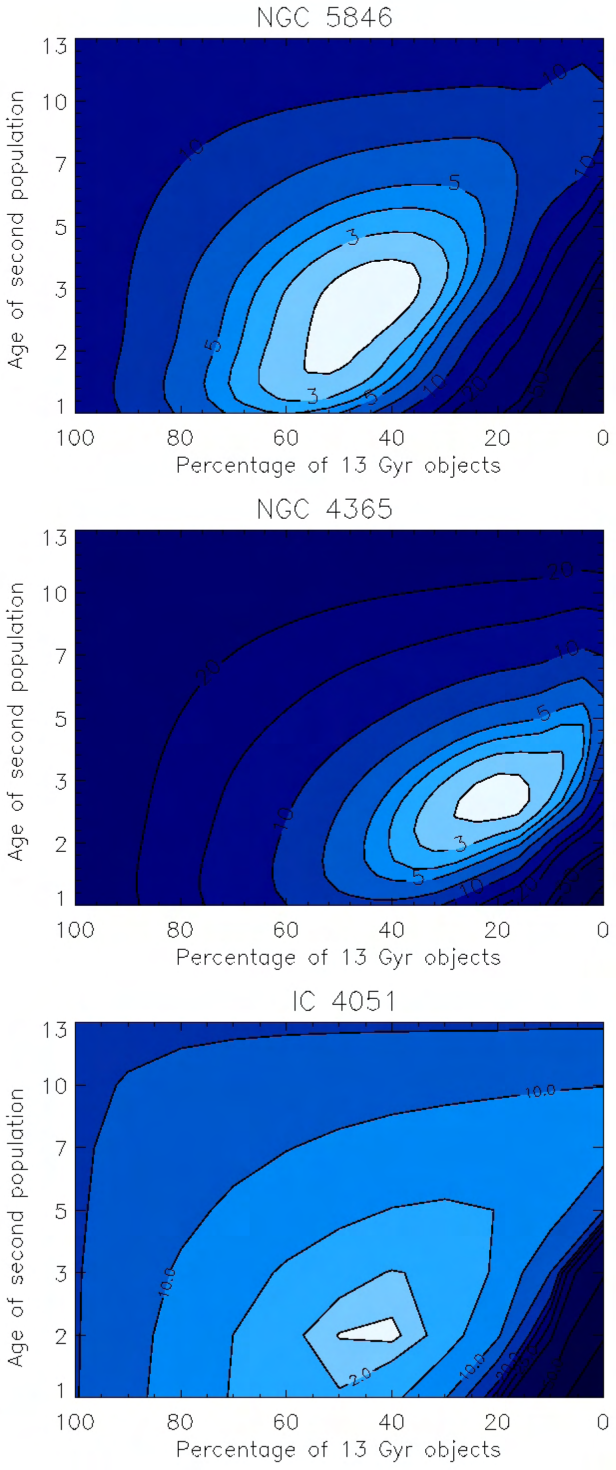

Fig. 7.7.— χ^2- contour plot for NGC 5846 (top), NGC 4365 (middle) and IC 4051 (bottom). The contours represent the χ^2 values for the comparison between the cumulative age distribution in the observed globular cluster systems and a system of 77 different simulations. In all three systems the best fitting model to the observed data contain a significant fraction of intermediate/young globular clusters. The surprisingly large contribution of this second generation globular clusters will be discussed later.

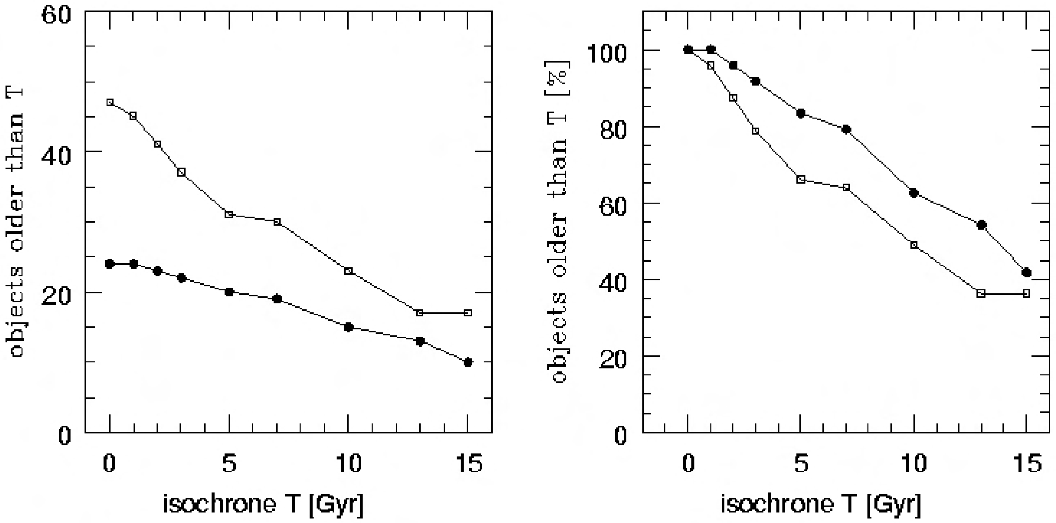

Fig. 7.8.— The cumulative age distribution for NGC 7192 (solid circles), NGC 3115 (open squares) in absolute values (left panel) and normalised to the total number of objects included (right panel).

References

Ashman, K.M. & Bird, C.M. 1993, AJ, 106, 2281

Binggeli, B. 1999, "The Virgo Cluster- Home of M87", in: Proceedings Ringberg Meeting, H.J. Röser, K. Meisenheimer (eds.), Springer Verlag Berlin

Bower, R.G., Lucey, J.R., Ellis, R.S. 1992, MNRAS, 254, 601

Brodie, J.P., Larsen, S. & Kissler-Patig, M. 2000, ApJ, 543, L19

Bruzual, G.A. & Charlot, S. 1993, ApJ, 405, 393B

Bruzual, G.A. & Charlot, S. 2000, private communication

Carretero, C., Vazdekis, A., Beckman, J.E. et al. 2004, ApJL, accepted

Cohen, J.G., Blakeslee, J.P. & Ryzhov, A. 1998, ApJ, 501, 554

Curtis, H.D. 1918,Publ. Lick Obs., 13, 9

Djorgovski, S. & Davies, M. 1987, ApJ, 313, 59

Djorgovski, S., Pahre, M.A. & de Carvalho, R.R. 1996, ASP Conference Ser., 86, 129

Dressler, A., Lynden-Bell, D., Burstein, D. et al. 1987, ApJ, 313, 42

Ellis, R.S., Smail, I., Dressler, A. et al. 1997, ApJ, 483, 582

Forbes, D.A., Brodie, J.P. & Grillmair, C.J. 1997, AJ, 113, 887

Goudfrooij, P. & Trichnieri, G. 1998, A&A, 330, 123

Harris, W.E. & van den Bergh, S. 1981, AJ, 86, 1627

Harris, W.E., Kavelaars, J.J., Hanes, D. A. et al. 2000, ApJ, 533, 137

Hibbard, J.E., Mihos, J.C. 1995, AJ, 110, 140

Hilker, M. 2002, in: Proceedings of the IAU Symp., "Extragalactic Star Clusters", eds. D.Geisler, E.K. Grebel, D.Minniti, 207, 281

Hilker, M. 2003, ASP Conf. Ser. 296, 583

Hilker,M 2003, ESO Astrophysical Symp.:"Extragalactic Globular Cluster Systems", 173

Jordán, A., Côte, P., West et al. 2002, ApJL, 576, 113

Kissler-Patig, M., Brodie, J.P. & Minniti, D. 2002, A&A, 491, 441

Kundu, A. Whitmore, B.C., Sparks, W. et al. 1999, ApJ, 513, 733

Larson, R.B. 1974, MNRAS, 166, 585

Lee, Y.-W., Demarque, P. & Zinn, R. 1994, ApJ, 423, 248

McLaughlin, D.E. 1994, PASP, 106, 47

McLaughlin, D.E. 1995, AJ, 109, 2034

Mehlert, D., Saglia, R.P., Bender, R. et al. 1998, A&A, 332, 33

Owen, F.N., Eilek, J.A. & Kassim, N. E. 2000, ApJ, 543, 611

Press, W.H. & Schechter, P. 1974, ApJ, 187, 425

Puzia, T.H., Kissler-Patig, M., Brodie, J.P. et al. 2000, AJ, 120, 777

Puzia, T.H., Zepf, S.E. , Kissler-Patig, M. et al. 2002, A&A, 391, 453

Renzini, A. & Ciotti, L. 1993, ApJ, 416, L49

Secker, J., Geisler, D., McLaughlin, D.E. et al. 1995, AJ, 109, 1019

Spergel, D.N., Verde, L., Peiris, H.V. et al. 2003, ApJS, 148, 175

Surma, P.& Bender, R. 1995, A&A, 298, 405

Tonry, J.L., Dressler, A., Blakeslee, J.P. et al. 2001, ApJ, 546, 681

Tully, R.B. 1988, “Nearby galaxies catalog”, Cambridge University Press

Västerberg, A. R., Lindblad, P. O.; Jorsater, S. 1991, A&A, 247, 335

Vazdekis, A. 1999, ApJ, 513, 224

White, S.D.M. & Frenk, C.S. 1991, ApJ, 379, 521

Worthey, G. 1994, ApJS, 95, 107

8 Summary

The work presented here deals with the age structure in globular cluster systems of early-type galaxies and aims at further clues about the formation and evolution of these galaxies. Hereby we turn our attention mainly to the detection of age sub-populations within the globular cluster systems, which are a clear signature of multiple star formation events and describe the major phases in the evolutionary history of the host galaxy. The basic ingredients to our semi-numerical approach are combined optical and near-infrared observations of various globular cluster systems and Single Stellar Population models.

Besides the introduction and the test of our semi-numerical method of deriving the age structure in globular cluster systems we are also interested in investigating an extended galaxy sample, i.e. their globular cluster systems in order to find systematic dependencies of the age structure. Since Single Stellar Population models are crucial for our project and various of these models are available we also to evcaluate the influence of our choice of SSP model on the final result.

In what follows we will summarize the major outcomes of this PhD project, draw final conclusions and give a brief outlook about the next steps which we think should complement our results.

8.1 Synopsis

Methodology

- Based on the model predictions for the time dependent evolution of single stellar population colors, represented by a globular cluster, color-color distributions can be used to derive their age distribution.
- Using the same SSP models the color distributions of globular cluster systems with a given composition, e.g. age and size of sub-populations, can be simulated and the corresponding cumulative age distribution can be derived.
- The comparison of observed and simulated age distributions via χ^2-test allows to set limits on age, and to some extend, on the relative size of age sub-populations. Due to the selection of objects included in this analysis, the size estimate will be at the most be a upper limit.
- The age rsolution can be increased by extending the observations into the short wavelength range, although this is paid for with stronger selection of globular clusters and henceforth a smaller sample. As our tests have shown below a model dependent limit the sample size becomes important as the χ^2-test are not stable.
- The application of different SSP models affects the final result in so far as the the age resolution and the required sample size are concened.

Age Structure in Globular Cluster Systems

- The age structure in globular cluster systems of early-type galaxies is more diverse than expected and sees indeed multiple star formation events in some elliptical galaxies.
- A set of eight early-type galaxies has been investigated, representing different classes of galaxy environments, such as the central regions of galaxy clusters (M87, NGC 3311, and NGC 4478), the less dense regions of smaller groups and cluster outskirts (NGC 5846, NGC 4365, IC 4051) as well as isolated field regions (NGC 7192 and NGC 3115). The cumulative age distributions for these galaxies and the comparison with simulated systems reveals a second generation of globular clusters in NGC 5846, NGC 4365, IC 4051 and NGC 3311, with a spectroscopic confirmation for NGC 5846 and NGC 4365.
- Assuming the first generation of globular clusters to be 13 Gyr old, the age distribution in NGC 5846 is best matched by a model containing 40-60 % of intermediate age (1-4 Gyr) globular clusters. In NGC 4365 the intermediate/young age fraction (within the observed sample) seems to be even larger and its age less uncertain, in the range between 2-3 Gyr.

- In case of IC 4051 the best fitting model to the cumulative age distribution assings about 50 % to an age of ∼2 Gyr. Although the χ^2-test results define the "best" model quite well, we have to be cautios in our interpretation. Compared to the previously discussed globular cluster systems the IC 4051 sample is relatively small and we can not exclude stability problems in the χ^2-test, which translate into a larger uncertainty in the age and size estimates.

- The globular cluster systems of isolated field galaxies, e.g. NGC 7192 and NGC 3115 are built by a population of old (10- 13 Gyr) and show no sign of a significant stellar population of younger age. Since in a low density environment galaxy interactions are rather unlikely this result is still consistent with the merger scenario for early-type galaxy formation.

- The situation for our galaxy sample in galaxy cluster core environment is less conclusive. The globular cluster sample of M87 and NGC 4478 follow the expectation of an dominant old population, although NGC 4478 is an extreme example for stability discussions. The age structure in NGC 3311 is atypical for a central cluster galaxy, hosting a large, spatial extended population of blue globular clusters which are, at least in the central region, about 10 Gyr younger than the first generation of globular clusters. The question remains whether these clusters belong to NGC 3311 very own globular cluster system or to the galaxy cluster core in general. and whether the blue population is uniformly built up be a young/ intermediate age population.

- The large differences in the age structure in the observed globular cluster systems change the picture of an passive evolution of these galaxies. Among other things we find the galaxy environment to be an important parameter, with galaxies in groups and outside the core of galaxy clusters being more likely to undergo interactions und boost second star formation events than field or cD galaxies.

8.2 Outlook

- So far the age distributions in observed globular cluster systems were compared to simulations assuming the first generation to be 15 and 13 Gyr old out of convinience and accordingly to to the latest WMAP results. Knowing that early-type galaxies show a surprisingly diverse age structure this approach should be replaced by a more galaxy specifc procedure. Taking advantage of the still higher accuracy of spectroscopic age estimates the age of a small sample supposedly old globular clusters (selected from the photometric data set) can be used for more realistic Monte-Carlo simulations.

- In the discussion of possible bias effects on the relative size of age sub-populations the spatial distributions plays a major role. Hence, if the size ratio between the globular cluster sub-populations is of special interest spatial extended samples need to be investigated.

- Morphological features hint to a rather exciting evolutionary history also in early-type galaxies. Nevertheless, also in a group environment galaxy interactions are likely but not compulsory events and a larger galaxy sample will be necessary to allow conclusions on the likelyhood of such events.
- Recent studies have shown that age estimation using SSP isochrones depends on the applied element abundance ratios. Although the mere detection of age sub-population should not be affected the age estimates will eventually change if different abundance ratios are applied.

Acknowledgments

The work presented in this thesis would not have been possible without the support and help of many people whom I would like to thank at this place.

Before all I am grateful to **Markus Kissler-Patig**, my supervisor at the European Southern Observatory, for his support, advice, encouragement when things didn't work out as fast or well as I would have liked them to do and last but not least for giving me the opportunity to start a PhD in astronomy. For this very reason I would also like to thank **Ralf Bender**, my supervisor at the LMU, as much as for his invaluable help in administrative challenges. Thanks to **Michael Hilker**, **Thomas Puzia** and **Søren Larsen** for answering many questions about astronomy or data reduction and sharing their knowledge and experience.

Soon I will leave the European Southern Observatory and it's due to countless staff members, fellows and students that this is going to be very hard. Besides everything I learned about astronomy in general, observing and data reduction I will take with me that there is nothing more exciting than spending time with people sharing my interest in astronomy and being generous with time, help and sometimes mental kick-offs. I'm deeply gratefully for Monday evening games, hiking tours, movie nights and simple "let's get together and chat" evenings, which added the necessary fun element to my student life. My special thanks goes to all the people I was lucky to share the office with. **Marina Rejkuba** and **Elena Pancino** welcomed me at ESO and showed endless patience telling me the secrets of IRAF and SuperMongo and how to express my dislike of "Fatal error" messages in Italian. I thank **Nicole Homeier** and **Nate Bastian** for interesting discussions about the relativity of ages in astronomy, the excitement of astronomical research, the beauty of IDL scripts and a bit off topic, about the emancipation of woman in science. To the Science Coffee Circle, **Bruno Leibundgut, Bob Fosbury, Harald Kuntschner, Chris Mullis, Maria-Rosa Cioni, Marina Rejkuba, Nicole Homeier, Markus Kissler-Patig, Gjis Verdoes** and many more, my sincere gratitude for showing me that there are other subjects in astronomy than the one my PhD is about. As a former Microsoft user I would like to thank the the **ESO Helpdesk** and especially **Antonello Piemonte** for their endless patience solving my computer problems and keeping my laptop alive.

I would like to thank the initiators, organizers and lecturers of the International Max-Planck Research School for Astronomy and Astrophysics for creating the environment where also students with no astronomy background, such as myself, are enabled to start a career in this scientific field.

I'm indebted to **Doug Geisler, Tom Richtler, Boris Dirsch and Ylva Schuberth** for their support and hospitality during my stay at the Universidad Concepción in Chile, which

filled these two month with interesting discussions as well as with unforgettable memories about a beautiful country.

I would also like to thank **Encarni Romero Colmenero, Stephen Potter, Sonja Vrielmann and Patrick Woudt**, my friends at the South African Astronomical Observatory and the University of Cape Town for letting me join them for observing nights, answering my endless questions in astronomy and of course encouraging me to move from solid state physics to astronomy. I wish I could also express my gratitude to the late **Duncan Elliot** for his advice: "If you want to do it- go for it.".

Meiner Familie, insbesondere meinen **Eltern** und meinen **Schwestern** danke ich für ihre Unterstützung, ihr Verständnis und ihre Liebe, und dafür daß sie mir immer das sichere Gefühl gaben, daß meine Entscheidungen für mich genau richtig sind. Ich weiß, daß einige davon für sie nicht einfach zu akzeptieren waren.

Lebenslauf

Name	Maren Hempel
Geburtsdatum	12. August 1967
Geburtsort	Karl- Marx- Stadt
Nationalität	deutsch
Familienstand	ledig

Ausbildung

- 1974- 1984 Polytechnische Oberschule Auerswalde-Oberlichtenau
- 1984- 1986 Erweiterte Oberschule, Karl-Marx-Stadt, Abitur
- 1986- 1991 Technische Universität Chemnitz, Physikstudium
- 1991 Erlangung des Physikdiploms
- 1996 Promotion an der Universität des Saarlandes zum Dr.rer.nat.

Bisherige Tätigkeiten

- >2001 Europäische Südsternwarte, Garching, Doktorand
- 2001 Nationales Beschleunigerzentrum, Somerset West, Republik Südafrika, wissenschaftlicher Mitarbeiter
- 1998- 2000 Universität Kapstadt, Cape Town, Republik Südafrika, Postdoktorand
- 1997- 1998 Universität des Saarlandes, Saarbrücken, wissenschaftlicher Mitarbeiter
- 1996- 1997 Fraunhofer Institut für Zerstörungsfreie Prüfverfahren, Dresden, freier Mitarbeiter
- 1992- 1996 Fraunhofer Institut für Zerstörungsfreie Prüfverfahren, Dresden, Doktorand
- 1992 Technische Universität Chemnitz, wissenschaftlicher Mitarbeiter

Forschungsaufenthalte

- 05/2003- 06/2003 Universität Concepćion, Chile
- 03/1995- 12/1995 Vereinigtes Institut für Kernforschung, Dubna, Russland
- 08/1994- 02/1995 Hahn- Meitner Institut, Berlin
- 01/1993- 08/1994 Vereinigtes Institut für Kernforschung, Dubna, Russland

Datum: Maren Hempel